RESEARCH ARTICLE

South American Nothochrysinae (Neuroptera, Chrysopidae): I. Description of *Nothochrysa ehrenbergi* sp. nov.

Catherine A. Tauber[1]

1 *Department of Entomology, Comstock Hall, Cornell University, Ithaca, NY 14853, USA* **2** *Department of Entomology and Nematology, University of California, Davis, CA, 95616, USA*

Corresponding author: *Catherine A. Tauber* (cat6@cornell.edu)

Citation: Tauber CA (2019) South American Nothochrysinae (Neuroptera, Chrysopidae): I. Description of *Nothochrysa ehrenbergi* sp. nov. ZooKeys 866: 1–18. https://doi.org/10.3897/zookeys.866.35394

Abstract

A new species, *Nothochrysa ehrenbergi* **sp. nov.**, is described from Chile; it is the first species of *Nothochrysa* to be reported from the Southern Hemisphere and only the second from the New World. The genus now contains six extant species as well as two species known from late Oligocene and Miocene fossils. An updated catalog of the valid *Nothochrysa* species is presented, and three *nomina dubia* are discussed. The inclusion of the new species in *Nothochrysa* is well supported by morphological features. However, it and other species currently in the genus also share significant features with *Archaeochrysa*, an older genus of Nothochrysinae which is known only from the Eocene (Ypresian) to the late Oligocene. It therefore appears that *N. ehrenbergi* is among the least derived *Nothochrysa* species, and that the separation of *Archaeochrysa* from *Nothochrysa* is open to question and further examination.

Keywords

Archaeochrysa, Chile, fossils, Green lacewing, wing venation

Introduction

The family Chrysopidae currently consists of three extant subfamilies. Chrysopinae, with approximately 75% of the known chrysopid genera, is by far the largest (N = ~80 genera). The other two subfamilies combined are much smaller (N =14 genera): Apochrysinae with five genera (Winterton and Brooks 2002) and Nothochrysinae

with nine (Adams 1967, Adams and Penny 1992). In addition, Nothochrysinae has 13 genera known only from fossils (Makarkin and Archibald 2013, Archibald and Makarkin 2015). Based on its morphological characters and substantial presence in the fossil record, the subfamily Nothochrysinae has long been considered the most basal of the extant chrysopids. However, recent molecular evidence does not consistently support this conclusion (Engel et al. 2018, Winterton et al. 2019).

Currently, there are records of four extant genera of Nothochrysinae from the New World, three of which are endemic to the region: *Asthenochrysa* Adams & Penny and *Leptochrysa* Adams & Penny (one species each) in South America, and *Pimachrysa* Adams (five species) in North America. The fourth genus, *Nothochrysa* McLachlan, is widespread throughout the Northern Hemisphere, but only one species is known from the New World (western North America).

During the last few years, several very interesting specimens of Nothochrysinae from the New World were found in museums. Among these specimens is a new species of *Nothochrysa*, the first from South America and the first from the Southern Hemisphere. The article here describes this new species and discusses its possible relationships with other genera of Nothochrysinae. Also included among the recently discovered New World specimens is the second known example of *Leptochrysa prisca* Adams & Penny. A separate article redescribes and provides images of this rare monotypic genus (Tauber 2019).

Systematics of *Nothochrysa* McLachlan

The genus *Nothochrysa* has had a tortuous taxonomic history that is well summarized by Tjeder (1966: 264). Briefly, over the years *Nothochrysa* has included a large number of species that correctly have been moved to other genera, mostly *Italochrysa* Principi. By the time this study began, the number of species in the genus *Nothochrysa* had been reduced to only ten – eight extant and two known from fossils (Oswald 2018). However, among the extant species there are three whose validity has been questioned. Thus, with the addition of the new species described here, there are eight confirmed, valid species of *Nothochrysa*: six extant and two from fossils (Table 1), as well as three *nomina dubia* (Appendix 1).

Table 1. Catalog of valid species names in the genus *Nothochrysa* McLachlan.

Extant species
californica Banks, 1892 [North America: southwestern Canada, western USA]
capitata (Fabricius, 1793) [Europe: widespread; northern Africa: Algeria, Tunisia]
ehrenbergi sp. nov. [South America: Chile]
fulviceps (Stephens, 1836) [Europe: widespread]
sinica Yang Chi-kun, 1986 [Asia: China]
turcica Kovanci & Canbulat, 2007 [Eurasia: Turkey]
Fossil species
praeclara Statz, 1936 [Miocene: Germany]
stampieni Nel & Séméria, 1986 [Oligocene: France]

Material and methods

Current usage of terms for veins in neuropteran wings is largely based on the classic studies of tracheal pathways by Tillyard (1916) and Comstock (1918, and his earlier studies with Needham), which were later modified and interpreted by others, e.g., Adams (1967), Kukalová-Peck (1991), Kukalová-Peck and Lawrence (2004), and most recently Breitkreuz et al. (2017). I did not examine tracheal pathways in the current study, and this report uses terminology for veins and cells based on a combination of the above studies. For example, as is customary, the names of the primary veins are abbreviated and capitalized (e.g., C, costa; Sc, subcosta; R, radius; M, media; Cu, cubitus; A1, A2, A3, first, second, and third anal veins; also Psm, pseudomedia and Psc, pseudocubitus). When veins split, I use A and P to indicate the anterior and posterior branches, as proposed by Breitkreuz et al. (2017). In addition, the term "furcation" and its italicized abbreviation "*f*" are useful in referring to the point on a vein where it forks or splits. Thus, for example, M*f* applies to the point on the media where it splits into two branches, the media anterior, MA, and the media posterior, MP.

The names of crossveins are in lowercase, contain a hyphen, and often begin with a number; for example, 1c-sc is the first (basal-most) costal-subcostal crossvein. Cell names are written in lowercase, italicized, and often appended with a number; e.g., *csc1* refers to the basal-most cell between C and Sc. For historical and grammatical consistency, I retained the traditional prefix "intra", rather than "inter" (as proposed by Breitkreuz et al. 2017), when referring to cells between two branches of the same major vein. For example, *im1* denotes the first "intramedian" cell, and *icu3* denotes the third "intracubital" cell. I also reversed the terms "eutriangular" and "pseudotriangular", as used by Breitkreuz et al. (2017) to categorize two types of *im1* cells. Their figure 17B, in which the *im1* is labeled "pseudotriangular", illustrates a triangular cell with three angles where three entities – two veins (MA, MP) and a crossvein (ma-mp) – intersect. This configuration is a true triangle and should carry the term "eutriangular". Similarly, their figure 17A illustrates another triangular-shaped *im1* cell, but this one has two curved sides (MA, MP) and only two angles where the veins intersect. They identified this configuration as "eutriangular", whereas it should be considered "pseudotriangular". The above changes do not affect the authors' interpretation of the venation, nor do they affect figures 17C or 17D. They merely help facilitate grammatical and user-friendly terminology.

The terminal traces of the various major veins were estimated by following the marginal branches basally to their origins on major veins (Fig. 2a, b). In some cases, it is not clear whether a pathway involves actual fusion and/or furcation of longitudinal veins versus the loss and/or insertion of a crossvein. In these cases, marginal veins can be traced to more than one basal origin. Thus, for consistency, the veins within the various areas indicated on Fig. 2a, b are those whose basal-most origin reasonably falls within the indicated field. Given the difficulty in deciphering the fusions and splitting of veins involved in the pseudomedia and pseudocubitus, it is understood that some

veins at the margins of each field may stem from more than one basal vein. [Note: For both the forewing and hindwing, I assume that the CuA actually extends distally towards and meets the MP, as opposed to being connected to it via a crossvein. It would be of value to confirm this assumption, via tracheal examination of both wings.]

To avoid uncertainty, it is also worthwhile to mention the terms that refer to the orientation of the wing: anterior – toward the elongate margin on the upper (costal) edge of the wing; posterior – toward the elongate margin along the lower edge of the wing; basal or proximal – toward the inner edge of the wing attached to the body; apical or distal – toward the far, outer edge of the wing.

The terminology for other body parts follows common usage.

Nothochrysa ehrenbergi Tauber, sp. nov.
http://zoobank.org/528B2ED3-82DF-4A61-8DF2-DD9DD5D77FED

Type material. The **holotype** (a male) is in the California Academy of Sciences (CAS). Its labels read: [1] "CHILE: Nuble [Ñuble] / Las Trancas / 20/25-II-1980 / Luis E. Pena [Peña]"; [2] "Suarius / flavescens / (Blanchard) / det. N. Penny, 1988"; [3] "HOLOTYPE / *Nothochrysa* / *ehrenbergi* / Tauber 2019" (Fig. 7f).

This single specimen was found in the CAS collection among the unidentified chrysopids. A subsequent search of the collection did not yield additional examples. Norm Penny's ID label remains on the specimen but was not included in Fig. 7f. It refers to *Suarius flavescens*, a species that now is placed in *Chrysopodes* (*Neosuarius*), and with which the new species shares similar coloration and appearance (see Tauber 2010).

When discovered, the specimen was discolored, and its wings were loosely folded around its body. One pair of wings was removed for study and is now attached with water-soluble hide glue to a card mounted on the pin below the specimen. The other pair fell off and was reattached to the specimen with hide glue. The abdomen was cleared and dissected; it is preserved in glycerin within a genitalia vial attached to the pin.

Diagnosis. Subfamily: This specimen exhibits the following diagnostic features of adult Nothochrysinae (cf.: Tjeder 1966, as Dictyochrysinae; Adams 1967; Brooks and Barnard 1990; Makarkin and Archibald 2013; Breitkreuz 2018): (i) wing-coupling mechanism consisting of a large jugal lobe on the forewing (here, folded ventrally; Fig. 1) and a frenulum on the hindwing (here, broken off); (ii) base of the forewing without tympanal organ (Fig. 1); (iii) forewing (and hindwing) with stem of the media extending basally, adjacent to the radius and not fused with it (Fig. 1a, b; cf. Breitkreuz et al. 2017: 32); (iv) first intramedian cell triangular, with boundaries formed by the MA, the MP, and the crossvein 1ma-mp ("pseudotriangular", sensu Breitkreuz et al. 2017); (v) pseudomedia ill-defined or appearing to merge with inner (not outer) series of gradates (Fig. 2); (vi) pseudocubitus appearing to merge with outer series of gradates (Fig. 2); (vii) forewing with basal subcostal crossvein present (Fig. 2); (viii) second m-cu crossvein stemming from the proximal half of the first intramedian cell (Fig. 2); (ix) each flagellomere having five or six whorls of setae (Figs 3e, 3f); and (x) anterodorsal surface of the metascutum displaying small, convex protrusion (Fig. 4b; cf. Breitkreuz 2018, Tauber 2019).
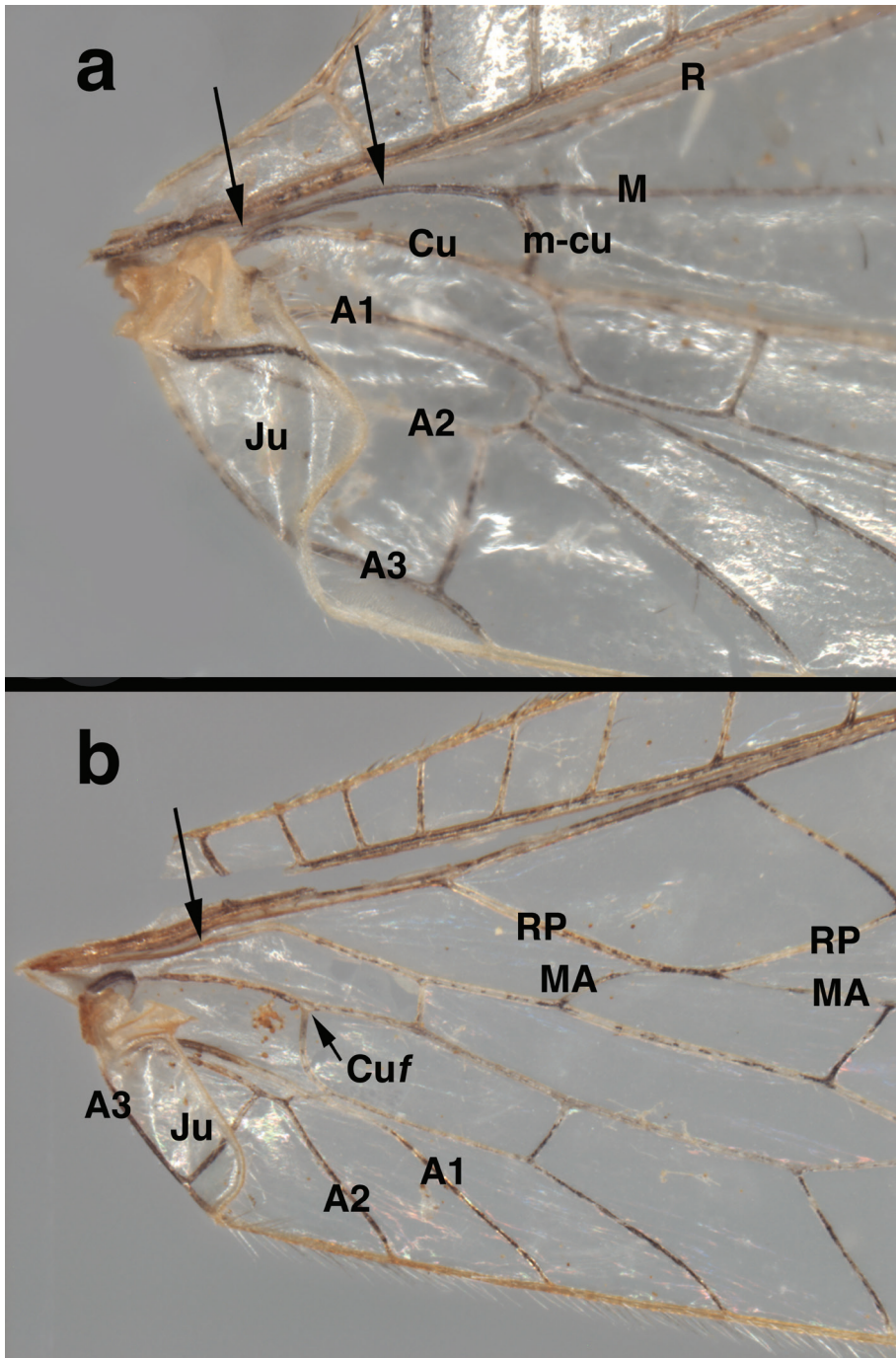
Figure 1. *Nothochrysa ehrenbergi* sp. nov. (Ñuble, Chile; Male, CAS): Venation at base of wings (**a**) left fore-wing, (**b**) left hindwing. Note the absence of a tympanal organ at the base of R in the forewing, the independent origin and trajectory of M along the base of R (arrows pointing downward, both wings), and the alignment of RP and MA in the hindwing. **A1, A2, A3** first, second, third anal veins **Cu** cubitus **Cu*f*** furcation (division) of cubitus **Ju** jugal lobe **M** media **MA** media anterior **m-cu** media-cubital crossvein **R** radius **RP** radius posterior.
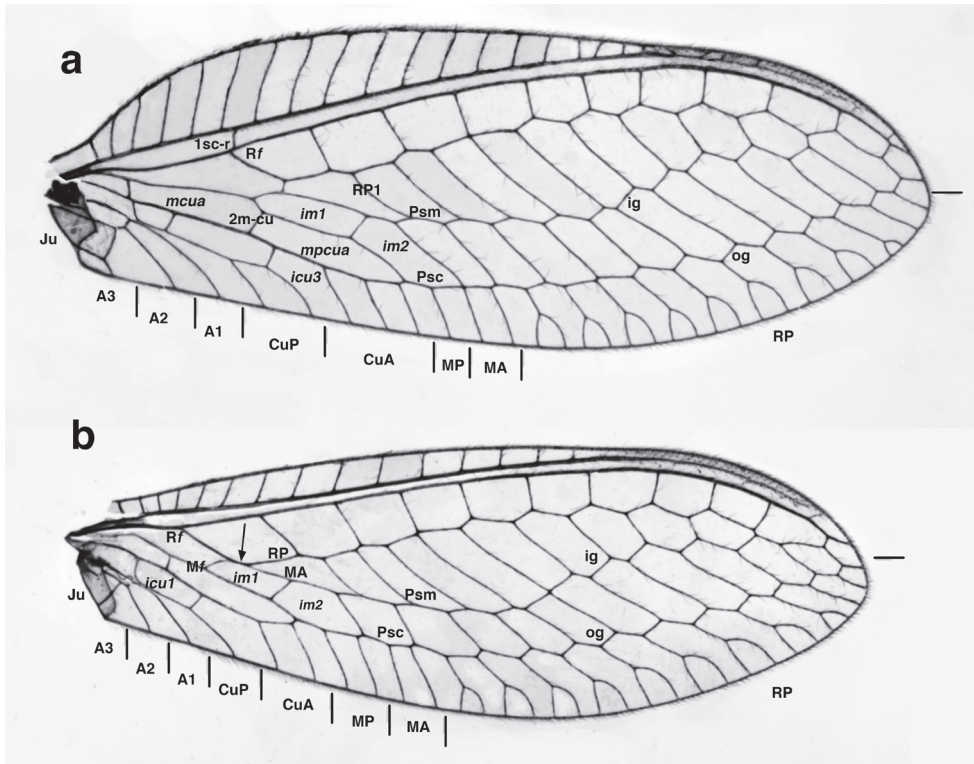
Figure 2. *Nothochrysa ehrenbergi* sp. nov. (Ñuble, Chile; Male, CAS): Wings with selected features labeled (**a**) left forewing, (**b**) left hindwing. Marginal traces of major veins demarcated; arrow (hindwing) indicates alignment of RP and MA along upper margin of first intramedian cell. **A1, A2, A3** first, second, third anal veins **CuA, CuP** anterior, posterior branches of cubitus **icu1, icu3** first, third intracubital cells **ig** inner gradate **im1, im2** first, second intramedian cells **Ju** jugal lobe **MA** media anterior **MP** media posterior **mcua, mpcua** second and third medial cells **Mf** furcation of media **og** outer gradate **Psc** pseudocubitus **Psm** pseudomedia **Rf** furcation of radius **RP** radius posterior **RP1** first branch of radius posterior **1sc-r** first crossvein between subcosta and radius **2m-cu** second crossvein between media and cubitus.

Genus placement: The Chilean specimen under study here falls into the genus *Nothochrysa* on the basis of the following features of its wings (Figs 1, 2): (i) forewing and hindwing having well developed pseudomedia and pseudocubitus; (ii) forewing and hindwing with two regular series of gradate veins (inner and outer); (iii) intramedian cell of forewing triangular, elongate, occupying approximately half the width between the pseudomedia and pseudocubitus; (iv) RP of forewing with 10 or more branches (Adams 1967; Makarkin and Archibald 2013; Archibald and Makarkin 2015; Breitkreuz 2018: 200). [Note: Some specimens of *N. californica* are known to have only eight or nine branches from the RP.]

Species placement: Apart from being the only known *Nothochrysa* species reported from South America, *N. ehrenbergi* is distinguishable from other species of *Nothochrysa* on the basis of a number of wing characters (Figs 1, 2; cf. Adams 1967; Aspöck et al.
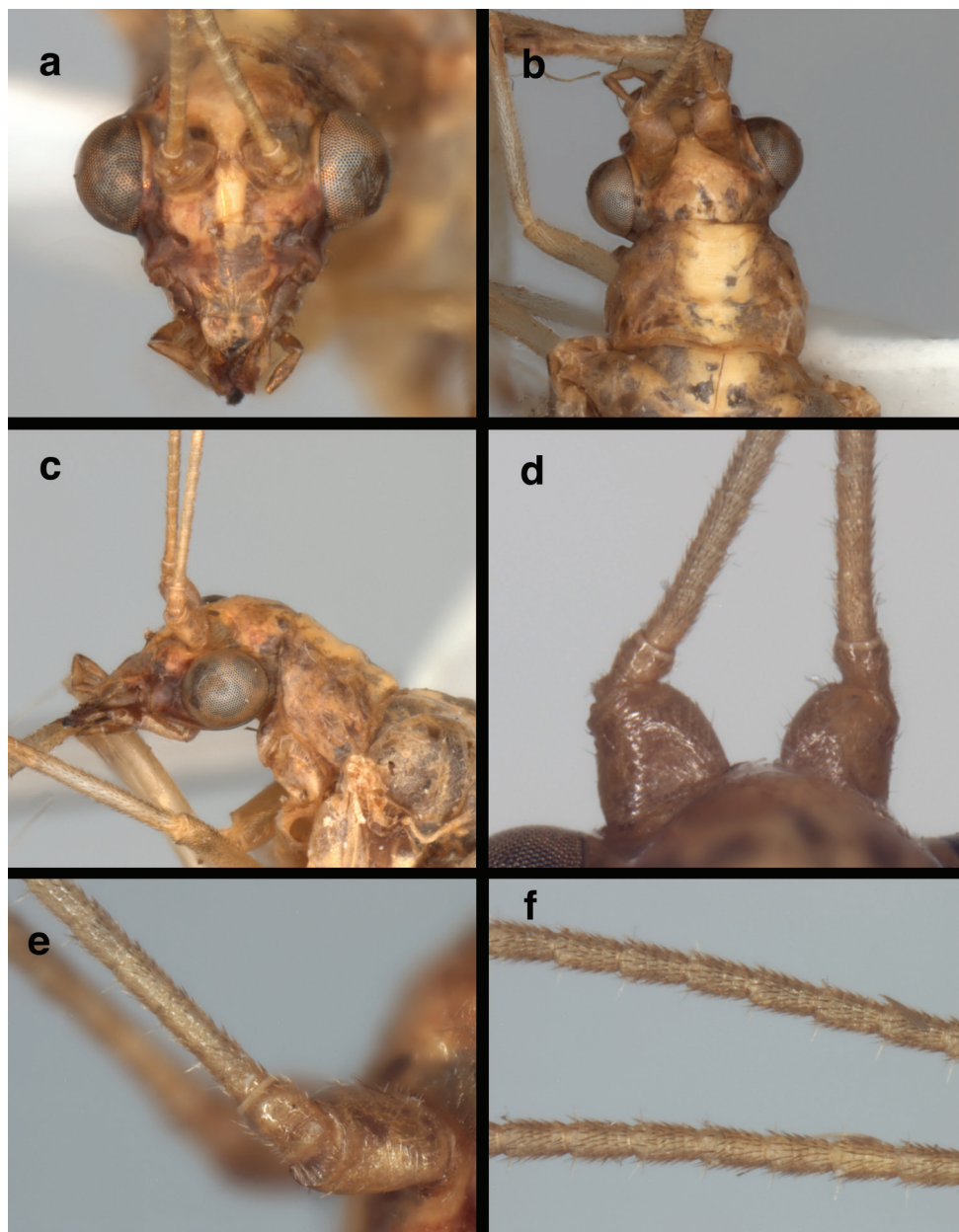
Figure 3. *Nothochrysa ehrenbergi* sp. nov. (Ñuble, Chile; Male, CAS): Head and prothorax (**a**) head, frontal (**b**) head and prothorax, dorsal (**c**) head and prothorax, lateral (**d, e**) base of antennae, dorsal, lateral (**f**) flagellar segments, mid antenna.

1980: figs 154, 155; Kovanci and Canbulat 2007: fig. 2): (i) the first anal vein is not forked; (ii) the basal subcostal crossvein is slightly distal to the furcation of the radius; (iii) as in most *Nothochrysa* species, the first intramedian cell is more wedge shaped
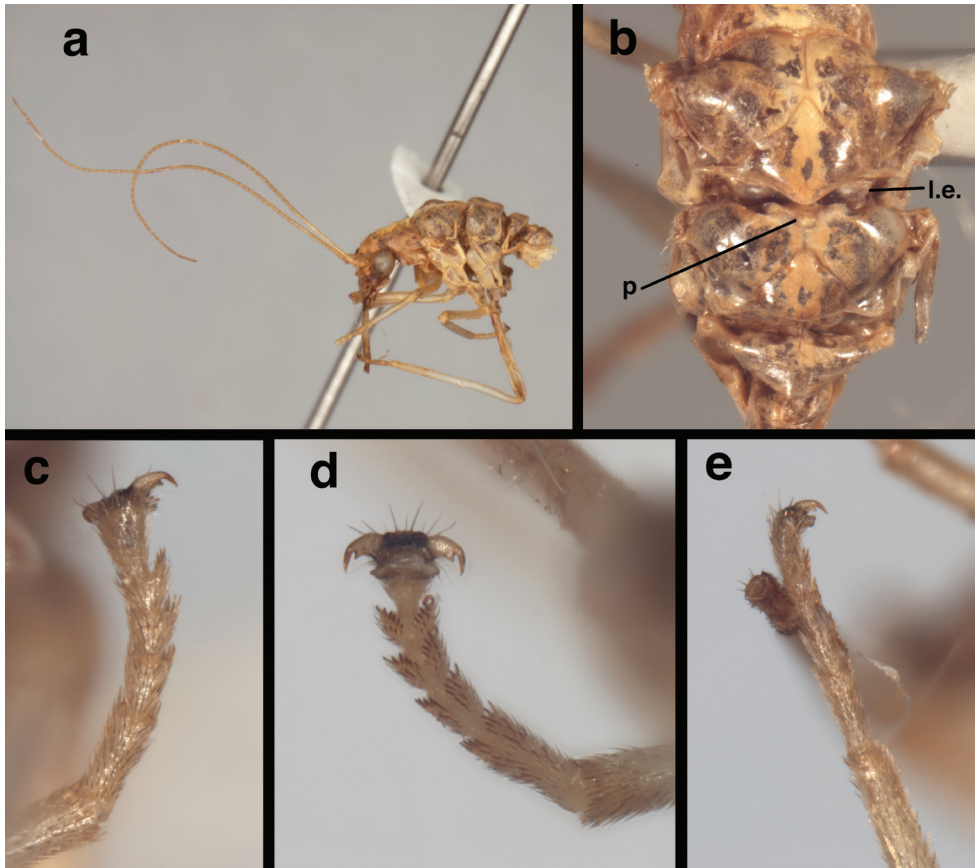
Figure 4. *Nothochrysa ehrenbergi* sp. nov. (Ñuble, Chile; Male, CAS): Habitus (**a**) antenna, head, and thorax, lateral (**b**) mesothorax, metathorax, dorsal (**c**) metatarsus, dorsal (**d**) metatarsus, ventral (**e**) mesotarsus, lateral. **p** raised metascutal protuberance **l.e.** mesoscutellar lobate expansion.

than truly quadrangular or triangular (i.e., the MA and MP meet basally at a broadly acute angle); and (iv) the third medial cell (directly below *im1*, Fig. 2a) is elongate and extends toward the pseudocubitus well beyond the distal edge of first intramedial cell.

Morphological characteristics. Head (Fig. 3): Width 1.6 mm (including eyes); ratio of head width to eye width = 3.0 : 1. Vertex raised, round; surface pitted anteriorly, with few or no setae, lacking prominent posterior fold. Distance between scapes 0.09 mm; distance between tentorial pits 0.36 mm; length of frons (midway between scapes – midway between tentorial pits) 0.33 mm. Frons relatively wide, with broad longitudinal ridge mesally; surface smooth, shiny, slightly rounded below toruli and at insertion of mouthparts; margin above clypeus straight. Clypeus tapering, with rounded sculpturing basally, indented mesally, slightly expanded distally, with distal margin straight to slightly convex; dorsal surface shiny, smooth, sculptured. Labrum about same width as clypeal margin, with small longitudinal ridge mesally; dorsal surface
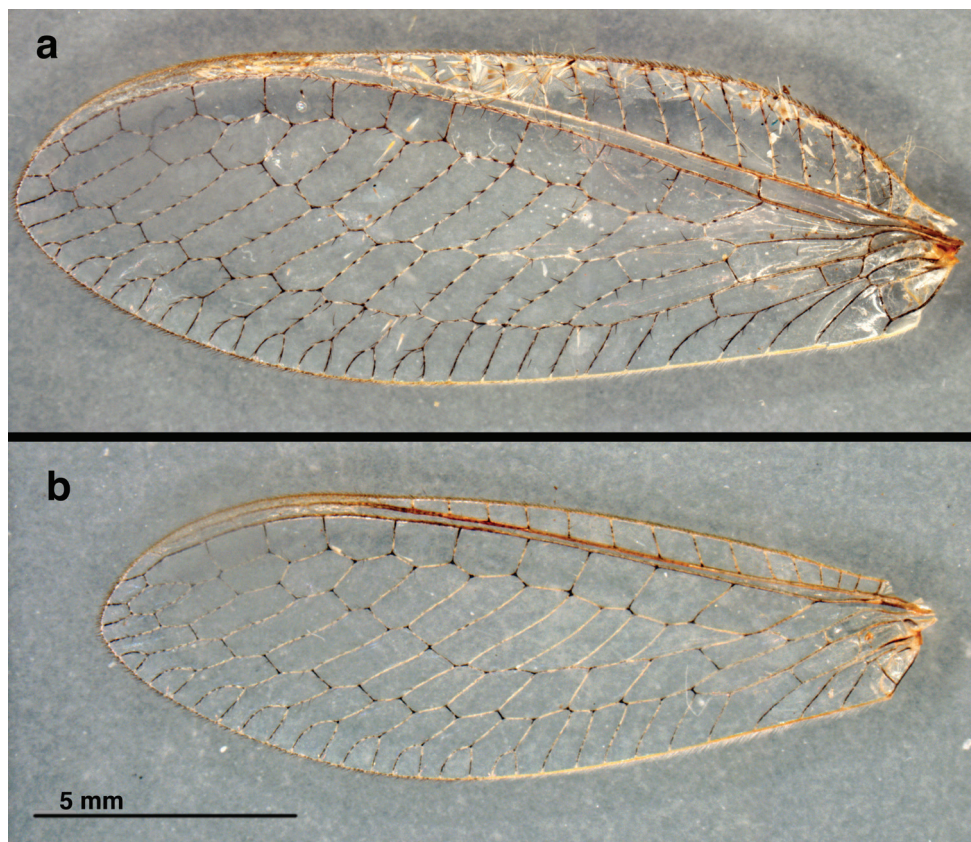
Figure 5. *Nothochrysa ehrenbergi* sp. nov. (Ñuble, Chile; Male, CAS): Wings, color slightly enhanced to emphasize pattern of vein markings (**a**) forewing (**b**) hindwing.

sculptured, shiny; distal margin bilobed, bearing numerous long setae distally. Antenna 9.7–9.8 mm long (~0.5× length of forewing); scape shorter than wide (0.23 mm long, 0.33 mm wide), lateral margin straight, mesal margin strongly convex, surface with short setae throughout; pedicel 0.17 mm long, 0.13 mm wide, with numerous short setae; flagellum with basal flagellomeres distinct, somewhat elongate (0.12–0.14 mm long, 0.07–0.08 mm wide), midantennal flagellomeres twice as long as broad (0.15 mm long, 0.07 mm wide), basal two flagellomeres with 4–5 partially indistinct whorls of thickset brown setae extending distally, third flagellomere and others distally all with five distinct whorls of thickset, brown setae extending distally, 0.3–0.5× width of flagellomere, distal whorl with one or two slender, elongate (~0.75× width of flagellomere), pale setae extending laterally.

Head coloration: Scape cream, with reddish spot on distolateral tip; pedicel, flagellum cream, unmarked; thickset setae in whorls mostly brown, elongate setae pale. Vertex cream, possibly tinged red laterally; dorsal torulus yellow to cream, apparently
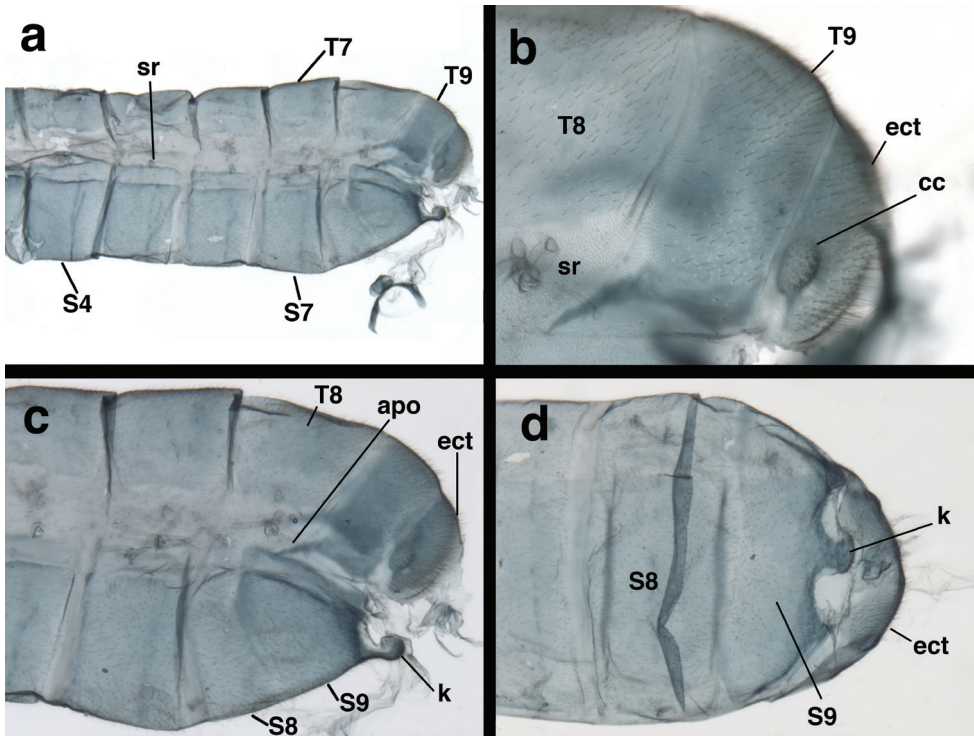
Figure 6. *Nothochrysa ehrenbergi* sp. nov. (Ñuble, Chile; Male, CAS): Abdomen, cleared (**a**) midsection-terminus, lateral (**b**) T8 (distal), T9, and ectoproct, lateral (**c**) terminal abdominal segments, lateral (**d**) terminal abdominal segments, ventral. **apo** dorsal apodeme extending below T8 **cc** callus cerci **ect** ectoproct **k** distal knob extending from S8+9 **sr** spiracle **S4, S7** fourth, seventh strenites **S8, S9** partially coalesced eighth and ninth sternites **T7, T8, T9** seventh, eighth, ninth tergites.

unmarked. Frons cream, probably with reddish tinge laterally below torulus; torulus cream, unmarked. Clypeus cream, possibly tinged red laterally; basal, distal margins straight. Genal mark dark red/brown throughout, extending to tentorial pit. Labrum probably cream. Palpomeres probably mostly cream, somewhat darkened distally.

Thorax (Fig. 4): Cervix not visible. Dorsal thoracic surface with pale longitudinal stripe mesally, probably with broad reddish or brownish stripes or coloration laterally. Prothorax broad, 0.9 mm long, 1.5 mm wide, ratio of length to width = 0.63 : 1; pronotum well sclerotized, with textured surface, transverse fold mesally, few or no setae. Legs elongate, slender, probably cream, unmarked, lacking prominent tibial spurs. Tarsus with basal three tarsomeres appearing coalesced, bearing spurs, setae intermixed along undersurface; middle three tarsomeres with expanded lateral lobes bearing spurs, setae in irregular rows; distal tarsomere narrow basally, enlarged distally, bearing numerous elongate, slender, dark setae laterally, distally, terminus bearing pair of claws laterally, large pad mesally; claw amber, with basal enlargement, acute slender hook terminally.
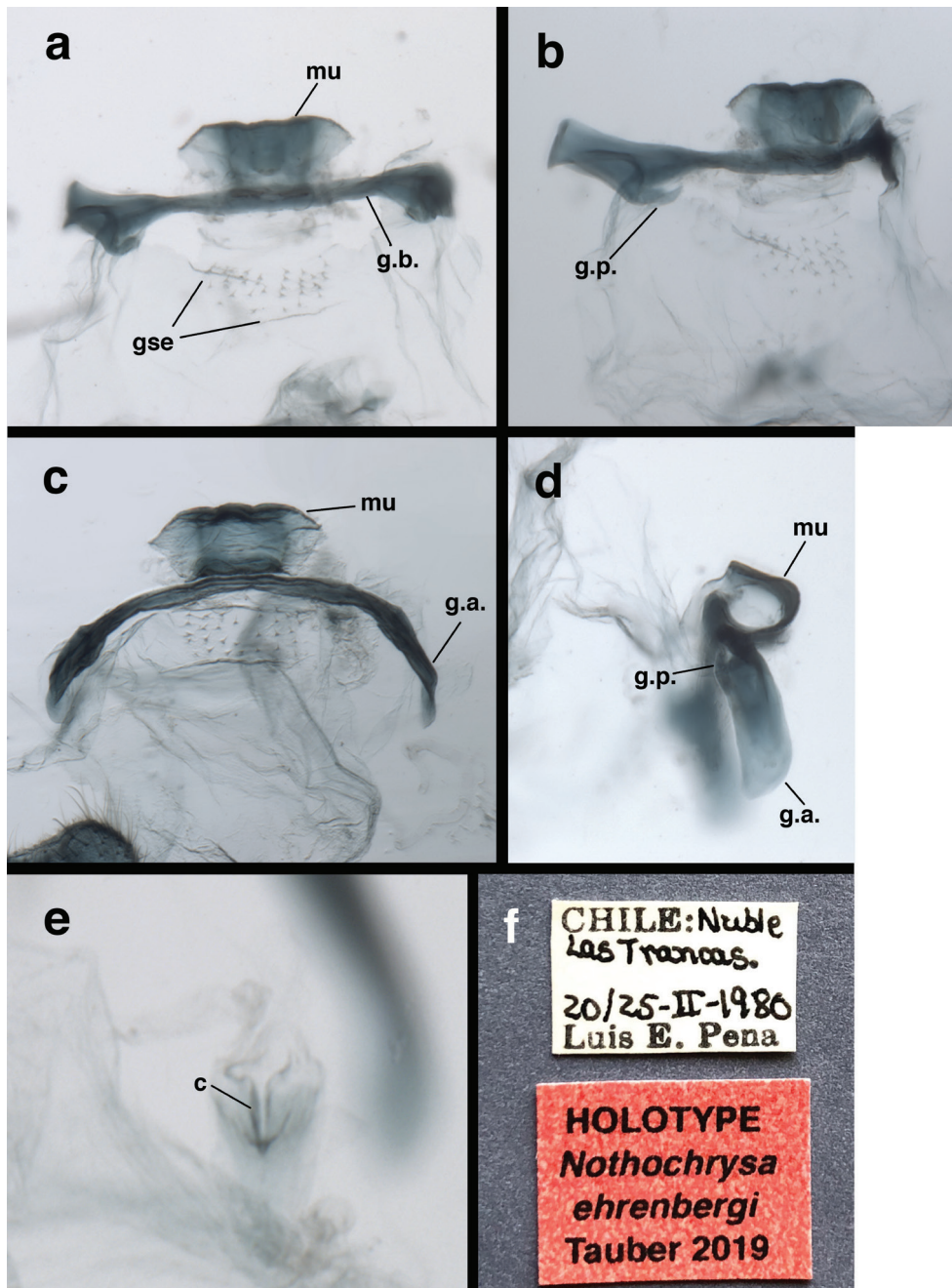
Figure 7. *Nothochrysa ehrenbergi* sp. nov. (Ñuble, Chile; Male, CAS): Male genitalia, cleared, and specimen labels (Penny's identification label not included) (**a**) gonarcal complex, dorsal (**b**) gonarcal complex, frontal, tilted (**c**) gonarcal complex, posterior (**d**) gonarcal complex, lateral (**e**) hypandrium internum (**f**) labels. **c** comes **g.a.** gonarcal apodeme **g.b.** gonarcal bridge **g.p.** gonarcal process **gse** gonosetae on membranous gonosaccus **mu** mediuncus.

Wings (Figs 1, 2, 5): *Forewing* 18.5 mm long, 6.5 mm wide (at widest point); ratio of length to maximum width = 2.9 : 1. Membrane clear, lacking markings; microtrichia present below base of every major vein, pale. Trichosors (sensu Makarkin and Archibald 2013: 140–142) absent. Costal area relatively enlarged; tallest costal cell (7th from base of wing) 1.8 mm tall, 2.7× width of cell, 0.28× height of wing; costal crossveins simple, six before 1sc-r, twelve after 1sc-r and before stigma, one (very small) after stigma, none within stigma. Sc extending into stigma, fading but not appearing to merge with C or RA; no crossveins in stigma; first sc-r crossvein slightly distal to R*f*, slightly basal to M*f*; RA with one very short veinlet extending to wing margin after stigma. Radial area between RA and RP with single row of ten closed cells; tallest cell (3rd from base of wing) 0.6× as tall as wide. Intramedian cell (*im1 = mamp1*) prominent, elongate, triangular, formed by MA, crossvein 1ma-mp, and two abscissae of MP, occupying approximately half the space between MA and CuA, with M*f* broadly acute, long sides (MA, MP) roughly parallel for most of span; crossvein 2m-cu proximal to midpoint of *im1*. Three medial cells present (*mcu, mcua, mpcua*), second, third of these elongate, with roughly parallel sides; MP merging into Psc well beyond *im1*. Two series of gradate veins parallel basally, diverging slightly medially, converging distally. Approximately nine inner gradates in regular, sinuous series, continuing from Psm in zigzag pattern across center of wing; approximately ten outer gradates continuing from Psc in regular, upturned series. RP with nine marginal forks beyond Psc. Cu furcated after m-cu crossvein, with two closed, four open *icu* cells. CuA with three furcations before meeting MP; CuP furcated below *icu2*; thus cubital trace having five terminal veinlets (three from CuA, two from CuP). A1, A2, A3 simple, unforked; a1-a2 and a2-a3 crossveins present; distal part of *a3* and jugal lobe with dense patch of microtrichia. Jugal lobe large, quadrate, folded beneath third anal cell, without internal vein; margin bearing long, slender setae basally.

Hindwing: 12.4 mm long, 4.2 mm wide. Costal area not enlarged; at least 15 c-sc crossveins before stigma, none within or after stigma. Radial area containing single row of eleven closed cells between RA and RP. Gradate veins in two roughly parallel series, slightly divergent distally; approximately seven inner gradates beyond Psm; approximately 11 outer gradates beyond Psc. Psc with nine marginal forks. MA aligned with RP for approximately one-third length of *im1*. CuA with two furcations before meeting MP; CuP undivided; thus, wing margin having three cubital veinlets (two from CuA, one from CuP). A1, A2, A3 simple, unforked; a1-a2 and a2-a3 crossveins present. Jugal lobe without internal vein, basal margin bearing long, slender setae.

Coloration of forewing, hindwing (Fig. 5): Membrane clear, somewhat glossy. Stigma slightly opaque, without coloration. Costal, subcostal, radial veins brownish; all other longitudinal veins pale with black marks at intersections and (forewing) at bases of setae. Forewing with posterior veinlets extensively marked black; basal inner gradates pale, others becoming increasingly marked black until entirely black distally; outer gradates mostly black. Hindwing with basal inner gradates pale, marked with black at intersections; outer gradates mostly black.

Abdomen (Male, Fig. 6; female unknown): Sclerites, integument of pleural region somewhat soft, flexible; tergites, sternites, pleural region covered with setae of uniformly short length; microsetae present, no microtholi. T6: length 0.78 mm, ~1.8× height; T7: length 0.80 mm, ~1.6× height; S6: length 0.67 mm, 0.72× height; S7: length 0.68 mm, ~0.70× height. Tergites roughly rectangular, edges acute or slightly rounded, ventral margins straight or slightly concave mesally. Spiracles located approximately in center of lateral membrane, roughly circular externally, not enlarged; atria slightly enlarged, rounded, with bifurcated tracheae. Coloration: body somewhat discolored; setae pale. Tergites probably green, without markings; pleuron mostly tan; sternites with green longitudinal stripe dorsally, tan ventrally; callus cerci white.

Male terminalia (Fig. 7): T8 broadly wedge shaped, with dorsal surface slightly rounded, length 0.83 mm, height 0.49 mm, considerably longer than dorsal surfaces of either T9 or ectoproct; lateral margins tapering inward ventrally, ventral margin roughly straight. T9 and ectoproct separate, not fused; callus cerci ovate, protruding basally from posterior margin of ectoproct, 0.18 mm length, 0.10 mm width, with ~30 trichobothria of various lengths. T9 rectangular, with distoventral margin rounded; elongate, lightly sclerotized ventral apodeme along ventral margin, extending proximally to midsection of A8. Ectoproct dome shaped, rounded distally, slightly convex basally, tightly curved ventrally, sloping dorsally; callus cerci situated on lower proximal margin. S8 and S9 partially fused, without internal ridge; S9 more heavily sclerotized than S8, posterior margin slightly more sclerotized than remainder of sternite. S8+9 (lateral view) with proximal margin straight ventrally, becoming broadly rounded dorsally, distal margin short, straight, ventral margin straight; terminal knob extending well beyond edge of S9, with elongate setae on ventral margin; dorsal surface of knob contiguous with heavy recurrent membrane attached to elongate gonarcal membrane. Subanal plate not found.

Gonarcus delicate, slender, broadly arcuate; lateral apodemes slender, quadrate (lateral view), rounded distally, with short, contiguous processes mesally, extending forward. Mediuncus closely attached to dorsal surface of gonarcal arch, flat, recurved into an almost fully circular hood, with two internal sclerotized "rods" extending roughly in parallel from mediuncal base to tip, converging slightly at tip; base of mediuncus quadrate (dorsal view), occupying approximately one-fourth span of gonarcal bridge; terminus of mediuncus with expanded lateral wings, rounded mesal protrusion. Gonosaccus transparent, immediately beneath gonarcal arch and mediuncus, with approximately 32 short setae on distinct setal bases uniformly distributed in two equal patches. Hypandrium internum small, located on delicate membrane extending well below gonosaccus, consisting of paired, curved lateral arms meeting mesally at narrow, rounded apex; comes lightly sclerotized, extending forward beyond apex. Gonapsis, gonocristae absent.

Biology. Nothing is known about the biology or larval morphology of this species. The gut of the *N. ehrenbergi* specimen did not contain noteworthy contents.

Larval descriptions of several *Nothochrysa* species are available for comparison if *N. ehrenbergi* larval specimens were to become available (see Tauber et al. 2014). *Nothochrysa* larvae generally are considered debris-carriers, but their packets of debris are small, and their morphology is only moderately modified for debris-carrying. In addition, detailed information on aspects of the developmental and reproductive biology of *N. californica* is available (Toschi 1965).

For generic-level comparisons, larval descriptions for genera within Nothochrysinae (*Kimochrysa*, *Pimachrysa*, *Dictyochrysa*, and *Hypochrysa*) have been published (see Tauber et al. 2014). Unfortunately, larvae of *Asthenochrysa, Leptochrysa, Pamochrysa,* and *Triplochrysa* are not described.

Known distribution. Currently, this species has only been reported from the type locality, which presumably is the Valle Las Trancas in the region of Ñuble, Chile.

Etymology. This species is named in honor of Ronald G. Ehrenberg, Irving M. Ives Professor of Industrial and Labor Relations and Economics at Cornell University, an esteemed and cherished colleague of the author and her late husband (Maurice J. Tauber).

Characteristics shared with *Archaeochrysa* species

As shown above, *N. ehrenbergi* shares many features with other extant *Nothochrysa* species, and its inclusion in the genus is well supported. However, the species also expresses many features that differ from *Nothochrysa* and that are shared by at least some of the five species in the fossil genus *Archaeochrysa*. I discuss four below:

First, in the *N. ehrenbergi* forewing, vein A1 is not forked, whereas it is forked in all other *Nothochrysa* species (Adams 1967; Aspöck et al. 1980: figs 154, 155; Makarkin and Archibald 2013: 135, 136). The feature is variable in *Archaeochrysa* specimens where A1 is visible. It is not forked in two species (Adams 1967: 237), forked in two species (Adams 1967: 230, Makarkin and Archibald 2013: 135), and missing from the specimen of the fifth species (Archibald and Makarkin 2015: 363).

Second, in *N. ehrenbergi* the basal sc-r crossvein arises distal to the furcation of the radius and almost directly above the furcation of the media. Both of these character states are shared with the fossil genus *Archaeochrysa* (Adams 1967, Makarkin and Archibald 2013), but not with other known *Nothochrysa* species.

Third, in *N. ehrenbergi* the distinction between the inner gradate series and the pseudomedia as well as between the outer gradate series and the pseudocubitus is indistinct. Rather, the gradate series and their respective pseudoveins tend to run together more smoothly as a curve, rather than at an angle as in other *Nothochrysa* species. Again, this feature of *N. ehrenbergi* is shared most closely with *Archaeochrysa* species (Adams 1967, Makarkin and Archibald 2013, Archibald and Makarkin 2015).

Fourth, currently the primary feature used to distinguish between *Nothochrysa* and *Archaeochrysa* is the presence or absence of a crossvein between RP and MA in the basal part of the hindwing. The crossvein is present in all known *Archaeochrysa* species and is reported to be absent from *Nothochrysa* (Makarkin and Archibald 2013: 134).

In *N. ehrenbergi*, MA aligns with RP for about one-third the length of the upper margin of the *im1* cell, and no crossvein is present (Figs 1b, 2b). However, even with this character there appears to be a possible exception. Figure 2 accompanying the original description of *Nothochrysa turcica* Kovanci and Canbulat shows a short crossvein between RP and MA; confirmation of the accuracy of this drawing is necessary.

Phylogenetic position of *Nothochrysa ehrenbergi* sp. nov.

Given the above, Archibald and Makarkin's (2015) discussion of the phylogeny of *Archaeochrysa* species is worthy of consideration here. Their paper evaluates how the various *Archaeochrysa* species express three features; each feature has several conditions ranging from presumably plesiomorphic to more derived. Below, the three features are considered, relative to their expression by *Nothochrysa* species, especially *N. ehrenbergi*.

(1) **The shape of the *im1* cell.** Archibald and Makarkin (2015) describe two configurations for this character; *N. ehrenbergi* expresses the second (more advanced) condition in which the sides of the *im1* cell are almost parallel for most of their span and converge basally at a relatively steep angle. The extant species of *Nothochrysa,* including *N. ehrenbergi,* share this feature with two species of *Archaeochrysa*.

(2) **The position of crossvein 2m-cu.** Archibald and Makarkin (2015) list six conditions for this character, each one considered more evolutionarily advanced than the preceding. *Nothochrysa ehrenbergi* falls into Condition 5, a derived condition in which 2m-cu is located distinctly in the proximal part of *im1* (as shown in fig. 2C of Archibald and Makarkin 2015). This character state is typical of at least two *Archaeochrysa* species, *A. creedi* (Adams) and *A. paranervis* (Adams), as well as several other extant genera in Nothochrysinae, including *Nothochrysa*.

(3) **The crossveins of Psc.** Archibald and Makarkin (2015: 366) describe and illustrate four character states for this feature; interested readers are referred to the original paper. Suffice it to say here, *N. ehrenbergi,* as well as three *Archaeochrysa* species but no other *Nothochrysa* species, fall into the second of the four conditions. This position is considered plesiomorphic among Nothochrysinae, both fossil and extant (Archibald and Makarkin 2015).

On the basis of the above information, it appears that *N. ehrenbergi* shares a very close phylogenetic relationship with the fossil genus *Archaeochrysa*. At this point, only one character (the absence of a crossvein between the RP and the MA above the first intramedial cell of the hindwing) supports its exclusion from *Archaeochrysa*, and this character may have exceptions within *Nothochrysa*. Indeed, there does not appear to be a synapomorphic character that consistently differentiates *Nothochrysa* from *Archaeochrysa*. Thus, given the overall similarity between *N. ehrenbergi* and the known *Archaeochrysa* species, I recommend that future studies examine the validity of maintaining the generic separation.

Acknowledgements

References

Adams PA (1967) A review of the Mesochrysinae and Nothochrysinae (Neuroptera: Chrysopidae). Bulletin of the Museum of Comparative Zoology 135: 215–238.

Adams PA, Penny ND (1992) New genera of Nothochrysinae from South America (Neuroptera: Chrysopidae). Pan-Pacific Entomologist 68: 216–221.

Archibald SB, Makarkin VN (2015) A new species of *Archaeochrysa* Adams (Neuroptera: Chrysopidae) from the early Eocene of Driftwood Canyon, British Columbia, Canada. Canadian Entomologist 147: 359–369. https://doi.org/10.4039/tce.2014.53

Aspöck H, Aspöck U, Hölzel H, Rausch H (1980) Die Neuropteren Europas, 2 vols. Goecke and Evers, Krefeld, 495 pp [vol. 1], 355 pp [vol. 2].

Aspöck H, Hölzel H, Aspöck U (2001) Kommentierter Katalog der Neuropterida (Insecta: Raphidioptera, Megaloptera, Neuroptera) der Westpaläarktis 2: 1–606.

Breitkreuz LCV (2018) Systematics and evolution of the family Chrysopidae (Neuroptera), with an emphasis on their morphology. PhD Thesis, University of Kansas, Lawrence, 661 pp.

Breitkreuz LCV, Winterton SL, Engel MS (2017) Wing tracheation in Chrysopidae and other Neuropterida (Insecta): a resolution of the confusion about vein fusion. American Museum Novitates 3890: 1–44. https://doi.org/10.1206/3890.1

Brooks SJ, Barnard PC (1990) The green lacewings of the world: a generic review (Neuroptera: Chrysopidae). Bulletin of the British Museum of Natural History, Entomology 59: 117–286.

Comstock JH (1918) The wings of insects: an exposition of the uniform terminology of the wing-veins of insects and a discussion of the more general characteristics of the wings of the several orders of insects. Comstock Publishing Co., Ithaca, New York, 430 pp. https://doi.org/10.5962/bhl.title.54605

Engel MS, Winterton SL, Breitkreuz LCV (2018) Phylogeny and evolution of Neuropterida: where have wings of lace taken us? Annual Review of Entomology 63: 531–551. https://doi.org/10.1146/annurev-ento-020117-043127

Ghosh SK (1990) Contribution to the taxonomical studies of Neuroptera (suborder Planipennia) from eastern India. III. Family Chrysopidae. Records of the Zoological Survey of India 86: 329–354.

Hölzel H (1966) Beschreibung einer neuen europäischen Neuropterenart – *Chrysopa raddai* sp. nov. (Planipennia - Chrysopidae). Entomologisches Nachrichtenblatt, Wien 13: 72–73.

Kovanci B, Canbulat S (2007) A new species of the genus *Nothochrysa* McLachlan 1868 from northwestern Turkey (Neuroptera: Chrysopidae) with a key to western Palaearctic species. Annales de la Société Entomologique de France (NS) 43: 165–168. https://doi.org/10.10 80/00379271.2007.10697507

Kukalová-Peck J (1991) Fossil history and the evolution of hexapod structures. In: Naumann ID (Ed.) The Insects of Australia (2nd edn), Vol. 1. Melbourne University Press, Melbourne, 141–179.

Kukalová-Peck J, Lawrence JF (2004) Relationships among coleopteran suborders and major endoneopteran lineages: evidence from hind wing characters. European Journal of Entomology 101: 95–144. https://doi.org/10.14411/eje.2004.018

Makarkin VN, Archibald SB (2013) A diverse new assemblage of green lacewings (Insecta, Neuroptera, Chrysopidae) from the Early Eocene Okanagan Highlands, western North America. Journal of Paleontology 87: 123–146. https://doi.org/10.1666/12-052R.1

Monserrat VJ (1985) Lista de los tipos de Mecoptera y Neuroptera (Insecta) de la colección L. Navás, depositados en el Museo de Zoología de Barcelona. Miscel·lània Zoològica 9: 233–243.

Navás L (1917) Insecta nova. I Series. Memorie dell'Accademia Pontificia dei Nuovi Lincei, Rome (2) 3: 1–11.

Needham JG (1909) Notes on the Neuroptera in the collection of the Indian Museum. Records of the Indian Museum, Calcutta 3: 185–210.

Oswald JD (2018) Neuropterida Species of the World. https://lacewing.tamu.edu/SpeciesCatalog/Main [Last accessed: April 11, 2019]

Tauber CA (2010) Revision of *Neosuarius*, a subgenus of *Chrysopodes* (Neuroptera, Chrysopidae). ZooKeys 44 (Special Issue): 1–104. https://doi.org/10.3897/zookeys.44.387

Tauber CA (2019) South American Nothochrysinae (Neuroptera: Chrysopidae): II. Redescription of *Leptochrysa prisca* Adams and Penny. ZooKeys, in press.

Tauber CA, Tauber MJ, Albuquerque GS (2014) Debris-carrying in larval Chrysopidae: unraveling its evolutionary history. Annals of the Entomological Society of America 107: 295–314. https://doi.org/10.1603/AN13163

Tillyard RJ (1916) Studies in Australian Neuroptera. No. 3. The wing-venation of the Chrysopidae. Proceedings of the Linnean Society of New South Wales 41: 221–248. https://doi.org/10.5962/bhl.part.15306

Tjeder B (1966) Neuroptera-Planipennia. The Lace-wings of Southern Africa. 5. Family Chrysopidae. In: Hanström B, Brinck P, Rudebec G (Eds) South African Animal Life. Vol. 12. Swedish Natural Science Research Council, Stockholm, 228–534.

Toschi CA (1965) The taxonomy, life histories, and mating behavior of the green lacewings of Strawberry Canyon (Neuroptera, Chrysopidae). Hilgardia 36: 391–433. https://doi.org/10.3733/hilg.v36n11p391

Winterton SL, Brooks SJ (2002) Phylogeny of the Apochrysinae green lacewings (Neuroptera: Chrysopidae: Apochrysinae). Annals of the Entomological Society of America 95: 16–28. https://doi.org/10.1603/0013-8746(2002)095[0016:POTAGL]2.0.CO;2

Winterton SL, Gillung JP, Garzón-Orduña IJ, Badano D, Breitkreuz LCV, Duelli P, Engel MS, Liu X, Machado RJP, Mansell M, Mochizuki A, Penny ND, Tauber CA, Oswald JD (2019) The evolution of green lacewings (Neuroptera: Chrysopidae): an anchored phylogenomics approach. Systematic Entomology https://doi.org/10.1111/syen.12347

Appendix 1. *Nomina dubia* within *Nothochrysa*

Nothochrysa indigena Needham, 1909

Although Ghosh (1990: 349) may be correct in his inclusion of this species in Nothochrysinae and *Nothochrysa*, his evidence as published remains questionable. The main characteristic that argues in favor of the identification is his report of a tympanum being absent. However, several other features contradict the identification and lead me to question whether the tympanum was overlooked. First, his report mentions flagellomeres with four whorls of setae (not five or six whorls as is typical of *Nothochrysa* and Nothochrysinae in general). Second, the images of the forewing and hindwing show no jugal lobe, no frenulum, and no basal subcostal crossvein; nor is there any mention of the presence of these structures – all of which are features of Nothochrysinae, including *Nothochrysa*. Third, the shape of the *im1* cell is not elongate, and the MA and MP that form the upper and lower margins of the cell are not parallel as described for other species of *Nothochrysa*. Fourth, Ghosh reports that the pseudomedia merges with the inner gradates; however, his figures illustrate the Psm intersecting (not merging) with the inner gradates well before the end of the Psm and at a much steeper angle than in any known *Nothochrysa* species (Ghosh 1990: figs 16, 17). While the configuration of the Psm in *Nothochrysa californica* Banks is similar to that of Chrysopinae, it does not resemble that which is depicted in the figure of *N. indigena*. Fifth and finally, the spinose tip of the male S8+9 (Ghosh 1990: fig. 19) is unusual for *Nothochrysa*, and the systematic importance of this structure is unknown.

Nothochrysa lefroyi Needham, 1909

No published information is available that helps identify the generic placement of this species, and apparently the type specimen has not been found (Needham 1909: 203, Ghosh 1990: 351).

Nothochrysa polemia Navás, 1917

The original description of this species is relatively detailed for its time, and it includes two illustrations. The type is reported from Mytilene, a city on the island of Lesbos in the North Aegean region (Navás 1917). Originally, the type was in Navás' collection; however, it is not there now (Monserrat 1985), and it is believed to have been destroyed. The name was treated as a *nomen dubium* by Aspöck et al. (2001: 314), who considered the species likely to be synonymous with *Rexa raddai* (Hölzel 1966). The designation of a neotype is necessary (Oswald 2018).

RESEARCH ARTICLE

South American Nothochrysinae (Neuroptera, Chrysopidae): II. Redescription of *Leptochrysa prisca* Adams & Penny

Catherine A. Tauber[1,2]

1 *Department of Entomology, Comstock Hall, Cornell University, Ithaca, NY, 14853, USA* **2** *Department of Entomology and Nematology, University of California, Davis, CA, 95616, USA*

Corresponding author: *Catherine A. Tauber* (cat6@cornell.edu)

Citation: Tauber CA (2019) South American Nothochrysinae (Neuroptera, Chrysopidae): II. Redescription of *Leptochrysa prisca* Adams & Penny. ZooKeys 866: 19–38. https://doi.org/10.3897/zookeys.866.35396

Abstract

Leptochrysa Adams & Penny is one of four genera of Nothochrysinae recorded from the New World. Previously, this genus and its only described species, *Leptochrysa prisca* Adams & Penny, were known from a single female specimen that is discolored and damaged by fungal infestation. Thus, accurate information on the taxon was limited mostly to the wings and some other external features. Here, I describe a recently collected, second female specimen with the goal of providing images of the adult coloration and elucidating characters (especially the female genitalia) that were unavailable earlier. Some variation between the two known specimens is also noted and used in interpreting venation characters. Finally, comparisons are made with other extant genera pertaining to the placement of the species within Chrysopidae.

Keywords

Female abdomen and genitalia, Green lacewing, Limaiinae, parasitoid

Introduction

This article is the second of two that focus on recently found specimens of South American Nothochrysinae (Neuroptera, Chrysopidae). The family Chrysopidae currently consists of four subfamilies: three with extant representatives (Apochrysinae, Chrysopinae, and Nothochrysinae) and a single subfamily (Limaiinae) known only

from fossils (see Archibald and Makarkin 2015). Among the extant Nothochrysinae the monotypic genus *Leptochrysa* Adams & Penny is the most enigmatic. Its systematic relationships are not well resolved; indeed, its assignment to Nothochrysinae is seriously questioned (Makarkin and Archibald 2013 and Discussion below). Moreover, because of its rarity, it has not been included in any molecular analyses.

This genus is known from only one species, *Leptochrysa prisca* Adams & Penny, and also from only one specimen, the badly damaged female holotype collected in Amazonas, Peru. Because this specimen was infested with fungal mycelia, Adams and Penny (1992b) mainly described external features, with emphasis on wing characteristics. Fortunately, an additional specimen, another female, has become available for study; below it is described with emphasis on abdominal and genital characters, as well as the color pattern of the exoskeleton. To allow the genus to be compared with those in recent morphology-based phylogenetic studies of the Chrysopoidea (e.g., Makarkin and Archibald 2013, Breitkreuz 2018), an effort was made to record relevant characters used in those studies.

Material and methods

As explained in the previous article on *Nothochrysa* McLachlan (Tauber 2019), I did not determine tracheal pathways in order to identify the various veins and cells of the wings. Here, I used the obvious pathways of the veins and the findings of previous authors (mainly Adams 1967, Makarkin and Archibald 2013, and Breitkreuz et al. 2017). The report uses prevailing terminology for veins and cells, as most recently modified by Breitkreuz et al. (2017), with exceptions and additions as described by Tauber (2019). The terminology for other body parts conforms to common usage. Measurements reported here are only from the undescribed specimen; some measurements of the holotype were reported by Adams and Penny (1992b).

Leptochrysa prisca **Adams & Penny, 1992**
Figs 1–10

Material studied. A single female specimen was found during a visit to the Florida State Collection of Arthropods (FSCA). Subsequent searches by L. A. Stange did not yield additional examples. The labels (all white) on the specimen read: [1] "PERU: Amazonas Dept / Huembo Lodge, Km / 315 on N5, 18-21-X- / 2012, 2078 m, JE Eger"; [2] "05°51'28.1S / 077°59'04.8W / MV & UV Light"; [3] "*Leptochrysa prisca* / Adams & Penny, det. / C. A. Tauber 2019".

The specimen is well preserved, and its wings are spread. After imaging, the abdomen was cleared for study; it is held in a microvial containing glycerin, attached to the pin. During clearing, several parasitoid larvae were discovered in the abdominal cavity. They were removed, imaged, and preserved in a separate genitalia vial with glycerin.
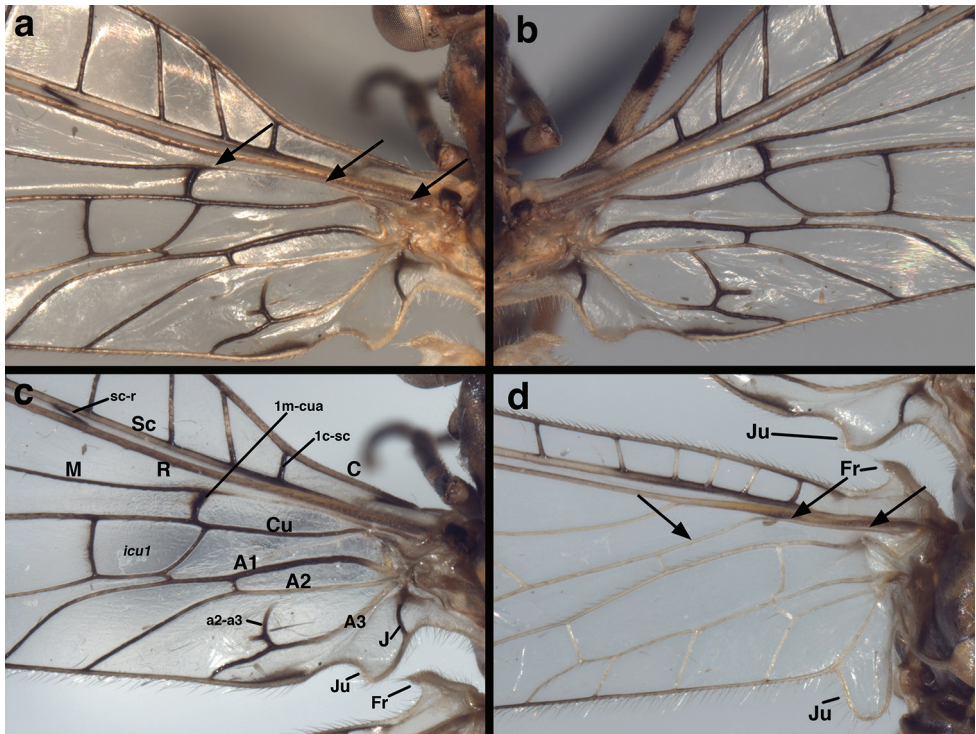
Figure 1. *Leptochrysa prisca* Adams & Penny (Peru, Amazonas, female, FSCA): Venation at base of wings (**a**) left forewing, (**b**) right forewing, (**c**) left forewing, labeled, (**d**) left hindwing, labeled. Note the absence of a tympanal organ at the base of R (forewing), the independent origin and trajectory of M along the base of R [forewing and hindwing; see arrows in (**a**) and (**d**), and the short break at the base of a2-a3 (forewing)]. Because of the natural pleating of the wings, the space below the Sc appears very small relative to its actual size. The sc-r crossvein is actually slanted as shown. **A1, A2, A3** first through third anal veins **a2–a3** crossvein between A2 and A3 **C** costa **Cu** cubitus **1c-sc** first crossvein between the costa and subcosta **Fr** frenulum **icu1** first intracubital cell **J** jugal vein (forewing only) **Ju** jugal lobe **M** media **1m-cua** first crossvein between the media and anterior cubital branch **R** radius **Sc** subcosta **sc-r** basal crossvein between the subcosta and radius.

For comparison, I examined the *L. prisca* holotype, which also was collected in the Peruvian region of Amazonas. The type locality is: "PERU. DEPT. AMAZONAS: 18 km N of Puente Engenio, km 320, alt 1750 m, 9 Oct. 1964, P. C. Hutchinson & J. K. Wright, collected on *Baccharis latifolia* #6380". As noted above, the abdomen of this specimen is in poor condition, and the body and wings are discolored by the intrusion of dark mycelia. However, the wings and external structure of the specimen are well preserved; the gut contents and cleared abdomen are held in separate vials in the unit tray holding the specimen.

Classification – subfamily. The holotype and the specimen described here exhibit the following diagnostic features of adult Nothochrysinae (cf.: Tjeder 1966, as Dictyochrysinae; Adams 1967; Brooks and Barnard 1990; Makarkin and Archibald 2013; Breitkreuz 2018): (i) wing-coupling mechanism consisting of a large jugal lobe on
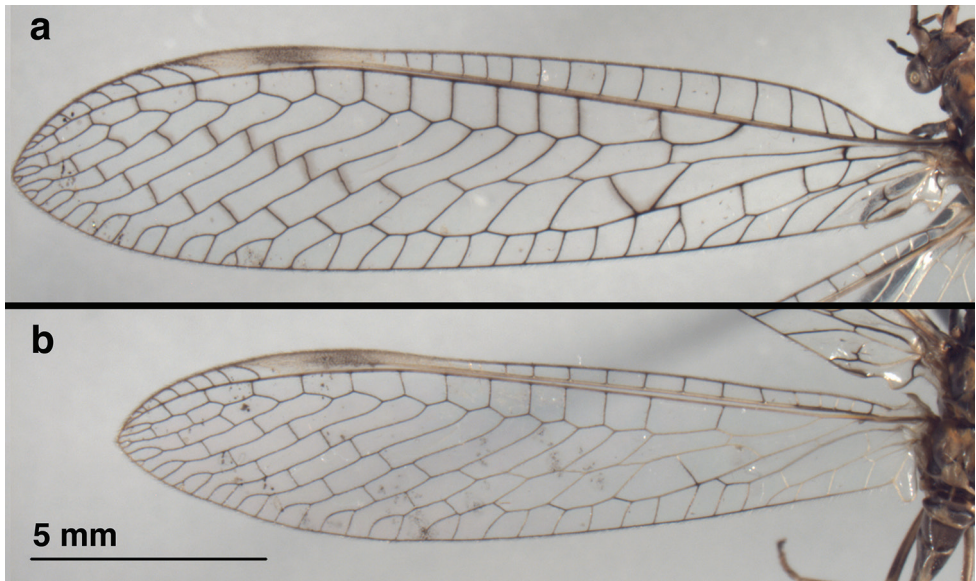
Figure 2. *Leptochrysa prisca* Adams & Penny (Peru, Amazonas, female, FSCA): Wings (**a**) forewing (**b**) hindwing.

the forewing and a frenulum on the hindwing (Figs 1, 2, 6); (ii) base of the forewing without tympanal organ (Fig. 1); (iii) forewing (and hindwing) with stem of the media (M) extending basally adjacent to the radius (R), not fused with it (see Fig. 1; cf. Breitkreuz 2018: 640); (iv) pseudomedia (Psm) merging (or appearing to merge) with inner gradates (not outer gradates) (Figs 2, 6); (v) pseudocubitus (Psc) merging with outer series of gradates (Figs 2, 6); (vi) forewing with subcostal crossvein present in basal section of wing (Fig. 1a–c); (vii) flagellomeres with five or six whorls of setae (Fig. 4c, d). However, as discussed later, the assignment of this species to Nothochrysinae is an "uncomfortable fit" (Makarkin and Archibald 2013: 125).

Classification – genus and species. This species' dark, mottled coloration, distinctive wing shape, and compressed venation make it highly recognizable among the Chrysopidae. Except in coloration (because of the fungal contamination in the holotype), the specimen reported here conforms completely to the generic description by Adams and Penny (1992b).

Redescription. Head (Figs 3, 4). Width 2.1 mm (including eyes); ratio of head width to eye width = 2.8 : 1. Vertex slightly raised, round anteriorly, without prominent posterior fold, surface rugose, pilose, with setae small, pale. Distance between scapes 0.26 mm; distance between tentorial pits 0.65 mm; length of frontal region (midway between scapes to midway between tentorial pits) 0.56 mm. Frons rounded laterally, well delineated, extending caudally between antennae, appearing to terminate in an acute apex at anterior margin of vertex; interantennal surface sculptured longitudinally, with longitudinal crease mesally, small rounded ridges fanning out from between scapes below frontal toruli; anterior section with weak transverse striation. Gena
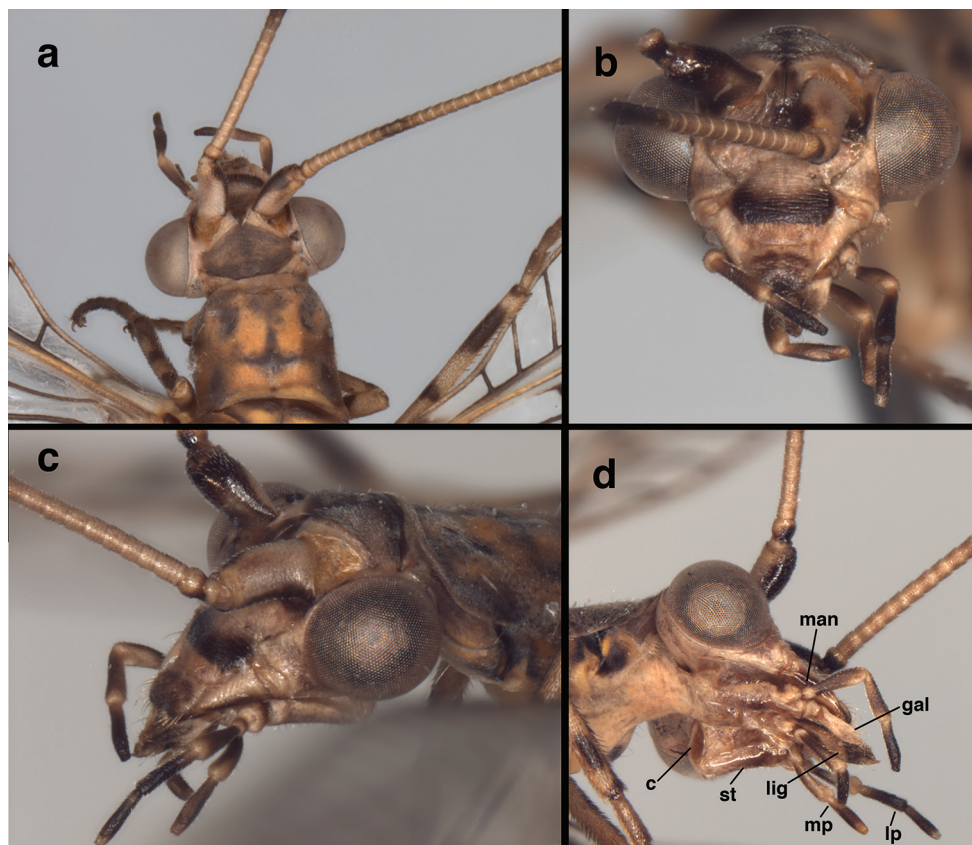
Figure 3. *Leptochrysa prisca* Adams & Penny (Peru, Amazonas, female, FSCA): Head and prothorax (**a**) head and prothorax, dorsal view (**b**) head, frontal view (**c**) head and anterior of prothorax, lateral view (**d**) head, posterolateral view. **c** cardo **gal** galea **lig** ligula **lp** labial palpus **man** mandible **mp** maxilary palpus **st** stipes.

(frontal view, Fig. 3b) appearing as rounded lobe from lateral base of scape to midsection of clypeus; tentorial pits on dorsal margin, near medial tip of lobe; insertion of mandibular base distinct, extending along full genal width. Clypeus relatively narrow basally, broader in center, narrowing distally; dorsal margin convex, lateral margins rounded, frontal margin straight; surface sculptured with transverse ridges except distally where ridges reduced, longitudinal. Frons, gena, base of clypeus rugose, without setae; distal part of clypeus, margins of mandibles with short to medium-length setae. Labrum narrower than clypeal margin, without ridges; dorsal surface somewhat sculptured; distal margin bilobed, with numerous long setae, especially on margin. Palpi elongate, tapered; venter of head with large, well-sclerotized cardo, stipes, narrow, elongate galea with conspicuous papilla; ligula elongate. Antenna length unknown (flagella broken); scape considerably longer than wide (length 0.57 mm, width 0.35 mm), with slight lateral bend; lateral margin slightly concave, mesal margin convex, surface with short setae throughout; pedicel length 0.23 mm, width 0.18 mm, with numer-
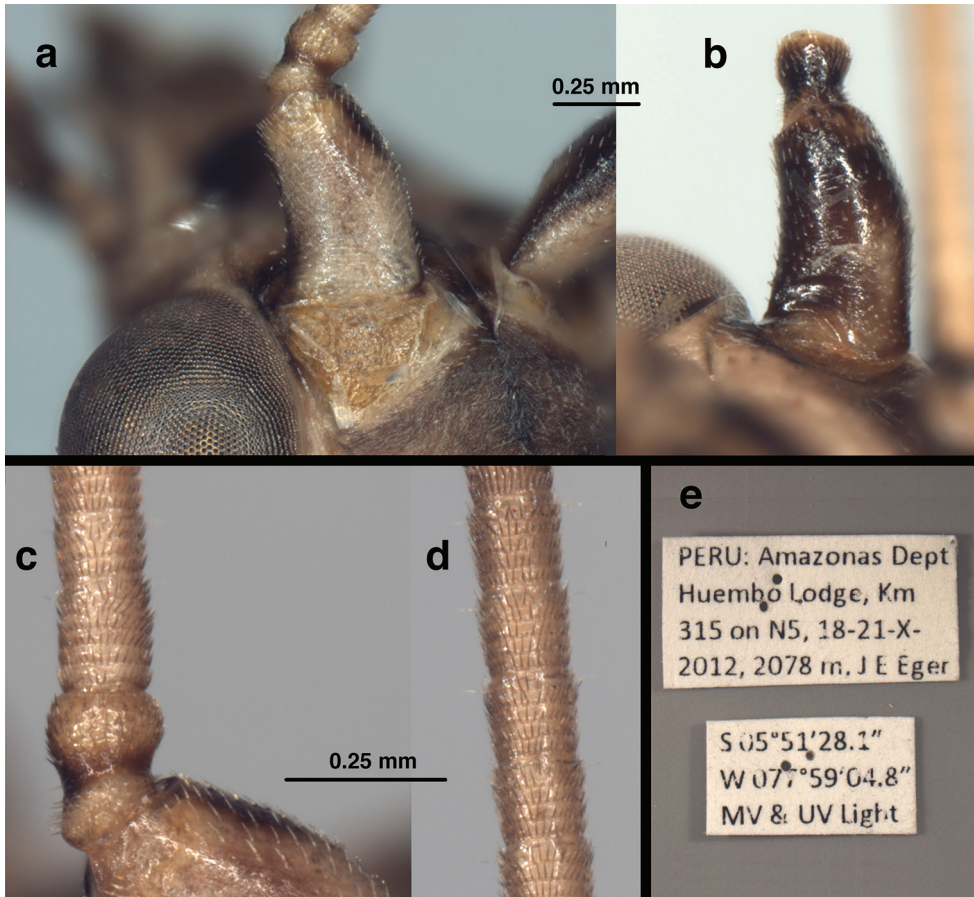
Figure 4. *Leptochrysa prisca* Adams & Penny (Peru, Amazonas, female, FSCA): Antenna and specimen labels (**a**) left scape, pedicel, dorsal torulus, tip of vertex, dorsal view (**b**) right scape, ventral view (**c**) pedicel, basal flagellar segments, dorsal view (**d**) distal flagellar segments, dorsal view (**e**) specimen labels. Scale between (**a**) and (**b**) applies to both (**a**) and (**b**); scale between (**c**) and (**d**) applies to both (**c**) and (**d**).

ous short setae; flagellum with basal flagellomere distinct, somewhat elongate (length 0.18 mm, width 0.15 mm), midantennal flagellomeres about as long as broad (length 0.13–0.14 mm, width 0.13–0.14 mm); basal flagellomere with six whorls of brown setae extending distally, second to fifth flagellomeres each with four whorls of brown setae extending distally; sixth to distal flagellomeres each with five whorls of brown setae; all flagellomeres each with two elongate setae extending laterally from distal whorl. Flagellar setae in whorls stouter, longer than setae on vertex.

Head coloration (Fig. 3). Antenna: dorsum, lateral sides of scape cream, with tan spot distolaterally; mesal, ventral sides dark brown; pedicel, cream to light brown with darker brown mesal band; flagellum cream to light brown, with eighth to twelfth segments dark brown; elongate setae, setae in whorls light brown to brown. Vertex dark brown; dorsal torulus golden tan; space between torulus and vertex cream; space

Figure 5. *Leptochrysa prisca* Adams & Penny (Peru, Amazonas, female, FSCA): Thorax (**a**) thorax and most of abdomen, lateral view (**b**) mesothorax and metathorax, dorsal view (**c**) mesoscutellum, metathorax, dorsal view (**d**) connection between mesoscutellum, metascutum (**e, f, g**) metatarsus, ventrolateral, ventral, lateral views, respectively. In (**d**), the lower arrow indicates the flat surface of the metascutum and its anterior quadrate protrusion; the upper arrow indicates the lobate lateral expansions of the mesoscutellum.

between vertex and eyes, cranial area behind eyes cream to light brown. Frons mostly cream, with dark brown mark along lateral base of scape, below scape along frontal margin of torulus, across dorsum of frons, between scapes, extending in an acute angle to brown mark on vertex; frontal torulus golden brown. Tentorial pits, frons between pits cream; gena cream with light brown mark at base of eye. Exposed lateral surface
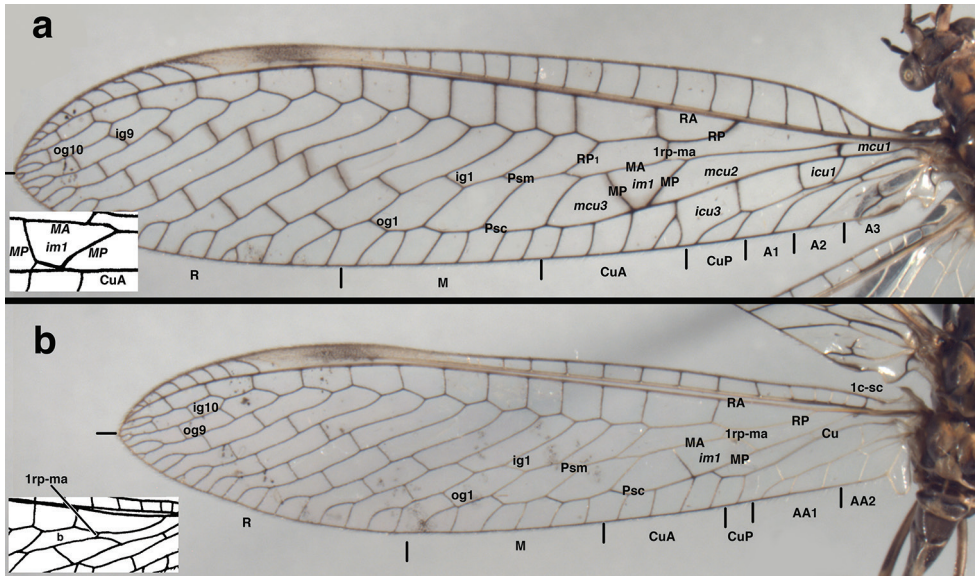
Figure 6. *Leptochrysa prisca* Adams & Penny (Peru, Amazonas, female, FSCA): Wings with selected features labeled (**a**) forewing, (**b**) hindwing. For comparison, the inserts depict the conditions on the *L. prisca* holotype for (**a**) the *im1* cell and (**b**) the proximal crossvein between RP and MA; images modified from Adams and Penny (1992b: fig 10). **A1, A2, A3** first, second, and third anal areas on wing margin, **1c-sc** first crossvein between the costa and subcosta **Cu** cubitus **CuA** anterior cubital area on wing margin **CuP** posterior cubital area on wing margin *icu1, icu3* first and third intracubital cells **ig, og** inner and outer gradate veins *im1* first intramedian cell **M** medial area on wing margin **MA, MP** anterior and posterior branches of the media *mcu1, mcu2, mcu3* first, second, and third medial cells **Psc** pseudocubitus **Psm** pseudomedia **R** radial area on wing margin **RA, RP** anterior and posterior branches of the radius **1rp-ma** first crossvein between RP and MA.

of mandible dark brown basally, brown to light brown distally. Clypeus cream to light brown, with large, dark brown band across mesal section. Labrum with basal, lateral margins cream to light brown, central and distal areas dark brown. Exposed dorsal section of labium (ligula) cream basally becoming dark brown distally; ventral surface of labium mostly light brown. Maxilla (ventral) mostly light brown, with galea cream, cardo brown, stipes brown distally. Maxillary, labial palpi brown to dark brown, with intersegmental connections cream to light brown.

Thorax (Figs 3a, 5). Cervix brownish, appearing sclerotized or partially so. Dorsal thoracic surface mostly smooth, with waxy coating, golden orange, mottled with large brown markings, bearing fine, pale setae throughout. Pronotum large, appearing well sclerotized, with small transverse depression mesally, slightly broader than long (dorsal view), length 1.2 mm; width 1.5 mm; ratio of length to width = 0.8 : 1. Mesothorax, metathorax with surface shiny, smooth, appearing well sclerotized; each segment with dark brown markings. Mesopostscutum with bilobed enlargement on posterior margin; anterior margin of metascutum without raised process on anterodorsal margin,
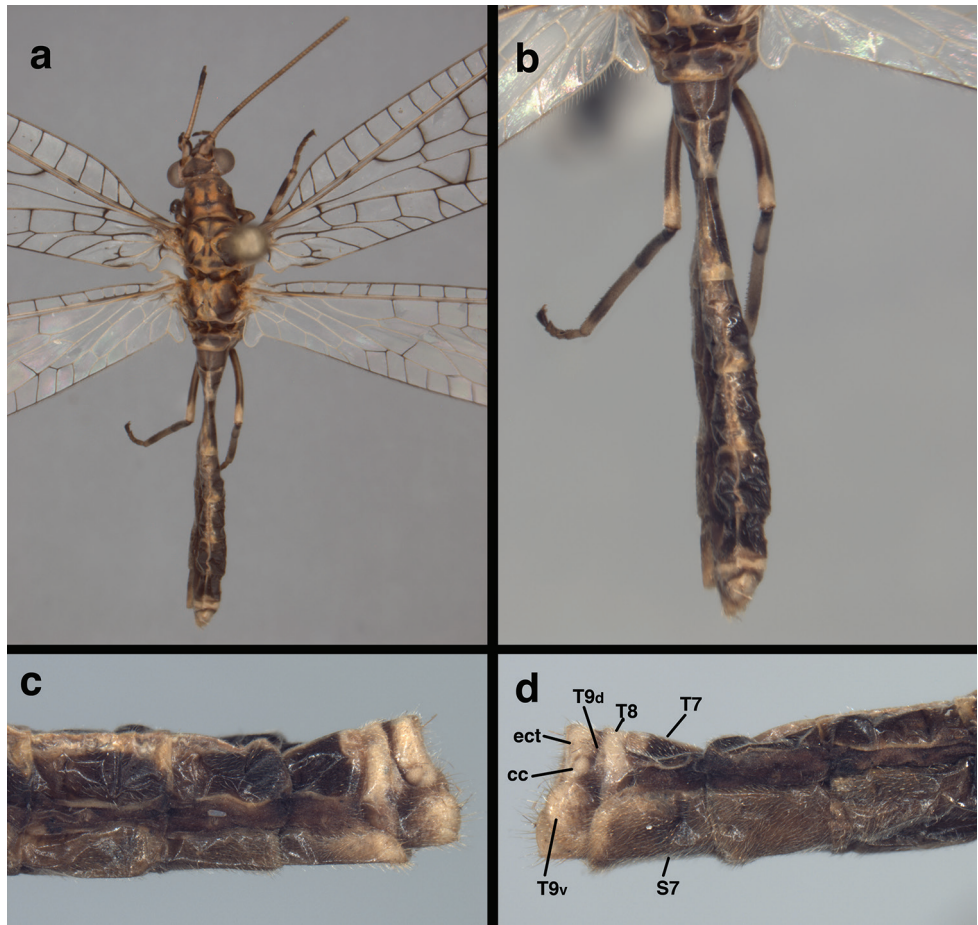
Figure 7. *Leptochrysa prisca* Adams & Penny (Peru, Amazonas, female, FSCA): Body and abdomen, external (**a**) body, dorsal view (**b**) abdomen, dorsal view (**c, d**) terminal abdominal segments, left and right, respectively, lateral views. **cc** callus cerci **ect** ectoproct **S7** seventh sternite **T7, T8** seventh, eighth tergites **T9d** dorsal section of large ninth tergite hidden beneath T8 **T9v** expanded ventral section of large ninth tergite encapsulating gonapophyses laterales.

but with quadrangular knob on anterior margin extending forward toward bilobed enlargement of mesopostscutum. Legs elongate, slender, cream; each femur, tibia marked with two elongate brown marks, without prominent tibial spurs. Tarsus (ventrolateral side, all legs) with dense, robust, dark brown setae ventrally, more slender setae dorsally; terminus with pair of curved claws laterally, large pad mesally; claw amber, without basal enlargement, acute slender hook terminally.

Wings (Figs 1, 2, 6). *Forewing:* Elongate, narrow, length 20.3 mm, maximum height 4.7 mm; ratio of length : maximum height = 4.3 : 1. Membrane transparent, uniformly covered with microtrichia. Trichosors (*sensu* Makarkin and Archibald 2013: 140–142) absent. Costal area narrow; tallest costal cell (#5) height 0.9 mm, 1.1 times
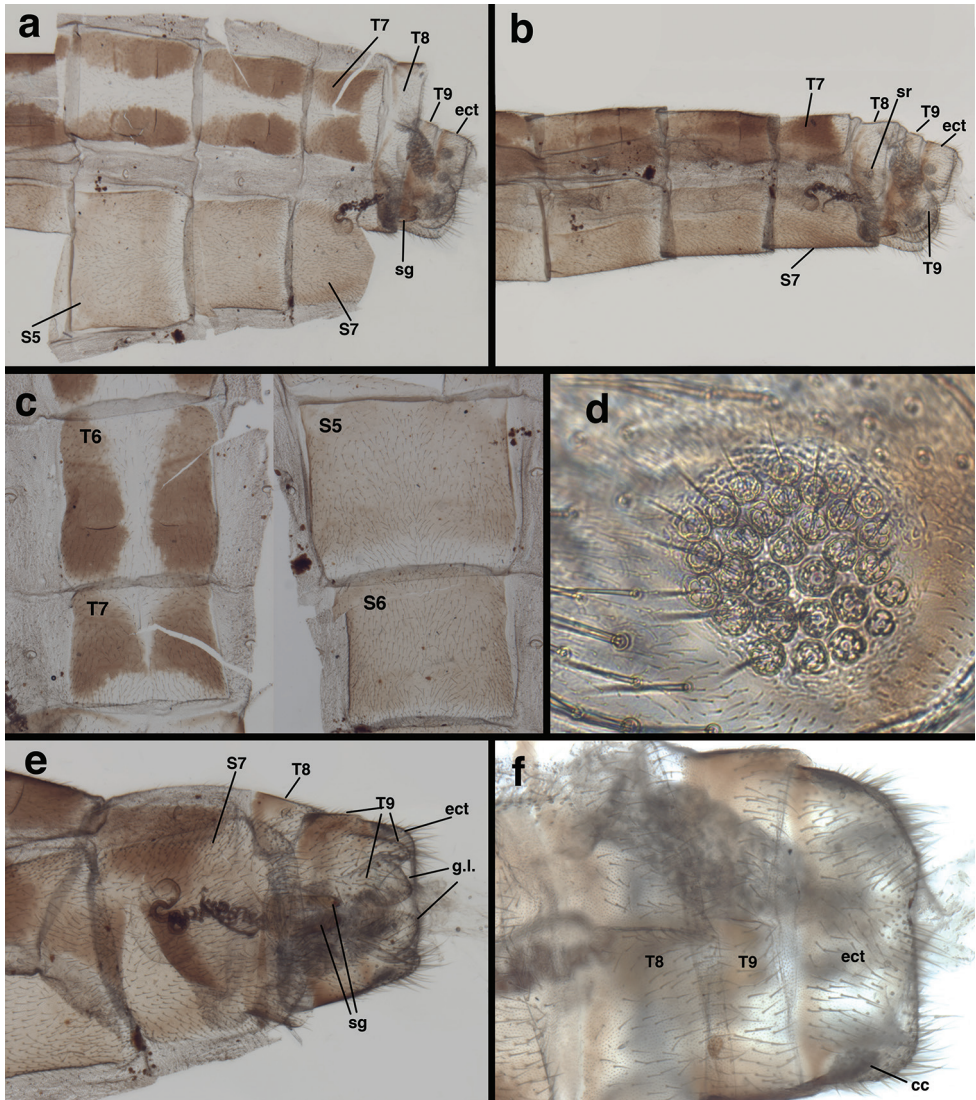
Figure 8. *Leptochrysa prisca* Adams & Penny (Peru, Amazonas, female, FSCA): Abdomen, cleared (**a**) abdominal integument dissected, segments A5-A7 with dorsal, lateral, and ventral surfaces in view, A8 with dorsal and lateral surfaces in view, A9, ectoproct in lateral view (**b**) segments A5-terminus, lateral view (**c**) abdominal integument, dorsal (T6-T7) and ventral (S5-S6) (**d**) callus cerci (**e**) terminal abdominal segments, ventral view (**f**) terminal abdominal segments, dorsal view. **cc** callus cerci **ect** ectoproct **g.l.** gonapophyses laterales **sg** subgenitale **sr** spiracle **S5, S6, S7** fifth, sixth, and seventh sternites **T6, T7, T8, T9** sixth, seventh, eighth, and ninth tergites.

width, 0.19 times height of wing; all costal crossveins simple, four c-sc crossveins before 1sc-r, fourteen c-sc after 1sc-r and before stigma, none within stigma. First sc-r crossvein (1sc-r) robust, angled basally; distal section of Sc extending into and fading within stigma, but not appearing to merge with C or RA; from no to two very faint
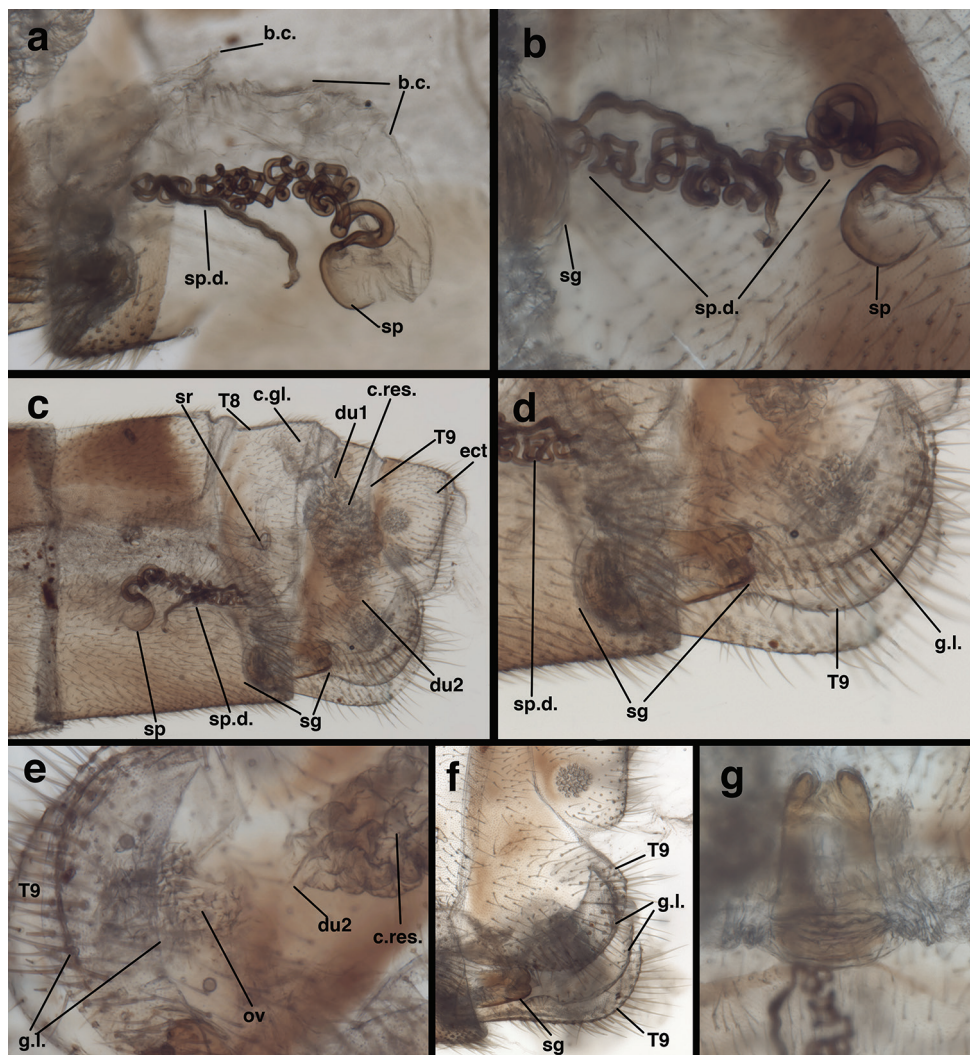
Figure 9. *Leptochrysa prisca* Adams & Penny (Peru, Amazonas, female, FSCA): Abdomen, genitalia, cleared (**a**) spermathecal complex (**b**) spermatheca and duct (**c**) terminalia, lateral view showing colleterial, spermathecal, and subgenitale complexes (**d**) subgenitale, lateroventral view (**e**) terminus, lateral view showing crescent-shaped gonapophysis lateralis (proximal and distal margins) encased between ventral extension of T9, spinose oviduct beneath (terminal end of duct 2 obscured) (**f**) gonapophyses laterales within extensions of T9, subgenitale beneath (**g**) subgenitale, dorsal view showing bilobed terminus. **b.c.** bursa copulatrix **c.gl.** colleterial gland (broken distally) **c.res.** colleterial reservoir **du1** large duct leading from colleterial gland to reservoir **du2** duct leading from colleterial reservoir to oviduct **ect** ectoproct **g.l.** gonapophysis lateralis nestled beneath T9 **ov** oviduct **sg** subgenitale **sp** spermatheca **sp.d.** spermathecal duct **sr** spiracle **T8, T9** eighth and ninth tergites.

sc-ra crossveins in stigma. Apical costal area (between C and RA) relatively broad apically; RA with ten to eleven anterior branchlets reaching apical region of wing margin. Furcation of R (R*f*) distal to 1sc-r crossvein, very much basal to furcation of M (M*f*). Radial area (between RA and RP) with single row of thirteen closed cells, only one
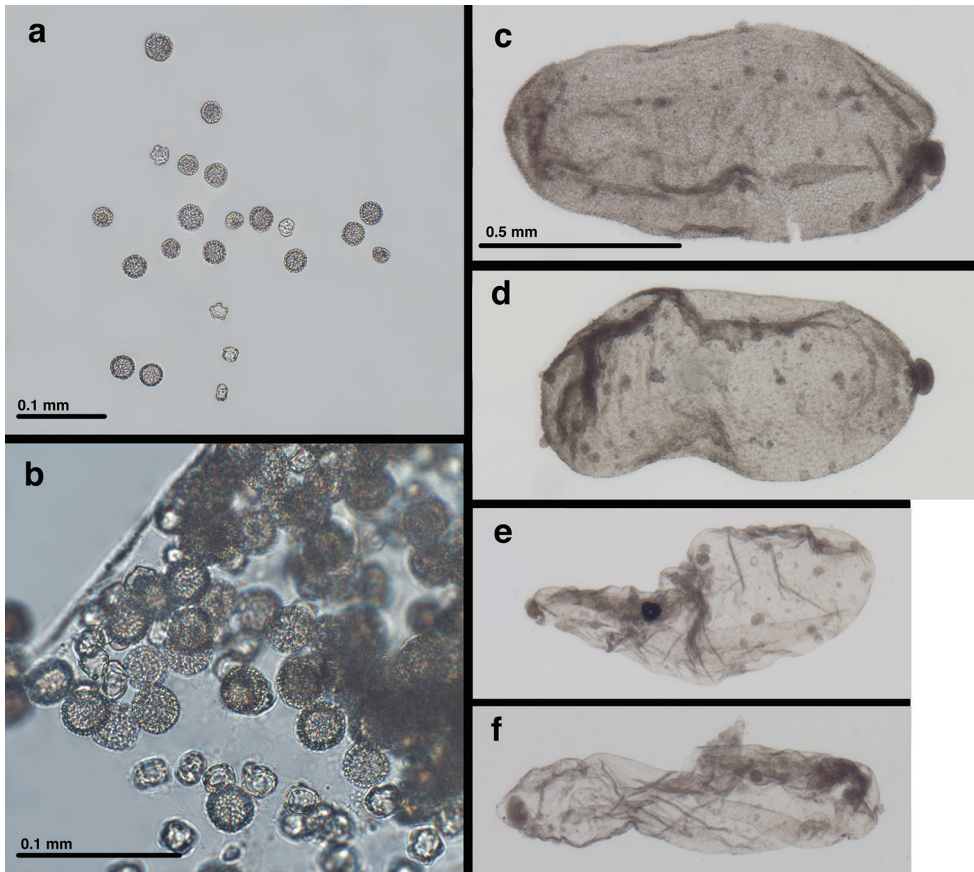
Figure 10. Contents of *Leptochrysa prisca* Adams & Penny abdomen (after clearing with KOH) (Peru, Amazonas, female, FSCA): Pollen and parasitoids. (**a, b**) pollen from gut (**c, d**) two of five robust parasitoid larvae from abdominal cavity (**e, f**) probably exuviae (two of five) from previous parasitoid instar. Scale on (**c**) applies to (**c, d, e, f**).

ra-rp anterior to the first branch (RP_1) stemming from RP; tallest cell (*rarp2*) height 0.9 mm, 0.9 times width; radial crossveins (ra-rp) straight. Radius with no crossveins to M before R*f*; 1rp-ma meeting MA at intramedian cell (*im1*). Media with one m-cu crossvein (therefore two medial cells, *mcu1*, *mcu2*) basal to *im1*. M*f* basal to first r-m crossvein (1rp-ma); angle of MA and MP broadly acute; MA becoming pale, diffuse and constricted between M*f* and insertion of 1rp-ma (both forewings) [holotype: MA thin in this area, but not pale]. Intramedian cell (*im1*) prominent, quadrangular in shape (but not *sensu* Breitkreuz et al. 2017: 29; see Discussion below), formed by MA anteriorly, MP basally, posteriorly, distally; anterior (MA) and posterior (MP) sides of *im1* roughly parallel for most of span; *im1* occupying entire vertical space between MA and CuA. MA and MP rejoining at anterodistal corner of *im1*, subsequently dividing at least once before meeting RP_1, and probably a second time before meeting RP_2.

Third medial cell (*mcu3*) distal to *im1*, triangular. Two series of gradate veins diverging medially, converging distally. Nine inner gradates (in regular, sinuous series), extending beyond pseudomedia (Psm) in zigzag pattern across center of wing; ten outer gradates in slightly upturned series beyond pseudocubitus (Psc). Radial branches from RP elongate, wavy before inner gradates, less so after. Gradate cells rectangular. Approximately eight primary marginal forks reaching posterodistal margin (radial field) of wing. Cubital furcation (Cu*f*) near, but basal to m-cua crossvein. CuA with two simple crossveins to CuP, a distal third vein forked, reaching wing margin, and probably three additional simple branches reaching wing margin beyond forked vein. Second cubital furcation (CuP*f*) below *icu2*; thus, posterior wing margin with seven to ten cubital veinlets total (five to eight from CuA, two from CuP). A1, A3 simple, unforked; A2 forked before a1–a2 crossvein, with anterior branch reaching wing margin, posterior branch extending to A3, with short distal veinlet ending within cell (both wings). Jugal lobe large, usually folded beneath anal region, with jugal vein dark, extending to basal margin; basal margin with elongate, pale setae.

Hindwing: Length 17.5 mm, maximum height 4.0 mm. Costal base with well-developed frenulum bearing cluster of elongate terminal setae. Costal area narrow, with 15 crossveins before stigma, eight radial veinlets extending to C after stigma; no veins within stigma. Subcostal area without crossveins. M parallel and attached to R until just past 1c-sc; R*f* distal to 3c-sc. Radial area with single row of thirteen closed cells between RA and RP (= 13 ra-rp crossveins). Two series of gradate veins, roughly parallel, regularly spaced; nine or ten inner gradates extending beyond Psm; nine or ten outer gradates, regularly spaced, extending beyond Psc. Approximately eight primary marginal forks reaching posterodistal margin (radial field) of wing. Only one r-m crossvein (1rp-ma). First intramedian cell with MA as anterior margin, with MP as posterior margin basally, MP+CuA distally, distal arm either MP, MA_1, or ma-mp crossvein). Cu sinuous, with two crossveins to A1, two branches reaching posterior wing margin before merging with MP. A1 with three veinlets reaching posterior wing margin; A2, A3 simple, unforked; one crossvein (a1–a2) between A1, A2; A3 forming base of jugal lobe; jugal lobe large, rounded.

Coloration of forewing, hindwing (Figs 1, 2, 6): Membrane of both wings appearing clear, somewhat glossy. Stigma prominent, dark brown medially, golden on both ends. All veins dark brown except forewing with Sc golden, anterior base of MA yellowish; hindwing with 1c-sc, 3c-sc3 to 6c-sc, Sc beyond 6c-sc, base of R (including base of RA and RP), base of M, most of MA and its branches, base of Cu, all anal veins golden. Forewing with brownish suffusion around MP, inner gradates, and outer gradates.

Abdomen (female, Figs 7–9; male unknown). Tergites, sternites, pleural region covered with relatively dense setae of uniformly short length; microsetae present, no microtholi. T6 (lateral view) length 1.2 mm, ~2.1× height, approximately same proportions as T7 (length 0.9 mm, ~1.7× height). S6 length 1.2 mm, ~2.0× height; S7 length 1.2 mm, approximately 2.0× height. Tergites roughly rectangular, with edges acute or slightly rounded, ventral margins straight; lateral (dark brown) regions more rigid and robust than mesal section. Sternites quadrate, uniformly colored and rigid

throughout. Spiracles located in pleural membrane, slightly closer to sternites than to tergites, roughly oval externally, not enlarged; atria slightly enlarged, rounded, with single tracheae. Coloration mostly dark brown with cream stripe on dorsal midline; distal tip of T7, T8, posterior region of T9, ectoproct, gonapophysis lateralis cream; setae, setal bases pale; callus cerci cream.

Female terminalia (Figs 7c, 7d, 8, 9c–f): Callus cerci (Fig. 8d) approximately circular, diameter 0.14-0.16 mm, with ~30 trichobothria of mixed length. Tergite 8 much narrower than T7 (lateral view), much taller than T7, extending well beyond distal margin of S7, with rounded ventral margins, bearing spiracle in lower sclerotized section. Tergite 9, ectoproct distinctly separate; T9 with dorsal margin narrow, less than half length of T7, becoming broad, bulbous ventrally, completely encasing gonapophyses laterales, ventral margin rounded, over three times length of dorsal margin. Sternite 7 roughly quadrate, with dorsal margin straight, approximately same height as S6, rounded and sloping abruptly in distal quarter, base at ventral margin extending distally as apical ledge, without knob; posteroventral setae slightly longer, more dense than other setae. Ectoproct with dorsal margin twice as long as dorsal margin of T9, ventral margin rounded, tucked below distal bulge of T9, bearing callus cerci near posterior margin; callus cerci about half width of segment. Gonapophysis lateralis well sclerotized, broadly crescent shaped, mostly enclosed by distal extension of T9 (Fig. 9f), with sparse distribution of small setae on distal, exposed surface only, not on basal surface.

Colleterial complex (***posterior to anterior***) (Fig. 9c, e): Oviduct immediately behind gonapophyses laterales, chamber setose (setae arising from large bulbous bases); no transverse sclerification found. Two sets of glands entering oviduct: posterior gland, fluted, with rough, setose surface, thin duct bearing secondary gland or small reservoir before opening to oviduct; anterior gland (probably the primary colleterial gland) distally with globate colleterial reservoir larger than width of T9, heavily textured surface with numerous rounded folds and some setae, entering oviduct via short, somewhat broad duct. Colleterial gland (anterior end missing) entering colleterial reservoir between T8 and T9 via broad, robust, membranous duct, gland probably large, with broad, structured, circular base, setose membranous sides, at least distally.

Bursal complex (Fig. 9a): Bursa copulatrix with two sections; larger section consisting of delicate, transparent membrane with transverse, angled folds, covering entire spermatheca and spermathecal duct; smaller section leathery, triangular, attached above membranous section; two sections fusing distally before entering chamber above subgenitale; bursal glands not found. Spermatheca bowl-shaped, somewhat transparent, invaginated, apparently open to large section of bursa via slit on basal (proximal) side of bowl and perhaps on spermathecal duct. Spermathecal duct well sclerotized, very long, with coiled section extending about 0.75 length of S7, straight section doubling back almost completely; basal section, tightly coiled, curved on itself, with smooth surface; distal section mostly straight, with some slight bending, dense, surface with brushy covering of setae; region between two sections in contact with subgenitale complex.

Subgenitale (Fig. 9d, g): Basal section well sclerotized, extending from leathery, partially sclerotized, membranous base; distal section elongate, rounded, robust laterally, flat

mesally, protruding distally between gonapophyses laterales, well beyond S7, with patch of approximately ten robust setae ventrally, shallow bilobed tip distally. Basal membranous section considerably shorter than sclerotized distal section, extending from sturdy membranous fold within ventral tip of S7, rounded proximally, folded throughout.

Biology. *Abdominal contents – pollen***:** A label on the type specimen indicated that it was taken from *Baccharis latifolia* (Ruiz & Pav.) Pers., a flowering shrub that is common throughout much of South America, including Peru. Adams and Penny (1992b) noted pollen in the gut contents. Thus, it is not surprising that both the foregut and hindgut of the female specimen studied here also were filled with pollen. The pollen grains were of several sizes and shapes: predominately large and round, but also small and round, as well as small and quadrate (Fig. 10a, b).

*Abdominal contents – parasitoids***:** After the abdomen was cleared, it was found to contain a number of parasitoid larvae (probably Hymenoptera). The parasitoids were also cleared during the process, and the resulting specimens consisted of two types. First, there were five robust larvae with a textured, scabriculous integument throughout, a rounded knob at one end, and a pair of small protrusions at the other end. The interior of these specimens appeared empty (Fig. 10c, d)); no mouthparts or other structures were visible. Second, there are five smaller, more delicate specimens, consisting of clear, smooth integuments without structures or setae (Fig. 10e, f). It is possible that these clear specimens are the exuviae of previous instars or a very different form or stage of parasitoid than the robust ones. It is noteworthy that the abdomen of the lacewing host was relatively slender for a well-sclerotized female (Fig. 7).

*Larvae***:** Discovery of *L. prisca* larvae would greatly help to decipher the phylogenetic relationships of the genus *Leptochrysa*. Unfortunately, the larvae of this genus remain unknown. Descriptions are available for comparison with the larvae of several Nothochrysinae genera: *Kimochrysa* Tjeder, *Pimachrysa* Adams, *Dictyochrysa* Esben-Petersen, *Hypochrysa* Hagen (one species each), and several species of *Nothochrysa* (see review by Tauber et al. 2014). The known *Nothochrysa* larvae are debris-carriers, whereas the known larvae of other genera are naked.

Known distribution. Thus far, there are only two records for this species, and both are from the Amazonas region of northern Peru. The specimen studied here is from Huembo Lodge, a reserve run by the Ecoan Andean Ecosystems Organization, and located on Hwy 5N southwest of Pomacochas.

Intraspecific variation. Other than the discoloration and damage caused by fungal growth on the holotype and some variation in the number of gradate cells, the two known *L. prisca* specimens show significant similarity. However, there is one notable area of variation in the forewing – the posterior margin of the intramedian (*im1*) cell. This variation, although subtle, proves to be useful in deciphering the venation of the *Leptochrysa* forewing.

In both specimens of *L. prisca*, the MP forms the posterior margin of the *im1* cell, and MP meets CuA at the posterobasal corner of *im1*. In the left and right wings of the holotype, MP and CuA clearly remain distinct (see insert on Fig. 6a). When the MP reaches the CuA, the two veins do not fuse; they extend distally along separate

trajectories. MP alone forms the posterior (lower) border of *im1*. CuA runs below MP and forms the base of a narrow triangular cell beneath the *im1*. A very short 2mp-cua crossvein or a branch of the MP extends anteriorly from the posterodistal corner of *im1*, and CuA continues distally.

In comparison, on the second specimen (left and right wings), MP and CuA appear as a single vein along the full posterior span of the *im1* cell. However, on the basis of the holotype's venation, I assume that the two veins remain juxtaposed, but separate along this span.

The configuration described above appears to be unusual within Nothochrysinae. Although variable, the *im1* in Nothochrysinae generally is triangular, being formed by MA, MP, and crossvein 1ma-mp. (Note: Breitkreuz et al. 2017 would consider this configuration as "pseudotriangular", but see reasons presented by Tauber (2019) for identifying this configuration as "triangular".). In contrast, the findings here indicate that the *im1* is composed entirely of the anterior and posterior branches of M, without a crossvein. Thus, the *im1* cell of *L. prisca* more closely aligns with a category of *im1* cells that is not usually reported for Nothochrysinae: shaped like a triangle or quadrangle, but without a crossvein forming a portion of the cell. Thus, the cell's quadrate shape and configuration in *L. prisca* elicit questions concerning the identity of the "crossvein" proposed to close the distal ends of the *im1* within other genera of Nothochrysinae. It is also noteworthy that on both the holotype and the second specimen of *L. prisca*, it is not clear whether the MP furcates at the posterodistal corner of the *im1*. If it does, then the CuA vein extending from the posterodistal corner of the *im1* would be a fused CuA+MP and thus part of the Psc.

Discussion

Leptochrysa prisca lacks several characteristics that are typically found in Nothochrysinae, and it also expresses some features that are unique among chrysopids or characteristic of ancient chrysopid subfamilies. As a result, the placement of the genus in Nothochrysinae remains unsettled (Makarkin and Archibald 2013). Below I discuss some of the features of interest.

Relative lengths of Sc and RA of forewing: In the elongated wings of *L. prisca* (both specimens), the Sc extends only partially into the stigma where it appears to dissipate, and the RA, which reaches well beyond the stigma almost to the apex of the wing, has numerous distinct veinlets that extend to the costa. According to Adams and Penny (1992a), the elongation of the wing and such a configuration are typical of species in two genera of Mesochrysopidae. And, according to Makarkin and Archibald (2013: 125), the *L. prisca* configuration of Sc and RA resembles that of the genus *Protochrysa* Willmann & Brooks in Limaiinae (Chrysopidae). In addition, aspects of the arrangement, e.g., veinlets on the posterior margin of the wings and perhaps the separation of the R and Sc near the tip of the wing, are typical of some Apochrysinae (see Winterton and Brooks 2002). In any case, none of the above features are known from other Nothochrysinae.

First intramedian cell of forewing: (i) Relationship of CuA to *im1*. In *L. prisca*, the MP runs parallel with the CuA, either in contact with it or very closely nearby, to form the posterior margin of the *im1*. Among the Nothochrysinae, such a close association between the *im1* and CuA is shared only with *Triplochrysa pallida* Kimmins. In this species, the *im1* cell is bounded posteriorly by MP and CuA (see New 1980: fig. 13); however, it is unknown if the two veins run separately and in parallel as they apparently do in the *L. prisca* studied here.

(ii) Vertical space between MP and CuA. In most Nothochrysinae, the *im1* occupies about one-half to two-thirds the vertical distance between MP and CuA (see New 1980, Brooks and Barnard 1990). In *L. prisca*, the *im1* cell, which is quadrate in shape, occupies the entire vertical space between MP and CuA. Among the Nothochrysinae, an *im1* that fills the entire vertical space between MP and CuA is shared only with *T. pallida* (see New 1980: fig. 13).

(iii) Modification of the second m-cu crossvein. As described above, the *L. prisca* holotype has a small second m-cu crossvein (mp-cua), and the second specimen entirely lacks a second m-cu crossvein. This reduction/loss appears to be unique among Nothochrysinae (see Adams 1967, Brooks and Barnard 1990, Archibald and Makarkin 2015: 361). Makarkin and Archibald (2013) consider this feature, as well as the basal tapering of the *im1* in *L. prisca*, to be suggestive of Limaiinae.

Rectangular gradate cells: Adams and Penny (1992a) noted that the gradate cells of *L. prisca* are clearly quadrangular in shape and very unlike the polygonical gradate cells typical of modern chrysopids. They considered such cells to represent a plesiomorphic condition among chrysopoids because even some mesochrysopids (e.g., *Mesypochrysa* Martynov) have gradate cells that are more typical of modern chrysopids. As they pointed out, the critical question is whether these cells are truly plesiomorphic or secondarily derived, perhaps associated with wing elongation.

White "break" in MA of forewing: The mostly dark wing venation of *L. prisca* accentuates a characteristic that is widespread among Nothochrysinae males and females, but apparently has been unreported. The media (MA), directly below or near the insertion of the rp-ma crossvein, is interrupted by a short span that is white and either broken or diffuse. The span contains what appears to be a tracheal branch. Distal to the white span the MA reassumes its normally defined, dark structure. These features are readily noticeable on the *L. prisca* specimen described here, less so on the holotype which has generally discolored (dark) venation. However, the holotype shows the narrowing of MA in the region.

The white "break" or narrowing of MA observed in *L. prisca* also occurs in all New World genera of Nothochrysinae: *Asthenochrysa* Adams & Penny, *Nothochrysa* McLachlan, *Pimachrysa* Adams (at least four species: *P. albicostalis* Penny, *P. fusca* Adams, *P. intermedia* Adams, and *P. nigra* Adams), and, as well as in *Dictyochrysa peterseni* Kimmins, *Hypochrysa elegans* (Burmeister), *Nothochrysa sinica* Yang, and perhaps other species in the Old World. The feature is readily seen in *Nothochrysa californica* Banks and *Pimachrysa* species because they, like *L. prisca*, have mostly dark veins. In *Asthenochrysa* and the South American species *Nothochrysa ehrenbergi* Tauber,

which have pale or mottled wing venation, the white span in the MA can be difficult to discern, but it is present. This character has not been reported for other chrysopids; its phylogenetic importance, if any, is unknown.

Proximal crossvein between RA and MA of hindwing: Adams and Penny (1992a, b) and Makarkin and Archibald (2013) reported that *Leptochrysa* is the only extant chrysopid genus in which the hindwing has a basal crossvein connecting RP and MA (rp-ma, identified and illustrated as the basal vein of the "b cell" by Adams and Penny; see insert on Fig. 6b). And, according to both sets of authors, this feature occurs in most Limaiinae and only in some early Eocene Nothochrysinae, perhaps most notably *Archaeochrysa* Adams. It was not reported from extant Nothochrysinae. However, some exceptions may have been overlooked: *Pimachrysa nigra* (Adams), *Kimachrysa africana* (Kimmins), and *Nothochrysa turcica* Kovanci & Canbulat, all of which are modern species in Nothochrysinae (Tjeder 1966, Adams 1967, Tauber 2019), and all of which appear to have an rp-ma crossvein. Thus, the value of the character as an indicator of phylogenetic position may not be as strong as originally thought.

Surface of the wings: *Leptochrysa prisca* is the only chrysopid known to have the membranous surfaces of its forewings and hindwings covered with microtrichia. As indicated by Adams and Penny (1992a, b), such an extensive covering of microtrichia occurs in Hemerobiidae and other Neuroptera but is not known in other chrysopids. Rather, in Chrysopidae, microtrichia are restricted to the bases of the forewings, and do not occur on other surfaces of the wings.

Metanotal expanded (raised) knob: A recent study by Breitkreuz (2018) reported that the dorsal surface of the anterior metascutum in Nothochrysinae typically has a raised expansion or knob. I have confirmed this feature for all New World genera and several Old World genera of Nothochrysinae. However, on the holotype and the specimen of *L. prisca* described here, the dorsal surface of the metascutum has no knob-like protrusion. In contrast, the anterior margin of the *L. prisca* metascutum is enlarged anteriorly as a flat, rectangular protrusion (Fig. 5c, d). Similarly, the metascutum of the holotype is depressed, and the anterior margin is slightly protruding and quadrate. This type of anterior extension/protrusion is only known for *L. prisca*, not for other Nothochrysinae. It is unknown whether this feature is independent or an alternate, homologous expression of the metascutal expansion/knob.

It should be noted that the paired, lobate structures on the posterior margin of the *L. prisca* mesoscutellum (where it meets the metanotum, Fig. 5c, d) are larger and more mesally located than those reported from *Nothochrysa* (cf., Tauber 2019, fig. 4b). Perhaps, the enlargement and placement of the above mesonotal and metanotal structures are associated with flight involving narrow wings.

Sclerotization of thoracic and abdominal tergites: Relative to other Nothochrysinae I have studied (mainly New World species), *L. prisca* seems to have an unusually well-sclerotized thorax (i.e., it has a rigid form and is sturdy). In other New World Nothochrysines, the thoracic integument is soft and flexible, and it often appears collapsed in pinned specimens. The feature is especially apparent in *Asthenochrysa*, but I do not know whether it occurs among Old World Nothochrysines.

Also, the presence of paired tergites and the pronounced softness along the dorsal abdominal midline of *L. prisca* (Fig. 8a, c) are unique, as far as I know. Chrysopid abdominal tergites are generally well sclerotized and rigid mesally and less so laterally. Both of the above features are in need of comparative study.

Conclusion

The phylogeny of *Leptochrysa* remains enigmatic, and the assignment of the genus to Nothochrysinae (indeed, to Chrysopidae) is unsettled. Resolution of its phylogenetic relationships within Neuroptera awaits studies of the larval stages and molecular analyses.

Acknowledgements

References

Adams PA (1967) A review of the Mesochrysinae and Nothochrysinae (Neuroptera: Chrysopidae). Bulletin of the Museum of Comparative Zoology 135: 215–238.

Adams PA, Penny ND (1992a) Review of South American genera of Nothochrysinae (Neuroptera: Chrysopidae). In: Canard M, Aspöck H, Mansell MW (Eds) Current Research in Neuropterology. Proceedings of the Fourth International Symposium on Neuropterology, Bagnéres-de-Luchon, Toulouse, France, 35–41.

Adams PA, Penny ND (1992b) New genera of Nothochrysinae from South America (Neuroptera: Chrysopidae). Pan-Pacific Entomologist 68: 216–221.

Archibald SB, Makarkin VN (2015) A new species of *Archaeochrysa* Adams (Neuroptera: Chrysopidae) from the early Eocene of Driftwood Canyon, British Columbia, Canada. Canadian Entomologist 147: 359–369. https://doi.org/10.4039/tce.2014.53

Breitkreuz LCV (2018) Systematics and evolution of the family Chrysopidae (Neuroptera), with an emphasis on their morphology. PhD Thesis, University of Kansas, Lawrence, 661 pp.

Breitkreuz LCV, Winterton SL, Engel MS (2017) Wing tracheation in Chrysopidae and other Neuropterida (Insecta): a resolution of the confusion about vein fusion. American Museum Novitates 3890: 1–44. https://doi.org/10.1206/3890.1

Brooks SJ, Barnard PC (1990) The green lacewings of the world: a generic review (Neuroptera: Chrysopidae). Bulletin of the British Museum of Natural History, Entomology 59: 117–286.

Makarkin VN, Archibald SB (2013) A diverse new assemblage of green lacewings (Insecta, Neuroptera, Chrysopidae) from the Early Eocene Okanagan Highlands, western North America. Journal of Paleontology 87: 123–146. https://doi.org/10.1666/12-052R.1

New TR (1980) A revision of the Australian Chrysopidae (Insecta: Neuroptera) Australian Journal of Zoology, Supplementary Series 77: 1–143. https://doi.org/10.1071/AJZS077

Tauber CA (2019) South American Nothochrysinae: I. Description of *Nothochrysa ehrenbergi* n. sp. (Neuroptera: Chrysopidae). ZooKeys (in press).

Tauber CA, Tauber MJ, Albuquerque GS (2014) Debris-carrying in larval Chrysopidae: unraveling its evolutionary history. Annals of the Entomological Society of America 107: 295–314. https://doi.org/10.1603/AN13163

Tjeder B (1966) Neuroptera-Planipennia. The Lace-wings of Southern Africa. 5. Family Chrysopidae. In: Hanström B, Brinck P, Rudebec G (Eds) South African Animal Life. Vol. 12. Swedish Natural Science Research Council, Stockholm, 228–534.

Winterton SL, Brooks SJ (2002) Phylogeny of the Apochrysine green lacewings (Neuroptera: Chrysopidae: Apochrysinae). Annals of the Entomological Society of America 95: 16–28. https://doi.org/10.1603/0013-8746(2002)095[0016:POTAGL]2.0.CO;2

RESEARCH ARTICLE

ZooKeys

A peer-reviewed open-access journal

Launched to accelerate biodiversity research

A peculiar new species of gall-inducing, clearwing moth (Lepidoptera, Sesiidae) associated with *Cayaponia* in the Atlantic Forest

Gilson R.P. Moreira[1], Oleg G. Gorbunov[2], Júlia Fochezato[3], Gislene L. Gonçalves[4,5]

1 *Departamento de Zoologia, Instituto de Biociências, Universidade Federal do Rio Grande do Sul, Av. Bento Gonçalves 9500, 91501-970 Porto Alegre, RS, Brazil* **2** *The A.N. Severtsov Institute of Ecology and Evolution, Russian Academy of Sciences, Leninsky Prospect, 33, Moscow 119071, Russia* **3** *PPG Biologia Animal, Departamento de Zoologia, Instituto de Biociências, Universidade Federal do Rio Grande do Sul, Av. Bento Gonçalves 9500, 91501-970 Porto Alegre, RS, Brazil* **4** *PPG Genética e Biologia Molecular, Departamento de Genética, Instituto de Biociências, Universidade Federal do Rio Grande do Sul, Av. Bento Gonçalves 9500, 91501-970 Porto Alegre, RS, Brazil* **5** *Departamento de Recursos Ambientales, Facultad de Ciencias Agronómicas, Universidad de Tarapacá, Casilla 6-D, Arica, Chile*

Corresponding author: *Gilson R.P. Moreira* (gilson.moreira@ufrgs.br)

Abstract

Larvae of most clearwing moths (Lepidoptera, Sesiidae) are endophagous borers of many angiosperms, including their fruits, stems, and roots. Their localized feeding may lead to swellings on those plant parts, but whether the structures produced should be considered true galls is still controversial. In this study we describe a peculiar sesiid moth, *Neosphecia cecidogena* **sp. nov.** whose larvae induce unusual, external galls on *Cayponia pilosa* (Vell.) Cogn. (Cucurbitaceae) in the Atlantic Forest of southernmost Brazil. The adults, egg, larva, pupa and the gall are described and illustrated based on light and scanning electron microscopy. Galls are cylindrical and unilocular; they are induced individually on axillary buds of the *C. pilosa* stem. Unlike larvae of other sesiids, those of *N. cecidogena* **sp. nov.** lack abdominal pseudopodia, and show reduced stemata and chaetotaxy. Pupation occurs inside the gall, after having overwintered in the last larval instar. A maximum likelihood tree constructed based on mitochondrial DNA (COI) sequences showed that *N. cecidogena* **sp. nov.** is monophyletic and has an average distance of 13% to species of *Melittia*. The genera *Neosphecia* Le Cerf, 1916 stat. rev., *Premelittia* Le Cerf, 1916 stat rev., and *Melittina* Le Cerf, 1917 stat. rev. are restored from synonyms of *Melittia* Hübner, 1819 ["1816"].

Introduction

The Sesiidae is a worldwide family with ca 160 valid genera and 1,452 species. Of these, 268 species are found in the Neotropical region (Pühringer and Kallies 2004, 2017) and 119 have been recorded in Brazil (Casagrande et al. 2018). These diurnal micromoths are well known by their morphological and behavioral modifications that have been associated with Batesian mimicry, particularly regarding bees and wasps (Duckworth and Eichlin 1974; Skowron et al. 2015). In the last decades, many of their species have been found by attracting the adults with the use of synthetic sex pheromones (Duckworth and Eichlin 1977b; Brown and Mizell 1993; Špatenka et al. 1999; Arita and Gorbunov 2000; Arita et al. 2009; Skowron et al. 2015; Gorbunov 2018).

In contrast to the adults, however, their immature stages are poorly known, especially in the tropical regions where the host plants for only a small proportion species have been documented (Heppner and Duckworth 1981; Eichlin 2003). The family is known to feed upon a wide variety of shrubs, trees, vines, and herbaceous plants (Heppner and Duckworth 1981; Brown and Mizell 1993; Špatenka et al. 1999). Most sesiid larvae are endophagous borers, and many are highly specific regarding host-plant use. They may be associated with various plant organs, including fruit (Harms and Aiello 1995; Lopes et al. 2003; Puchi 2005), trunks/stems (Bruch 1941; Eichlin and Passoa 1983; Brown and Mizell 1993; Eichlin 1995, 2003), and roots (e.g. Lima 1945; Gorbunov 2015, 2019). Their feeding may lead occasionally to localized swellings on plants, but whether these structures should be considered true galls has been controversial (Eichlin 1995; Hanson et al. 2014). As far we know, none has been associated with the induction of external galls yet.

This study concerns a new species of clearwing moth that induces conspicuous, external galls on the stem of a vine, *Cayaponia pilosa* (Vell.) Cogn. (Cucurbitaceae) in the Atlantic Forest of southernmost Brazil. A preliminary comparison of genitalia structures suggested that it belongs to a genus closely related to *Melittia* Hübner, 1819 ["1816"], but does not conform to any species within it. We describe and illustrate the gall, the immature stages and adults of this moth under both light and scanning electron microscopy, and provide information on its natural history. By conducting a phylogenetic analysis of mitochondrial DNA (COI) sequences using representative members of Melittini (*Melittia*), we provide further support for the proposition of the new taxon, as well as its genus validation.

After careful examination of the habitus we came to the conclusion that this species is congeneric with *Neosphecia combusta* Le Cerf, 1916, which is the type species of the monotypic genus *Neosphecia* Le Cerf, 1916. This genus was formally synonymized with *Melittia* by Duckworth and Eichlin (1977a), but without concrete arguments. Also in this work, by the same reason, we formally restore this and two other names

from synonymy with *Melittia* Hübner, 1819 ["1816"]: *Premelittia* Le Cerf, 1916, stat. rev., *Neosphecia* Le Cerf, 1916, stat. rev., and *Melittina* Le Cerf, 1917, stat. rev.

Material and methods

All specimens used in this study were either dissected or reared from galls in small plastic vials, which were maintained under controlled conditions (14 h light/10 h dark; 25 ± 2 °C) in the Laboratório de Morfologia e Comportamento de Insetos (LMCI), Departamento de Zoologia, Universidade Federal do Rio Grande do Sul (UFRGS). Galls were collected from *C. pilosa* during the autumn seasons of 2014–2018 in the Centro de Pesquisas e Conservação da Natureza (CPCN Pró-Mata/PUCRS; 29°28'36"S, 50°10'01"W), 900 m elevation, São Francisco de Paula Municipality, Rio Grande do Sul State, Brazil. Pupae were obtained later (September) by dissecting some galls under a stereomicroscope in the laboratory. Adults were pin-mounted and dried. Chorionated eggs were obtained by dissection of females used in genitalia preparations. Immature stages were fixed in Dietrich's fluid and preserved in 75% ethanol. Additional larvae used for DNA extraction were preserved in 100% ethanol at –20 °C.

For descriptions of genital morphology, larvae were cleared in a 10% potassium hydroxide (KOH) solution, stained with either Eosin or Chlorazol black E and slide-mounted in either glycerin jelly or Canada balsam. Last instar larvae were prepared similarly for description of chaetotaxy. Observations were performed with the aid of a Leica M125 stereomicroscope. Structures selected to be drawn were previously photographed with a Sony Cyber-shot DSC-H10 digital camera attached to the stereomicroscope. Vectorized line drawings were then made with the software Corel Photo-Paint X7, using the corresponding digitalized images as a guide. Additional specimens were used for scanning electron microscope analyses. They were dehydrated in a Bal-tec CPD030 critical-point dryer, mounted with double-sided tape on metal stubs, coated with gold in a Bal-tec SCD050 sputter coater and examined and photographed in a JEOL JSM6060 scanning electron microscope at the Centro de Microscopia Eletrônica (CME) of UFRGS.

Molecular analysis

DNA was extracted from four larvae (specimens LMCI 263-33A, B, C, and D) of the new taxon using the PureLink Genomic DNA extraction kit (Invitrogen). Extracted DNA was resuspended in 50 mL Tris: EDTA (10 mm Tris-HCl, 1 mm EDTA, pH 5 8.0). Mitochondrial DNA PCR was conducted using primers LCO1490 and HCO2198 (Folmer et al. 1994), which amplified approximately 650 bp of the cytochrome oxidase I gene (COI), a fragment entitled DNA barcode. PCR reactions were conducted using 2 μL of the extracted DNA. The thermal cycler profile for CoI consisted of 35 cycles of 94 °C for 45 s, 48 °C for 45 s and 72 °C for 45 s. Excess dNTPs and primers were removed and the amplified DNA concentrated using exonuclease I and FastAP thermosensitive alkaline phosphatase (Thermo Fisher Scientific,

Waltham, USA). Samples were sequenced using BigDye Terminator v. 3.1 Cycle Sequencing kit (Thermo Fisher Scientific) and analyzed in an ABI3730XL automatic sequencer. The new data were deposited in the GenBank and BOLD Systems (http://www.boldsystems.org/) under the project MISA (Table 1). The COI sequences were initially aligned using Clustal W (Thompson et al. 1994) and subsequently refined by eye using CodonCode Aligner (CodonCode Corp, Massachusetts, USA).

The final dataset included 12 specimens: four individuals originally sequenced and six species of *Melittia*, the only representative of Melittini available, chosen based on morphologically established relationships with the new taxon. In addition, two species of Synanthedonini were used as outgroup to Melittini according to relationships proposed based on previous molecular phylogenies (e.g. McKern et al. 2008; Hansen et al. 2012; Lait and Hebert 2018).

The specific status of the new taxon was tested through a COI tree relying on monophyly. Tree reconstruction was based on the maximum likelihood (ML) algorithm performed in PHYML v. 3.0 (Guindon et al. 2010), using 1,000 replicates of heuristic search with random addition of sequences and TBR branch swapping. The substitution model GTR+I+G was selected based on the Akaike Information Criterion run in MEGA v. 7 (Kumar et al. 2016). Monophyly confidence limits were assessed with the bootstrap method at a 50% cutoff after 1000 iterations. Sequence divergences were quantified using the Kimura 2-parameter model in MEGA v. 7.

Museum collections

Abbreviations of the institutions from which specimens were examined are:

MCTP Museu de Ciências e Tecnologia da Pontifícia Universidade Católica do Rio Grande do Sul, Porto Alegre, Rio Grande do Sul, Brazil.

LMCI Laboratório de Morfologia e Comportamento de Insetos, Universidade Federal do Rio Grande do Sul, Porto Alegre, Rio Grande do Sul, Brazil.

Table 1. DNA barcode sequences of Sesiidae specimens used to infer the relationship of *Neosphecia cecidogena* (BOLD dataset DS-NEOSESII) within the tribe Melittiini.

Group	Genus	Species	Specimen voucher	Accession number	
				GenBank	**BOLD**
Ingroup	*Melittia*	*brabanti* Le Cerf, 1917	NS-RR051	JN304556	LNOUE514-11
		calabaza Duckworth & Eichlin, 1973	USNM ENT 00831286	MH592747	LNAUS302-12
		cucurbitae (Harris, 1828)	USNM ENT 00831289	MH592773	LNAUS305-12
		grandis (Strecker, 1881)	USNM ENT 00831295	MH592813	LNAUS310-12
		gloriosa Edwards, 1880	USNM ENT 00831292	MH592712	LNAUS308-12
		snowii Edwards, 1882	CSU-CPG-LEP001016	GU685631	ABLCU016-09
	Neosphecia	*cecidogena* sp. nov.	LMCI 263-33A	MK210242	MISA037-18
			LMCI 263-33B	MK210243	MISA038-18
			LMCI 263-33C	MK210244	MISA039-18
			LMCI 263-33D	MK210241	MISA040-18
Outgroup	*Carmenta*	*bassiformis* (Walker, 1856)	USNM ENT 00831360	MF124173	LNAUS376-12
	Synanthedon	*exitiosa* (Say, 1823)	06-JKA-0240	MH592851	LSEU240-06

Results

Molecular phylogeny

Sequencing of COI resulted in an average amplicon size of 633 bp. The aligned data matrix including all genera resulted in 668 characters. Of these, 189 (28%) were phylogenetically informative. Maximum likelihood analysis recovered an optimal ML tree = 5897 with nucleotide frequencies of A = 29.1%, C = 16.5%, G = 14.8%, and T = 39%. The four LMCI 263-33 specimens grouped in the COI tree as a single lineage, which was placed close to the genus *Melittia* (Fig. 1). *Melittia grandis* was the closest taxon (89% similarity) retrieved from online blast tools of Genbank and BOLD. Pairwise K2P distances estimated from the new taxon and *Melittia* ranged from 13% to 16% (*M. grandis* and *M. calabaza*, respectively) (Table 2). Divergence to the outgroup varied from 18% to 22%.
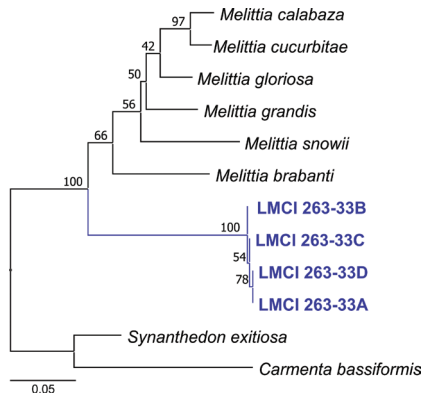

Figure 1. Maximum likelihood consensus tree of *Neosphecia cecidogena* (LMCI 263-33) and related Melittiini taxa. The monophyly and relationships were inferred based on 668 base pairs of cytochrome oxidase subunit gene I (COI) sequences (using six species of *Melittia*, one from *Synanthedon* and *Carmenta* from databases; the later genera of the related subfamily Synanthedonini were surveyed as outgroups). Numbers above branches indicate statistical support (bootstrap values).

Table 2. Genetic distance between *Neosphecia cecidogena* and other members of Melittini based on a 668 base pair sequence of the cytochrome oxidase I (COI) gene using the Kimura 2-parameter model. Comparisons with the outgroup Synanthedonini (*Synanthedon* and *Carmenta*) are indicated as well. Intragroup distances are shown in brackets.

	1	2	3	4	5	6	7	8	9
1. *Neosphecia cecidogena*	0.00								
2. *Melittia snowii*	0.14	–							
3. *Melittia brabanti*	0.15	0.11	–						
4. *Melittia calabaza*	0.13	0.08	0.11	–					
5. *Melittia gloriosa*	0.13	0.08	0.08	0.05	–				
6. *Melittia grandis*	0.12	0.09	0.09	0.06	0.06	–			
7. *Melittia cucurbitae*	0.14	0.09	0.10	0.02	0.05	0.06	–		
8. *Synanthedon exitiosa*	0.18	0.16	0.16	0.18	0.15	0.16	0.18	–	
9. *Carmenta bassiformis*	0.22	0.21	0.19	0.19	0.19	0.18	0.20	0.12	–

Taxonomy

Melittina **Le Cerf, 1917, stat. rev.**

"Genre *Melittina* gen. nov." Le Cerf, 1917: 239. Type species: *Melittina nigra* Le Cerf, 1917, by original designation.

Dalla Torre and Strand 1925: 136 (as a distinct genus); Zukowsky 1936: 1248 (as a distinct genus); Duckworth and Eichlin 1977a: (as a synonym of *Melittia*); Heppner and Duckworth 1981: 26 (as a synonym of *Melittia*); Eichlin and Duckworth 1988: 50 (as a synonym of *Melittia*); Pühringer and Kallies 2004: 15 (as a synonym of *Melittia*).

Diagnosis (after Le Cerf 1917: 239; pl. 477, fig. 3933). Head with antenna strongly clavate but without a hook apically, short, slightly shorter than half forewing; vertex with hair-like scales; proboscis well developed, functional. Legs with hind tibia and tarsus with slightly elongated scales. Forewing with transparent areas well developed; veins R_4 and R_5 long stalked; hindwing transparent, anal lobe undeveloped. Abdomen smooth scaled with anal tuft poorly developed.

    Differential diagnosis. Despite the fact that Le Cerf placed *Melittina* in the subfamily Aegeriinae sensu Le Cerf, 1917 [= Sesiini + Osminiini + Paranthrenini + Synanthedonini], by the venation of the hindwing this genus belongs to the tribe Melittiini. Superficially *Melittina* resembles the Afrotropical genus *Agriomelissa* Meyrick, 1931 (type species: *Agriomelissa gypsospora* Meyrick, 1931), but it can be differed by the practically undeveloped hair-like tuft of the hind leg (vs hair-like tuft of the hind leg well-developed in *Agriomelissa*) and undeveloped anal lobe of the hindwing (vs well-developed in the genus compared). *Melittina* can be easily distinguished from *Premelittia* and *Neosphecia* by the well-developed proboscis (proboscis undeveloped in both these compared genera) and shape of the antenna (antenna strongly clavate, short, slightly shorter than a half of forewing in *Melittina*, vs antenna fusiform, slightly longer than middle of forewing in *Premelittia* and *Neosphecia*). From all other genera in Melittiini, including species of New World so-called "Melittia" (Arita and Gorbunov 1996), *Melittina* differs by the shape of the antenna (antenna clavate with a hook apically in compared Melittiini) and by the undeveloped anal lobe of the hindwing (anal lobe of the hindwing well developed in all genera compared Melitiini).

    Composition. Presently this genus contains only a single species: *Melittina nigra* Le Cerf, 1916, stat. rev.

    Remarks. The genus *Melittina* was described by Le Cerf (1917) based on a single female specimen of the type species, *Melittina nigra* Le Cerf, 1917. Fortunately, the original description is rather complete and supplemented with a fairly accurate figure of the type species, *Melittina nigra* (Le Cerf 1917: 239; pl. 477, fig. 3933). They contain important characters (venation of the hindwing), which clearly put this genus in the tribe Melittiini. As we have mentioned above, this genus was synonymized with *Melittia* by Duckworth and Eichlin (1977a) without concrete arguments. After a careful re-examination of the original description (Le Cerf 1917: 239) and the figure of the type

species (Le Cerf 1917: pl. 477, fig. 3933), we conclude that *Melittina* is a distinct genus and restore it from synonymy with *Melittia*. Besides this, we also transfer *Melittia nigra* (Le Cerf, 1917) back to its original combination, *Melittina nigra* Le Cerf, 1917.

Premelittia Le Cerf, 1916, stat. rev.

"*Premelittia rufescens* ♀ nov. sp." — Le Cerf 1916: 9. Type species: *Premelittia rufescens* Le Cerf, 1916, by original designation.

Dalla Torre and Strand 1925: 136 (as a distinct genus); Zukowsky 1936: 1248 (as a distinct genus); Duckworth and Eichlin 1977a: (as a synonym of *Melittia*); Heppner and Duckworth 1981: 25 (as a synonym of *Melittia*); Eichlin and Duckworth 1988: 50 (as a synonym of *Melittia*); Špatenka et al. 1999: 89 (as a synonym of *Melittia*); Pühringer and Kallies 2004: 15 (as a synonym of *Melittia*).

Diagnosis (after Le Cerf 1916: pl. 375, fig. 3136, 1917: 234). Head with antenna fusiform without a hook distally, slightly longer than half forewing; vertex smooth scaled; proboscis undeveloped. Legs with hind tibia and tarsus smoothly scaled. Forewing with transparent areas well-developed; veins R_4 and R_5 short stalked; hindwing transparent, anal lobe very small. Abdomen smoothly scaled with anal tuft poorly developed.

Differential diagnosis. Without any doubt, by the venation of the hindwing this genus belongs to the tribe Melittiini. By the undeveloped proboscis and fusiform antenna this genus seems to be closely related to the genus *Neosphecia* Le Cerf, 1916, but it can be separated from it by the smoothly scaled vertex (vs vertex covered with hair-like scales in the compared genus) and venation of the forewing (veins R_4 and R_5 short stalked in *Premelittia* vs veins R_4 and R_5 separate basally in *Neosphecia*). It is easily distinguished from all other Melittiini, including species of New World so-called "Melittia" (Arita and Gorbunov 1996), by the smoothly scaled vertex (vs vertex with hair-like scales in all genera of Melittiini), form of the antenna (antenna clavate with a hooked apex in all other Melittiini), absence of the proboscis (proboscis well developed and functional in all other Melittiini), and form of the hind leg (with a tuft of hair-like scales in all other Melittiini).

Composition. Presently this genus contains the single species: *Premelittia rufescens* Le Cerf, 1916.

Remarks. The generic name *Premelittia* was first introduced in the legends of figures as the binominal "*Premelittia pufescens* nov. sp." (Le Cerf 1916: 9). The original description of this genus was published a year later (Le Cerf 1917: 234). Unfortunately, it was based on a single female specimen of the type species, *Premelittia pufescens* Le Cerf, 1916, but it is rather complete and contains important characters, which clearly separate this genus from the genus *Melittia*. This genus was also synonymized with *Melittia* by Duckworth and Eichlin (1977a) without concrete arguments. After a careful re-examination of the description (Le Cerf 1917: 234) and the figure of the type species (Le Cerf 1916: pl. 375, fig. 3136) we conclude that *Premelittia* is a distinct

genus of the tribe Melittiini and restore it from synonymy with *Melittia*. Besides this, we also transfer *Melittia rufescens* (Le Cerf, 1916) back to its original combination, *Premelittia rufescens* Le Cerf, 1916.

Neosphecia Le Cerf, 1916, stat. rev.

"*Neosphecia combusta* ♀ nov. sp." — Le Cerf 1916: 9. Type species: *Neosphecia combusta* Le Cerf, 1916, by original designation.

Dalla Torre, Strand 1925: 136 (as a distinct genus); Zukowsky 1936: 1247 (as a distinct genus); Duckworth and Eichlin 1977a (as a synonym of *Melittia*); Heppner and Duckworth 1981: 26 (as a synonym of *Melittia*); Eichlin and Duckworth 1988: 50 (as a synonym of *Melittia*); Pühringer and Kallies 2004: 15 (as a synonym of *Melittia*).

Diagnosis (after Le Cerf 1916: pl. 375, fig. 3137, 1917: 236). Head relatively broad; antenna fusiform without a hook distally, slightly longer than half forewing; vertex covered with hair-like scales; proboscis undeveloped. Legs with hind tibia and tarsus smoothly scaled. Forewing with transparent areas undeveloped or very small; veins R_4 and R_5 separate basally; hindwing transparent, anal lobe undeveloped or extremely small. Abdomen smooth scaled with anal tuft poorly developed.

Differential diagnosis. Like the two previous taxa, on the basis of the venation of the hindwing this genus belongs to the tribe Melittiini. By the fusiform antenna and undeveloped proboscis this genus is closely related to the genus *Premelittia* Le Cerf, 1916, stat. rev., but it can be distinguished the forewing venation (veins R_4 and R_5 shortly stalked in *Premelittia* vs veins R_4 and R_5 separate basally in *Neosphecia*). *Neosphecia* differs from *Melittina* by the undeveloped proboscis (well developed and functional in the compared genus), shape of the antenna (strongly clavate and short, not reaching the middle of the forewing in *Melittina* vs fusiform, long, slightly longer than half forewing in *Neosphecia*), and the venation of the forewing (veins R_4 and R_5 long stalked in *Melittina* vs veins R_4 and R_5 separate basally in *Neosphecia*). From all other genera of the Melittiini, including New World so-called "Melittia" (Arita and Gorbunov 1996), it differs by the shape of the antenna (clavate with a hook apically in all other Melittiini vs fusiform in *Neosphecia*), completely undeveloped proboscis (vs well developed in all other Melittiini), and venation of the forewing (veins R_4 and R_5 separate basally in *Neosphecia* vs veins R_4 and R_5 stalked in all genera of Melittiini).

Composition. Currently, we include two species in this genus: *Neosphecia combusta* Le Cerf, 1916 (type species) and *N. cecidogena* sp. nov.

Remarks. Like the genus *Premelittia* (see above), the genus name *Neosphecia* was firstly introduced in the legends of the figures as the binomen "*Neosphecia combusta* nov. sp." (Le Cerf 1916: 9). The original description of this genus was published a year later (Le Cerf 1917: 236). Unfortunately, it was based on a single female specimen of the type species, *Neosphecia combusta* Le Cerf, 1916, but it is rather complete and contains

important characters, which clearly separate this genus from *Melittia*. This genus was also synonymized with *Melittia* by Duckworth and Eichlin (1977a) without concrete arguments, as with the two previous genera. After careful re-examination of the description (Le Cerf 1917: 236) and the figure of the type species (Le Cerf 1916: pl. 375, fig. 3137) we conclude that *Neosphecia* is a distinct genus of the tribe Melittiini and restore it from synonymy with *Melittia*. Besides this, we also transfer *Mellittia combusta* (Le Cerf, 1916) back to its original combination, *Neosphecia combusta* Le Cerf, 1916.

Neosphecia cecidogena Moreira & Gorbunov, sp. nov.
http://zoobank.org/116E59F8-44F9-4F1A-9CAD-6C32C068E4E4
Figs 2–9

Description. Male (holotype) (Fig. 2A–D). Alar expanse 23.1 mm; body length 10.8 mm; forewing 10.5 mm; antenna 5.8 mm.

Head with antenna dark brown to black dorso-externally and yellow ventro-externally; scapus yellow and narrowly lined with dark brown dorsally; frons entirely dark brown with purple-blue sheen; vertex black with dark-blue sheen and an admixture of individual white and yellow hair-like scales; proboscis completely undeveloped; labial palpus dark brown to black with an admixture of yellow scales dorsally and white, long, hair-like scales ventrally in distal half; occipital black with a few white scales dorsally.

Thorax with patagia dark brown to black with a small, yellow, transverse spot anterior-ventrally; tegula dark brown to black with yellow, hair-like scales distally; mesothorax entirely dark brown to black; metathorax dark brown to black with two tufts of yellow, hair-like scales laterally; thorax laterally dark gray-brown with bronze-violet sheen. Legs with neck plate dark brown to black; fore coxa dark brown to black with a narrow, yellow exterior margin; hind tibia dark yellow with an admixture of black elongated scales on basal half; spurs dark yellow with golden sheen and a few black scales exterior-basally; hind tarsus dark yellow with a dense admixture of elongated black scales dorso-externally. Forewing: dorsally dark brown with dark-violet sheen and an admixture of individual yellow-orange scales, more dense distally and at anal margin; transparent areas present but very small: anterior and posterior ones very narrow, external one divided into two very short cells; cilia dark brown to black with dark violet-purple sheen. Hindwing transparent; veins broadly covered with dark brown and a few yellow-orange scales; discal spot undeveloped; outer margin about as broad as cilia, dark yellow and narrowly dark brown distally; cilia dark brown with dark violet sheen.

Abdomen including anal tuft black with dark blue sheen and a few yellow scales at base of second tergite.

Male genitalia (Fig. 3A–D). Tegumen-uncus complex relatively broad; uncus bilobed distally, with a relatively large semi-oval plate of strong, short, pointed setae internally on each side distally; gnathos rather small, membranous, with a small, narrow, slightly sclerotized plate medio-basally; valva broad, subrectangular, with dorsal margin
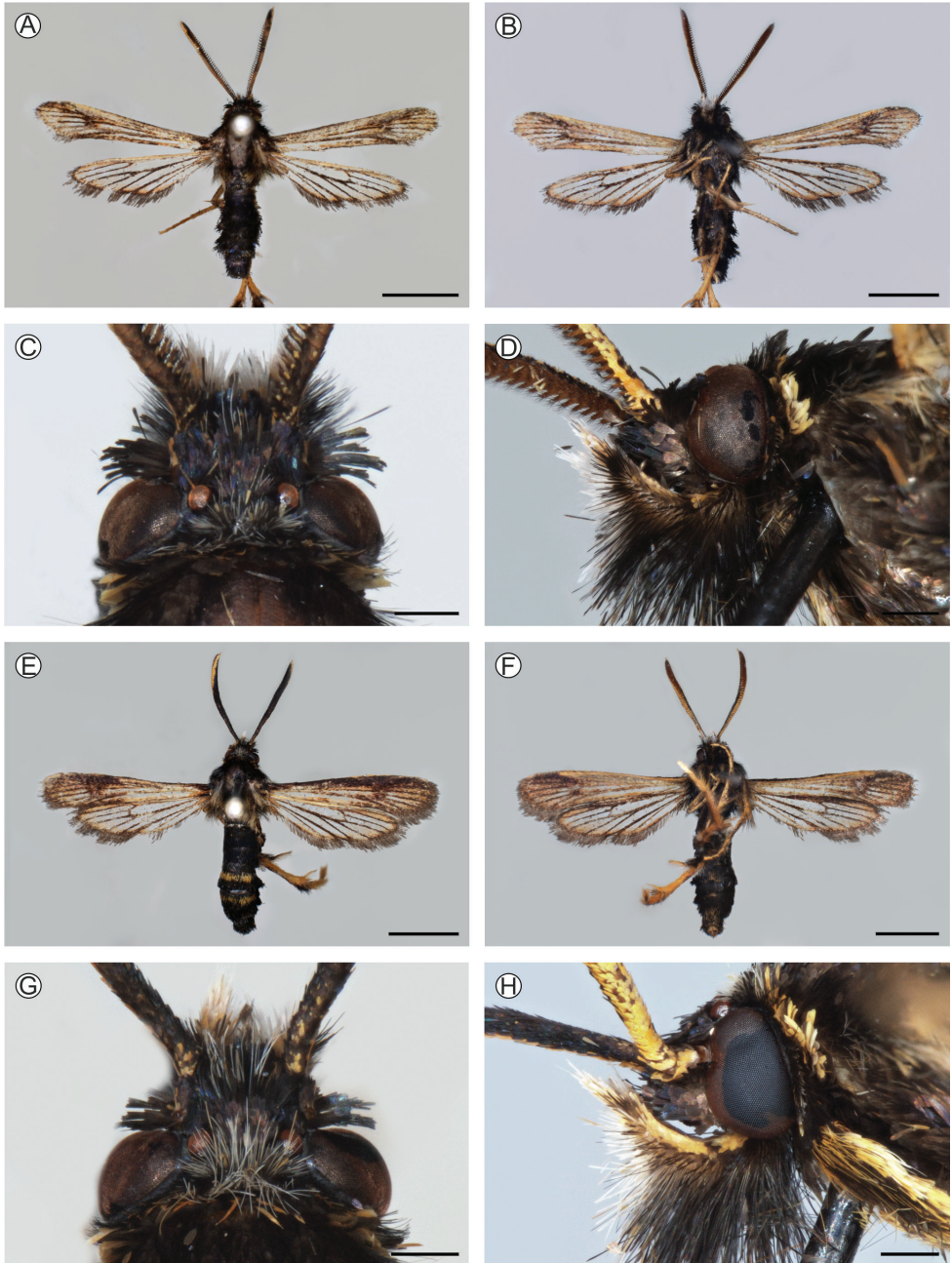
Figure 2. Pinned-dried *Neosphecia cecidogena* adults, with corresponding heads in detail **A–D** male (holotype, LMCI 319-83) **E–H** female (paratype, LMCI 319-85); dorsal (**A, C, E, G**), ventral (**B, F**) and lateral (**D, H**) views. Scale bars = 0.5mm (**C, D, G, H**); 4mm (**A, B, E, F**).
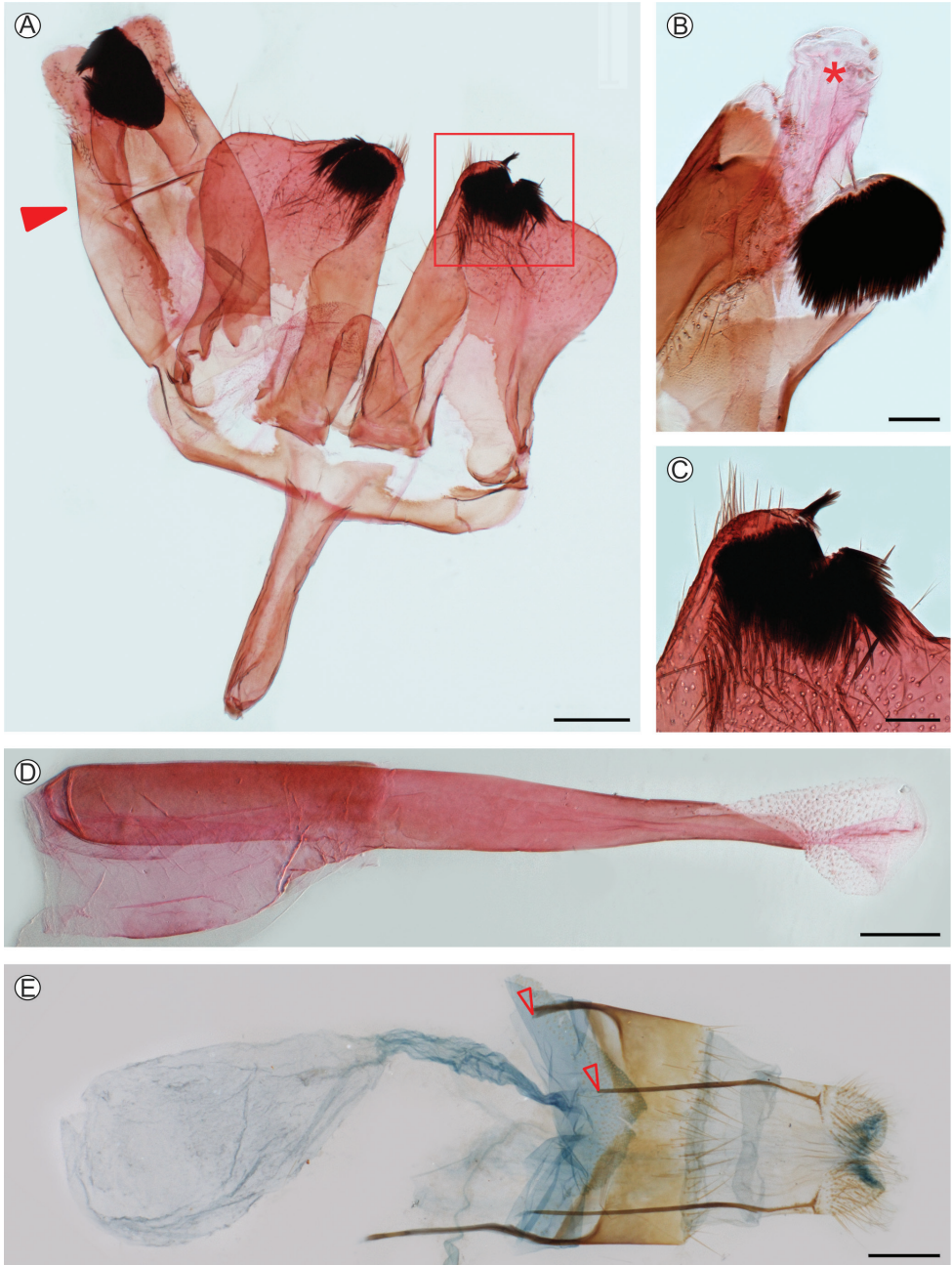
Figure 3. *Neosphecia cecidogena* genitalia morphology under light microscopy **A** male (LMCI 319-84), general, ventral view (unrolled preparation, sensu Pitkin 1986; aedeagus omitted) **B** right half of the tegumen-uncus complex, mesal (pointed by closed arrow in **A** asterisk indicates anal tube) **C** distal portion of left valva in detail (enlarged area marked with a rectangle in **A**), ventral **D** aedeagus, lateral **E** female (LMCI 306-19), general, ventral (open arrow points to missing distal portion of the right anterior apophysis, broken off during preparation). Scale bars = 0.1 mm (**B–D**); 0.3 mm (**A, E**).
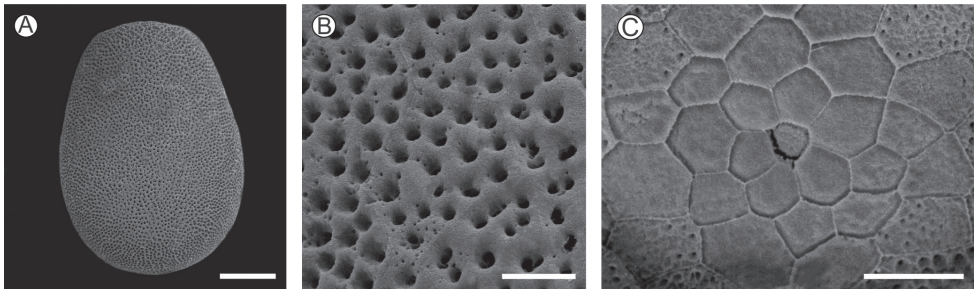
Figure 4. Egg of *Neosphecia cecidogena* under scanning electron microscopy **A** general view **B** chorion in detail **C** micropyle area. Scale bars: 100, 15, 20 μm, respectively.

concave mesally and rounded distally; distal field of setae not developed; setae of medial field restricted to a path on ventro-distal margin; ventral lobe relatively broad on 2/3 basal section, narrowed distally; saccus narrow, ca 0.7 valva in length; aedeagus tubiform, narrowed distally, ca 1.3× valva length; vesica with numerous minute cornuti.

Female (paratype) (Fig. 2E–H). Antenna with more broad yellow stripe ventro-externally; vertex with more numerous white hair-like scales; labial palpus with more numerous yellow scales dorsally; patagia with more yellow scales anteriorly; legs with more numerous yellow scales; both tergites 4 and 5 with a sparse, dark yellow stripe medially. Color patterns otherwise as in male.

Female genitalia (Fig. 3E). Papillae anales membranous, covered with short and a few long setae; eighth tergite relatively broad with relatively long setae distally; posterior apophyses about 1.2× longer than anterior apophyses; ostium bursae opening near posterior margin of sternite seven, slightly funnel-shaped; antrum membranous, narrow and short; ductus bursae narrow, slightly broadened medially, about as long as anterior apophyses; corpus bursae membranous, elongate-ovoid, ca 1.5× as long as anterior apophyses, without signum.

Individual variability. The type series practically invariable in individual size and in the coloration of various parts of the body and wings.

Differential diagnosis. This new species looks like *Melittina nigra* Le Cerf, 1917 (type locality: "Brésil, ex E. Le Moult, Coll. F. Le Cerf"; Le Cerf 1917: 240), from which it can be easily distinguished by the absence of the proboscis (well developed in *M. nigra*) and poorly developed transparent areas of the forewing (large, well developed, external transparent area divided into seven cells between veins R$_3$–CuA$_2$ in *M. nigra*; compare Fig. 2 with Le Cerf 1917: pl. 477, fig. 3933). From *N. combusta* Le Cerf, 1916 (type locality: "Bolivie, Cochabamba, Yunga del Espiritu-Santo; ex P. Germain (1888–1889)"; Le Cerf 1916: 9) this new species differs by the presence of transparent areas of the forewing (completely opaque in *N. combusta*), by the coloration of the abdomen (dorsally tergite 3 with a narrow yellow stripe anteriorly in *N. combusta*), and by the coloration of the hind tarsus (dark brown to black in the compared species; compare Fig. 2 with Le Cerf 1916: pl. 375, fig. 3137). *Neosphecia cecidogena* sp. nov. cannot be confused with any other Melittiini of the Neotropical region by its generic characters.
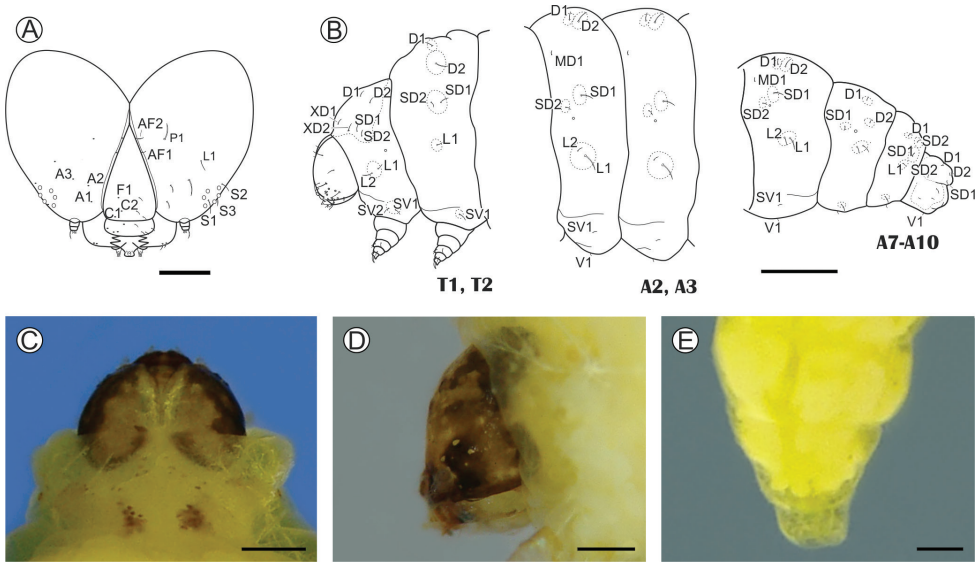
Figure 5. *Neosphecia cecidogena* last larval instar under light microscopy **A** cephalic chaetotaxy, frontal view **B** thoracic and abdominal chaetotaxy, lateral **C, D** head in detail, anterior and lateral, respectively. **E** last abdominal segments in detail, dorsal. Scale bars: 200 μm (**A, D**); 0.4 mm (**E**); 0.5 mm (**C**); 1 mm (**B**).

Etymology. The species name, an adjective, is derived from a composition between the Portuguese "Cecidia" (a gall) and the suffix *gena* (derived from the Latin verb "gigno", be born). Thus, the epithet refers to the cecidogenous habit of the new described clearwing moth.

Material examined. All specimens were either dissected or reared from galls associated with *Cayaponia pilosa* (Vell.) Cogn. (Cucurbitaceae), from the Centro de Pesquisas e Conservação da Natureza Pró-Mata (CPCN Pró-Mata, 29°28'36"S, 50°10'01"W, São Francisco de Paula Municipality, Rio Grande do Sul State (RS), Brazil; 04–06. IV.2014, G.R.P. Moreira & R. Brito legs., LMCI 263; 21–24.VI.2016, G.R.P. Moreira, R. Brito, J. Fochezato legs, LMCI 306; 28–30.VI.2017, G.R.P. Moreira and J. Fochezato legs., LMCI 319; 01–02.VIII.2017, G.R.P. Moreira and J. Fochezato, LMCI 320; 20–23.III.2018, G.R.P. Moreira, V. Becker, A. Moser, R. Brito & J. Fochezato legs., LMCI 326.

Type material (all pinned-dried adults). *Holotype*: ♂ LMCI 319-83; *Paratypes*: 1♂, LMCI 319-84, with genitalia preparation on slide; 1♀, LMCI 263-52, with genitalia preparation on slide; 1♀, LMCI 319-82, donated to MCTP (64103); 1♀, LMCI 319-85.

Non-type material. Adults (pinned-dried): 1♂, with genitalia preparation on slide, LMCI 319-81; 1♀, with genitalia preparation on slide, LMCI 306-19. Immature stages (fixed in Dietrich's fluid and preserved in 70% ethanol): ca 30 eggs, dissected from female during genitalia preparation, LMCI 263-52b; 2 last instar larvae (LMCI 263-49 and 326-148); 2 pupae (LMCI 263-51 and 309-02); 12 dis-

sected, mature galls (LMCI 263-35); 5 empty, senescent galls with pupal exuviae (LMCI 319-86). Also, 6 last instar larvae, preserved in 100% ethanol at –20 °C, used for DNA extraction (4 specimens, LMCI 263-33; 2 specimens, 326-146), and 2 last instar larvae preparations, mounted in Canada balsam on a slide (LMCI 263-42, 43).

Description of immature stages. Eggs (Fig. 4): light brown, obovoid, with the anterior end slightly flattened; maximum length (average ± standard deviation) = 0.05 ± 0.01 mm, maximum width = 0.39 ± 0.01 mm, *n* = 6. Surface of chorion with faint carenae, delimiting irregular, mostly hexagonal cells and minutely pitted, forming a continuous meshwork-like plastron (sensu Hinton 1981), except for the anterior end where corresponding holes are sparse. Micropylar area on anterior pole, consisting of a subtrapezoidal indentation in the center, which is surrounded by a rosette of about 20 subpentagonal cells that increase in size centrifugally.

Last instar larva (Figs 5, 6, 9D): head capsule width (average ± standard deviation) = 2.39 ± 0.06 mm; body length = 10.34 ±2.45 mm, *n* = 4. Body light yellow; head tan-brown, with a clearer, dorsal, irregularly shaped area, covering the frontoclypeus, adfrontal area and adjacent portions; this area projects latero-posteriorly, ending close to the posterior margin of the head. Prothoracic shield slightly melanized except for a pair of faint patches formed by pigmented spots, located mesally on posterior margin. Anal plate and prothoracic legs not melanized (Figs 5C, D, 9D). Setae mostly reduced in size, on pinacula (Fig. 6G, K) that are inconspicuous under light microscopy (same color as body) (Fig. 5C–E). Head: wider than long, with lateral margins convex, slightly hypognathus; frontoclypeus subtriangular, higher than wide, extending to three-quarters of epicranial notch; ecdysial line weakly defined, reaching close to epicranial notch and delimiting a narrow adfrontal area (Fig. 5A–D). Six poorly developed, laterally located stemmata (Fig. 6A, C). Antennae (Fig. 6B) two-segmented; basal segment with four sensilla on distal margin, two short and stout, one minute and one long, ca 10× the length of the others; distal segment much thinner and shorter, bearing three short sensilla on distal margin. Labrum slightly bilobed, with three pairs of setae laterally on distal margin, and one pair centrally on proximal base. Mandible well developed, with four cusps along distal margin and two small setae mesally on external surface. Maxilla (Fig. 6D, E) with palpus and galea well developed. Spinneret short, conical (Fig. 6D, E). Labial palpus (Fig. 6E) bisegmented; distal segment thinner and shorter, with well-developed apical seta. Thorax (T) and abdomen (A): integument covered with microtrichia, except on pinacula (Fig. 6G, K, L). Thoracic legs well developed, with stout tarsal claw (Fig. 6H, I). Circular spiracles with slightly elevated peritreme, laterally on T1, A1–8. Abdominal pseudopodia absent, replaced by pairs of ambulatory calli (Fig. 6L) on A3–6 and A10, without crochets.

Chaetotaxy (Fig. 5A, B). Head with F unisetose; C group bisetose; A group trisetose, forming an obtuse triangle with A3 closest to stemmata; AF group bisetose; P unisetose; Md group absent; L unisetose; S trisetose; SS trisetose (not drawn). A3 and P1 about equal in length, longest setae on head. T1 with D group bisetose; XD bise-

tose; SD bisetose; L bisetose; SV bisetose. T2–3 with D group bisetose; SD unisetose; L1 unisetose; SV unisetose. A1–7 with D group bisetose; MD unisetose; SD bisetose; L bisetose; SV and V unisetose. A8 with D group bisetose; MD unisetose; SD1 unisetose; L bisetose; V unisetose. A9 with D group unisetose, SD bisetose; L unisetose. A10 with D group bisetose; SD bisetose; V unisetose, and three pairs of unnamed setae on lateral of calli.

Pupa (Figs 7, 8). Body length (average ± standard deviation) = 11.52 ± 0.67 mm; n = 5. Yellowish brown, becoming dark brown near adult emergence (Fig. 7C). Head with stout, short, bow-shaped frontal gall-cutter process in dorsal view (Figs 7A, C), which is continued latero-caudally up to eye margin by slightly elevated ridges that limit depressions on frons under lateral view. Vertex with two pairs of small setae laterally. Clypeus little pronounced, with one pair of small setae laterally; labrum short, slightly bilobed (Fig. 8B). Antennae clubbed at the end, reaching anterior portion of third abdominal segment. Mandibles small, rounded, meso-anterior to the eyes. Maxillary palpi small, rounded, latero-posteriorly to the eyes. Proboscis shorter than and laterally margined by the prothoracic legs; galea converging mesally along the second half portion. Labial palpi contiguous on the center, extending to half length of the galea. Pronotum fairly developed, bearing a central ridge that extends caudally along the meso- and metanotum. Hindwings concealed by forewings, both extending to sixth abdominal segment. Protho-, meso-, and methatoracic legs reaching the second, fifth, and seventh abdominal segments, respectively. Thoracic and abdominal setae extremely reduced in size: one pair, latero-dorsally, on meso- and metathorax, and A2–A9; another pair, subspiracular, on A2–A7. Abdominal spiracles rounded, with slightly elevated peritreme (Fig. 8E), laterally on A2–A7; spiracle on A8 closed. Basal and caudal transverse rows of spines (Figs 8D, F) present from abdominal segments two to seven on males; only one row of such spines is found on segment seven of females, and also on segments eight and nine on both sexes. Last abdominal segment with four pairs of stout, scaly spines on caudal margin: two pairs in latero-dorsal and two pairs in latero-ventral position (Fig. 8H, G).

Distribution. This new species is known only from the type locality, the humid forest portions of the CPCN Pró-Mata, São Francisco de Paula municipality, Rio Grande do Sul State, Brazil.

Host plant. Galls of *N. cecidogena* have been found only in association with *Cayaponia pilosa* (Vell.) Cogn. (Cucurbitaceae), which is distributed in the ombrophilous Atlantic Forest of southern Brazil (from Minas Gerais to Rio Grande do Sul State) (Gomes-Klein et al. 2015). Biology and natural history of this cucurbit are poorly known. It is a herbaceous, prehensile vine (Fig. 9A), which bears pairs of forked, axillary tendrils, simple, alternate leaves with lamina that may vary from entire, to three to five lobed; flowers are solitary, axillary, and with penduncles varying from 7 to 9 cm long; fruits are ellipsoid and ca 2 cm in length, which are initially green (Fig. 9B) but changing to wine-colored when mature (Porto 1974; Villagra and Romaniuc Neto 2011). At the type locality, *C. pilosa* plants are found scattered on forest borders, particularly along trails.
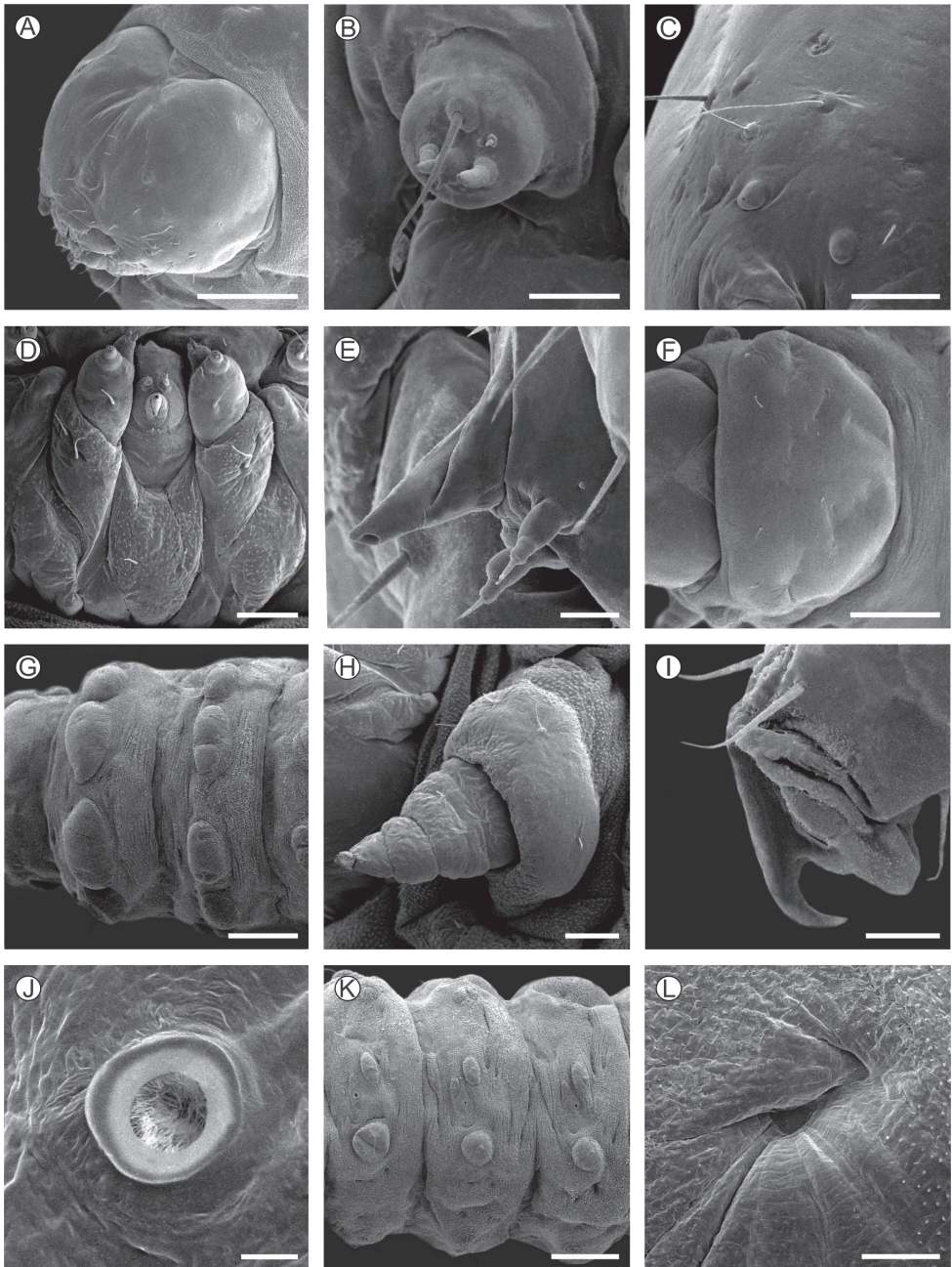
Figure 6. Morphology of *Neosphecia cecidogena* last larval instar under scanning electron microscopy **A** head, antero-dorsal view **B** antenna, anterior **C** stemmata, lateral **D** maxillae and labium, ventral **E** spineret, lateral **F** prothoracic shield, dorsal **G** meso- and metathoracic segments, dorsal **H** prothoracic leg, posterior **I** tarsal claw in detail, posterior **J** prothoracic spiracle, lateral **K** second to fourth abdominal segments, lateral **L** abdominal callus in detail, ventral. Scale bars: 20 μm (**E, I, J**); 40 μm (**B**), 100 μm (**C, D, H, L**); 0.5 mm (**A, G, K**).
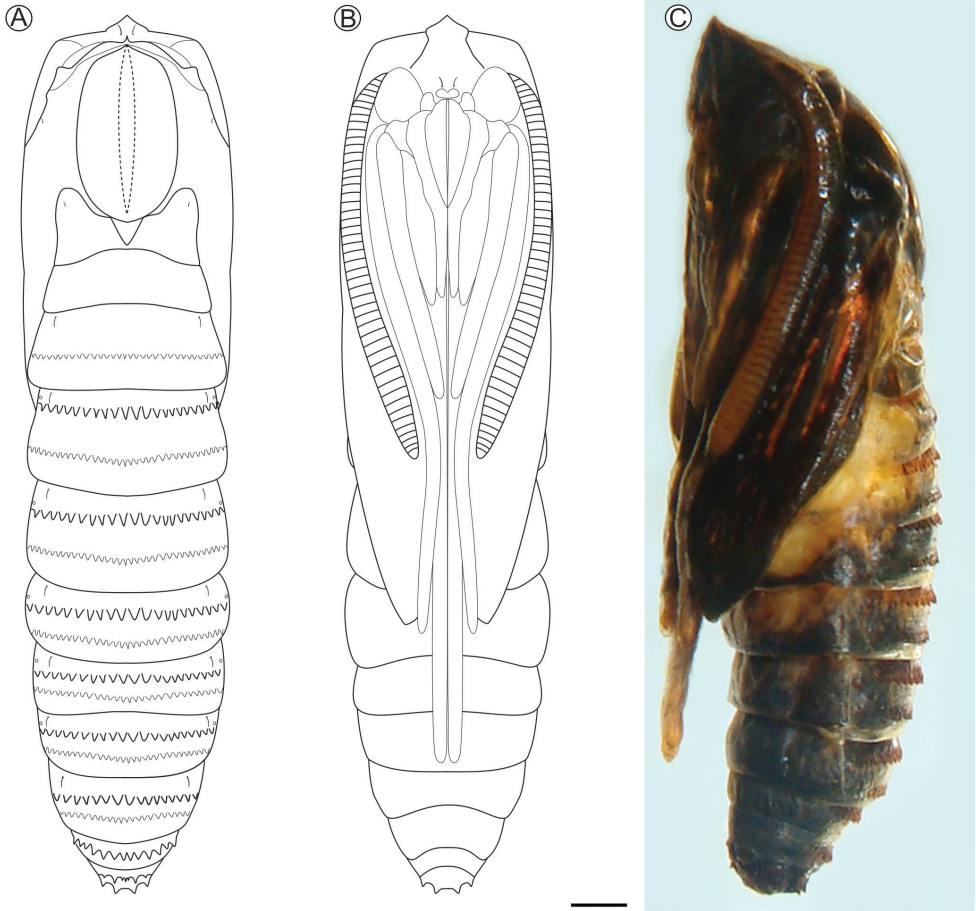
Figure 7. *Neosphecia cecidogena* pupa under light microscopy, in dorsal (**A**), ventral (**B**) and lateral (**C**) views. Scale bar:1 mm.

Natural history. The unilocular, cylindrical galls of *N. cecidogena* measure on average (± standard deviation) 3.44 ± 2.51 cm (*n* = 9) in length when mature. They appear individually and from the beginning develop externally on axillary buds of *C. pilosa* vines. Contrary to the oval *C. pilosa* fruits (Fig. 9B), *N. cecidogena* galls are not pedunculate (Fig. 9C). They are green during development and later turn dark brown with the progress of senescence (Fig. 9I). The internal chamber is filled with a yellowish nutritive tissue (Fig. 9D, E) which is consumed by larvae during development. With the end of feeding, the last larval instar builds a blackish, circular operculum (Fig. 9F–H) that splits the chamber into two sections, one distal, where the frass is deposited, and one basal, which has the distal portion of the wall lined with light-gray silk (Fig. 9E) and where pupation occurs. Achieving maturation, the wall of the gall hardens with the exception of the distal, pointed end, which remains thin and soft and through
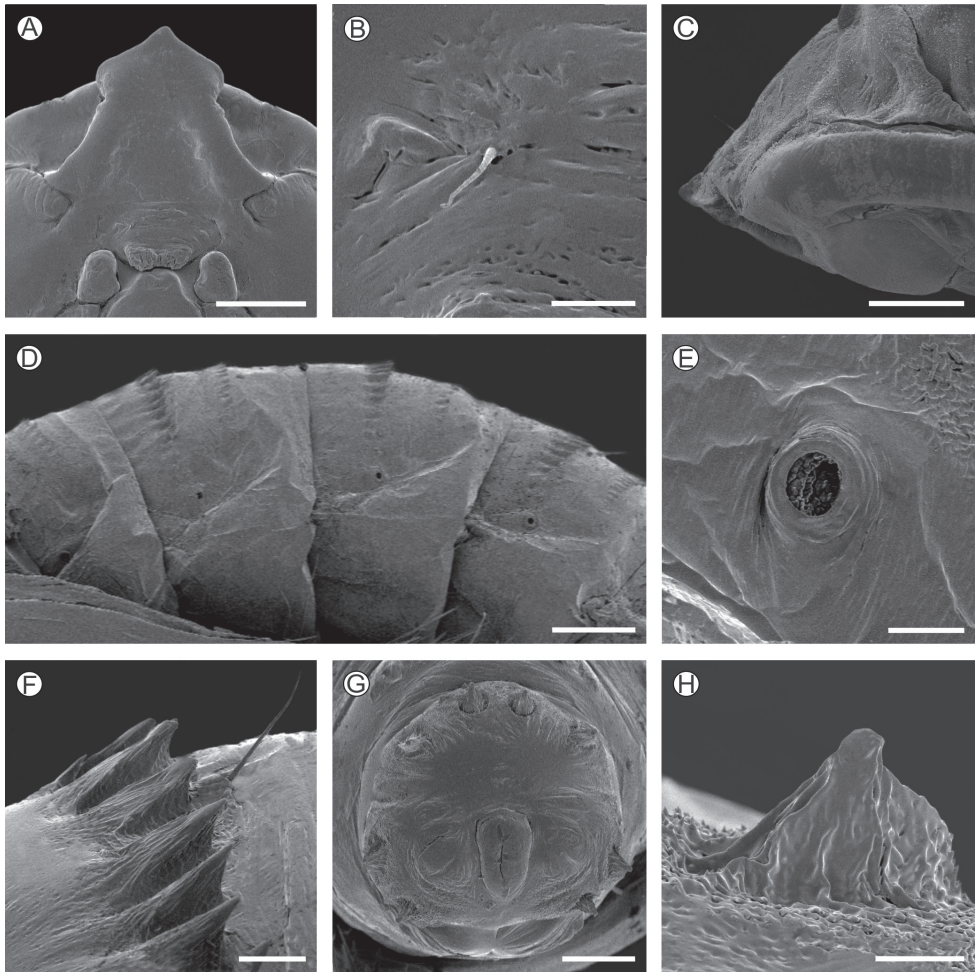
Figure 8. *Neosphecia cecidogena* pupal morphology under scanning electron microscopy **A, C** head, ventral and lateral views, respectively **B** clipeal seta in detail **D** third to sixth abdominal segments, lateral **E** fourth abdominal spiracle, lateral **F** spines of fourth abdominal segment in detail, lateral **G** last abdominal segments, posterior **H** spine of last abdominal segment, mesal. Scale bars: 40 μm (**H**); 50 μm (**B, E**); 100 μm (**F**); 200 μm (**C, G**); 0.4 mm (**A**); 0.5 mm (**D**), respectively.

which adult emergence occurs (Fig. 9I). During emergence, with the action of the frontal process and body contortions, the pupa detaches the operculum and ruptures the distal, weaker portion of the wall. By continuing these movements and anchoring the body laterally with its abdominal spines, the pupa pushes itself partially out of the gall. During this process, the anterior portion of the exuviae is split, allowing adult emergence. In all cases of adult emergence under laboratory conditions, the anterior part of the pupal exuviae (head and thorax) was found protruding to the outside (Fig. 9J), while the posterior third remained in the chamber.
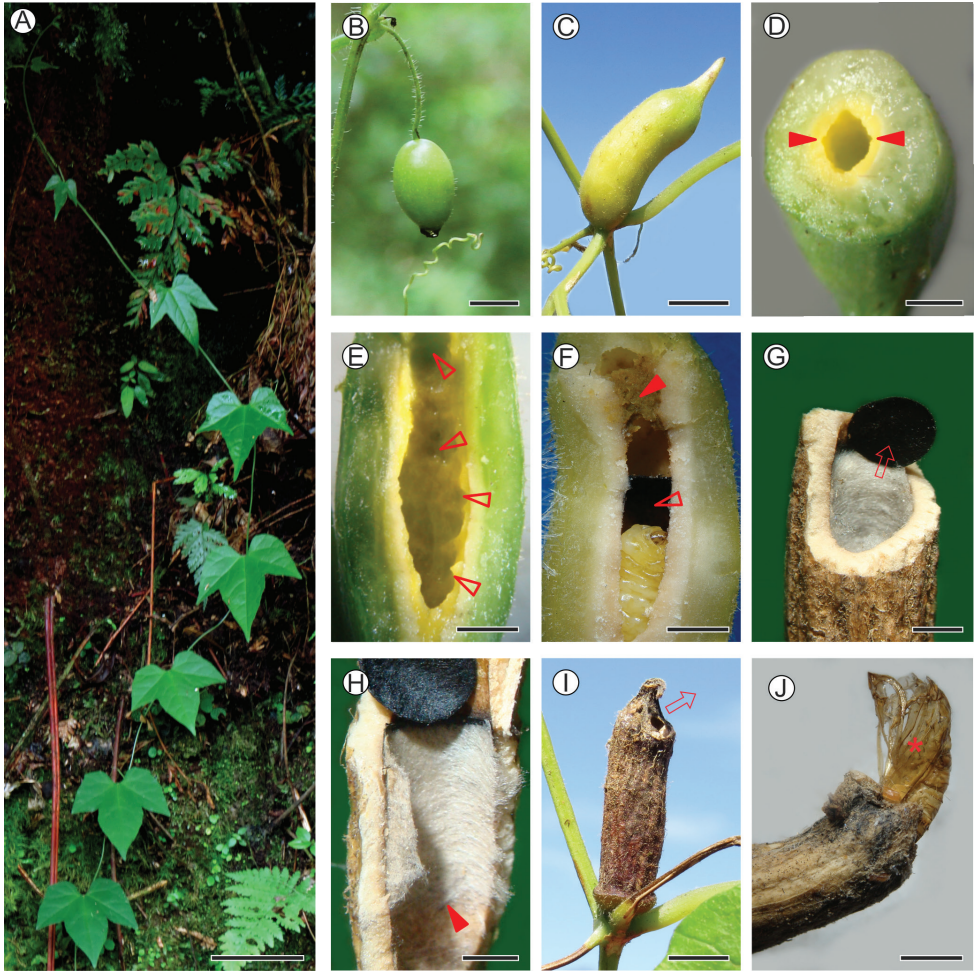
Figure 9. Natural history of *Neosphecia cecidogena* on *Cayaponia pilosa* **A** host plant at the type locality **B** young fruit, lateral **C** fully developed gall on axillary region, lateral **D, E** basal portion of median-sized gall sectioned transversally, showing yellowish nutritive tissue (pointed by closed arrows) (**D**) longitudinally sectioned medium-sized galls, showing larval feeding scars on nutritive tissue (some are indicated by open arrows) **F** longitudinally sectioned mature gall, with last instar larva (asterisk) inside (closed and open arrows indicate frass and operculum, respectively) **G** transversally sectioned, senescent gall showing detached operculum (indicated by seta) and internal wall covered by silk **H** longitudinally sectioned senescent gall showing internal silk covering (proximal limit pointed by closed arrow) **I** senescent, overwintering gall, lateral (seta indicates direction of adult emergence) **J** distal portion of senescent gall, showing pupal exuvium left partially protruded after adult emergence (marked with asterisk). Scale bars: 2 mm (**G, H**); 3mm (**D–F**); 4mm (**J**); 6 mm (**I**); 9 mm (**C**); 1 cm (**B**); 9 cm (**A**).

A few *C. pilosa* plants have been found at the type locality bearing from one to five *N. cecidogena* galls per plant. Field collections carried out during five consecutive years at the type locality indicated that it is a univoltine species, larvae growing during the summer

when young galls are seen on *C. pilosa* vines. Fully developed galls containing last instar larvae have been collected mainly during autumn. When brought to the laboratory, these remained larvae during the winter, apparently in a diapause state. Pupation in this case occurred during the first week of September and emergence a few days later during early spring. The absence of a proboscis suggests that adults of *N. cecidogena* are not active feeders. The appearance of a substantial number of corionated eggs in the abdomen of dissected females shortly after emergence in the laboratory indicates that reproduction occurs early in adult life, and thus, adults may not live long.

Discussion

A few molecular phylogenies have been proposed for Sesiidae, particularly including Melittini (McKern et al. 2008; Hans et al. 2012; Lait and Hebert 2018), which present a controversial relationship within Sesiinae, placed in the basal position. *Melittia* is the main representative of the tribe so far sequenced, and in this study presented high internal divergence (6–11%), which suggests that distinct lineages have been lumped into this genus. This seems to hold true particularly for the "New World" lineages that were separated from *Melittia* based on genitalia (Arita and Gorbunov 1996). Molecular data presented here gave further support in the sense that the genus *Neosphecia* is closely related to *Melittia*, from which COI sequences of *N. cecidogena* diverged ca 13%. Corresponding divergences between the genera *Synanthedon* and *Carmenta* were 18 and 22%, respectively. Unfortunately, DNA sequences are not available for the genera *Premelittia* and *Melittina*, which precludes further comparison within the Neotropical Melitiini, whose phylogenetic relationships are still controversial, as already mentioned.

Premelittia and *Melittina* are poorly known monotypic genera, with data available restricted to the original taxonomic description, and observations on morphology made *a posteriori* based also on the adult female holotypes only by Arita and Gorbunov (1996). According to these authors, the Nearctic and Neotropical Melittini as a whole are in need of revision, and thus, the taxonomic positioning of these groups within the family is still pending. Results presented in the present study demonstrate that variation among the immature stages of Sesiidae, especially the larva and its feeding habits, is broader than previously thought and should be taken into account in future phylogenetic studies involving these lineages. We demonstrate clearly that not only internal damage related to mobile (borer) activity is to be found among clearwing moths, but also typical, external galls containing differentiated nutritive tissues as induced by *N. cecidogena*.

Sesiid eggs have been described as ventrally flat, being laid with the longitudinal axis parallel to the substrate and having the lower surface less ornamented than the upper one (Duckworth and Eichlin 1974; Eichlin and Passoa 1983; Eichlin 1995; Puchi 2005). This may not the case in *N. cecidogena*, a situation that should be better examined under natural conditions. Eggs dissected in this study were transversally nearly elliptical and uniformly covered by a continuous plastron, with the exception of the anterior pole where the micropyles are located, as already mentioned. We could not

identify differentiated aeropyles on the chorion surface of *N. cecidogena* eggs, which are supposedly located underneath such a plastron.

Unlike larvae of other sesiids that have pseudopodia bearing crochets (Heppner and Duckworth 1981; Heppner 1987), those of *N. cecidogena* lack such structures. It is still uncertain whether this reduction is unique to *Neosphecia* species. It may represent an evolutionary loss, associated with the stationary way of life within a gall. This hypothesis should be tested further by comparing this species with other representatives including those having similar cecidogenous habit (sessile, confined life style) where corresponding convergences to *N. cecidogena* is expected, and to different life habits like borers (more mobile life style), where pseudopodia bearing crochets are expected to be found. This could be also the case of setae that are reduced in size and in number, and which are tentatively named here. For example, P and Md groups are well developed in the head of other sesiids (e.g. Eichlin and Passoa 1983) but absent in *N. cecidogena,* except for P1. Heppner and Duckworth (1981) and Heppner (1987) stated that the L group is trisetose on the protorax of sesiids in general, which is not the case in *N. cecidogena* where this group is bisetose, also on abdominal segments A1–8. Furthermore, we could not find any trace of SV2 setae on *N. cecidogena*, except for the prothoracic segment; the SV3 and MV setae were not found.

Pupae of *N. cecidogena* showed the general integument morphology usually found in the family (Patočka and Turčani 2005). Pads of galea are well differentiated externally on *N. cecidogena* pupa, but contrary to other buccal appendages that are filled with the corresponding adult buccal appendages, they are empty later in pupal development, thus suggesting that the proboscis is in fact being lost during that ontogenetic stage in this species. Additional differences exist in the pupal stage of *N. cecidogena* in relation to the absence of a differentiated frontal process on the head, which is well developed and bow-shaped, for example, in *Melittia gilberti* Eichlin (Eichlin 1992). It also slightly differs regarding the shape, size, and arrangement of A10 spines, compared for example to those described for *Carmenta* species (Eichlin and Passoa 1983; Puchi 2005). Most sesiids pupate internally, within the gallery opened by larval feeding (e.g. Bruch 1941; Duckworth and Eichlin 1974; Eichlin 1995; Harms and Aiello 1995; Newland and Sawyer 2014). In this case, the larva may either tunnel to the plant surface prior to pupation, leaving a thin exterior covering through which emergence occurs later (Duckworth and Eichlin 1974), or build a cocoon within the feeding site that is surrounded by the frass (e.g. Lopes et al. 2003). However, other species leave the feeding site later in development, weaving a silk cocoon in the soil within which pupation occurs (e.g. Heppner and Duckworth 1981; Gorbunov 2015). In *N. cecidogena* pupation happens inside the gall, which is used as the pupal chamber after being closed distally with a silk-made operculum and deprived of frasses, and thus without tunneling or building a typical cocoon. Variation in this life history trait among other sesiid lineages should be also evaluated further from a phylogenetic perspective.

Finally, the galls described here appeared figured twice in association with *Cayaponia* spp. in a survey carried out at the type locality by Toma and Mendonça (2013). The one in early development stage that was illustrated by them (green color;

Toma and Mendonça 2013: fig. 1P) had the induction attributed to an unidentified species of Coleoptera, which resulted from misidentification. The one that appears in a senescent stage (brown color; Toma and Mendonça 2013: fig. 1Q) had the induction correctly associated by these authors to an unidentified Lepidoptera. Similar galls are also found on *C. pilosa* plants in Parque Nacional do Itatiaia Nacional, Rio de Janeiro, as illustrated by Maia and Mascarenhas (2017: fig. 139). However, it is unlikely in this case that they are conspecific to *N. cecidogena* as the galls are differently shaped; they are pedunculate and present five conspicuous filiform projections distally. Bruch (1941) showed the feeding damage made by larvae of *Melittia tayuyana* Bruch, 1941, which appears externally as swellings on the stems of *Cayaponia ficifolia* (Vell.) Cogn. [= *C. bonariensis* (Mill.) Mart. Crov.] in Argentina, a plant that is sympatric to *C. pilosa* (Gomes-Klein et al. 2015). Possible tuberculate galls that are induced by an unidentified species of *Sincara* Walker, 1856 on the roots of *Wilbrandria verticillata* (Vell.) Cogn. (Cucurbitaceae) were illustrated by Lima (1945), also for the Atlantic Forest in Brazil. Recently, Gorbunov (2015) suggested the existence of a gregarious feeding habit on galls induced by *Melittia ambo* Gorbunov, 2015 at the root collar of *Citrullus colocynthis* (L.) Schrad. (Cucurbitaceae) in Ethiopia. These few records suggest cucurbit galls are associated with more than one lineage of sesiid moths, and may vary in general shape, host plant species, plant parts where they are induced, and the density of larvae they bear inside.

Acknowledgements

References

Arita Y, Gorbunov OG (1996) A revision of Ferdinand Le Cerf's clearwing moth types (Lepidoptera, Sesiidae), kept at the Paris Museum. I. The genus *Melittia* Hübner, [1819] in the Oriental and Australian Regions. Japanese Journal of Systematic Entomology 2: 137–187.

Arita Y, Gorbunov OG (2000) Notes on the tribe Osminiini (Lepidoptera, Ssiidae) from Vietnam, with descriptions of new taxa. Transactions of the Lepidopterological Society of Japan 51: 49–74.

Arita Y, Kimura M, Owada M (2009) Two new species of the clearwing moth (Sesiidae) from Okinawa-jima, the Ryukyus. Transactions of the Lepidopterological Society of Japan 60: 189–192.

Brown LN, Mizell RF (1993) The clearwing borers of Florida (Lepidoptera: Sesiidae). Tropical Lepidoptera 4 (Suppl. 4): 1–21.

Bruch C (1941) Observaciones biológicas sobre "*Melittia bergi*" Edwards (Lepidoptera: Aegeriidae). Notas del Museo de La Plata 4: 157–163.

Casagrande MM, Dias FMS, Carneiro E (2018) Sesiidae. Catálogo da Fauna do Brasil. http://fauna.jbrj.gov.br/fauna/faunadobrasil/153512 [Accessed on: 2018-9-27]

Dalla Torre KW von, Strand E (1925) Aegeriidae. In: Strand E (Ed.) Lepidopterorum Catalogus. Pars 31. W. Junk, Berlin, 1–202. https://doi.org/10.5962/bhl.title.143714

Duckworth WD, Eichlin TD (1974) Clearwing moths of Australia and New Zealand (Lepidoptera: Sesiidae). Smithsonian Contributions to Zoology 180: 1–45. https://doi.org/10.5479/si.00810282.180

Duckworth WD, Eichlin TD (1977a) A classification of the Sesiidae of America north of Mexico. Occasional Papers in Entomology 26: 1–54.

Duckworth WD, Eichlin TD (1977b) Two new species of clearwing moths (Sesiidae) from eastern North America clarified by sex pheromones. Journal of the Lepidopterists' Society 31: 191–196.

Eichlin TD (1992) Clearwing moths of Baja California, Mexico (Lepidoptera: Sesiidae). Tropical Lepidoptera 3: 135–150.

Eichlin TD (1995) New data and a redescription for *Melittia oedipus*, an African vine borer (Lepidoptera: Sesiidae). Tropical Lepidoptera 6: 47–51.

Eichlin TD (2003) *Carmenta guayaba*, a new clearwing moth from Peru (Lepidoptera: Sesiidae). Tropical Lepidoptera 11: 44–45.

Eichlin TD, Duckworth WD (1988) The Moths of America North of Mexico. Fascicle 5.1. Sesioidea, Sesiidae. Washington, DC, 176 pp.

Eichlin TD, Passoa S (1983) A new clearwing moth (Sesiidae) from Central America: a stem borer in *Mimosa pigra*. Journal of the Lepidopterists' Society 37: 193–206.

Folmer O, Black M, Hoeh W, Lutz R, Vrijenhoek R (1994) DNA primers for amplification of mitochondrial cytochrome c oxidase subunit I from diverse metazoan invertebrates. Molecular Marine Biology and Biotechnology 3: 294–299.

Gomes-Klein VL, Lima LFP, Gomes-Costa GA, Medeiros ES (2015) Cucurbitaceae. In: Lista de Espécies da Flora do Brasil. Jardim Botânico do Rio de Janeiro. http://floradobrasil.jbrj.gov.br/jabot/floradobrasil/FB82111 [Accessed on: 2018-9-24]

Gorbunov OG (2015) Contributions to the study of the Ethiopian Lepidoptera. I. The genus *Melittia* Hübner, 1819 ["1816"] (Lepidoptera: Sesiidae) with description of a new species. Zootaxa 4033: 543–554. https://doi.org/10.11646/zootaxa.4033.4.5

Gorbunov OG (2018) New data on the clearwing moth fauna of the Altai Mountains, Russia, with the description of two new species (Lepidoptera, Sesiidae). Zootaxa 4425: 263–282. https://doi.org/10.11646/zootaxa.4425.2.4

Gorbunov O.G. (2019) A new species of the genus *Bembecia* Hübner, 1819 ["1916"] from the European part of Russia (Lepidoptera, Sesiidae), with remarks on the *Bembecia dispar* (Staudinger, 1891) species group. Zoological Journal 98: 393–406. https://doi.org/10.1134/S0044513419040081

Guindon S, Dufayard JF, Lefort V, Anisimova M, Hordijk W, Gascuel O (2010) New algorithms and methods to estimate maximum-likelihood phylogenies: assessing the performance of PhyML 3.0. Systematic Biology 59: 307–321. https://doi.org/10.1093/sysbio/syq010

Hansen JA, Klingeman WE, Moulton JK, Oliver JB, Windham MT, Zhang A, Trigiano RN (2012) Molecular identification of Synanthedonini members (Lepidoptera: Sesiidae) using cytochrome oxidase I. Annals of the Entomological Society of America 105: 520–528. https://doi.org/10.1603/AN11028

Hanson P, Nishida K, Gómez-Laurito J (2014) Insect galls of Costa Rica and their parasitoids. In: Fernandes GW, Santos JC (Eds) Neotropical Insect Galls. Springer, Dordrecht, 497–517. https://doi.org/10.1007/978-94-017-8783-3_23

Harms KE, Aiello A (1995) Seed-boring by tropical clearwing moths (Sesiidae): Aberrant behavior or widespread habit? Journal of the Lepidopterists' Society 49: 43–48.

Heppner JB (1987) Sesiidae (Sesioidea). In: Stehr FW (Ed) Immature Insects, vol. 1. Kendall/Hunt Publishing Company, Dubuque, 411–412.

Heppner JB, Duckworth WD (1981) Classification of the Superfamily Sesioidea (Lepidoptera: Ditrysia). Smithsonian Contributions to Zoology 314: 1–144. https://doi.org/10.5479/si.00810282.314

Hinton HE (1981) Biology of insect eggs. Vol. I. Pergamon Press, Oxford. 473pp.

Kumar S, Stecher G, Tamura K (2016) MEGA7: Molecular Evolutionary Genetics Analysis Version 7.0 for Bigger Datasets. Molecular Biology and Evolution 33: 1870–1874. https://doi.org/10.1093/molbev/msw054

Lait LA, Hebert PDN (2018) A survey of molecular diversity and population genetic structure in North American clearwing moths (Lepidoptera: Sesiidae) using cytochrome c oxidase I. PloS ONE 13(8): e0202281. https://doi.org/10.1371/journal.pone.0202281

Le Cerf F (1916) Explication des planches. In: Oberthür C (Ed.) Études de Lépidoptérologie Comparée 12 (1): 7–14. [pls 373–381] https://doi.org/10.5962/bhl.title.8792

Le Cerf F (1917) Contributions à l'étude des Aegeriidae. Description et iconographie d'espèces et de formes nouvelles ou peu connues. In: Oberthür C (Ed.) Études de Lépidoptérologie Comparée 14: 137–388. [pls 475–481] https://doi.org/10.5962/bhl.title.8792

Lima AC (1945) Insetos do Brasil. 5° Tomo. Lepidópteros, 1ª Parte. (Série Didática 5). Escola Nacional de Agronomia, Rio de Janeiro, 379 pp.

Lopes PSN, Souza JC, Reis JR, Oliveira JM, Rocha IDF (2003) Caracterização do ataque da broca dos frutos do pequizeiro. Revista Brasileira de Fruticultura 25: 540–543. https://doi.org/10.1590/S0100-29452003000300046

Maia VC, Mascarenhas B (2017) Insect galls of the Parque Nacional do Itatiaia (southeast region, Brazil). Anais da Academia Brasileira de Ciencias 89(suppl.): 505–575. https://doi.org/10.1590/0001-3765201720160877

McKern JA, Szalanski AL, Johnson DT, Dowling APG (2008) Molecular phylogeny of Sesiidae (Lepidoptera) inferred from mitochondrial DNA sequences. Journal of Agricultural and Urban Entomology 25: 165–177. https://doi.org/10.3954/1523-5475-25.3.165

Newland DE, Sawyer TJ (2014) Eclosion mechanics, mating and ovipositing behaviour of *Sesia apiformis* (Clerck, 1759) (Lepidoptera: Sesiidae). Entomologist's Gazette 65: 217–230

Patočka J, Turčani M (2005) Lepidoptera pupae: Central European species. Vol. 1. Apollo Books, Stenstrupp, 321 pp.

Pitkin LM (1986) A technique for the preparation of complex male genitalia in microlepidoptera. Entomologist's Gazette 37: 173–179.

Porto ML (1974) Cucurbitaceae. Boletim do Instituto Central de Biociências 31: 1–64.

Puchi ND (2005) Caracterización morfológica de los Sesiidae (Insecta: Lepidoptera) perforadores del fruto del cacao (*Theobroma cacao* L.), presentes en la región costera del estado Aragua, Venezuela. Entomotropica 20: 97–111.

Pühringer F, Kallies A (2004) Provisional checklist of the Sesiidae of the world (Lepidoptera: Ditrysia). Mitteilungen der Entomologischen Arbeitsgemeinschaft Salzkammergut 4: 1–85. [Updated by F. Pühringer, 2017-1- 28] http://www.sesiidae.net/Checklst.htm

Pühringer F, Kallies A (2017) Checklist of the Sesiidae of the world (Lepidoptera: Ditrysia). http://www.sesiidae.net/Checklst.htm [Accessed on: 2018-4-26]

Skowron MA, Munisamy B, Hamid SB, Wegrzyn G (2015) A new species of clearwing moth (Lepidoptera: Sesiidae: Osminiini) from Peninsular Malaysia, exhibiting bee-like morphopholgy and behavior. Zootaxa 4032: 426–434. https://doi.org/10.11646/zootaxa.4032.4.7

Špatenka K, Gorbunov O, Laštůvka Z, Toševski I, Arita Y (1999) Sesiidae, clearwing moths. In: Naumann CM (Ed.) Handbook of Palaearctic Macrolepidoptera. Vol. 1. Gem Publishing Company, Wallingford, 569 pp.

Thompson JD, Higgins DG, Gibson TJ (1994) CLUSTAL W: improving the sensitivity of progressive multiple sequence alignment through sequence weighting, position-specific gap penalties and weight matrix choice. Nucleic Acids Research 22: 4673–4680. https://doi.org/10.1093/nar/22.22.4673

Toma TSP, Mendonça MSJr (2013) Gall-inducing insects of an *Araucaria* Forest in southern Brazil. Revista Brasileira de Entomologia 57: 225–233. https://doi.org/10.1590/S0085-56262013005000001

Villagra BLP, Romaniuc Neto S (2011) Plantas trepadeiras do Parque Estadual das Fontes do Ipiranga (São Paulo, Brasil). Hoehnea 38: 325–384. https://doi.org/10.1590/S2236-89062011000300001

Zukowsky B (1936) Family: Aegeriidae. In: Seitz A (Ed.), 1935–1936 Die Gross-Schmetterlinge der Erde: eine systematische Bearbeitung der bis jetzt bekannten Gross-Schmetterlinge. II Abteilung: die Gross-Schmetterlinge des Amerikanischen Faunengebietes. Bd. 6. Die amerikanischen Spinner und Schwärmer. A. Kernen Verlag, Stuttgart, 1215–1262. [pls 176–180, 185] https://doi.org/10.5962/bhl.title.9400

RESEARCH ARTICLE

The genus *Macrobrachium* (Crustacea, Caridea, Palaemonidae) with the description of a new species from the Zaomu Mountain Forest Park, Guangdong Province, China

Xiao-Zhuang Zheng[1], Wen-Jian Chen[1], Zhao-Liang Guo[1]

1 *Department of Animal Science, School of Life Science and Engineering, Foshan University, Nanhai 528231, Guangdong Province, China*

Corresponding author: *Zhao-Liang Guo* (zlguo@fosu.edu.cn)

Citation: Zheng X-Z, Chen W-J, Guo Z-L (2019) The genus *Macrobrachium* (Crustacea, Caridea, Palaemonidae) with the description of a new species from the Zaomu Mountain Forest Park, Guangdong Province, China. ZooKeys 866: 65–83. https://doi.org/10.3897/zookeys.866.32708

Abstract

Evidence-based information is the foundation for addressing urgent global challenges in conservation and sustainable management of the freshwater biodiversity. The present study expands current knowledge of the genus *Macrobrachium* in Zaomu Mountain Forest Park, Guangdong Province based on the morphology, colouration, distribution, and molecular characteristics of *Macrobrachium maculatum*, *M. inflatum*, *M. nipponense,* and an undescribed new species, *M. laevis. Macrobrachium laevis* **sp. nov.** can be distinguished from its congeners by a combination of characters, which includes the shape of rostrum, smooth carapace, and male second pereiopod. *Macrobrachium laevis* **sp. nov.** displays striking colour pattern, which could help to distinguish this species from other congeneric species in living specimen. Furthermore, the molecular characteristics of mitochondrial cytochrome c oxidase subunit I (COI) showed that this species has a sufficient interspecific divergence from its congeners.

Keywords

biodiversity, freshwater prawn, molecular phylogeny, morphology, oriental region, taxonomy

Introduction

The genus *Macrobrachium* Spence Bate, 1868 comprises 242 species and subspecies inhabiting fresh to brackish environments (De Grave and Fransen 2011). *Macrobrachium* species are native to all continents except for Europe (Holthuis and Ng 2010). Prawns of the genus *Macrobrachium* are widely distributed in China. They can be found in various water bodies, including lakes, reservoirs, rivers, ponds, streams, ditches, swamps, and subterranean waters.

Interest in *Macrobrachium* as a food has emerged throughout the world because of their delicious and unique flavor, and large size. *Macrobrachium* species have become an attractive food source, with good economic potential and high commercial interest in China. In addition, some colourful members of the genus *Macrobrachium* have attracted attention as ornamental pet prawn, and are traded in the ornamental fish market. Li et al. (2007) confirmed the existence of 33 species of the genus *Macrobrachium* in China. Recently, Guo and He (2008), He et al. (2009) and Chen et al. (2018) reported three new species from Guangdong Province, southern China. Furthermore, three new troglobitic species were reported in Guangxi Zhuang Autonomous Region, southwest China (Li and Luo 2001; Li et al. 2006; Pan et al. 2010; Lan et al. 2017; Cai and Ng 2018). A total of 39 species of the genus *Macrobrachium* have been recorded from China. The continued description of new species within *Macrobrachium* is a strong indication that there is still undiscovered species richness across the full taxonomic spectrum of *Macrobrachium* in China. The taxonomy of the genus *Macrobrachium* is mainly based on morphological characters, such as the relative length of the articles of the second pereiopods in fully developed males, rostrum shape and indentation, and colouration (Holthuis 1950; Chace and Bruce 1993). Some of these morphological characteristics have been proven highly variable within the species (e.g., rostrum shape and colouration). Furthermore, the second chelipeds in particular show a very high level of developmental and sexual variation, including allometric growth in males (Short 2004). This makes it a challenge to identify and distinguish different species, and almost impossible to identify juvenile, immature and adult female specimens. Thus, comprehensive molecular characterisations have become a crucial step towards resolving these longstanding taxonomic issues (Liu et al. 2007; Jose and Harikrishnan 2019).

The Zaomu Mountain Forest Park (22°43'–22°45'N, 112°45'–112°47'E) was rated as national 4A scenic area in 2012 (Zhang 2014). In recent years, tourism in the Zaomu Mountain Forest Park has been fast growing. The park has been reconstructed with newly climbing trestles, streams for drifting, and amusement facilities. However, the increasing exploitation of tourist resources has failed to recognise the conservation needs of different species that are found in this ecosystem. These may have negatively affected the species biodiversity of the prawn fauna in the scenic area. So far, the *Macrobrachium* fauna of the Zaomu Mountain Forest Park has not been accurately surveyed. To understand the diversity of the prawn fauna in the scenic area, intensive field surveys were carried out in the period from 2017 to 2018. The results of these field surveys have shown that there are four species of *Macrobrachium*; one of them is considered as a new species to science, *M. laevis* sp. nov.

Materials and methods

Study area

The Zaomu Mountain Forest Park (112°45'–112°47'E, 22°43'–22°45'N) is located in the Youngmei Town, Gaoming District, 38 km West Foshan, Guangdong Province. The area stretches approximately 11 km from north to south and is 5 km wide. The total area is 55 square km. The main mountain peak is 804.5 meters above sea level, and is known as the highest peak of Foshan City (Zhang 2014). The Zaomu Mountain Forest Park has a subtropical maritime monsoon climate, which is warm and humid throughout the year. The mean annual temperature and precipitation are 22.5 °C and 1681.2 mm, respectively (Lu et al. 2003). There are many streams, ponds and reservoirs spread out the Zaomu Mountain Forest Park, and the Yangmei River runs through near the west. The locations of the sampling stations are shown in Figure 1.

Collecting specimens

Samples were collected by a hand net with a mesh size of 0.8 mm. All specimens obtained were fixed in 95 % ethanol. Ethanol was replaced after 24 h with fresh 75 % ethanol. The drawings were made with the aid of a drawing tube mounted on an Olympus BX-41 compound microscope.

Genetic analyses

Genomic DNA was isolated from the muscle tissue of the abdomen by using the Universal Genomic DNA Kit (Beijing, China). A fragment of the COI (619bp) gene was amplified with conventional polymerase chain reaction (PCR) using two primers LCO1490 (5'-GGTCAACAAATCATAAAGATATTGG-3') and HCO2198 (5'-TAAACTTCAGGGTGACCAAAAAATCA-3') (Folmer et al. 1994).

PCR cycling conditions consisted of a 3 min denaturation at 94 °C, followed by 35 cycles of denaturation at 94 °C for 30 s, annealing at 45–47 °C for 60 s, extension at 72 °C for 60 s, and a final extension at 72 °C for 5 min. PCR amplification sequences were obtained by sanger dideoxy sequencing (Applied Biosystems 3730), after verification with the complementary strand. The sequenced fragments were edited and aligned using Codon Code Aligner v. 8.0.2 (Codon Code Corporation, Dedham, MA, USA) and corrected by the naked eye. All sequences of this study have been deposited in GenBank Nucleotide Sequence Database (see Table 1 for accession numbers).

Six specimens of *Macrobrachium laevis* sp. nov. and 21 specimens of nine described species, namely *Macrobrachium maculatum*, *M. formosense*, *M. meridionalis*, *M. nipponense*, *M. inflatum*, *M. dongaoensis*, *M. asperulum*, *M. fukienense,* and *Palaemon modestus* were analysed in the prensent study. Sequences of *M. asperulum*
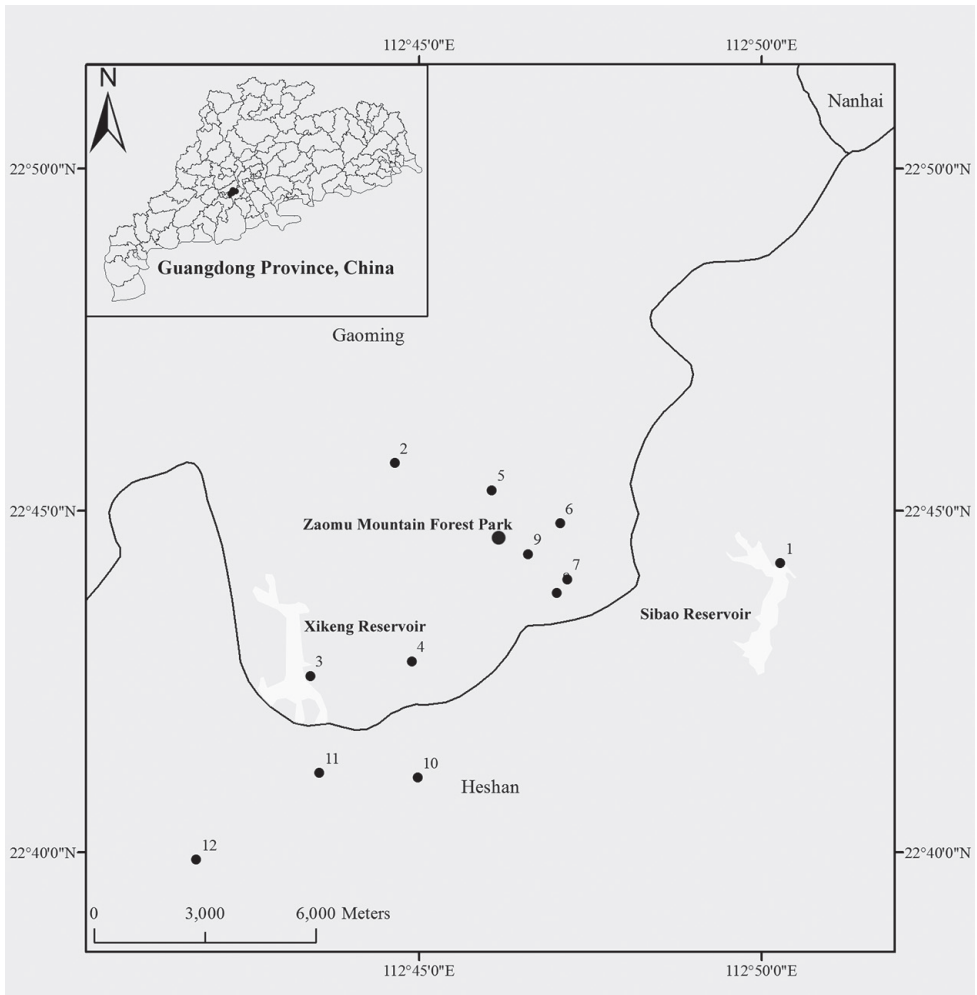
Figure 1. A schematic map of Guangdong Province, China. The expanded map shows locations of the Zaomu Mountain Forest Park and the 12 sampling sites.

and *M. fukienense* were obtained from GenBank for comparative and phylogenetic analyses. Two phylogenetic methods, maximum likelihood (ML) and neighbor-joining (NJ) were implemented. The best-fitting model for sequence evolution was determined by Modelgenerator (Goss et al. 2014) and selected by the Akaike Information Criterion (AIC). Pairwise genetic distances were calculated using the Kimura 2-parameter model with the pairwise deletion option in the MEGA 5 program. The phylogenetic tree was estimated using a NJ and ML method by MEGA 5 (Tamura et al. 2011), and the confidence level in the generated tree was obtained by using 1,000 bootstraps.

Table 1. List of locality, geographical coordinates, and GenBank accession numbers of eight palaemonid species used in the present study.

Species	Locality	Geographical coordinates	GenBank accession numbers
M. dongaoensis	Dong'ao Island, Zhuhai	22°01'39"N, 113°42'54"E	MK412789
M. formosense	Chancheng, Foshan	22°56'39"N, 112°53'41"E	MK412773
	Chancheng, Foshan	22°56'39"N, 112°53'41"E	MK412780
M. inflatum	Dongfang, Hainan	18°52'50"N, 108°59'29"E	MK412787
	Dongfang, Hainan	18°52'50"N, 108°59'29"E	MK412788
M. laevis sp. nov.	Gaoming, Foshan	22°43'60"N, 112°47'10"E	MK412774
	Gaoming, Foshan	22°43'60"N, 112°47'10"E	MK412775
	Heshan, Jiangmen	22°41'06"N, 112°44'59"E	MK412776
	Heshan, Jiangmen	22°41'06"N, 112°44'59"E	MK412777
	Gaoming, Foshan	22°43'60"N, 112°47'10"E	MK412781
	Gaoming, Foshan	22°43'60"N, 112°47'10"E	MK412782
M. maculatum	Gaoming, Foshan	22°45'18"N, 112°46'04"E	MK412770
	Gaoming, Foshan	22°45'18"N, 112°46'04"E	MK412771
	Gaoming, Foshan	22°45'18"N, 112°46'04"E	MK412785
	Gaoming, Foshan	22°45'18"N, 112°46'04"E	MK412786
M. meridionalis	Chancheng, Foshan	22°56'39"N, 112°53'41"E	MK412778
	Chancheng, Foshan	22°56'39"N, 112°53'41"E	MK412779
M. nipponense	Gaoming, Foshan	22°39'54"N, 112°41'45"E	MK412772
	Gaoming, Foshan	22°45'18"N, 112°46'04"E	MK412783
	Gaoming, Foshan	22°44'49"N, 112°47'04"E	MK412784
Outgroup			
P. modestus	Wulanhaote, Neimenggu	46°19'20"N, 121°54'45"E	MK412768
	Wulanhaote, Neimenggu	46°19'20"N, 121°54'45"E	MK412769

Abbreviations

The following abbreviations are used throughout the text:

alt altitude,
b breadth,
c carpus,
cl carapace length, measured from the postorbital margin to the posterior margin of the carapace,
f finger,
i ischium,
l length,

m merus,
p palm,
rl rostral length, measured from the rostral tip to the postorbital margin,
stn sampling station,
tl total length, measured from the rostral tip to the posterior margin of the telson.

All measurements are in millimetres. Specimens were deposited in the Department of Animal Science, School of Life Science and Engineering, Foshan University (**FU**).

Systematic accounts

Palaemonidae Rafinesque, 1815
Genus *Macrobrachium* Spence Bate, 1868

Macrobrachium laevis sp. nov.
http://zoobank.org/E4A945BD-0988-40FB-B8E7-5199396E62D1
Figs 2, 3

Material examined. Holotype: Adult male (FU, 2018-01-15-01), tl 66.2 mm, cl 18.8 mm, rl 9.4 mm; a stream near the bamboo park, the Zaomu Mountain Forest Park, Guangdong Province China (22°43'60"N, 112°47'10"E, alt. 182 m, stn. 7), 15 January 2018. **Paratypes:** 7 males (FU, 2018-01-15-02) tl 45.0–61.1 mm, cl 11.8–16.4 mm, rl 7.2–9.3 mm. 14 females, 2 ovigerous females (FU, 2018-01-15-03), tl 39.8–61.5 mm, cl 9.9–17.3 mm, rl 6.5–9.3 mm, same data as for holotype. **Paratypes:** 2 males (FU, 2018-01-15-04), tl 32.1–48.8 mm, cl 8.0–14.2 mm, rl 5.0–8.0 mm. 1 female, tl 40.0 mm, cl 11.0 mm, rl 5.9 mm, a small stream near the Luohan hill, Heshan, Jiangmen City, Guangdong Province China (22°41'10"N, 112°43'33"E, alt. 140 m, stn.11), 12 May 2018. **Paratypes:** 8 males (FU, 2018-01-15-05), tl 43.3–51.2 mm, cl 11.8–14.4 mm, rl 8.5–10.1 mm. 14 female, 10 ovigerous females, tl 39.2–60.1mm, cl 10.1–16.5 mm, rl 6.5–9.6 mm, Longquan Gorge near Heshan, Jiangmen City, Guangdong Province China (22°41'6"N, 112°44'59"E, alt. 180 m, stn. 10), 12 May 2018.

Diagnosis. Rostrum 0.51–0.71 of cl, tip slightly bent downwards, reaching to end of third segment of antennular peduncle. Rostral formula: 3-4+5-8/2-3 (usually 3), teeth equally spaced. Cephalothorax, abdomen, and second pereiopods smooth, without microspinules. Second pereiopods shorter than tl in both sexes; merus 1.0–1.2 times as long as the ischium; carpus 4.5–5.2 times as long as width, 1.2–1.4 times as long as merus and 0.8–1.0 times as long as palm. Palm not inflated, 4.8–5.3 times as long as wide. Movable finger 0.66–0.86 times as long as palm, without any gape when crossed. Fixed finger with one proximal tooth; moveable finger with two proximal teeth. All segments smooth, with only a small amount of spines along the lateral surfaces of the palm. Eggs large; size 1.1–1.4 × 1.5–1.8 mm diameter.

Description. Rostrum (Fig. 2A, B) rl 0.51–0.71 of cl, high, reaching downward to end of third segment of antennular peduncle. Dorsal margin with 8–12 teeth, three or four equally spaced teeth behind orbit; ventral margin with two or three teeth (usually three).

Carapace (Fig. 2A) smooth; antennal spine well developed, situated below lower orbital angle. Hepatic spine slightly larger than antennal spine, and slightly above level of antennal spine.

Antennule (Fig. 2A, B) bearing sharp stylocerite, reaching end of eye; anterior margin of basal segment distinctly convex, second segment 0.46 times as long as basal segment, 0.83 time as long as distal segment. All segments with submarginal plumose setae.

Antenna (Fig. 2A, B) bearing scaphocerite large, rectangular, 2.4–2.6 times as long as wide. Outer margin almost straight, ending with a strong spine, overreached by lamella.
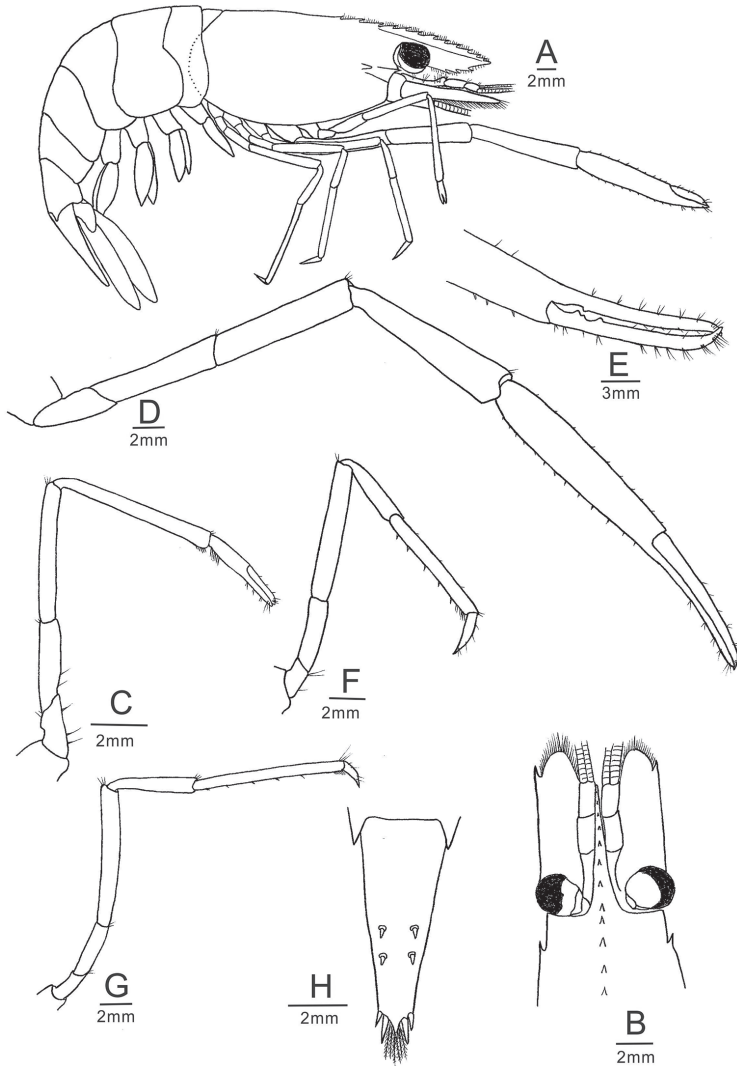
Figure 2. *Macrobrachium laevis* sp. nov., holotype male (FU, 2018-01-15-01), cl 18.8 mm. **A** Entire animal, lateral view **B** cephalothorax and cephalic appendages, dorsal view **C** first pereiopod **D** second pereiopod **E** fingers of second pereiopod **F** third pereiopod **G** fifth pereiopod **H** telson.

Mandibles, maxillulae, maxillae, first maxillipeds, second maxillipeds and branchial formula typical for genus. *Third maxillipeds* with robust endopod and ischiomerus slightly bow-shaped, with rows of long simple setae on distal inner and outer margins. Carpus 0.70 times length of ischiomerus, with row of long simple setae on inner margin and sparse row of simple setae on outer margin; distal segment 0.83 times of penultimate segment, with long simple setae on inner margin. Exopod reaching distal end of ischiomerus, with plumose setae distally, basal with well-developed oval lateral plate; two arthrobranchs, one rudimentary, obscured by the larger one.

First pereiopods (Fig. 2C) slender, overreaching antennal scale by carpus; carpus 1.6–2.0 times as long as chela; fingers shorter than palm, 0.80–0.90 times as long as palm.

Second pereiopods (Fig. 2D, E) shorter than tl. Shape and segment ratios of left and right second pereiopods similar in both sexes, extending beyond the antennal scale by 1/2 of carpus; merus 1.0–1.2 times as long as ischium; carpus 4.5–5.2 times as long as wide, 1.2–1.4 times as long as merus, 0.80–1.0 times as long as palm; palm not inflated, 4.8–5.3 times as long as wide, movable finger 0.66–0.86 times as long as palm; fingers not gaping when crossed; fixed finger with one tooth at proximal, moveable finger with two proximal teeth; all segments smooth, only small amount of spines along lateral surfaces of palm.

Third pereiopods (Fig. 2F) extending to end of third segment of antennular peduncle by distal propodus; propodus 2.5–3.3 times as long as dactylus, with 5–7 spines on posterior margin; dactylus 5.5 times as long as wide, terminating in small claw.

Fourth pereiopods (Fig. 2A) extending to end of third antennular peduncle segment by distal propodus, somewhat similar to third pereiopods.

Fifth pereiopods (Fig. 2G) extending to end of third segment of antennular peduncle; propodus 3.4–6.5 times as long as dactylus, with 5–7 spines on posterior margin; dactylus 3.5 times as long as wide, terminating in small claw.

First pleopods of male with endopod of approximately half-length of exopod, slightly concave at inner margin, tip rounded, without appendix interna.

Second pleopods with well-developed appendix masculina, reaching middle of endopod, approximately twice as long as appendix interna with numerous stiff setae.

Abdomen (Fig. 2A) glabrous, smooth, pleura of first to third somites broadly rounded; pleura of fourth and fifth somites also rounded, but with almost rectangular posterolateral angle; sixth somite 1.2–1.4 times as long as fifth somite, 0.59–0.67 times as long as telson.

Telson (Fig. 2H) smooth, 0.46–0.61 times of cl, longer than sixth abdominal segment; dorsal surface furnished with two pairs of stout, movable, spine; posterior margin tapering regularly to a sharp point with two pairs of posterior a spine; numerous plumose setae present between inner pair of spine.

Uropodal diaeresis with a spine shorter than lateral angle.

Eggs large, size 1.1–1.4 × 1.5–1.8 mm.

Live colour patterns. The juvenile was yellowish and semi-transparent (Fig. 3E); the adult male had a few indistinct longitudinal yellow stripes on the carapace, with one transverse yellow band on the first abdominal somite. All segments of the second pereiopods were golden (Fig. 3A, B). The ovigerous females had a pale yellow longitudinal stripe on the mid-dorsal surface from the rostrum to the tail, which extended to both sides of the abdominal somites. The palms of the third to fifth pereiopods had black and white rings (Fig. 3D). The eggs were brown (Fig. 3C).

Molecular phylogenetic results. Neighbour-joining (NJ) and maximum likelihood (ML) trees inferred from partial COI sequences (619 bp) from ten species of Palaemonidae, including the new species, are shown in Figure 4. *Macrobrachium laevis* sp. nov. is clustering
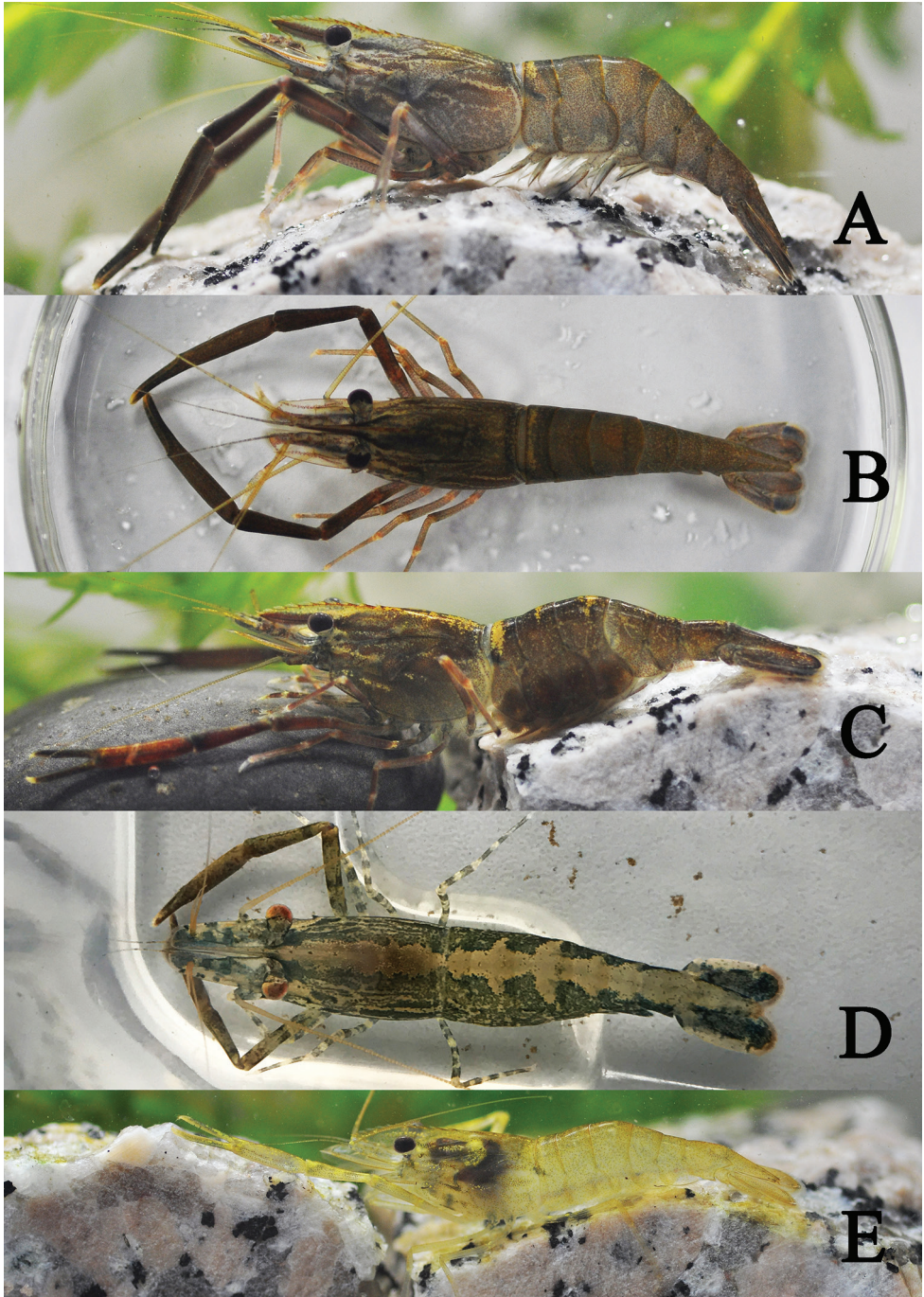
Figure 3. The colour of living *Macrobrachium laevis* sp. nov. **A** Lateral view of adult male **B** dorsal view of adult male **C** lateral view of ovigerous female **D** dorsal view of the fresh moulting female **E** lateral view of the immature male.
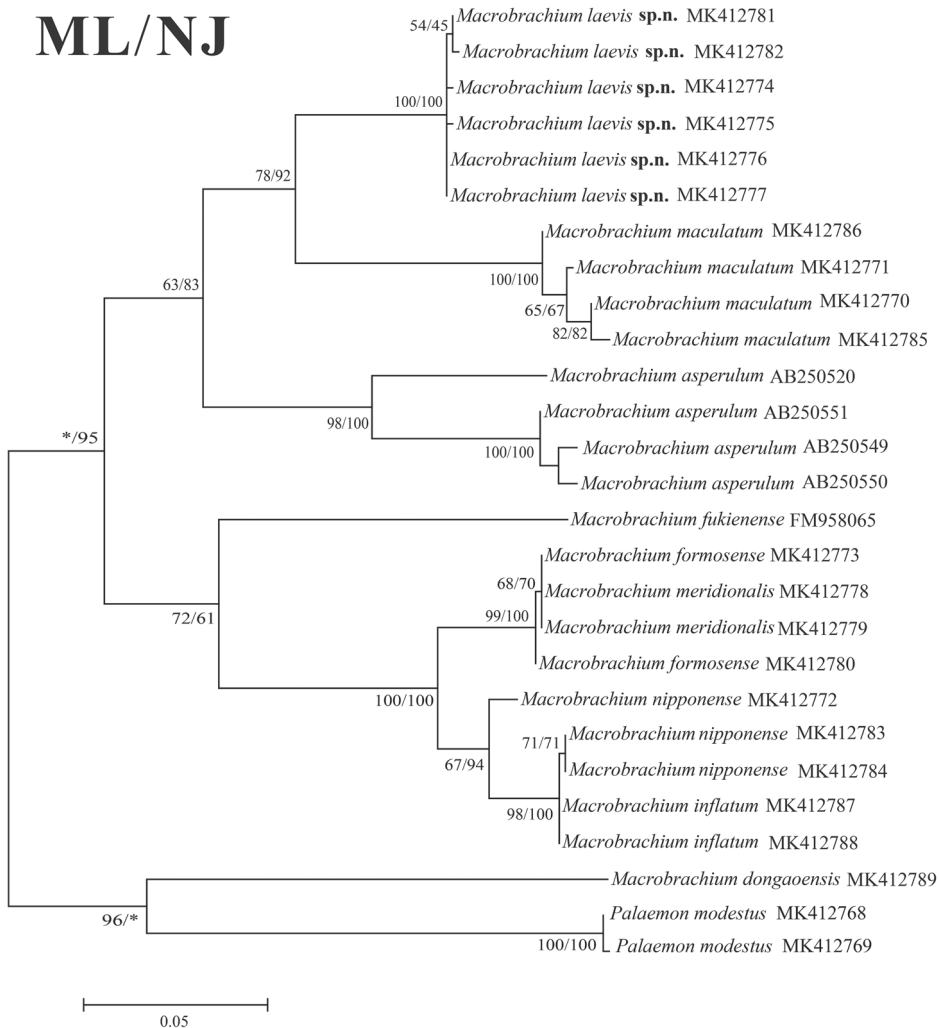
ML/NJ

Figure 4. Phylogenetic relationships among *Macrobrachium laevis* sp. nov. and the other nine species, analysed by maximum likelihood (ML) and neighbour-joining (NJ) methods with *Palaemon modestus* as the out-group taxa. Bootstrap values of ML (left) and NJ (right) are indicated above the branches of the clades.

with *M. maculatum* with high bootstrap support (96 % in ML tree and 96 % in NJ tree). Interspecific genetic divergence (K2P) among these ten species is summarised in Table 2. The pairwise distance was 0.15–0.62%. The new species was closest to *M. asperulum* (0.1475–0.1496) and *M. maculatum* (0.1095–0.1154), and the morphological characters supported this relationship. Moreover, the genetic divergence between *M. laevis* sp. nov., *M. inflatum*, *M. nipponense* and *M. dongaoensis* were 0.1558–0.1598, 0.1576–0.1617 and 0.2154–0.2218, respectively, supporting the morphological differentiation of the three species. Of the species analysed, *M. dongaoensis* was most genetically divergent from the new species (0.2154–0.2218).

Table 2. Pairwise genetic distance among nine *Marobrachium* prawn species based on the COI gene.

	1	2	3	4	5	6	7	8	9
(1) *M. maculatum*		0.138	0.169	0.166	0.167	0.167	0.192	0.171	0.103
(2) *M. asperulum*	0.138		0.162	0.160	0.171	0.171	0.203	0.151	0.135
(3) *M. inflatum*	0.169	0.162		0.014	0.053	0.053	0.197	0.146	0.148
(4) *M. nipponense*	0.166	0.160	0.014		0.050	0.050	0.193	0.144	0.145
(5) *M. formosense*	0.167	0.171	0.053	0.050		0.001	0.208	0.147	0.137
(6) *M. meridionalis*	0.167	0.171	0.053	0.050	0.001		0.208	0.146	0.138
(7) *M. dongaoensis*	0.192	0.203	0.197	0.193	0.208	0.208		0.207	0.182
(8) *M. fukienense*	0.171	0.151	0.146	0.144	0.147	0.146	0.207		0.155
(9) *M. laevis* sp. nov.	0.103	0.135	0.148	0.145	0.137	0.139	0.192	0.155	

Etymology. Species name is derived from *laevis* (Latin) in reference to the smoothness of the segments of the second pereiopod, carapace, and abdomen.

Remarks. *Macrobrachium laevis* sp. nov. shows close similarity with *M. maculatum* Liang and Yan 1980 regarding the ratios of various segments of the second pereiopods and in the rostral shape. *Macrobrachium laevis* sp. nov. can be distinguished from *M. maculatum* by the smooth second pereiopod whose margin of the palm has scattered microspinules (versus second pereiopod with microspinules on its whole surface); the second tooth of the movable finger placed on the proximal one-quarter (versus on the proximal one-fifth); the lack of papillae along the cutting edges (versus numerous papillae along the cutting edges); the finger slightly longer than the merus (versus the finger distinctly shorter than merus); the wider scaphocerite (2.4–2.6 times as long as wide) (versus 3.5 times); and ovigerous females carrying smaller eggs (1.1–1.4 × 1.5–1.8 mm) (versus larger egg sizes, 1.60–1.68 × 2.12–2.36 mm). *Macrobrachium laevis* sp. nov. is morphologically close to *M. asperulum* von Martens 1868 regarding the form of the rostrum and egg size. *Macrobrachium laevis* sp. nov. can be distinguished from *M. asperulum* by its smooth carapace and second chelipeds and lack of denticles on the cutting edges (versus with rough carapace and chelipeds, and the presence of approximately ten denticles on the cutting edges), and the second tooth of the movable finger at about proximal one-quarter (versus second tooth of the movable finger on the proximal two-fifths). *Macrobrachium laevis* sp. nov. superficially resembles *M. inflatum* Liang & Yan, 1985; however, *Macrobrachium laevis* sp. nov. can be distinguished from *M. inflatum* by its shorter rostrum with fewer dorsal teeth and reaching beyond the end of the third antennular peduncle segment, with 8–12 dorsal teeth (versus rostrum reaching beyond the scaphocerite, with 12–17 dorsal teeth); the palm of male second pereiopod being not inflated (versus inflated) and 4.8–5.3 times as long as wide (versus 3.5–3.6 times); the finger distinctly longer than merus (versus the finger as along as the merus); the ischium shorter than the merus (versus the ischium distinctly longer than the merus); and the ovigerous females bearing larger-sized eggs (1.1–1.4 × 1.5–1.8 mm) (versus 0.53–0.59 × 0.62–0.69 mm). *Macrobrachium laevis* sp. nov. is closely related to *M. fukienense* Liang & Yan, 1980. It is possible to distinguish *Macrobrachium laevis* sp. nov. from *M. fukienense* by the presence of more dorsal and postorbital teeth (8–12 dorsal and 3–4 postorbital teeth) (versus 7–8 dorsal and 1–2 postorbital teeth); the second tooth of the

Table 3. Morphological characteristics of *Macrobrachium laevis* sp. nov. and the congeners.

	M. laevis sp. nov.	M. maculatum	M. asperulum	M. fukienense	M. inflatum	M. nipponense	M. dongaoensis
Rostrum							
Number of dorsal teeth	8–12	9–14	8–12	7–9	12–17	9–13	10–13
Number of postal orbit teeth	3–4	3–5	2–3	1–2	3–4	2–3	4–5
Number of ventral teeth	2–3	3–5	2–3	1–2	3–5	2–3	1–3
Ratio of RL/CL	0.5–0.7	0.6–0.7	0.6–0.7	0.6	1.0	0.6–0.8	0.5–0.7
First periopod Ratio of f/p	0.73–0.97	0.76–0.83	0.78	0.85	0.83–0.91	0.8	1.0
Second pereiopod							
Ratio of palm L/b	4.8–5.3	4.5–6.0	5.0–6.5	4.3	3.5–3.6	4.7–7.0	4.3–4.9
Ratio of f/p	0.66–0.86	0.62–0.78	0.5–0.6	0.4–0.5	0.82–1.0	0.6–0.7	0.69–0.78
Ratio of c/p	0.8–1.0	0.8–0.9	0.79–0.84	0.76–0.87	1.4	1.4	0.93–1.0
Ratio of c/m	1.2–1.4	1.1–1.3	1.3–1.4	1.1	1.4–1.5	1.6–1.7	1.1–1.4
Ratio of i/m	0.83–1.0	0.76–1.0	0.78	0.6–0.7	1.1	0.74–0.9	0.9
Ratio of f/m	≥1	<1	<1	<1	=1	<1	>1
Microspinules on every segment	Smooth, except margins of palm with scattered microspinules	All segments with	All segments with	All segments with	All segments without, except pout margin of palm with	All segments with	All segments with
Distribution of the second tooth of moveable finger	On the proximal 1/4	On the proximal 1/5	On the proximal 2/5	On the proximal 1/2	On the proximal 1/7	On the proximal 1/5	On the proximal 1/5
Eggs size (mm)	1.1–1.4 × 1.5–1.8	1.6–1.7 × 2.1–2.4	1.08–1.26 × 1.50–1.76	1.5–1.6 × 2.1–2.2	0.53–0.59 × 0.62–0.69	0.54–0.68 × 0.72–0.86	0.33–0.42 × 0.37–0.44
Scaphocerite l/b	2.4–2.6	3.5	2.8–3.2	2.5–2.8	3.4	2.7–3.1	3.4

movable finger of the male second pereiopods on the proximal one-quarter (versus on the proximal half). *Macrobrachium laevis* sp. nov. is also closely related to *M. nipponense* De Haan, 1849. *Macrobrachium laevis* sp. nov. can be distinguished from *M. nipponense* by morphological characters of the male second pereiopods. The second pereiopods of *Macrobrachium laevis* sp. nov. are distinctly shorter than those of *M. nipponense*; the finger are distinctly longer than the merus (versus the finger shorter than the merus), and without setae on the cutting edge (versus the cutting edge with the long dense setae) (Fig. 3A, B versus Fig. 6A). It is possible to distinguish living *Macrobrachium laevis* sp. nov. from other congeners by its striking colour pattern (Fig. 3). Morphological differences between these congeneric species are presented in Table 3.

Habitat. Specimens of *Macrobrachium laevis* sp. nov. were collected from two streams and a river. The stream was near bamboo park, the Zaomu Mountain Forest Park, Foshan City (22°43'60"N, 112°47'10"E, alt. 182 m, stn. 7) (Fig. 5A). This stream runs through land covered with a secondary forest, with beds of rock and patches of gravel. The stream width and depth were 2.0–3.5 m and 0.6–0.9 m, respectively, with fast flowing water. The water parameters of the stream at the time of collection (15 January 2018) were: temperature 13.8 °C, pH 7.0, dissolved ammonia nitrogen 0.2 mg/l, and dissolved oxygen 4.0 mg/l. The prawns were found at the bottom of the streams together with an atyid shrimp, *Caridina cantonensis* Yu 1938. The specimens were also collected from another small stream near the Luohan hill, Heshan, Jiangmen City, Guangdong Province (22°41'10"N, 112°43'33"E, atl. 140 m, stn. 11). The environmental conditions were very similar to the first stream. The water parameters of the stream at the time of collection (12 May 2018) were: temperature 25.6 °C, pH 6.5, dissolved ammonia nitrogen 0.2 mg/l, and dissolved oxygen 4.5 mg/l. Additional specimens were collected from the Longquan Gorge, near Heshan, Jiangmen City (22°41'6"N, 112°44'59"E, atl. 180 m, stn. 10) (Fig. 5B). It is a small river, with a total length of 6 km. The total drop of the river is 108 meters. The river resembles a jade belt and is deeply embedded at the bottom of the Zaomu Mountain. The river has flowing water, with rocks interspersed with sand patches at its bottom. The water parameters of the river at the time of collection (12 May 2018) were temperature of 26.1 °C, pH 7.0, dissolved ammonia nitrogen 0.2 mg/l, and dissolved oxygen 6.0 mg/l.

Distribution. So far only known from the type locality and nearby localities in the Guangdong Province, southern China.

Macrobrachium nipponense **(De Haan, 1849)**
Fig. 6A

Material examined. Five females, tl 48.5–52.8 mm, cl 14.2–16.3 mm, 4 males, tl 51.3–65.9 mm, cl 18.0–25.6mm, Sibao Reservoir, Heshan, Jiangmen City (22°44'14"N, 112°50'17"E, alt. 84 m, stn. 1), 3 September 2017; 2 females, tl 48.5–50.4 mm, cl 15.2–16.4 mm, 1 male, tl 51.3 mm, cl 17.3mm, Lingshan Garden, Gaoming, Foshan City (22°45'42"N, 112°44'39"E, alt. 44.9 m, stn. 2), 17 May 2018; 3 females, tl 46.3–49.2

Figure 5. Habitats of *Macrobrachium laevis* sp. nov. **A** Stream near bamboo park, Zaomu Mountain Forest Park, Foshan City (type locality) **B** the Longquan Gorge, near Heshan, Jiangmen City. Both localities are situated in the Guangdong Province, southern China.

Figure 6. Photographs of *Macrobrachium* species. **A** *M. nipponense*, living specimen, male **B** *M. maculatum*, living specimen, male **C** *M. inflatum*, living specimen, female.

mm, cl 14.1–15.3 mm, 2 males, tl 51.3–61.4 mm, cl 18.2–23.4 mm, Xikong Reservoir, Gaoming, Foshan City (22°42'35"N, 112°43'25"E, alt. 22.4 m, stn. 3), 17 May 2018; 2 females, tl 42.5–44.1 mm, cl 13.2–14.6 mm, 4 males, tl 48.3–59.4 mm, cl 17.4–22.9 mm, Yangmei River, Gaoming, Foshan City (22°45'18"N, 112°46'04"E, alt. 49 m, stn. 5), 9 September 2017; 4 females, tl 41.4–50.3 mm, cl 12.3–16.3 mm, 3 males, tl 47.2–65.5 mm, cl 17.5–24.5 mm, stream near Hengkong Village, Gaoming, Foshan City (22°44'49"N, 112°47'04"E, alt. 72 m, stn. 6), 9 September 2017; 1 female, tl 42.5 mm, cl 13.2, 1 male, tl 48.3 mm, cl 16.7 mm, a stream near Datian Village, Gaoming, Foshan City (22°44'22"N, 112°46'36"E, alt. 56 m stn. 9), 17 May 2018.

Remarks. *Macrobrachium nipponense* were found in reservoirs, streams, rivers, and ponds of the Zaomu Mountain Forest Park. The species is native and broadly distributed throughout East Asia (i.e. China, Japan, Korea, Vietnam, and Myanmar),

(Cai and Ng 2002; Li et al. 2007). *Macrobrachium nipponense* was introduced into Singapore, Philippines, Uzbekistan, Iraq, Russia, Belarus, Moldova, and Iran (Chong et al. 1987; Alekhnovich and Kulesh 2001; Mirabdullaev and Niyazov 2005; Cai and Shokita 2006; De Grave and Ghane 2006; Salman et al. 2006). *Macrobrachium nipponense* is commercially important in Guangdong Province where it is sold live in local fish markets, and is locally consumed at home and in restaurants as a special dish.

Colouration. The body has a lighter green and transparent colour, and the carapace has an M-shaped mark on the side (Fig. 6A).

Distribution. China, Japan, Korea, Myanmar, and Vietnam.

Macrobrachium maculatum Liang & Yan, 1980
Fig. 6B

Material examined. Three females, tl 45.8–54.0 mm, cl 12.0–18.3 mm, 4 males, tl 35.6–75.8 mm, cl 9.6–19.8 mm, Yangmei River, Gaoming, Foshan City (22°45'18"N, 112°46'04"E, alt. 49 m, stn. 5), 9 September 2017.

Remarks. The present specimens are consistent with the original description and illustration by Liang and Yan (1980) and Liu et al. (1990). This species is widely distributed in the southeastern China. *Macrobrachium maculatum* has an economic importance and is usually found in the same habitat with *M. nipponense*. *Macrobrachium maculatum* inhabits freshwater and has been found in rivers, reservoirs, and streams. This species seeks shelter among aquatic vegetation.

Colouration. The body is very dark brown, the cephalothorax has diagonal yellow stripes, and the abdomen has large spots (Fig. 6B).

Distribution. Southeastern China (Anhui, Hunan, Fujian, and Guangdong Provinces).

Macrobrachium inflatum Liang & Yan, 1985
Fig. 6C

Material examined. Two females, tl 46.8–50.2 mm, cl 13.8–15.3 mm, 1 male, tl 52.1 mm, cl 14.2 mm, Qianlonggu, Gaoming, Foshan City (22°42'48"N, 112°44'54"E, alt. 124 m, stn. 4), 9 September 2017; 2 females, tl 45.5–51.0 mm, cl 13.4–16.1 mm, 3 males, tl 46.5–60.1 mm, cl 15.2–21.3 mm, Yangmei River, Gaoming, Foshan City (22°45'18"N, 112°46'04"E, alt. 49 m, stn. 5), 9 September 2017; 3 females, tl 40.5–54.3 mm, cl 12.5–20.6 mm, 2 males, tl 41.5–65.2 mm, cl 16.2–23.7 mm, Sibao Reservoir, Heshan, Jaingmen City (22°44'14"N, 112°50'17"E, alt. 84 m, stn.1), 17 August 2017.

Remarks. Specimens were confidently assigned to the present species due to their inflated palm, the upturned rostrum and the rostral formula, as well as the ratio of the segments in the male second pereiopods. *Macrobrachium inflatum* is usually found together with *M. nipponense*.

Colouration. The body is translucent and light green. The rostrum is transparent to almost colourless. The cephalothorax has blue-black diagonal strips, and the abdomen shows blue-black transverse strips. The second pereiopods have transversal yellow bands on the merus and carpus. All joints of third to fifth pereiopods have transversal yellow bands. The eggs are yellow (Fig. 6C).

Distribution. Southeastern China (Jiangsu, Anhui, Hunan, Guangdong, and Yunnan Provinces).

Acknowledgements

References

Alekhnovich AV, Kulesh VF (2001) Variation in the parameters of the life cycle in prawns of the genus *Macrobrachium* Bate (Crustacea, Palaemonidae). Russian Journal of Ecology 32: 454–459. https://doi.org/10.1023/A:1012586218096

Cai YX, Ng PKL (2002) The freshwater palaemonid prawns (Crustacea: Decapoda: Caridea) of Myanmar. Hydrobiologia 487: 59–83. https://doi.org/10.1023/A:1022991224381

Cai YX, Ng PKL (2018) Freshwater shrimps from karst caves of southern China, with descriptions of seven new species and the identity of *Typhlocaridina linyunensis* Li and Luo, 2001 (Crustacea: Decapoda: Caridea). Zoological Studies 57: 1–33.

Cai YX, Shokita S (2006) Report on a collection of freshwater shrimps (Crustacea: Decapoda: Caridea) from the Philippines, with descriptions of four new species. Raffles Bulletin of Zoology 54: 245–270.

Chace FA, Bruce AJ (1993) The caridean shrimps (Crustacea: Decapoda) of the 'Albatross' Philippine Expedition 1907–1910, part 6: Superfamily Palaemonoidea. Smithsonian Contributions to Zoology 543(543): 1–152. https://doi.org/10.5479/si.00810282.543

Chen QH, Chen WJ, Guo ZL (2018) Caridean prawn (Crustacea, Decapoda) from Dong'ao Island, Guangdong, China. Zootaxa 4399(3): 315–328. https://doi.org/10.11646/zootaxa.4399.3.2

Chong SSC, Khoo HW, Ng PKL (1987) Presence of the Japanese freshwater prawn *Macrobrachium nipponense* (De Haan, 1849) (Decapoda: Caridea: Palaemonidae) in Singapore. Zoologische Mededelingen Leiden 61: 313–317.

De Grave S, Fransen CHJM (2011) Carideorum catalogus: the recent species of the dendrobranchiate, stenopodidean, procarididean and caridean shrimp (Crustacea: Decapoda). Zoologische Mededelingen Leiden 89(5): 195–589.

De Grave S, Ghane A (2006) The establishment of the Oriental River Prawn, *Macrobrachium nipponense* (de Haan, 1849) in Anzali Lagoon (Iran). Aquatic Invasions 1(4): 204–208. https://doi.org/10.3391/ai.2006.1.4.2

De Haan W (1833–1850) Crustacea. In: von Siebold PF (Ed.) Fauna Japonica sive descriptio animalium, quae in itenere per Japoniam, jussu et auspiciis superiorum, qui summum in India Batava imperium tenent, suscepto, annis 1823–1830 collegit, notis, observationibus et admumbrationibus illustravit. Lugduni-Batavorum, 243 pp. [I–xxxi, plates A–J, L–Q, 1–55]

Folmer O, Black M, Hoeh W, Lutz R, Vrijenhoek R (1994) DNA primers for amplification of mitochondrial cytochrome c oxidase subunit i from diverse metazoan invertebrates. Molecular Marine Biology and Biotechnology 3(5): 294–299.

Goss EM, Tabima JF, Cooke DEL, Restrepo S, Fry WE, Forbes GA (2014) The Irish potato famine pathogen *Phytophthora infestans* originated in central Mexico rather than the Andes. Proceedings of the National Academy of Sciences of the United States of America 111(24): 8791–8796. https://doi.org/10.1073/pnas.1401884111

Guo ZL, He SL (2008) One new and four newly recorded species of the genus *Macrobrachium* (Decapoda: Caridea: Palaemoindae) from Guangdong Province, southern China. Zootaxa 1961: 11–25.

He SL, Gao J, Guo ZL (2009) *Macrobrachium pentazona*, a new freshwater palaemonid prawn (Decapoda: Caridea: Palaemoindae) from Guangdong Province, China. Zootaxa 2140: 38–44.

Holthuis LB (1950) The Decapoda of the Siboga expedition. Part 10. The Palaemonidae collected by the Siboga and Snellius Expeditions with remarks on other species. I. Subfamily Palaemonidae. Siboga-Expeditie Leiden 39a(9): 1–268.

Holthuis LB, Ng PKL (2010) Nomenclature and taxonomy. In: New MB, Valenti WC, Tidwell JH, D'Abramo LR, Kutty MN (Eds) Freshwater Prawns: Biology and Farming (1st edn). Wiley-Blackwell, Oxford, 12–17. https://doi.org/10.1002/9781444314649.ch2

Jose D, Harikrishnan M (2019) Evolutionary history of genus *Macrobrachium* inferred from mitochondrial markers: a molecular clock approach. Mitochondrial DNA Part A 30: 92–100. https://doi.org/10.1080/24701394.2018.1462347

Lan C, Wu Z, Li W (2017) A new troglobitic shrimp from Guangxi Zhuang Autonomous Region: *Macrobrachium duanensis* sp. Journal of Jishou University 38(2): 61–62.

Li JC, Cai YX, Clarke A (2006) A new species of troglobitic freshwater prawn of the genus *Macrobrachium* from southern China (Crustacea: Decapoda: Palaemonidae). Raffles Bulletin of Zoology 54: 277–282.

Li W, Luo Z (2001) A new troglobitic shrimp from Guangxi. Journal of Guangxi Normal University 19(12): 72–74. [in Chinese with English abstract]

Li XZ, Liu RY, Liang XQ, Chen GX (2007) Fauna Sinica. Invertebrata. Vol. 44. Crustacea Decapoda Palaemonoidea. Science Press, Beijing, 381 pp. [in Chinese with English abstract]

Liang XQ, Yan SL (1980) Description of two new species of *Macrobrachium* (Decapoda Caridea) from Fujian, China. Acta Zootaxonomica Sinica 5(1): 30–34. [in Chinese with English abstract]

Liang XQ, Yan SL (1985) New species and new record of Palaemoninae from China (Crustacea Decapoda). Acta Zootaxonomica Sinica 10(3): 253–258. [in Chinese with English abstract]

Liu MY, Cai YX, Tzeng CS (2007) Molecular systematics of the freshwater prawn genus Macrobrachium Bate, 1868 (Crustacea: Decapoda: Palaemonidae) inferred from mtDNA sequences, with emphasis on east Asian species. Zoological Studies 46(3): 272–289.

Liu RY, Liang XQ, Yan SL (1990) A study of the Palaemoninae (Crustacea Decapoda) from China I. *Macrobrachium, Leander* and *Leandrites*. Transactions of The Chinese Crustacean Society No. 2: 102–134. [in Chinese with English abstract]

Lu YD, Xue KN, Li ZK (2003) Investigation on the wild ornamental plants in Gaoming City, Guangdong. Guangdong Forestry Science and Technology 19(3): 35–37.

Mirabdullaev IM, Niyazov DS (2005) Alien decapods (Crustacea) in Uzbekistan. Abstracts of the II International Symposium Invasion of alien species in Holarctic (BOROK-2), Borok, Russia, 27 September 27–1 October, 113–114.

Pan YT, Hou Z, Li SQ (2010) Description of a new *Macrobrachium* species (Crustacea: Decapoda: Caridea: Palaemonidae) from a cave in Guangxi, with a synopsis of the stygobiotic Decapoda in China. Journal of Cave and Karst Studies 72: 86–93. https://doi.org/10.4311/jcks2009lsc0087

Rafinesque CS (1815) Analyse de la Nature, ou Tableau de l'Univers et des Corps Organisés. L'Imprimerie de Jean Barravecchia, Palermo, 224 pp. https://doi.org/10.5962/bhl.title.106607

Salman SD, Page TJ, Naser MD, Yasser AG (2006) The invasion of *Macrobrachium nipponense* (De Haan, 1849) (Caridea: Palaemonidae) into the Southern Iraqi marshes. Aquatic Invasions 1: 109–115. https://doi.org/10.3391/ai.2006.1.3.2

Short JW (2004) A revision of Australian river prawn, *Macrobrachium* (Crustacea: Decapoda: Palaemonidae). Hydrobiologia 525: 1–100. https://doi.org/10.1023/B:HYDR.0000038871.50730.95

Spence Bate CS (1868) On a new genus, with four new species of freshwater prawns. Proceedings of the Zoological Society of London 1868: 363–368.

Tamura K, Dudley J, Nei M, Kumar S (2011) MEGA5: molecular evolutionary genetics analysis using maximum likelihood, evolutionary distance, and maximum parsimony methods. Molecular Biology & Evolution 28(10): 2731–2739. https://doi.org/10.1093/molbev/msr121

Von Martens E (1868) Über einige ostasiatische Süsswasserthiere. Archiv für Naturgeschichte Berlin 34(1): 1–67. https://doi.org/10.5962/bhl.part.20475

Yu SC (1938) Studies on Chinese *Caridina* with descriptions of five new species. Bulletin of the Fan Memorial Institute of Biology, Zoology 8: 275–310.

Zhang YL (2014) Charming Yang He: Building the town in the scenery. Insight China 9: 60–62.

Pollinators on the polar edge of the Ecumene: taxonomy, phylogeography, and ecology of bumble bees from Novaya Zemlya

Grigory S. Potapov[1,2], Alexander V. Kondakov[1,2], Boris Yu. Filippov[1,2],
Mikhail Yu. Gofarov[1,2], Yulia S. Kolosova[1,2], Vitaly M. Spitsyn[1,2],
Alena A. Tomilova[2], Natalia A. Zubrii[1,2], Ivan N. Bolotov[1,2]

1 *Northern Arctic Federal University, 163002, Northern Dvina Emb. 17, Arkhangelsk, Russia* **2** *Federal Center for Integrated Arctic Research, Russian Academy of Sciences, 163000, Northern Dvina Emb. 23, Arkhangelsk, Russia*

Corresponding author: *Grigory S. Potapov* (grigorij-potapov@yandex.ru)

Abstract

The High Arctic bumble bee fauna is rather poorly known, while a growing body of recent molecular research indicates that several Arctic species may represent endemic lineages with restricted ranges. Such local endemics are in need of special conservation efforts because of the increasing anthropogenic pressure and climate changes. Here, we re-examine the taxonomic and biogeographic affinities of bumble bees from Novaya Zemlya using historical samples and recently collected materials (1895–1925 *vs.* 2015–2017). Three bumble bee species inhabit the Yuzhny (Southern) Island and the southern edge of Severny (Northern) Island of this archipelago: *Bombus glacialis* Friese, 1902, *B. hyperboreus* Schönherr, 1809, and *B. pyrrhopygus* Friese, 1902. *Bombus glacialis* shares three unique COI haplotypes that may indicate its long-term (pre-glacial) persistence on Novaya Zemlya. In contrast, *Bombus hyperboreus* and *B. pyrrhopygus* share a rather low molecular divergence from mainland populations, with the same or closely related haplotypes as those from Arctic Siberia and Norway. A brief re-description of *Bombus pyrrhopygus* based on the newly collected topotypes is presented. Habitats, foraging plants and life cycles of bumble bees on Novaya Zemlya are characterized, and possible causes of extremely low bumble bee abundance on the archipelago are discussed. The species-poor bumble bee fauna of Novaya Zemlya is compared with those in other areas throughout the Arctic. The mean bumble bee species richness on the Arctic Ocean islands is three times lower than that in the mainland Arctic areas (3.1 *vs.* 8.6 species per local fauna, respectively).

General linear models (GLMs) indicate that this difference can be explained by specific environmental conditions of insular areas. Our findings highlight that the insularity is a significant factor sharply decreasing species richness in bumble bee assemblages on the Arctic Ocean archipelagoes through colder climate (lower summer temperatures), prevalence of harsh Arctic tundra landscapes with poor foraging resources, and in isolation from the mainland.

Introduction

Novaya Zemlya is an Arctic archipelago comprising two large islands, i.e., the Yuzhny (Southern) and Severny (Northern) islands, and numerous small islets. This huge insular area has a harsh Arctic climate (Coulson et al. 2014). Dwarf-shrub tundra and moss wetlands are the most typical assemblages for the coastal areas of the Yuzhny Island, while rocky mountain tundra covers its central range. Large mountain glaciers occupy the Severny Island, but its southern margin and narrow coastal areas are ice-free and covered by Arctic tundra landscapes (Walker et al. 2005). It was thought that Novaya Zemlya has a low level of endemism of vascular plants and terrestrial animals (Brochmann et al. 2003) and that extensive Pleistocene ice sheets did not cover the Yuzhny Island (Mangerud et al. 2008; Coulson et al. 2014).

The terrestrial invertebrate fauna of the Novaya Zemlya Archipelago is relatively poorly known, because there were few researchers compared with other areas of the Arctic (Coulson et al. 2014). However, several groups of large insects such as bumble bees have attracted the full attention of collectors even during the initial exploration period of Novaya Zemlya (Holmgren 1883; Jacobson 1898). Later, the bumble bee fauna of Novaya Zemlya was examined in a series of taxonomic and ecological works (Friese 1902, 1905, 1908, 1923; Sparre-Schneider 1909; Høeg 1924) and was discussed in subsequent reviews on bumble bees from various northern Palearctic areas (Pittioni 1942, 1943; Løken 1973; Rasmont and Iserbyt 2014; Potapov et al. 2014; Rasmont et al. 2015). Finally, a recent study confirms the status of *Bombus glacialis* as a divergent phylogenetic lineage and a putative endemic species to the Arctic Ocean islands including Novaya Zemlya (Potapov et al. 2018a).

This paper aims to re-examine the taxonomic and biogeographic affinities of bumble bees from Novaya Zemlya using newly collected samples from two sites on the Yuzhny Island. Based on our novel phylogeographic data, we suggest putative historical biogeographic scenarios explaining the origin of bumble bee fauna on Novaya Zemlya and other Arctic Ocean islands. We compare the species richness of bumble bees on the Arctic Ocean islands with that in the mainland Arctic areas and estimate a possible influence of polar climate and harsh landscapes on the low species richness of bumble bee faunas in the High Arctic using general linear modeling approach. Finally, issues concerning the current taxonomy of *Bombus glacialis*, *B. hyperboreus*, *B. pyrrhopygus*, and the entire subgenus *Alpinobombus* are critically discussed with a special focus to the newly obtained molecular sequence data from Novaya Zemlya and adjacent areas.

Materials and methods

Data sampling and morphological study

A bumble bee sample from Novaya Zemlya typically represents a daily sampling effort of a single collector in most cases, while only a few samples represent a bumble bee collection during several days (Table 1). The historical samples of bumble bees from Novaya Zemlya were studied by Grigory S. Potapov in the Natural History Museum [**NHMUK**], London, UK; Tromsø University Museum [**TMU**], Tromsø, Norway; Zoological Museum of Moscow University [**ZMMU**], Moscow, Russia; Zoological Institute of the Russian Academy of Sciences [**ZISP**], Saint Petersburg, Russia. The type locality of *B. hyperboreus* is given according to the database of the Swedish Royal Museum of Natural History (Naturhistoriska riksmuseet) [**NRM**], Stockholm, Sweden.

The recent samples of bumble bees were collected by Vitaly M. Spitsyn from two sites on the Yuzhny Island of Novaya Zemlya: Malye Karmakuly Station, 27.vii-9.viii.2015 (*N* = 13 specimens); and Bezymyannaya Bay, 19–26.vii.2017 (*N* = 23 specimens) (Figs 1–3, Tables 1–2, and Suppl. material 2: Table S3). These samples were pinned and deposited in the Russian Museum of the Biodiversity Hotspots [**RMBH**] of the Federal Center for Integrated Arctic Research of the Russian Academy of Sciences (Arkhangelsk, Russia).

The bumble bee specimens were studied using a stereomicroscope Solo 2070 (Carton Optical (Siam) Co., Ltd., Thailand). For the morphological study of samples, we applied a standard approach and terminology described by Løken (1973) and Williams et al. (2008, 2014). Images of the morphological details were taken using a stereomicroscope Leica EZ4D (Leica Microsystems GmbH, Germany).

Laboratory protocols and searching for the nearest neighbor sequences

We obtained new sequences of the *cytochrome c oxidase subunit I* (COI) gene from 27 bumble bee specimens, including the topotypes of *Bombus pyrrhopygus* (Table 3). The laboratory protocols were as described in Potapov et al. (2018a). Resulting COI gene sequences were checked manually using a sequence alignment editor (BioEdit v. 7.2.5; Hall 1999). Phylogenetic relations of the COI haplotypes were checked with the BOLD COI Full Database (BOLD thereafter) (Ratnasingham and Hebert 2007) and with the NCBI's GenBank using a Basic Local Alignment Search Tool, BLAST (Altschul et al. 1990).

Phylogeographic analyses

We used a median-joining network approach using Network v. 4.6.1.3 with default settings (Bandelt et al. 1999). Additional COI sequences of *Bombus pyrrhopygus*, *B. hyperboreus* and *B. natvigi* were obtained from the BOLD and GenBank databases (*N* = 26; Suppl. material 1, Table S1). The alignment of COI sequences was performed using the ClustalW algorithm implemented in MEGA7 (Kumar et al. 2016).
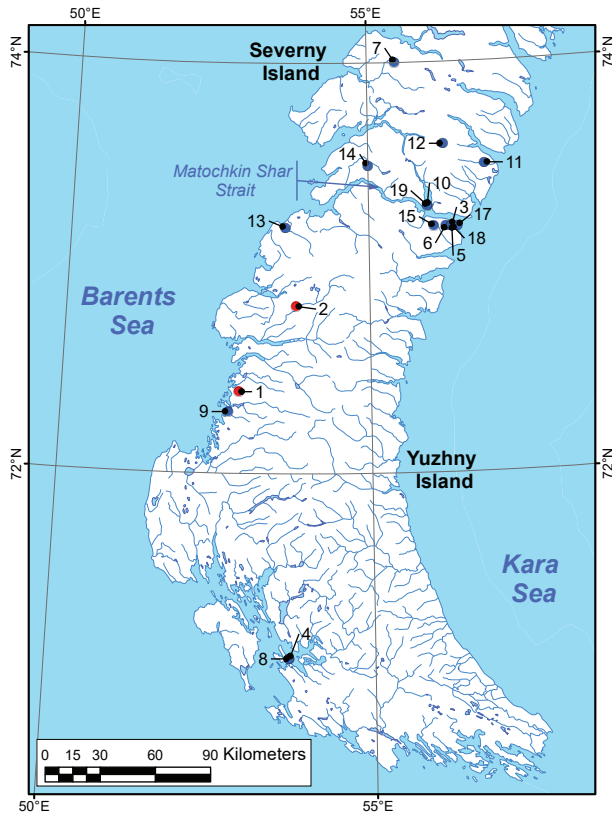
Figure 1. Map of bumble bee collecting localities on Novaya Zemlya (YI – Yuzhny Island, NI – Severny Island). Recent samples (red circles): 1 – Malye Karmakuly (YI); 2 – Bezymyannaya Bay (YI). Historical samples (blue circles): 3 – Matochkin Shar Strait (YI); 4 – Kostin Shar Strait (YI); 5 – Matochkin Shar Strait, broadcast station (YI); 6 – Matochkin Shar Strait, Nochuev Stream (YI); 7 – Krestovaya Bay (NI); 8 - Kostin Shar Strait, Propashchaya Bay (YI); 9 – Malye Karmakuly (YI); 10 – Verkhnyaya Tyulenya Bay (NI); 11 – Chekin Bay (NI); 12 – Novosiltsev Lake (NI); 13 – Peschanka River (YI); 14 – Bychkov River (NI), 15 – Matochkin Shar Strait, Poperechniy Cape (YI); 16 – Matochkin Shar Strait, coast (YI); 17 – Matochkin Shar Strait, Blizhnyaya Mountain (YI); 18 – Matochkin Shar Strait, observatory (YI).

Phylogenetic analyses

For phylogenetic analyses, we used the dataset with unique COI haplotypes of *Alpinobombus* taxa from Novaya Zemlya (Table 3) and other areas (*N* = 43; Suppl. material 1, Table S2). *Bombus ignitus*, *B. terrestris audax*, and *B. cryptarum* were used as outgroup (GenBank acc. nos. HQ228365, KT074036, and AY530013, respectively). The COI sequences were aligned using the MUSCLE algorithm of MEGA7 (Kumar et al. 2016). The phylogenetic modeling was performed with IQ-TREE (Nguyen et al. 2015) through an online web server (http://iqtree.cibiv.univie.ac.at) (Trifinopoulos et al. 2016). The best-fit evolutionary model (K3Pu+F+G4) was identified with Model Finder based on Bayesian Information Criterion (BIC) (Kalyaanamoorthy et al. 2017). Boot-

strap support (BS) values were estimated by means of an ultrafast bootstrap (UFBoot2) approach (Hoang et al. 2018). We used IQ-TREE software, because it achieves the best likelihoods compared with other similar phylogenetic programs (Zhou et al. 2018).

Species delimitation modeling

Molecular Operational Taxonomic Units (MOTUs) for the subgenus *Alpinobombus* were obtained using the multi-rate Poisson tree processes (mPTP) model of Kapli et al. (2017) for single-locus species delimitation through online mPTP server (http://mptp.h-its.org). A phylogenetic input tree was obtained from IQ-TREE analysis (see above). The mean genetic divergences (uncorrected *p*-distances) between COI haplotypes were computed in MEGA7 (Kumar et al. 2016).

Species richness modeling

To estimate the possible role of climatic parameters and insular environment for the bumble bee species richness throughout the Arctic, we applied the general linear models (GLMs; Statistica v. 13.3, Stat Soft Inc., USA). We used species richness plotted against mean air temperature as a covariate and geographic position as a factor with two levels (island *vs.* mainland) (Bolotov et al. 2018). Additionally, we computed models using type of biome as a factor with three levels (Arctic tundra *vs.* tundra *vs.* forest tundra). Monthly and annual mean air temperatures were obtained from the CRU TS v. 4.01 climate database (Climatic Research Unit, University of East Anglia) as gridded variables (0.5° resolution), which were based on weather station records during the period from 1 January 1901 to 31 December 2010 (Harris et al. 2014). Estimations of bumble bee species richness in various sites throughout the Arctic Ocean islands and the mainland were compiled from the body of reliable literature sources. The GLMs were simplified to the minimal adequate models using sequential exclusion of insignificant factors from the model (Crawley 2002). Correlation of species richness with climatic and geographic variables was calculated using Spearman's coefficients with Statistica v. 13.3.

Results

Bumble bee assemblages on Novaya Zemlya

Bumble bees are not abundant on Novaya Zemlya, with the mean value of 2.77 and 3.26 specimens per recent and historical sample, respectively (no significant differences, Mann-Whitney test: $U = 189$, $N_{recent} = 13$, $N_{historical} = 31$, $P = 0.74$) (Table 1). While three bumble bee species are known from Novaya Zemlya, i.e., *Bombus glacialis*, *B. pyrrhopygus* and *B. hyperboreus* (Table 2), the mean number of recorded species per sample is 1.62 and 1.35 in recent and historical samples, respectively (no significant differences, Mann-

Table 1. Collecting localities and samples of bumble bees from Novaya Zemlya.

Locality	N	E	Date	Collector	Number of specimens	Number of species	Depository
Recent samples							
Malye Karmakuly (YI)	72.3992	52.8671	27.vii.2015	Spitsyn	5	3	RMBH
Malye Karmakuly (YI)	72.3742	52.7806	28.vii.2015	Spitsyn	4	2	RMBH
Malye Karmakuly (YI)	72.3754	52.7241	30.vii.2015	Spitsyn	1	1	RMBH
Malye Karmakuly (YI)	72.3739	52.7167	5.viii.2015	Spitsyn	1	1	RMBH
Malye Karmakuly (YI)	72.4229	52.8143	6.viii.2015	Spitsyn	1	1	RMBH
Malye Karmakuly (YI)	72.3905	52.7167	9.viii.2015	Spitsyn	1	1	RMBH
Bezymyannaya Bay (YI)	72.8169	53.7843	21.vii.2017	Spitsyn	1	1	RMBH
Bezymyannaya Bay (YI)	72.8338	53.3781	23.vii.2017	Spitsyn	6	2	RMBH
Bezymyannaya Bay (YI)	72.8120	53.8411	23.vii.2017	Spitsyn	1	1	RMBH
Bezymyannaya Bay (YI)	72.8781	53.6303	23.vii.2017	Spitsyn	1	1	RMBH
Bezymyannaya Bay (YI)	72.8667	53.6335	19-21.vii.2017	Spitsyn	2	2	RMBH
Bezymyannaya Bay (YI)	72.8528	53.7134	19-26.vii.2017	Spitsyn	8	2	RMBH
Bezymyannaya Bay (YI)	72.8335	53.7339	19-26.vii.2017	Spitsyn	4	3	RMBH
Mean ± s.e.m.					**2.77±0.66**	**1.62±0.22**	
Historical samples							
n/a	n/a	n/a	n/a	n/a	6	2	NHMUK
Matochkin Shar Strait (YI)*	73.2	56.4	12.vii.1925	Vakulenko	1	1	HNMUK
n/a	n/a	n/a	n/a	n/a	1	1	TMU
Kostin Shar Strait (YI)*	71.1	53.7	19.vii.1895	n/a	1	1	TMU
Krestovaya Bay (NI)	74.0	55.5	10-12.viii.1909	Rusanov	1	1	ZMMU
Matochkin Shar Strait, broadcast station (YI)	73.2	56.4	3.vii.1924	Tolmachev	1	1	ZMMU
Matochkin Shar Strait, Nochuev Stream (YI)	73.2	56.3	31.vii.1925	Vakulenko	1	1	ZMMU
Kostin Shar Strait, Propashchaya Bay (YI)*	71.1	53.7	16.viii.1925	Pokrovskiy	1	1	ZMMU
Matochkin Shar Strait (YI)*	73.2	56.4	11.viii.1925	Pokrovskiy	1	1	ZMMU
Malye Karmakuly (YI)	72.3	52.7	23.vii.1896	Jacobson	10	2	ZISP
Verkhnyaya Tyulenya Bay (NI)*	73.3	56.0	9.vii.1901	Timofeev	9	1	ZISP
Chekin Bay (NI)	73.5	57.0	27.vii.1901	Timofeev	2	2	ZISP
Novosiltsev Lake (NI)*	73.6	56.3	2.viii.1901	Timofeev	1	1	ZISP
Peschanka River (YI)	73.2	53.6	22.viii.1902	n/a	1	1	ZISP
Bychkov River (NI)*	73.5	55.0	5.viii.1907	n/a	1	1	ZISP
Krestovaya Bay (NI)	74.0	55.5	10-12.viii.1909	Rusanov	5	1	ZISP
Krestovaya Bay (NI)	74.0	55.5	22.vii.1910	Sosnovskiy	7	1	ZISP
Kostin Shar Strait, Propashchaya Bay (YI)*	71.1	53.7	1-9.viii.1913	Skribov	2	2	ZISP
Matochkin Shar Strait, broadcast station (YI)	73.2	56.4	21.vi.-11.viii.1924	Tolmachev	6	2	ZISP
Matochkin Shar Strait (YI)*	73.2	56.4	13-15.vii.1924	Tolmachev	4	3	ZISP
Matochkin Shar Strait, Nochuev Stream (YI)	73.2	56.3	23.vii.1924	Tolmachev	2	2	ZISP
Matochkin Shar Strait, Poperechniy Cape (YI)	73.2	56.1	5.viii.1924	Tolmachev	5	2	ZISP
Matochkin Shar Strait (YI)*	73.2	56.4	2.vii.1925	Tolmachev	14	1	ZISP
Matochkin Shar Strait, Nochuev Stream (YI)	73.2	56.3	18.vii.1925	Tolmachev	2	1	ZISP
Matochkin Shar Strait, Nochuev Stream (YI)	73.2	56.3	1.viii.1925	Tolmachev	1	1	ZISP
Plateau (YI)*	73.2	56.3	1.viii.1925	Tolmachev	1	1	ZISP
Matochkin Shar Strait, coast (YI)*	73.2	56.4	9.vi.1925	Vakulenko	1	1	ZISP
Matochkin Shar Strait, Blizhnyaya Mountain (YI)*	73.2	56.5	21.vi.1925	Vakulenko	3	1	ZISP
Matochkin Shar Strait, observatory (YI)	73.2	56.4	29.vi.1925	Vakulenko	1	1	ZISP
Matochkin Shar Strait (YI)*	73.2	56.4	6.-15.vii.1925	Vakulenko	7	3	ZISP
Belushya Bay (NI)	73.3	56.0	5.-7.vii.1925	Vakulenko	2	1	ZISP
Mean ± s.e.m.					**3.26±0.59**	**1.35±0.11**	

Key: YI – Yuzhny Island, NI – Severny Island of the Novaya Zemlya Archipelago, *Coordinates of these localities are approximate, n/a – not available (locality, date, or collector are unknown).

Whitney test: $U = 164$, $N_{recent} = 13$, $N_{historical} = 31$, $P = 0.25$) (Table 1). Based on the recent and historical samples, *Bombus glacialis* seems to be the most commonly occurring species, while *B. pyrrhopygus* and *B. hyperboreus* have lower abundance (Table 2).

Bumble bee habitats and primary foraging resources on Novaya Zemlya

The recent samples of bumble bees were collected in three habitat types, representing rather small patches within a continuous mountain tundra landscape: (1) meadow-like associations (17 specimens, 47.2% of a total sample), (2) herb tundra patches with *Astragalus alpinus* (16 specimens, 44.4% of a total sample), and (3) herb tundra patches with *Hedysarum arcticum* (3 specimens, 8.3% of a total sample) (Fig. 2 and Suppl. material 2, Table S3). Bumble bees were not recorded beyond these types of habitats (Vitaly M. Spitsyn, personal observations, 2015–2017). The bumble bees in recent samples were primarily collected from three legume species (*Astragalus alpinus*, *A. umbellatus*, and *Hedysarum arcticum*), and one willowherb species (*Chamaenerion latifolium*) (Fig. 3). These four plant species seems to be the most important foraging resources for bumble bees in Malye Karmakuly and Bezymyannaya Bay.

Table 2. Bumble bee assemblages (total number of specimens) in historical and recent collections from Novaya Zemlya.

Locality	Year	*Bombus glacialis*		*Bombus pyrrhopygus*		*Bombus hyperboreus*	
		N	Caste composite	N	Caste composite	N	Caste composite
Recent samples							
Malye Karmakuly (YI)	2015	7	4♀, 1♂, 2☿	5	4♀, 1♂	1	1♀
Bezymyannaya Bay (YI)	2017	16	1♀, 15☿	5	4♀, 1♂	2	2♀
Total		**23**	**5♀, 1♂, 17☿**	**10**	**8♀, 2☿**	**3**	**3♀**
Historical samples							
Kostin Shar Strait (YI)	1895	1	1♀	–	–	–	–
Malye Karmakuly (YI)	1896	–	–	8	7♂,1☿	2	2♀
Verkhnyaya Tyulenya Bay (NI)	1901	9	9☿	–	–	–	–
Chekin Bay (NI)	1901	1	1♀	–	–	1	1♀
Novosiltsev Lake (NI)	1901	–	–	–	–	1	1♀
Peschanka River (YI)	1902	1	1♂	–	–	–	–
Bychkov River (NI)	1907	–	–	1	1♂	–	–
Krestovaya Bay (NI)	1909	5	1♀, 4♂,	–	–	1	1♂
Krestovaya Bay (NI)	1910	7	1♀, 4♂, 2☿,	–	–	–	
Kostin Shar Strait, Propashchaya Bay (YI)	1913	–	–	1	1♂	1	1♀
Matochkin Shar Strait (YI)	1924	2	2♀	1	1♀	1	1♀
Matochkin Shar Strait, broadcast station (YI)	1924	6	6♀	1	1♀		
Matochkin Shar Strait, Nochuev Stream (YI)	1924	1	1♀	–	–	1	1♀
Matochkin Shar Strait, Poperechniy Cape (YI)	1924	4	1♀, 2♂, 1☿	1	1☿	–	–
Matochkin Shar Strait	1925	21	11♀, 10☿	1	1♀	2	2♀
Matochkin Shar Strait, Nochuev Stream (YI)	1925	4	1♀, 1♂, 2☿	–	–	–	–
Matochkin Shar Strait, Blizhnyaya Mountain (YI)	1925	3	3♀	–	–	–	–
Matochkin Shar Strait, observatory (YI)	1925	–	–	–	–	1	1♀
Kostin Shar Strait, Propastshaya Bay (YI)	1925	–	–	–	–	1	1♀
Belushya Bay (NI)	1925	2	2♀	–	–	–	–
Total		**67**	**31♀, 12♂, 24☿**	**14**	**3♀, 9♂, 2☿**	**12**	**11♀, 1♂**

Key: YI – Yuzhny Island, NI – Severny Island of the Novaya Zemlya Archipelago. "–" indicates the lack of a species in a given sample.

Figure 2. Habitats of bumble bees on Novaya Zemlya (Yuzhny Island). (**A**) Herb tundra patch with Alpine milkvetch (*Astragalus alpinus*), Bezymyannaya Bay, 20.vii.2017. (**B**) Herb tundra patch with Arctic sweetvetch (*Hedysarum arcticum*), Bezymyannaya Bay, 29.vii.2017. (**C**) Meadow-like association with dwarf fireweed (*Chamaenerion latifolium*) along a stream valley, Bezymyannaya Bay, 26.vii.2017. (**D**) Meadow-like association on a mountain terrace, Malye Karmakuly, 28.vii.2015. Photographs by Vitaly M. Spitsyn (**A, C–D**), Elena Y. Churakova (**B**).

Phylogeny and species delimitation model for the subgenus *Alpinobombus*

The maximum likelihood phylogeny reveals that two COI haplotypes of *Bombus hyperboreus* from Novaya Zemlya cluster together with those from Norway (Fig. 4). The mPTP species-delimitation model supports almost all valid species in this genus, but the clade containing haplotypes of *Bombus hyperboreus*, *B. natvigi*, and *B. kluanensis* was considered a single MOTU (Fig. 4). The mean uncorrected COI *p*-distance between *Bombus hyperboreus* and *B. natvigi* is 1.6% (rather intraspecific difference), while those between these taxa and *B. kluanensis* are 2.1–2.4% (rather interspecific differences).

Phylogeography

Bombus hyperboreus and *B. pyrrhopygus* from Novaya Zemlya share a low molecular divergence from mainland populations, with the same or closely related haplotypes as those from Arctic Siberia and Norway (Fig. 5A–B). In particular, *Bombus pyrrhopygus* from Novaya Zemlya (Fig. 6) shares a single COI haplotype, which also occurs in
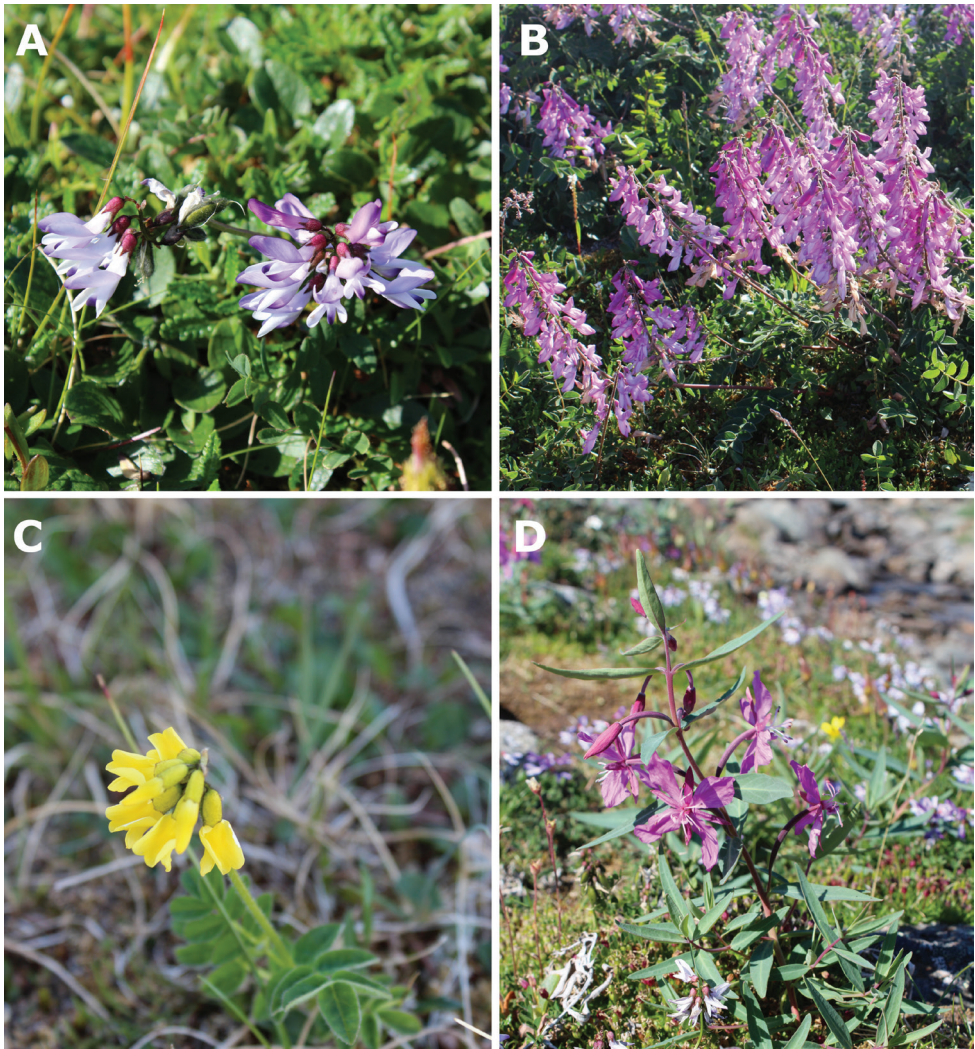
Figure 3. Primary foraging resources of bumble bees on Novaya Zemlya (Yuzhny Island, Bezymyannaya Bay). (**A**) Alpine milkvetch (*Astragalus alpinus*), 26.vii.2017. (**B**) Arctic sweetvetch (*Hedysarum arcticum*), 27.vii.2017. (**C**) Tundra milkvetch (*Astragalus umbellatus*), 20.vii.2017. (**D**) Dwarf fireweed (*Chamaenerion latifolium*), 26.vii.2017. Photographs by Vitaly M. Spitsyn.

Norway and Kamchatka (Fig. 5B). *Bombus hyperboreus* from Novaya Zemlya (Fig. 7) shares two COI haplotypes, one of which is also known from the Arctic Siberia (Yakutia), while the second haplotype was not recorded anywhere, but is genetically close to the Norwegian lineage (Fig. 5A). *Bombus glacialis* shares three unique COI haplotypes (Fig. 5C). The first haplotype (GL1) was found in 14 specimens from both recent localities, while the other two haplotypes were recorded only in three specimens from Bezymyannaya Bay (Table 3).
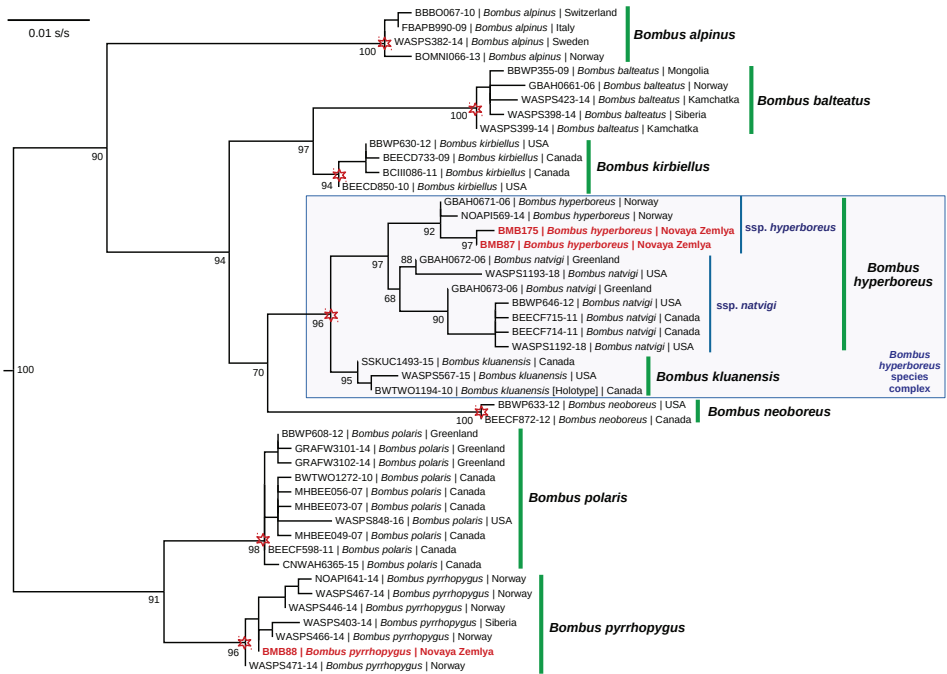
Figure 4. Maximum likelihood (IQ-TREE) phylogeny of the subgenus *Alpinobombus* based on the COI gene haplotypes. The red asterisks indicate the putative species-level clades supported by mPTP species-delimitation model. The black numbers near nodes are ultrafast bootstrap support values. The haplotypes from Novaya Zemlya are colored red. The *Bombus hyperboreus* species complex with two valid species is colored light blue. Outgroup is not shown.

Bumble bee species richness in the Arctic

The number of bumble bee species on islands of the Arctic Ocean varies from one (Devon Island, Canadian Arctic Archipelago) to seven (Iceland) species, while local faunas in the mainland Arctic areas contains from three (Taymyr Peninsula, Arctic Siberia) to 15 (Pechora River Delta in Arctic European Russia) species (Table 4). We found that the mean bumble bee species richness on the Arctic islands is three times lower than that in the mainland Arctic areas: 3.1 *vs.* 8.6 species per local fauna, respectively (Mann-Whitney test: $U = 16.5$, $N_{island} = 14$, $N_{mailand} = 16$, $P = 0.0001$) (Table 4). The mean temperature of July in the Arctic Ocean island localities is almost two times lower than that in the mainland Arctic localities: 6.7 °C *vs.* 12.0 °C, respectively (Mann-Whitney test: $U = 22.0$, $N_{island} = 14$, $N_{mailand} = 16$, $P = 0.0002$) (Table 4). The annual mean temperature in the insular localities is also slightly lower than that in the mainland localities: -11.7 °C *vs.* -7.5 °C, respectively (Mann-Whitney test: $U = 64.0$, $N_{island} = 14$, $N_{mailand} = 16$, $P = 0.0472$) (Table 4).
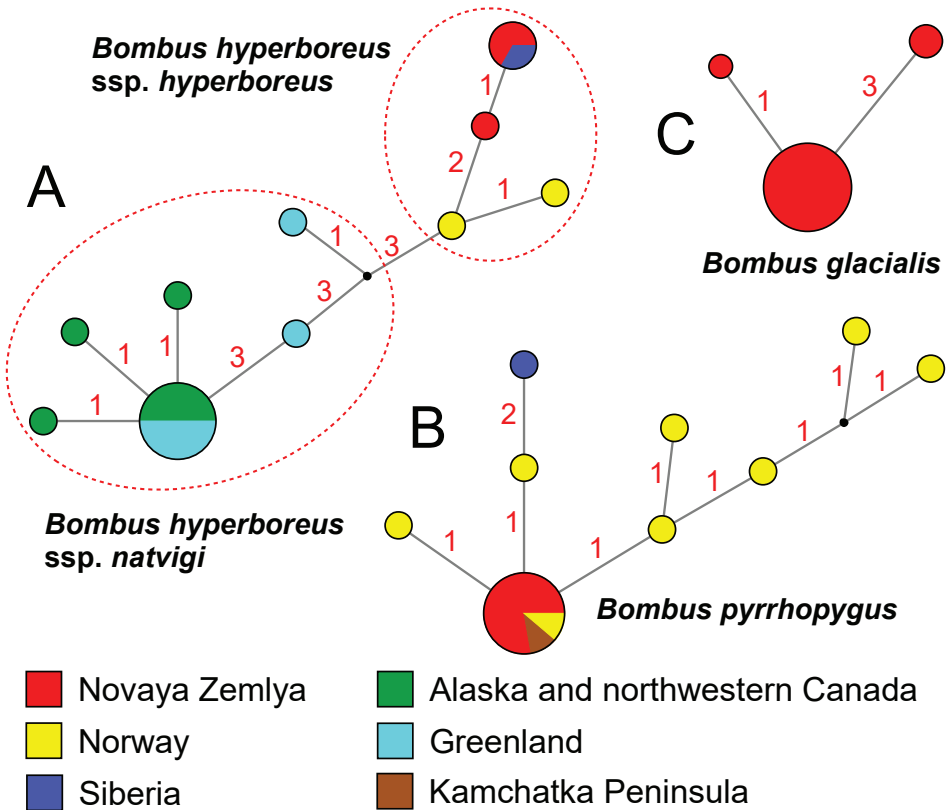
Figure 5. Median-joining haplotype networks of the available COI sequences of bumble bees from Novaya Zemlya and other Arctic areas. (**A**) *Bombus hyperboreus*. (**B**) *B. pyrrhopygus*. (**C**) *B. glacialis*. The circle size is proportional to the number of available sequences belonging to a certain haplotype (smallest circle = one sequence). The small black dots indicate hypothetical ancestral haplotypes. Red numbers near branches indicate the number of nucleotide substitutions between haplotypes.

The bumble bee species richness is correlated with latitude (Spearman R = -0.39, N = 30, P = 0.0325), annual mean air temperature (Spearman R = 0.4219, N = 30, P = 0.0202), and July mean air temperature (Spearman R = 0.7537, N = 30, P < 0.0001). As the mean temperature of July was found to be the most influential factor based on the nonparametric correlation analyses, we have used this parameter in the general linear models (GLMs) (Table 5). Results of the GLMs indicate that the bumble bee species richness in the Arctic is significantly influenced by the mean temperature of July (Table 5). The island position is an indirect significant factor, which is associated with the lower mean temperature of July in the insular areas. Furthermore, the species richness of bumble bees is influenced by type of biome independently of the mean temperature of July.

Table 3. List of COI sequences for bumble bee specimens from Novaya Zemlya (Yuzhny Island). The list of additional sequences of bumble bees from other regions used in this study is presented in Suppl. material 1, Table S1.

Species	COI haplotype code	GenBank accession number	Specimen voucher [RMBH]	Locality
B. glacialis	GL1	KY202838	BMB78	Malye Karmakuly
B. glacialis	GL1	KY202839	BMB79	Malye Karmakuly
B. glacialis	GL1	KY202840	BMB80	Malye Karmakuly
B. glacialis	GL1	KY202841	BMB82	Malye Karmakuly
B. glacialis	GL1	KY202842	BMB83	Malye Karmakuly
B. glacialis	GL1	KY202843	BMB84	Malye Karmakuly
B. glacialis	GL1	MK530672	BMB158	Bezymyannaya Bay
B. glacialis	GL1	MK530674	BMB162	Bezymyannaya Bay
B. glacialis	GL1	MK530669	BMB153	Bezymyannaya Bay
B. glacialis	GL1	MK530670	BMB154	Bezymyannaya Bay
B. glacialis	GL1	MK530675	BMB164	Bezymyannaya Bay
B. glacialis	GL1	MK530676	BMB165	Bezymyannaya Bay
B. glacialis	GL1	MK530677	BMB166	Bezymyannaya Bay
B. glacialis	GL1	MK530678	BMB167	Bezymyannaya Bay
B. glacialis	GL2	MK530671	BMB157	Bezymyannaya Bay
B. glacialis	GL2	MK530673	BMB161	Bezymyannaya Bay
B. glacialis	GL3	MK530683	BMB172	Bezymyannaya Bay
B. pyrrhopygus [Topotype]	PY1	MK530667	BMB88	Malye Karmakuly
B. pyrrhopygus [Topotype]	PY1	MK530668	BMB90	Malye Karmakuly
B. pyrrhopygus	PY1	MK530679	BMB168	Bezymyannaya Bay
B. pyrrhopygus	PY1	MK530680	BMB169	Bezymyannaya Bay
B. pyrrhopygus	PY1	MK530681	BMB170	Bezymyannaya Bay
B. pyrrhopygus	PY1	MK530682	BMB171	Bezymyannaya Bay
B. pyrrhopygus	PY1	MK530684	BMB173	Bezymyannaya Bay
B. hyperboreus	HY1	MK530666	BMB87	Malye Karmakuly
B. hyperboreus	HY2	MK530685	BMB174	Bezymyannaya Bay
B. hyperboreus	HY2	MK530686	BMB175	Bezymyannaya Bay

Table 4. Species richness of bumble bees on the Arctic Ocean islands and the mainland.

Region	Latitude	Longitude	Biome type**	JMT, °C*	AMT, °C*	Number of species	References
Islands							
Novaya Zemlya	72.3N	52.8E	Arctic tundra	10.42	-7.48	3	This study
Vaigach Island	70.2N	59.0E	Tundra	11.38	-7.00	5	Potapov et al. (2017)
Kolguev Island	68.8N	49.2E	Tundra	13.45	-3.42	5	Kolosova and Potapov (2011); Potapov et al. (2014)
Wrangel Island	71.0N	178.5W	Arctic tundra	2.29	-12.18	3	Berezin (1990); Proshchalykin and Kupianskaya (2005)
Banks Island	71.5N	123.8W	Arctic tundra	4.45	-14.21	2	Williams et al. (2014)
Victoria Island	69.1N	105.0W	Tundra	7.46	-14.99	4	Williams et al. (2014)
Prince Patrick Island	76.1N	121.7W	Arctic tundra	3.52	-17.54	3	Williams et al. (2014)
Melville Island	75.2N	109.0W	Arctic tundra	4.03	-17.33	1	Williams et al. (2014)
Devon Island	74.6N	82.4W	Arctic tundra	3.29	-17.69	1	Chernov (2004)
Baffin Island	72.6N	77.9W	Arctic tundra	4.41	-15.98	5	Williams et al. (2014)
Southampton Island	64.2N	83.2W	Arctic tundra	8.55	-11.66	4	Williams et al. (2014)
Ellesmere Island	80.0N	85.9W	Arctic tundra	4.41	-20.38	4	Williams et al. (2014)
Greenland	69.2N	50.0W	Arctic tundra	5.44	-8.05	2	Pape (1983); Vilhelmsen (2015)
Iceland	64.0N	21.6W	Tundra	10.45	3.69	1[+6]***	Prŷs-Jones et al. (2016); Potapov et al. (2018b)

Region	Latitude	Longitude	Biome type**	JMT, °C*	AMT, °C*	Number of species	References
Mean ± s.e.m.				**6.7±1.0**	**-11.7±1.8**	**3.1±0.4**	
Mainland							
Finnmark, Norway	70.8N	29.0E	Tundra	11.66	-0.85	8	Løken (1973, 1984)
Kola Peninsula (north)	69.0N	33.1E	Tundra	12.34	-0.19	7	Paukkunen and Kozlov (2015)
Kanin Peninsula (north)	67.8N	44.1E	Tundra	14.25	-1.57	5	Kolosova and Potapov (2011); Potapov et al. (2014)
Kanin Peninsula (south)	66.6N	44.6E	Forest tundra	14.65	-1.27	14	Kolosova and Potapov (2011); Potapov et al. (2014)
Pechora River Delta	67.6N	53.0E	Forest tundra	13.09	-3.72	15	Ross (2000); Kolosova and Potapov (2011); Potapov et al. (2014)
Pymvashor Hot Springs	67.0N	60.5E	Tundra	12.82	-5.55	12	Kolosova et al. (2016)
Yugorsky Peninsula	69.7N	61.6E	Tundra	11.60	-7.08	11	Potapov et al. (2017)
Polar Ural	66.9N	65.7E	Tundra	12.71	-6.48	5	Kaygorodova (1978); Bogacheva and Shalaumova (1990); Olshvang (1992)
Taymyr Peninsula (south)	73.2N	90.5E	Tundra	10.49	-12.49	3	Chernov (1978)
Tiksi, Yakutia	71.6N	128.8E	Tundra	13.88	-16.54	6	Davydova (2003)
Indigirka River Delta	71.0N	149.0E	Tundra	10.67	-14.45	8	Shelokhovskaya (2009)
Chukotka Peninsula	64.7N	177.4E	Tundra	10.70	-7.54	7	Proshchalykin and Kupianskaya (2005)
Alaska (north)	69.4N	152.1W	Tundra	10.66	-9.17	13	Williams et al. (2014)
Mackenzie River Delta	67.5N	134.1W	Tundra	13.92	-8.98	14	Williams et al. (2014)
Coppermine River Delta	67.7N	115.1W	Tundra	9.75	-11.45	4	Williams et al. (2014)
Bathurst Inlet	66.5N	108.0W	Tundra	9.59	-12.87	5	Williams et al. (2014)
Mean ± s.e.m.				**12.0±0.4**	**-7.5±1.3**	**8.6±1.0**	

Key: *JMT – July mean temperature; AMT – annual mean temperature. Mean temperature values (1901-2010) were obtained from the CRU TS v. 4.01 climate database (Climatic Research Unit, University of East Anglia). **Types of biomes were determined using available classification schemes (Aleksandrova 1976; Olson et al. 2001; Walker et al. 2005). ***The one native bumble bee species, *Bombus jonellus*, inhabits Iceland; the other six species have recently colonized this island via human-mediated dispersal or direct introduction events (Prŷs-Jones et al. 2016; Potapov et al. 2018b). We used only the one native species in our subsequent calculations and species richness modeling.

Table 5. Results of general linear models (GLMs) of bumble bee species richness on the Arctic Ocean islands and the mainland. Regression models were simplified to the minimal adequate models (Crawley 2002).

Response variable	Source	SS	d.f.	F	P
Species richness (R² = 0.72)	Intercept	–	–	–	n.s.
	July mean temperature	734.75	1	87.02	<0.0001
	Geographic position (island vs mainland)	–	–	–	n.s.
	July mean temperature × Geographic position	60.11	1	7.12	0.0125
	Error	236.42	28		
Species richness (R² = 0.72)	Intercept	888.43	1	102.25	<0.0001
	July mean temperature	–	–	–	n.s.
	Type of biome	259.40	2	14.93	<0.0001
	July mean temperature × Type of biome	–	–	–	n.s.
	Error	234.60	27		

Taxonomic account

Order Hymenoptera
Family Apidae
Genus *Bombus* Latreille, 1802

Subgenus *Alpinobombus* Skorikov, 1914

Type species. *Apis alpina* Linnaeus (by subsequent designation)

Bombus pyrrhopygus Friese, 1902
Fig. 6A–G

Bombus kirbyellus subsp. *pyrrhopygus* Friese (1902): 495; Friese (1905): 515.
Bombus kirbyellus var. *pleuralis* sensu Friese, 1902 non Nylander, 1848: Friese (1902):
    495; Friese (1905): 515; Friese (1923): 4.
Bombus kirbyellus var. *cinctus* Friese (1911a): 456; Friese (1923): 6.
Bombus kirbyellus var. *cinctellus* Friese (1911a): 456; Friese (1923): 6.
Bombus alpinus var. *diabolicus* Friese (1911b): 571.
Bombus alpinus var. *pretiosus* Friese (1911b): 571.
Bombus kirbyellus var. *semljaensis* Friese (1923): 4.
Bombus arcticus var. *alpiniformis* Richards (1931): 13.

Type locality. Nowaja Semlja [Novaya Zemlya] (Friese 1902). It is most likely that the exact type locality was situated somewhere around the Malye Karmakuly Station, because the type series has been collected by G.G. Jacobson in the year 1896 (Friese 1905). Jacobson (1898) noted that he collected the sample of bumble bees near Malye Karmakuly.

    Type. Whereabouts unknown. Rasmussen and Ascher (2008) noted that the type is in Heinrich Friese collections, but we were unable to find it in available museums, including the NHMUK and TMU.

    Material examined (pinned specimens). *Topotypes:* NOVAYA ZEMLYA, YUZHNY ISLAND: Malye Karmakuly, 72.3992°N, 52.8671°E, meadow-like association in tundra, 2♀, Spitsyn leg. [RMBH: voucher nos. BMB88 and BMB90]; Malye Karmakuly, 72.3742°N, 52.7806°E, meadow-like association in tundra, 28.vii.2015, 1☿, Spitsyn leg. [RMBH]; Malye Karmakuly, 72.3754°N, 52.7241°E, meadow-like association in tundra, 30.vii.2015, 1♀, Spitsyn leg. [RMBH]; Malye Karmakuly, 72.3905°N, 52.7167°E, meadow-like association in tundra, 9.viii.2015, 1♀, Spitsyn leg. [RMBH]. *Other recent material examined:* NOVAYA ZEMLYA, YUZHNY ISLAND: Bezymyannaya Bay, 72.8169°N, 53.7843°E, tundra with *Astragalus alpinus*, 21.vii.2017, 1♀, Spitsyn leg. [RMBH]; Bezymyannaya Bay, 72.8338°N, 53.3781°E, tundra with *Astragalus alpinus*, 23.vii.2017, 1♀, Spitsyn
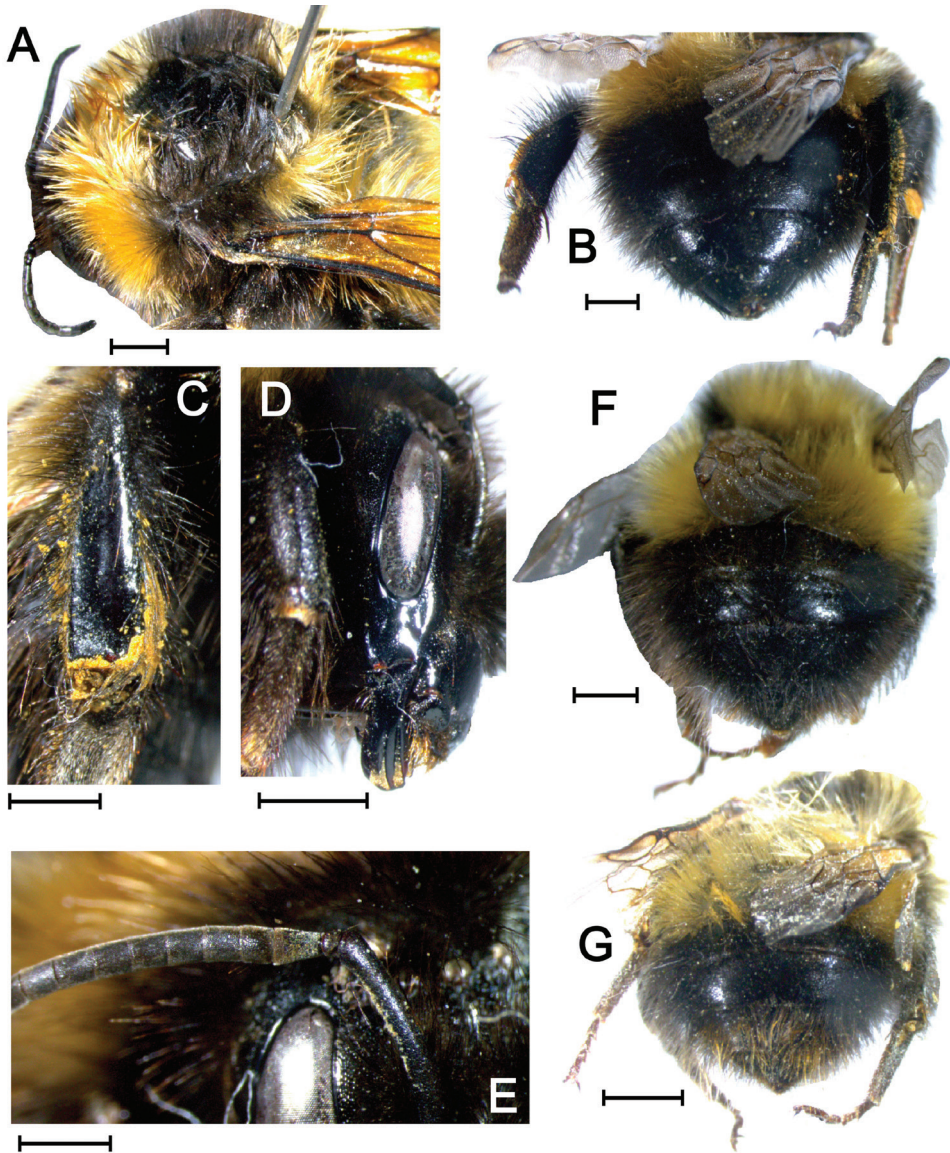
Figure 6. Morphological patterns of *Bombus pyrrhopygus* from Malye Karmakuly, Yuzhny Island, Novaya Zemlya: (**A**) Thorax (prospective topotype RMBH BMB90, queen). (**B**) Metasoma (same topotype queen). (**C**) Hind tibia (same topotype queen). (**D**) Surface of malar space (same topotype queen). (**E**) Flagellum (same topotype queen). (**F**) Metasoma (RMBH BMB88, worker). (**G**) Metasoma (RMBH BMB86, worker). Scale bars 2 mm (A-D, F-G); 1 mm (E). Photographs by Grigory S. Potapov.

leg. [RMBH]; Bezymyannaya Bay, 72.8781°N, 53.6303°E, tundra with *Hedysarum arcticum*, 23.vii.2017, 1⚥, Spitsyn leg. [RMBH]; Bezymyannaya Bay, 72.8667°N, 53.6335°E, tundra with *Hedysarum arcticum*, 19–21.vii.2017, 1♀, Spitsyn leg.

[RMBH]; Bezymyannaya Bay, 72.8335°N, 53.7339°E, meadow-like association with *Artemisia tilesii* and *Salix lanata*, 19–26.vii.2017, 1♀, Spitsyn leg. [RMBH]. *Historical material examined:* NOVAYA ZEMLYA, YUZHNY ISLAND: Matochkin Shar Strait, 11.viii.1925, 1♀, Pokrovskiy leg. [ZMMU]; Malye Karmakuly, 23.vii.1896, 1☿, 7♂, Jacobson leg. [ZISP]; Kostin Shar Strait, Propashchaya Bay, meadow-like habitat on coast, 9.viii.1913, 1♂, Skribov leg. [ZISP]; Matochkin Shar Strait, 13–15.vii.1924, 1♀, Tolmachev leg. [ZISP]; Matochkin Shar Strait, near broadcast station, 18.vii.1924, 1♀, Tolmachev leg. [ZISP]; Matochkin Shar Strait, Poperechniy Cape, 5.viii.1924, 1☿, Tolmachev leg. [ZISP]. NOVAYA ZEMLYA, SEVERNY ISLAND: Bychkov River, 5.viii.1907, 1♂, collector unknown [ZISP]. NOVAYA ZEMLYA: exact locality and date unknown, 5♀, Pittioni det. [NHMUK].

Description of the topotypes. *Queen morphology:* Malar space slightly longer than the distal width. Central part of clypeus with rather sparse puncturing, while puncturing becomes gradually denser laterally and in the lower part of clypeus. Supra-orbital line transecting ocelli. A3 distinctly longer than A4, A4 shorter than A5. Outer surface of the hind tibia distinctly alutaceous, dull. T4 and T5 chagrinated and punctured. *Queen color pattern*: Head and face black, vertex with slight admixture of yellow hairs. Collar, scutellum, T1 and T2 ochreous-yellow. T3 – T6 black. T6 with slight admixture of ferruginous hairs, which is more distinct in the specimen BMB88.

Color variations. Other specimens collected on Novaya Zemlya (Table 1 and Suppl. material 2, Table S3) share variation in an admixture of ferruginous hairs of T4 – T6. It ranges from black coloring of these tergites without ferruginous hairs to quite distinct ferruginous T4 – T6 in a worker (specimen BMB86). The latter type of coloration clearly matches the protologue of Friese (1902: 495): "Segment 4 – 6 rot behaart (ano rufo)".

Phenology. This species differs from the other Novaya Zemlya bumble bees by the shortest flight period from mid-July to mid-August, with workers and males emerging in late July (Fig. 8B).

Distribution. Arctic Eurasia from Scandinavia to Chukotka Peninsula (Williams et al. 2015, Williams 2018), including the Yuzhny Island and the southern edge of Severny Island of the Novaya Zemlya Archipelago.

Taxonomic comments. Friese (1902) briefly described this taxon as the subspecies *Bombus kirbyellus pyrrhopygus*. Later, Friese (1905) provided the primary diagnostic features of this subspecies. Currently, *B. pyrrhopygus* was considered a valid species, which is closely related to the Nearctic *B. polaris* Curtis, 1835 (Williams et al. 2015, 2016, Williams 2018). This conclusion is fully supported by our modeling (Fig. 4). Martinet et al. (2018) recently placed this species as a subspecies of *Bombus polaris* based on the similarity of the major compounds in the male cephalic labial gland secretions (CLGS). However, we disagree with this solution, because the level of genetic distance between these taxa (uncorrected COI *p*-distance = 3.2%) is too high for subspecies-level differences. Here, we consider *Bombus polaris* and *B. pyrrhopygus* as two separate species.

Bombus hyperboreus Schönherr, 1809
Fig. 7A–E

Bombus hyperboreus Schönherr (1809): 57.

Type locality. Lapponia [Lapland], Sweden

Type. Holotype NHRS-HEVA000004559, Swedish Royal Museum of Natural History (Naturhistoriska riksmuseet), Stockholm, Sweden.

Material examined (pinned specimens). *Recent material examined:* NOVAYA ZEMLYA, YUZHNY ISLAND: Malye Karmakuly, 72.3992°N, 52.8671°E, meadow-like association in tundra, 27.vii.2015, 1♀, Spitsyn leg. [RMBH]; Bezymyannaya Bay, 72.8528°N, 53.7134°E, tundra with *Astragalus alpinus*, 19–26.vii.2017, 1♀, Spitsyn leg. [RMBH]; Bezymyannaya Bay, 72.8335°N, 53.7339°E, meadow-like association with *Artemisia tilesii* and *Salix lanata*, 19–26.vii.2017, 1♀, Spitsyn leg. [RMBH]. *Historical material examined:* NOVAYA ZEMLYA, YUZHNY ISLAND: exact locality and date unknown, 1♀, Pittioni det. [NHMUK]; Kostin Shar Strait, Propashchaya Bay, 16.viii.1925, 1♀, Pokrovkiy leg. [ZMMU]; Malye Karmakuly, 23.vii.1896, 2♀, Jacobson leg. [ZISP]; Kostin Shar Strait, Propashchaya Bay, 1.viii.1913, 1♀, Skribov leg. [ZISP]; Matochkin Shar Strait, 13–15.vii.1924, 1♀, Tolmachev leg. [ZISP]; Matochkin Shar Strait, slope near Nochuev Stream, 23.vii.1924, 1♀, Tolmachev leg. [ZISP]; Matochkin Shar Strait, near observatory, 29.vi.1925, 1♀, Vakulenko leg. [ZISP]; Matochkin Shar Strait, 6.vii.1925, 12.vii.1925, 2♀, Vakulenko leg. [ZISP]. NOVAYA ZEMLYA, SEVERNY ISLAND: Krestovaya Bay, 10–12.viii.1909, 1♂, Rusanov leg. [ZMMU]; Chekin Bay, 27.vii.1901, 1♀, Timofeev leg. [ZISP]; Novosiltsev Lake, 2.viii.1901, 1♀, Timofeev leg. [ZISP].

Phenology. This species flights from late June to late August, with male appearance in mid-August (Fig. 8C), while its worker caste is lacking throughout the Arctic (Løken 1973; Lhomme and Hines 2018).

Distribution. The nominative subspecies inhabits Arctic Eurasia, including the Yuzhny Island and the southern edge of Severny Island of the Novaya Zemlya Archipelago, while *Bombus hyperboreus natvigi* is known from Arctic North America, and Greenland (Williams et al. 2015, Williams 2018; this study).

Taxonomic comments on the *Bombus hyperboreus* species complex. Three taxa belong to the *Bombus hyperboreus* species complex: *B. hyperboreus* from Arctic Eurasia (including Novaya Zemlya), *B. natvigi* from Arctic North America and Greenland, and *B. kluanensis* from Alaska and Yukon (Williams et al. 2015, 2016). These taxa are phylogenetically close to each other (Fig. 4). While Williams et al. (2015, 2016) considered *Bombus natvigi* to be a valid species using the COI gene fragment, Martinet et al. (2018) suggested that it is a subspecies of *B. hyperboreus* because of similarity in the major CLGS compounds. We used an expanded data set of COI sequences of *Bombus hyperboreus* and *B. natvigi* with two additional intermediate haplotypes from Greenland and USA that filled the molecular gap between these taxa discovered by
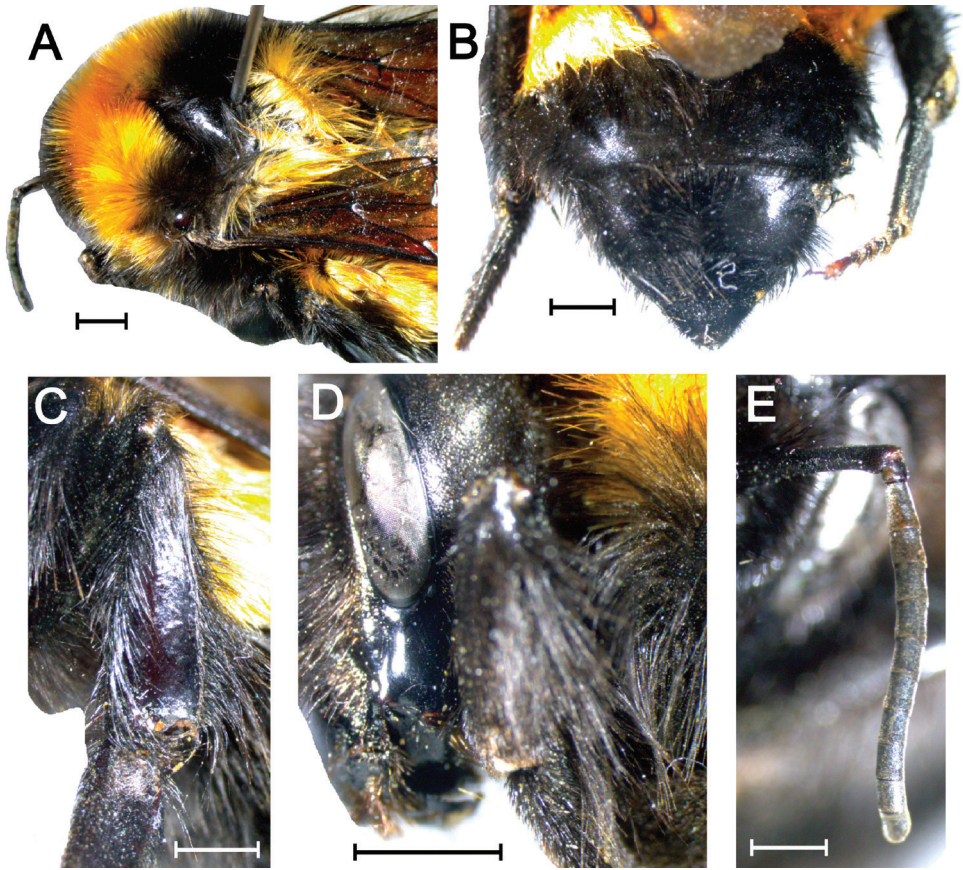
Figure 7. Morphological patterns of *Bombus hyperboreus* from Malye Karmakuly, Yuzhny Island, Novaya Zemlya (RMBH BMB87, queen). (**A**) Thorax. (**B**) Metasoma. (**C**) Hind tibia. (**D**) Surface of malar space. (**E**) Flagellum. Scale bars 2 mm (**A-D**); 1 mm (**E**). Photographs Grigory S. Potapov.

Williams et al. (2015, 2016). Our mPTP species-delimitation model houses the haplotypes of *Bombus hyperboreus*, *B. natvigi*, and *B. kluanensis* within a single MOTU (Fig. 4). Taking into account a shallow genetic divergence between *Bombus hyperboreus* and *B. natvigi*, we consider these taxa as two geographic races within the widespread *Bombus hyperboreus* that agrees with the CLGS-based concept of *Alpinobombus* developed by Martinet et al. (2018). However, *Bombus kluanensis* shares a rather high level of genetic divergence from *B. hyperboreus* and *B. natvigi* (mean uncorrected COI *p*-distances = 2.1–2.4%), and it must be considered valid species.

Subgenus *Pyrobombus* Dalla Torre, 1880

Type species. *Apis hypnorum* Linnaeus (by monotypy)

Bombus glacialis Friese, 1902

Bombus lapponicus subsp. *glacialis* Friese (1902): 495 [introduced as Sparre-Schneider's manuscript name]; Friese (1905): 515.

Bombus lapponicus sensu Friese, 1923 non Fabricius, 1793. – Friese (1923): 4.

Bombus lapponicus var. *errans* Friese, 1923: 4.

Bombus lapponicus var. *errans* var. *aberrans* Friese, 1923: 4 [intrasubspecific name (Art. 45.6.1 of ICZN), unavailable (Art. 45.5 of ICZN)].

Pratibombus glacialis Sparre-Schneider, 1902. – Skorikov (1937): 60.

Bombus glacialis Sparre-Schneider, 1902. – Panfilov (1978): 512.

Bombus glacialis Friese, 1902. – Rasmont and Iserbyt (2014); Rasmont et al. (2015): 172; Potapov et al. (2018a): 635.

Type locality. Nowaja Semlja [Novaya Zemlya] (Friese 1902).

Type. Syntype ♀ No. TSZX 7288 labelled "Nova Semlja. v. *glacialis* Sp. Schn.", Sparre-Schneider's type collection, Tromsø University Museum, Norway [examined and re-described by us (Potapov et al. 2018a)].

Material examined (pinned specimens). *Recent material examined:* NOVAYA ZEMLYA, YUZHNY ISLAND: Malye Karmakuly, 72.3992°N, 52.8671°E, meadow-like association in tundra, 27.vii.2015, 1♀, 1♂, Spitsyn leg. [RMBH]; Malye Karmakuly, 72.3742°N, 52.7806°E, meadow-like association in tundra, 28.vii.2015, 2♀, 1☿, Spitsyn leg. [RMBH]; Malye Karmakuly, 72.3739°N, 52.7167°E, meadow-like association in tundra, 5.viii.2015, 1♀, Spitsyn leg. [RMBH]; Malye Karmakuly, 72.4229°N, 52.8143°E, meadow-like association in tundra, 6.viii.2015, 1☿, Spitsyn leg. [RMBH]; Bezymyannaya Bay, 72.8338°N, 53.3781°E, tundra with *Astragalus alpinus*, 23.vii.2017, 5☿, Spitsyn leg. [RMBH]; Bezymyannaya Bay, 72.8120°N, 53.8411°E, tundra with *Astragalus alpinus*, 23.vii.2017, 1☿, Spitsyn leg. [RMBH]; Bezymyannaya Bay, 72.8667°N, 53.6335°E, tundra with *Hedysarum arcticum*, 19–21.vii.2017, 1☿, Spitsyn leg. [RMBH]; Bezymyannaya Bay, 72.8528°N, 53.7134°E, tundra with *Astragalus alpinus*, 19–26.vii.2017, 1♀, 6☿, Spitsyn leg. [RMBH]; Bezymyannaya Bay, 72.8335°N, 53.7339°E, meadow-like association with *Artemisia tilesii* and *Salix lanata*, 19–26.vii.2017, 2☿, Spitsyn leg. [RMBH]. *Historical material examined:* NOVAYA ZEMLYA, YUZHNY ISLAND: Matochkin Shar Strait, 12.vii.1925, 1♀, Vakulenko leg. [NHMUK]; Kostin Shar Strait, 19.vii.1895, 1♀, collector unknown [TMU]; Matochkin Shar Strait, near broadcast station, 3.vii.1924, 1♀, Tolmachev leg. [ZMMU]; Matochkin Shar Strait, slope near the mouth of Nochuev Stream, on *Polemonium boreale*, 31.vii.1925, 1♂, Vakulenko leg. [ZMMU]; Peschanka River, 22.viii.1902, 1♂, collector unknown [ZISP]; Matochkin Shar Strait, near broadcast station, 21.vi.1924, 3.vii.1924, 12.vii.1924, 18.vii.1924, 11.viii.1924, 5♀, Tolmachev leg. [ZISP]; Matochkin Shar Strait, 13–15.vii.1924, 2♀, Tolmachev leg. [ZISP]; Matochkin Shar Strait, slope near Nochuev Stream, 23.vii.1924, 1♀, Tolmachev leg. [ZISP]; Matochkin Shar Strait, Poperechniy Cape, 5.viii.1924, 1♀,

1♀, 2♂, Tolmachev leg. [ZISP]; Matochkin Shar Strait, on *Salix arctica*, 2.vii.1925, 2♀, Tolmachev leg. [ZISP]; Matochkin Shar Strait, on *Saxifraga oppositifolia*, 2.vii.1925, 1♀, Tolmachev leg. [ZISP]; Matochkin Shar Strait, nest of bumble bee, 2.vii.1925, 1♀, 10♀, Tolmachev leg. [ZISP]; Matochkin Shar Strait, Nochuev Stream, on *Astragalus umbellatus*, 18.vii.1925, 2♀, Tolmachev leg. [ZISP]; Matochkin Shar Strait, Nochuev Stream, 1.viii.1925; 1♀, Tolmachev leg. [ZISP]; plateau, 1.viii.1925, 1♀, Tolmachev leg. [ZISP]; Matochkin Shar Strait, coast, 9.vi.1925, 1♀, Vakulenko leg. [ZISP]; Matochkin Shar Strait, slope of Blizhnyaya Mountain, 21.vi.1925, 3♀, Vakulenko leg. [ZISP]; Matochkin Shar Strait, 6.vii.1925, 9.vii.1925, 10.vii.1925, 4♀, Vakulenko leg. [ZISP]; Matochkin Shar Strait, burrow of lemming, 15.vii.1925, 1♀, Vakulenko leg. [ZISP]. NOVAYA ZEMLYA, SEVERNY ISLAND: Verkhnyaya Tyulenya Bay, nest of bumble bee, 9.vii.1901, 9♀, Timofeev leg. [ZISP]; Chekin Bay, 27.vii.1901, 1♀, Timofeev leg. [ZISP]; Krestovaya Bay, 10–12.viii.1909, 1♀, 4♂, Rusanov leg. [ZISP]; Krestovaya Bay, 22.vii.1910, 1♀, 2♀, 4♂, Sosnovskiy leg. [ZISP]; Belushya Bay, 5.vii.1925, 7.vii.1925, 2♀, Vakulenko leg. [ZISP].

Phenology. This species has the longest flight period among Novaya Zemlya bumble bees that lasts from early June or mid-June to late August (Fig. 8A). Its workers are appeared in early July, while the flight of males starts in late July.

Distribution. Yuzhny Island and the southern edge of Severny Island of the Novaya Zemlya Archipelago, probably also Wrangel Island (Berezin 1990; Chernov 2008; Potapov et al. 2018a). The records from the Kanin Peninsula and Kolguev Island (Poppius 1908; Pittioni 1943) are highly questionable (Potapov et al. 2018a).

Taxonomic comments. The results of our previous integrative study indicate that *Bombus glacialis* is a separate bumble bee species that is phylogenetically and morphologically distinct from the other taxa in the *B. lapponicus* complex (Potapov et al. 2018a).

Discussion

Bumble bee fauna of Novaya Zemlya with taxonomic remarks on historical checklists

Three species of bumble bees were recorded from Novaya Zemlya based on recent and historical samples: *Bombus pyrrhopygus*, *B. hyperboreus*, and *B. glacialis* (Table 2). These three species were recorded from the Yuzhny Island and the southern edge of Severny Island of the Novaya Zemlya Archipelago up to 74° N (Table 1). This estimation disagrees with previous authors, whose listed two more taxa, i.e., *Bombus kirbyellus* s. lato (= *B. balteatus*) (Friese 1902, 1911a, b, 1908, 1923; Høeg 1924) and *B. lapponicus* (e.g., Friese 1908, 1923; Høeg 1924; Rasmont and Iserbyt 2014).

It is known that old European entomologists often confused *Bombus pyrrhopygus* with *B. balteatus* (= *B. kirbyellus* s. lato) due to the high levels of variability in external coloration patterns (fide Richards 1931). Based on the coloration of the 5th and 6th tergites, Friese (1902, 1908, 1923) recognised three forms of *Bombus kirbyellus*: white tailed, red tailed, and black tailed. The two latter forms were commonly recorded from Novaya Zemlya, while the white-tailed form (typical form of *B. kirbyellus* sensu Friese,
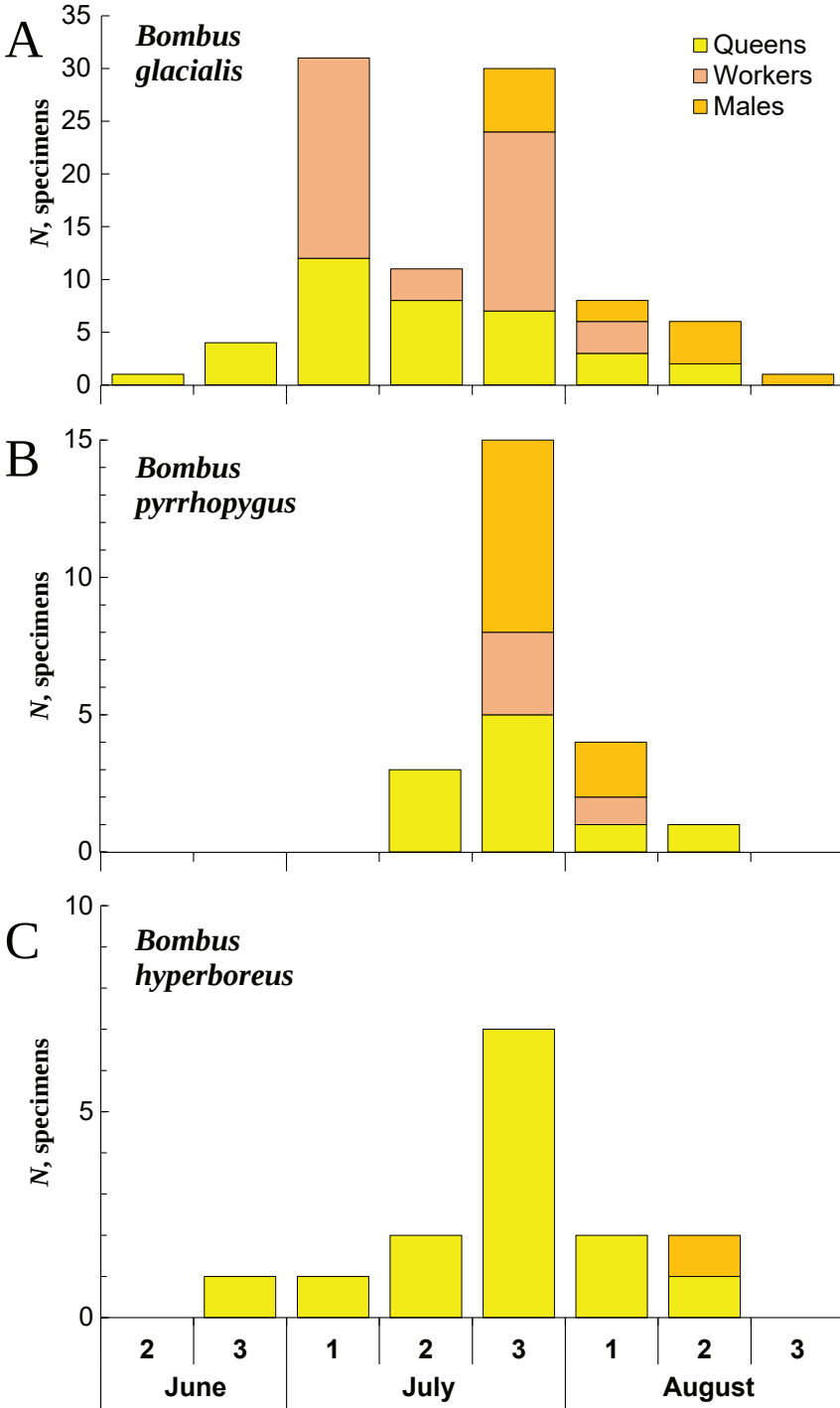
Figure 8. Phenology of bumble bees from Novaya Zemlya by ten-day periods (summary data from the historical and recent samples). (**A**) *Bombus glacialis* (*N* = 92 specimens). (**B**) *B. pyrrhopygus* (*N* = 23 specimens). (**C**) *B. hyperboreus* (*N* = 15 specimens).

1923) was not found on the archipelago (Friese 1923). Based on the morphological descriptions of Friese (1902, 1908, 1923), his white-tailed form of *Bombus kirbyellus* must be considered *B. balteatus*, while his red-tailed and black-tailed forms represent morphological varieties of *B. pyrrhopygus* (Williams et al. 2015, 2016, Williams 2018). We were also unable to find *Bombus balteatus* in recent and historical samples from Novaya Zemlya, and this species should not be included to the fauna of the archipelago.

Specimens of *Bombus lapponicus* are also lacking in recent and historical samples from Novaya Zemlya (Tables 1–3 and Suppl. material 2, Table S3), while *B. glacialis* has a quite distinct set of morphological features that allows to distinguish it from *B. lapponicus* (Chernov 2008; Potapov et al. 2018a). Based on this evidence, we can conclude that all historical records of *Bombus lapponicus* and its varieties from Novaya Zemlya (Friese 1908, 1923; Høeg 1924; Rasmont and Iserbyt 2014) actually refer to *B. glacialis*. In this study, we provide an updated synonymy of *Bombus glacialis* that includes one additional subspecific name, i.e., *B. lapponicus errans*, introduced by Friese (1923) for this biological species.

Taxonomic comments on the subgenus *Alpinobombus*

Based on newly obtained results, we suggest that this subgenus includes eight valid species as follows:

(1) *B. alpinus* (Linnaeus, 1758) [supported by the COI (Williams et al. 2015, 2016; this study) and CLGS data (Martinet et al. 2018)]

   =*B. alpinus helleri* von Dalla Torre, 1882 [Martinet et al. (2018) placed this taxon as a subspecies of *B. alpinus*. However, its molecular divergence from the Arctic populations is very shallow, and it must be treated as a synonym of *B. alpinus*]

(2)*B. balteatus* Dahlbom, 1832 [supported by the COI (Williams et al. 2015, 2016; this study) and CLGS data (Martinet et al. 2018)]

(3) *B. hyperboreus* Schönherr, 1809 [supported by the COI (Williams et al. 2015, 2016; this study) and CLGS data (Martinet et al. 2018)]

   ssp. *hyperboreus* Schönherr, 1809 [Arctic Eurasia]

   ssp. *natvigi* Richards, 1931 [Arctic North America and Greenland]

(4) *B. kluanensis* Williams & Cannings, 2016 [supported by the high level of the COI divergence (Williams et al. 2016; this study); not supported by the mPTP model (this study)]

(5) *B. kirbiellus* Curtis, 1835 [supported by the COI (Williams et al. 2015, 2016; this study) and CLGS data (Martinet et al. 2018)]

(6) *B. neoboreus* Sladen, 1919 [supported by the COI (Williams et al. 2015, 2016; this study) and CLGS data (Martinet et al. 2018)]

(7) *B. polaris* Curtis, 1835 [supported by the COI (Williams et al. 2015, 2016; this study) and CLGS data (Martinet et al. 2018)]

(8) *B. pyrrhopygus* Friese 1902 [supported by the COI data (Williams et al. 2015, 2016; this study), not supported by the CLGS data (Martinet et al. 2018)]

Comparison of the bumble bee species richness on Novaya Zemlya with other Arctic areas

Based on our assessment (Table 4), the low number of species on Novaya Zemlya seems to be a rather typical feature for the Arctic insular bumble bee faunas. A much higher species richness of bumble bees in the Icelandic fauna reflects multiple human-mediated dispersal and introduction events (Prŷs-Jones et al. 2016; Potapov et al. 2018b). Several common Eurasian Arctic species are lacking in the fauna of Novaya Zemlya, e.g., *Bombus balteatus*, *B. lapponicus*, and *B. flavidus*, while these species are known from the nearest Vaygach Island (Potapov et al. 2017). Perhaps, the Kara Strait separating the Vaigach Island from the Yuzhny Island serves as a 50 km wide marine barrier and prevents further expansion of widespread bumble bees to Novaya Zemlya and backward dispersal of *Bombus glacialis* from the archipelago. In contrast, the narrow Matochkin Shar Strait (0.6–3 km wide) between the two main islands of the archipelago does not hamper the dispersal of bumble bees as all the three species were recorded from the Severny Island (Fig. 1).

As for the mainland, sites with the highest number of bumble bee species are situated in river and mountain valleys having species-rich flowering plant associations that allows environment-induced local expansions of boreal bumble bees (e.g., *Bombus distinguendus*, *B. hortorum*, and *B. consobrinus*) to the Arctic (Shvartsman and Bolotov 2008; Kolosova and Potapov 2011; Potapov et al. 2014). In general, *Bombus lapponicus*, *B. pyrrhopygus*, *B. balteatus*, and the nominative subspecies of *B. hyperboreus* prevail in bumble bee assemblages throughout the Eurasian Arctic, with the exception of Novaya Zemlya. *Bombus glacialis*, in its turn, is the most abundant species on the Yuzhny Island of Novaya Zemlya (Potapov et al. 2018a), and probably on the Wrangel Island (Berezin 1990). *Bombus sylvicola*, *B. polaris*, *B. kirbiellus*, and *B. hyperboreus natvigi* are the most common species in the American Arctic (Proshchalykin and Kupianskaya 2005; Williams et al. 2015; Potapov et al. 2014, 2017, 2018a).

We found that the mean species richness of bumble bees on the Arctic Ocean islands is three times lower than that in the mainland Arctic areas (3.1 *vs.* 8.6 species per local fauna, respectively). Our GLMs revealed that this difference could be explained by specific environmental conditions of insular areas, i.e., the colder climate (lower mean summer temperature) and the prevalence of harsh Arctic tundra landscapes with extremely poor foraging resources. These results support the conclusion of Chernov (2008) that the level of species richness of terrestrial invertebrates (e.g., butterflies and ground beetles) in high latitudes primarily reflects summer temperatures, i.e., the mean temperature of July.

Historical biogeographic scenarios

Bombus pyrrhopygus was described from Novaya Zemlya, and we have sequenced the prospective topotypes of this species from Malye Karmakuly. The topotypes share the same COI haplotype as samples from Norway and Kamchatka, indicating a broad

range of this species across the Arctic Eurasia in the Late Pleistocene or Early Holocene. The phylogeographic pattern discovered in *Bombus hyperboreus* is similar to that in *B. pyrrhopygus*, with similar haplotypes in Novaya Zemlya and the mainland areas (Fig. 5).

The populations of *Bombus glacialis* from Novaya Zemlya share three COI haplotypes, indicating its long-term persistence on the archipelago that agrees with the hypothesis of Potapov et al. (2018a) that this species may represent a relict Pleistocene lineage adapted to living in the Arctic desert environment. These results indicate that the Yuzhny Island was ice-free during the last glacial maximum and that this remote land could have served as a cryptic glacial refugium for terrestrial and freshwater invertebrates and terrestrial plants (Serebryanny and Malyasova 1998; Mangerud et al. 2008; Coulson et al. 2014; Potapov et al. 2018a; Makhrov et al. 2019). However, several paleogeographic models suggest that Novaya Zemlya was almost completely covered with ice sheet, at least from the mid-Pleistocene (Svendsen et al. 2004; Patton et al. 2016; Ivanova et al. 2016; Hughes et al. 2016).

At first glance, we could assume that *Bombus pyrrhopygus* and *B. hyperboreus* spread across the emerged Eurasian shelf margin in the Late Pleistocene, with subsequent fragmentation of their continuous ranges in the Holocene. *Bombus glacialis* shares another phylogeographic pattern, with at least three unique COI haplotypes in Novaya Zemlya's population, while this species was not found from the mainland areas (Potapov et al. 2018a). This pattern could be explained by specific environmental preferences of this species, which is clearly linked to the Arctic desert areas (Chernov 2008; Potapov et al. 2008a). This species has the longest flight period (early June or mid-June to late August) among Novaya Zemlya bumble bees that probably reveals its better life cycle adaptation to the hard climate of the archipelago.

Low abundance of bumble bees on Novaya Zemlya and environmental features

Bumble bees are extremely scarce on Novaya Zemlya, with only a few specimens being collected per sampling effort (Table 1). This seems to be a natural feature of this area, because the mean number of specimens and species per sample does not share significant differences between the historical and recent samples (1895–1925 *vs.* 2015–2017). While the harsh polar climate itself could significantly decrease the abundance of bumble bees (see results of the GLMs above), this phenomenon could have been caused by two additional reasons. First, *Bombus glacialis* and *B. pyrrhopygus* have small colonies producing few workers (Jacobson 1898; Potapov et al. 2018a), while *B. hyperboreus* is a social parasite in the nests of *B. pyrrhopygus* and has no workers (Lhomme and Hines 2018). Second, foraging resources are patchily distributed through mountain tundra landscapes of Novaya Zemlya, and bumble bees are primarily associated with meadow-like and herb tundra communities, occupying rather small and highly fragmented areas (Figs 2–3) (Jacobson 1898; Potapov et al. 2018a; this study). The number of flowering plant species supporting bumble bees on Novaya Zemlya is low, with *Astragalus alpinus*, *A. umbellatus*, *Hedysarum arcticum*, *Oxytropis*

campestris, *Chamaenerion latifolium*, *Pedicularis sudetica*, *Silene acaulis*, and *Saxifraga oppositifolia* serving as the primary foraging resources (Jacobson 1898; Friese 1908; Høeg 1924; this study). Taking into account the low abundance of bumble bees on Novaya Zemlya, human-mediated loss of natural habitats and climate changes may seriously alter the island populations of these insects in the future.

Acknowledgements

References

Aleksandrova VD (1976) Arcticae et Antarcticae divisio geobotanica. Nauka, Leningrad, 189 pp.

Altschul SF, Gish W, Miller W, Myers EW, Lipman DJ (1990) Basic local alignment search tool. Journal of Molecular Biology 215(3): 403–410. https://doi.org/10.1016/S0022-2836(05)80360-2

Bandelt HJ, Forster P, Röhl A (1999) Median-joining networks for inferring intraspecific phylogenies. Molecular Biology and Evolution 16(1): 37–48. https://doi.org/10.1093/oxford-journals.molbev.a026036

Berezin MV (1990) Ecology and nesting of bumblebees on Wrangel Island. In: Kipyatkov VE (Ed.) Proceedings of Colloquia of All-Union Entomological Society Section for the Study of Social Insects, 1st Colloquium, Leningrad (USSR), October 1990. VIEMS, Leningrad, 19–28.

Bogacheva IA, Shalaumova EV (1990) Daily rhythm of bumblebee activity in the Polar Urals. In: Utochkin AS (Ed.) Fauna and ecology of insects in Ural: Inter-university collection of scientific papers. Perm State University, Perm, 17–26.

Bolotov IN, Makhrov AA, Gofarov MY, Aksenova OV, Aspholm PE, Bespalaya YV, Kabakov MB, Kolosova YS, Kondakov AV, Ofenböck T, Ostrovsky AN, Popov IY, von Proschwitz T, Rudzīte M, Rudzītis M, Sokolova SE, Valovirta I, Vikhrev IV, Vinarski MV, Zotin AA (2018) Climate warming as a possible trigger of keystone mussel population decline in oligotrophic rivers at the continental scale. Scientific Reports 8: 35. https://doi.org/10.1038/s41598-017-18873-y

Brochmann C, Gabrielsen TM, Nordal I, Landvik JY, Elven R (2003) Glacial survival or tabula rasa? The history of North Atlantic biota revisited. Taxon 52(3): 417–450. https://doi.org/10.2307/3647381

Chernov YI (1978) Anthophilous insects in the subzone of typical tundra in Western Taymyr and their role for pollination. In: Tikhomirov BA, Tomilin BA (Eds) Structure and function of biogeocenoses in Taymyr. Nauka, Leningrad, 264–290.

Chernov YI (2004) Terrestrial animals of polar desert in the Devon Island Plateau (the Canadian Arctic Archipelago). Zoologicheskii Zhurnal 83(5): 604–614.

Chernov YI (2008) Ecology and Biogeography. Selected works. KMK Scientific Press Ltd., Moscow, 580 pp.

Coulson SJ, Convey P, Aakra K, Aarvik L, Ávila-Jiménez ML, Babenko A, Biersma E, Boström S, Brittain JE, Carlsson A, Christoffersen KS, De Smet WH, Ekrem T, Fjellberg A, Füreder L, Gustafsson D, Gwiazdowicz DJ, Hansen LO, Hullé M, Kaczmarek L, Kolicka M, Kuklin V, Lakka H-K, Lebedeva N, Makarova O, Maraldo K, Melekhina E, Ødegaard F, Pilskog HE, Simon JC, Sohlenius B, Solhøy T, Søli G, Stur E, Tanasevitch A, Taskaeva A, Velle G, Zawierucha K, Zmudczyńska-Skarbek K (2014) The terrestrial and freshwater invertebrate biodiversity of the archipelagoes of the Barents Sea; Svalbard, Franz Josef Land and Novaya Zemlya. Soil Biology and Biochemistry 68: 440–470. https://doi.org/10.1016/j.soilbio.2013.10.006

Crawley MJ (2002) Statistical computing, an introduction to data analysis using S-plus. John Wiley and Sons Ltd., Chichester, 772 pp.

Davydova NG (2003) Fauna of bees (Hymenoptera, Apoidea) of Yakutia. PhD thesis. Saint-Petersburg, Russia: Zoological Institute of RAS.

Fabricius JC (1793) Entomologia systematica emendata et aucta. Secundum classes, ordines, genera, species adjectis synonimis, locis observationibus, descriptionibus. Tom 2. Impensis Christ. Gottl. Proft., Hafniae, 519 pp. https://doi.org/10.5962/bhl.title.122153

Friese H (1902) Die arktischen Hymenopteren, mit Ausschluss der Tenthrediniden. In: Römer F, Schaudinn F (Eds) Fauna Arctica: eine Zusammenstellung der arktischen Tierformen, mit besonderer Berücksichtigung des Spitzbergen-Gebietes auf Grund der Ergebnisse der Deutschen Expedition in das Nördlichen Eismeer im Jahre 1889. Band 2. Verlag von Gustav Fischer, Jena, 439–500.

Friese H (1905) Neue oder wenig bekannte Hummeln des Russischen Reiches (Hymenoptera). Annuaire du Musée Zoologique de l'Académie Impériale des Sciences de St.-Pétersbourg 9: 507–523.

Friese H (1908) Ueber die Bienen (Apidae) der Russischen Polarexpedition 1900–1903 und einigen anderen Arktischen Ausbeuten. Mémoires de L'Académie Impériale des Sciences de St.-Pétersbourg. VIII Série. Classe Physico-mathématique 8(13): 1–19.

Friese H (1911a) Neue Varietäten von *Bombus*. (Hym.) II. Deutsche entomologische Zeitschrift 1911: 456–457. https://doi.org/10.1002/mmnd.48019110415

Friese H (1911b) Neue Varietäten von *Bombus*. (Hym.) III. Deutsche entomologische Zeitschrift 1911: 571–572. https://doi.org/10.1002/mmnd.48019110510

Friese H (1923) Hymenoptera, Apidae. Report of the scientific results of the Norwegian expedition to Novaya Zemlya 1921 14: 3–9.

Hall TA (1999) BioEdit: a user-friendly biological sequence alignment editor and analysis program for Windows 95/98/NT. Nucleic Acids Symposium 41: 95–98.

Harris I, Jones PD, Osborn TJ, Lister DH (2014) Updated high-resolution grids of monthly climatic observations – the CRU TS 3.10 Dataset. International Journal of Climatology 34: 623–642. https://doi.org/10.1002/joc.3711

Holmgren AE (1883) Insecta a viris Doctissimis Nordenskiöld illum ducem sequentibus in insulis Waigatsch et Novaja Semlia anno 1875 collecta. Hymenoptera and Diptera. Entomologisk Tidskrift 4: 140–190.

Hoang DT, Chernomor O, von Haeseler A, Minh BQ, Vinh LS (2018) UFBoot2: Improving the Ultrafast Bootstrap Approximation. Molecular Biology and Evolution 35(2): 518–522. https://doi.org/10.1093/molbev/msx281

Hughes AL, Gyllencreutz R, Lohne ØS, Mangerud J, Svendsen JI (2016) The last Eurasian ice sheets – a chronological database and time-slice reconstruction, DATED-1. Boreas 45(1): 1–45. https://doi.org/10.1111/bor.12142

Høeg O (1924) Pollen on humble-bees from Novaya Zemlya. Report of the Scientific Results of the Norwegian Expedition to Novaya Zemlya 1921 27: 3–18.

Ivanova EV, Murdmaa IO, Emelyanov EM, Seitkalieva EA, Radionova EP, Alekhina GN, Sloistov SM (2016) Postglacial paleoceanographic environments in the Barents and Baltic seas. Oceanology 56(1): 118–130. https://doi.org/10.1134/S0001437016010057

Jacobson GG (1898) Zoological investigation on Novaya Zemlya in 1896. The insects of Novaya Zemlya. Mémoires de L'Académie Impériale des Sciences de St. Pétersbourg 8(1): 171–244.

Kalyaanamoorthy S, Minh BQ, Wong TKF, von Haeseler A, Jermiin LS (2017) Model Finder: fast model selection for accurate phylogenetic estimates. Nature Methods 14(6): 587–589. https://doi.org/10.1038/nmeth.4285

Kapli P, Lutteropp S, Zhang J, Kobert K, Pavlidis P, Stamatakis A, Flouri T (2017) Multi-rate Poisson tree processes for single-locus species delimitation under maximum likelihood and Markov chain Monte Carlo. Bioinformatics 33 (11): 1630–1638. https://doi.org/10.1093/bioinformatics/btx025

Kaygorodova MS (1978) Antecology of plants in tundra of the Polar Ural. II. The relationship between entomophilous plants and bumblebee. In: Bannikova VA (Ed.) Ecology of pollination: Inter-university collection of scientific papers. Perm State University, Perm, 3–13.

Kolosova YS, Potapov GS (2011) Bumblebees (Hymenoptera, Apidae) in the forest-tundra and tundra of Northeast Europe. Entomological Review 91(7): 830–836. https://doi.org/10.1134/S0013873811070049

Kolosova YS, Potapov GS, Skyutte NG, Bolotov IN (2016) Bumblebees (Hymenoptera, Apidae, *Bombus* Latr.) of the thermal spring Pymvashor, north-east of European Russia. Entomologica Fennica 27(4): 190–196.

Kumar S, Stecher G, Tamura K (2016) MEGA7: Molecular Evolutionary Genetics Analysis Version 7.0 for Bigger Datasets. Molecular Biology and Evolution 33(7): 1870–1874. https://doi.org/10.1093/molbev/msw054

Lhomme P, Hines HM (2018) Ecology and evolution of cuckoo bumblebees. Annals of the Entomological Society of America 1–19. https://doi.org/10.1093/aesa/say031

Løken A (1973) Studies of Scandinavian bumblebees (Hymenoptera, Apidae). Norsk Entomologisk Tidsskrift 20(1): 1–218.

Makhrov AA, Bolotov IN, Spitsyn VM, Gofarov MY, Artamonova VS (2019) Resident and anadromous forms of Arctic charr (*Salvelinus alpinus*) from North-East Europe: An example of high ecological variability without speciation. Doklady Akademii Nauk 485(2): 1–4. https://doi.org/10.1134/S1607672919020066

Mangerud J, Kaufman D, Hansen J, Svendsen JI (2008) Ice-free conditions in Novaya Zemlya 35000–30000 cal years B.P., as indicated by radiocarbon ages and amino acid racemization evidence from marine molluscs. Polar Research 27(2): 187–208. https://doi.org/10.3402/polar.v27i2.6176

Martinet B, Brasero N, Lecocq T, Biella P, Valterová I, Michez D, Rasmont P (2018) Adding attractive semio-chemical trait refines the taxonomy of *Alpinobombus* (Hymenoptera: Apidae). Apidologie 49(6): 838–851. https://doi.org/10.1007/s13592-018-0611-1

Nguyen LT, Schmidt HA, von Haeseler A, Minh BQ (2015) IQ-TREE: a fast and effective stochastic algorithm for estimating maximum-likelihood phylogenies. Molecular Biology and Evolution 32(1): 268–274. https://doi.org/10.1093/molbev/msu300

Nylander W (1848) Adnotationes in expositionem monographicam apum borealium. Meddelanden af Societatis pro fauna et flora Fennica 1: 165–282. https://doi.org/10.5962/bhl.title.66897

Olshvang VN (1992) The structure and dynamics of the insect population of the South Yamal. Nauka, Ekaterinburg, 104 pp.

Olson DM, Dinerstein E, Wikramanayake ED, Burgess ND, Powell GVN, Underwood EC, D'Amigo JA, Itoua I, Strand HE, Morrison JC, Loucks CJ, Allnutt TF, Ricketts TH, Kura Y, Lamoreux JF, Wettengel WW, Hedao P, Kassem KR (2001). Terrestrial Ecoregions of the World: A New Map of Life on EarthA new global map of terrestrial ecoregions provides an innovative tool for conserving biodiversity. BioScience 51(11), 933–938. https://doi.org/10.1641/0006-3568(2001)051[0933:TEOTWA]2.0.CO;2

Panfilov DV (1978) The keys for the species of Family Apidae – Bees. In: Medvedev GS (Ed.) The keys for insects of the European part of USSR 3(1). Nauka, Leningrad, 508–519.

Pape T (1983) Observations on nests of *Bombus polaris* Curtis usurped by *B. hyperboreus* Schönherr in Greenland (Hymenoptera: Apidae). Entomologiske Meddelelser 50: 145–150.

Paukkunen J, Kozlov MV (2015) Stinging wasps, ants and bees (Hymenoptera: Aculeata) of the Murmansk region, Northwest Russia. Entomologica Fennica 26: 53–73.

Patton H, Hubbard A, Andreassen K, Winsborrow M, Stroeven AP (2016) The build-up, configuration, and dynamical sensitivity of the Eurasian ice-sheet complex to Late Weichselian climatic and oceanic forcing. Quaternary Science Reviews 153: 97–121. https://doi.org/10.1016/j.quascirev.2016.10.009

Pittioni B (1942) Die boreoalpinen Hummeln und Schmarotzerhummeln (Hymen., Apidae, Bombinae). Teil 1. Mitteilungen aus den Königlichen Naturwissenschaftlichen Instituten in Sofia 15: 155–218

Pittioni B (1943) Die boreoalpinen Hummeln und Schmarotzerhummeln (Hymen., Apidae, Bombinae). Teil 2. Mitteilungen aus den Königlichen Naturwissenschaftlichen Instituten in Sofia 16: 1–78.

Poppius B (1908) Zur Kenntnis der Hummel-Fauna der Halbinsel Kanin. Meddelanden af Societas pro Fauna et Flora Fennica 34: 85–89.

Potapov GS, Kolosova YS, Gofarov MY (2014) Zonal distribution of bumblebee species (Hymenoptera, Apidae) in the North of European Russia. Entomological Review 94 (1): 79–85. https://doi.org/10.7868/S0044513413100103

Potapov GS, Kolosova YS, Zubriy NA, Filippov BY, Vlasova AA, Spitsyn VM, Bolotov IN, Kondakov AV (2017) New data on bumblebee fauna (Hymenoptera: Apidae, *Bombus* Latr.) of Vaygach Island and the Yugorsky Peninsula. Arctic Environmental Research 17 (4): 346–354. https://doi.org/10.17238/issn2541-8416.2017.17.4.346

Potapov GS, Kondakov AV, Spitsyn VM, Filippov BY, Kolosova YS, Zubrii NA, Bolotov IN (2018a) An integrative taxonomic approach confirms the valid status of *Bombus glacialis*, an endemic bumblebee species of the High Arctic. Polar Biology 41 (4): 629–642. https://doi.org/10.1007/s00300-017-2224-y

Potapov GS, Kondakov AV, Kolosova YS, Tomilova AA, Filippov BY, Gofarov MY, Bolotov IN (2018b) Widespread continental mtDNA lineages prevail in the bumblebee fauna of Iceland. ZooKeys 774: 141–153. https://doi.org/10.3897/zookeys.774.26466

Proshchalykin MY, Kupianskaya AN (2005) The bees (Hymenoptera, Apoidea) of the northern part of the Russian Far East. Far Eastern Entomologist 153: 1–39.

Prŷs-Jones OE, Kristjánsson K, Ólafsson E (2016) Hitchhiking with the Vikings? The anthropogenic bumblebee fauna of Iceland – past and present. Journal of Natural History 50(45–46): 2895–2916. https://doi.org/10.1080/00222933.2016.1234655

Rasmont P, Iserbyt S (2014) Atlas of the European Bees: genus *Bombus*. 3d Edition. STEP Project, Atlas Hymenoptera, Mons, Gembloux. Available at http://www.atlashymenoptera.net/page.asp?ID=169

Rasmont P, Franzén M, Lecocq T, Harpke A, Roberts SPM, Biesmeijer JC, Castro L, Cederberg B, Dvořák L, Fitzpatrick U, Gonseth Y, Haubruge E, Mahé G, Manino A, Michez D, Neumayer J, Ødegaard F, Paukkunen J, Pawlikowski T, Potts SG, Reemer M, Settele J, Straka J, Schweiger O (2015) Climatic risk and distribution atlas of European bumblebees. Biorisk 10: 1–246. https://doi.org/10.3897/biorisk.10.4749

Rasmussen C, Ascher JS (2008) Heinrich Friese (1860–1948): Names proposed and notes on a pioneer melittologist (Hymenoptera, Anthophila). Zootaxa 1833: 1–118. https://doi.org/10.11646/zootaxa.1833.1.1

Ratnasingham S, Hebert PDN (2007) BOLD: The Barcode of Life Data System (www.barcodinglife.org) Molecular Ecology Notes 7: 355–364. https://doi.org/10.1111/j.1471-8286.2007.01678.x

Richards OW (1931) Some notes on the humble-bees allied to *Bombus alpinus*, L. Tromsø Museums Årshefter 50: 1–32.

Ross M (2000) Butterflies, bumblebees and wasps. In: Eerden MRV (Ed.) Pechora Delta: structure and dynamics of the Pechora Delta ecosystems (1995–1999). University of Groningen, Groningen, 139–145.

Schönherr CJ (1809) Entomologiska anmärkningar och beskrifningar på några for Svenska fauna nya insecter. Kungliga Svenska vetenskapsakademiens handlingar 30: 48–58.

Shelokhovskaya LV (2009) Fauna and ecology of bees (Hymenoptera, Apoidea) in the tundra zone of the lower reaches of Indigirka River (north-eastern Yakutia). PhD thesis. Yakutsk, Russia: Yakutia State University.

Shvartsman YG, Bolotov IN (2008) Spatio-temporal heterogeneity of the taiga biome in the Pleistocene continental glaciations. The Ural Branch of the RAS, Ekaterinburg, 302 pp.

Serebryanny L, Malyasova E (1998) The Quaternary vegetation and landscape evolution of Novaya Zemlya in the light of palynological records. Quaternary International 45: 59–70. https://doi.org/10.1016/S1040-6182(97)00007-4

Skorikov AS (1937) Die grönländischen Hummeln im Aspekte der Zirkumpolarfauna. Entomologiske Meddelelser 20: 37–64.

Sparre-Schneider J (1909) Hymenoptera aculeata im arktischen Norwegen. Tromsø Museums Aarshefter 29: 81–160.

Svendsen JI, Alexanderson H, Astakhov VI, Demidov I, Dowdeswell JA, Funder S, Gataullin V, Henriksen M, Hjort C, Houmark-Nielsen M, Hubberten HW, Ingolfsson O, Jakobsson M, Kjær KH, Larsen E, Lokrantz H, Lunkka JP, Lyså A, Mangerud J, Matiouchkov A, Murray A, Möller P, Niessen F, Nikolskaya O, Polyak L, Saarnisto M, Siegert C, Siegert MJ, Spielhagen RF, Stein R (2004) Late Quaternary ice sheet history of northern Eurasia. Quaternary Science Reviews 23: 1229–1271. https://doi.org/10.1016/j.quascirev.2003.12.008

Trifinopoulos J, Nguyen LT, von Haeseler A, Minh BQ (2016) W-IQ-TREE: a fast online phylogenetic tool for maximum likelihood analysis. Nucleic Acids Research. 44(1): 232–235. https://doi.org/10.1093/nar/gkw256

Vilhelmsen L (2015) Apidae (Apoidea) (Bees) In: Böcher J, Kristensen NP, Pape T, Vilhelmsen L (Eds.) The Greenland entomofauna: an identification manual of insects, spiders and their allies. Fauna Entomologica Scandinavica 44: 254–256.

Walker DA, Raynolds MK, Daniëls FJA, Einarsson E, Elvebakk A, Gould WA, Katenin AE, Kholod SS, Markon CJ, Melnikov ES, Moskalenko NG, Talbot SS, Yurtsev BA (2005) The Circumpolar Arctic vegetation map. Journal of Vegetation Science 16: 267–282. https://doi.org/10.1111/j.1654-1103.2005.tb02365.x

Williams PH, Cameron SA, Hines HM, Cederberg B, Rasmont P (2008) A simplified subgeneric classification of the bumblebees (genus *Bombus*). Apidologie 39: 46–74. https://doi.org/10.1051/apido:2007052

Williams PH, Thorp RW, Richardson LL, Colla SR (2014) Bumble Bees of North America: An Identification Guide. Princeton University Press, Princeton, 208 pp.

Williams PH, Byvaltsev AM, Cederberg B, Berezin MV, Ødegaard F, Rasmussen C, Richardson LL, Huang J, Sheffield CS, Williams ST (2015) Genes Suggest Ancestral Colour Polymorphism are Shared Across Morphologically Cryptic Species in Arctic bumblebees. PLoS ONE 10(12): e0144544 1–26 pp. https://doi.org/10.1371/journal.pone.0144544

Williams PH, Cannings SG, Sheffield CS (2016) Cryptic subarctic diversity: a new bumblebee species from the Yukon and Alaska (Hymenoptera: Apidae). Journal of natural history 50 (45–46): 2881–2893. https://doi.org/10.1080/00222933.2016.1214294

Williams PH (2018) Bumblebees of the World. London. http://www.nhm.ac.uk/research-curation/projects/bombus/index.html

Zhou X, Shen XX, Hittinger CT, Rokas A (2018) Evaluating Fast Maximum Likelihood-Based Phylogenetic Programs Using Empirical Phylogenomic Data Sets. Molecular Biology and Evolution 35 (2): 486–503. https://doi.org/10.1093/molbev/msx302

Supplementary material 1

Tables S1–S2. Lists of the COI gene sequences

Authors: Grigory S. Potapov, Alexander V. Kondakov, Boris Yu. Filippov, Mikhail Yu. Gofarov, Yulia S. Kolosova, Vitaly M. Spitsyn, Alena A. Tomilova, Natalia A. Zubrii, and Ivan N. Bolotov

Data type: molecular sequence data

Link: https://doi.org/10.3897/zookeys.866.35084.suppl1

Supplementary material 2

Table S3. Samples of bumble bees from Novaya Zemlya examined in this study

Authors: Grigory S. Potapov, Alexander V. Kondakov, Boris Yu. Filippov, Mikhail Yu. Gofarov, Yulia S. Kolosova, Vitaly M. Spitsyn, Alena A. Tomilova, Natalia A. Zubrii, and Ivan N. Bolotov

Data type: specimen data

Link: https://doi.org/10.3897/zookeys.866.35084.suppl2

RESEARCH ARTICLE

A new species of *Pheidole* (Formicidae, Myrmicinae) from Dominican amber with a review of the fossil records for the genus

Alexandre Casadei-Ferreira[1], Julio C.M. Chaul[2], Rodrigo M. Feitosa[1]

1 *Laboratório de Sistemática e Biologia de Formigas, Departamento de Zoologia, Universidade Federal do Paraná, Avenida Francisco Heráclito dos Santos, s/n, Centro Politécnico, Mailbox 19020, 81531-980, Curitiba, Brazil* **2** *Pós-Graduação em Ecologia, Departamento de Biologia Geral, Universidade Federal de Viçosa, 36570-900, Viçosa, MG, Brazil*

Corresponding author: *A Casadei-Ferreira* (alexandrefrreira@gmail.com)

Citation: Casadei-Ferreira A, Chaul JCM, Feitosa RM (2019) A new species of Pheidole (Formicidae, Myrmicinae) from Dominican amber with a review of the fossil records for the genus. ZooKeys 866: 117–125. https://doi.org/10.3897/zookeys.866.35756

Abstract

Pheidole comprises approximately 1,000 extant species distributed worldwide, being particularly diverse in the New World. In addition to its high diversity and ecological prevalence, the genus is also characterized by the predominantly intraspecific dimorphism, with major and minor workers. Currently, five fossil species are known, all of which are represented only by minor workers. A new species, †*Pheidole anticua* **sp. nov.**, is described from Dominican amber, based on a major worker. Additionally, the identity of the currently known fossil species in *Pheidole* is discussed and †*P. cordata* from Baltic amber is considered as incertae sedis, resulting in no *Pheidole* species currently recognized for Baltic amber

Keywords

Miocene, morphological diversity, new status, taxonomy

Introduction

Pheidole Westwood 1839 is the largest myrmicine ant genus with 1,047 species worldwide (Bolton 2019). Species in this genus are generally characterized by conspicuous dimorphism, with major and minor workers. Currently, five fossil species of *Pheidole* are

known: †*Pheidole primigenia* Baroni Urbani, 1995 and †*Pheidole tethepa* Wilson, 1985 from Dominican amber (Early Miocene) dated from 16–19 mya (Seyfullah et al. 2018); †*Pheidole tertiaria* Carpenter, 1930 based on compression fossils from the Florissant in Colorado (Late Eocene) dating from 34.07 ± 10 mya (Evanoff et al. 2001); †*Pheidole rasnitsyni* Dubovikoff, 2011 originally described as a Baltic amber fossil, but now recognized as a copal inclusion (Perkovsky 2016); and †*Pheidole cordata* (Holl 1829) described from the Baltic amber (Late Eocene) dating from 34–48 mya (Seyfullah et al. 2018). All fossil records mentioned for *Pheidole* so far are exclusively represented by minor workers. Here we describe a new species of *Pheidole* for the Dominican amber based on a major worker. We also propose changes to the status of the other fossil species in the genus.

Material and methods

The studied inclusion was originally immersed in a 26 × 14 × 14 mm, orange, oval Dominican amber piece with a fragmentary specimen of Psocoptera as a syninclusion, which was lost after treatment of the stone. This piece was faceted and polished for better visualization using increasingly finer sandpapers and, lastly, liquid silver polishing on a soft, clean, and dry cloth. The specimen was bought from the eBay store "ambergalleryboutique1" in July 2017. The seller confirmed that the specimen was mined in "La Toca" site. The specimen had the morphospecies code "*Pheidole* ufv-65" from 2017 to 2019 on Antweb.

The holotype is deposited at the Padre Jesus Santiago Moure Entomological Collection of the Universidade Federal do Paraná, Curitiba, Brazil (**DZUP**). Observations were made at 80× magnification with a Zeiss SteREO Discovery.V8 dissecting microscope. Measurements were made with a dual-axis micrometer stage with output in increments of 0.001 mm. All measurements are given in mm. The high-resolution images were made with an Axiocam 305 color camera coupled to a Zeiss SteREO Discovery.V20. Extended depth focus was made with Zen Blue v.2.3 and subsequently treated to correct for brightness and contrast. Digital vectorization was based on original photographs.

We adopted morphological terminology and measurements proposed by Longino (2009) and sculpture terminology by Harris (1979).

Results

†*Pheidole anticua* sp. nov.
http://zoobank.org/DB5554BA-36B6-4105-988E-DF1D2F284E93
Figures 1, 2

Holotype major worker. Dominican Republic, "La Toca" mine (ANTWEB1038178) [DZUP].

Holotype conditions. After treatment, the amber piece is now a 15 × 10 × 5 mm, roughly pyramidal structure, glued in a perspex card, and pinned. The specimen pre-
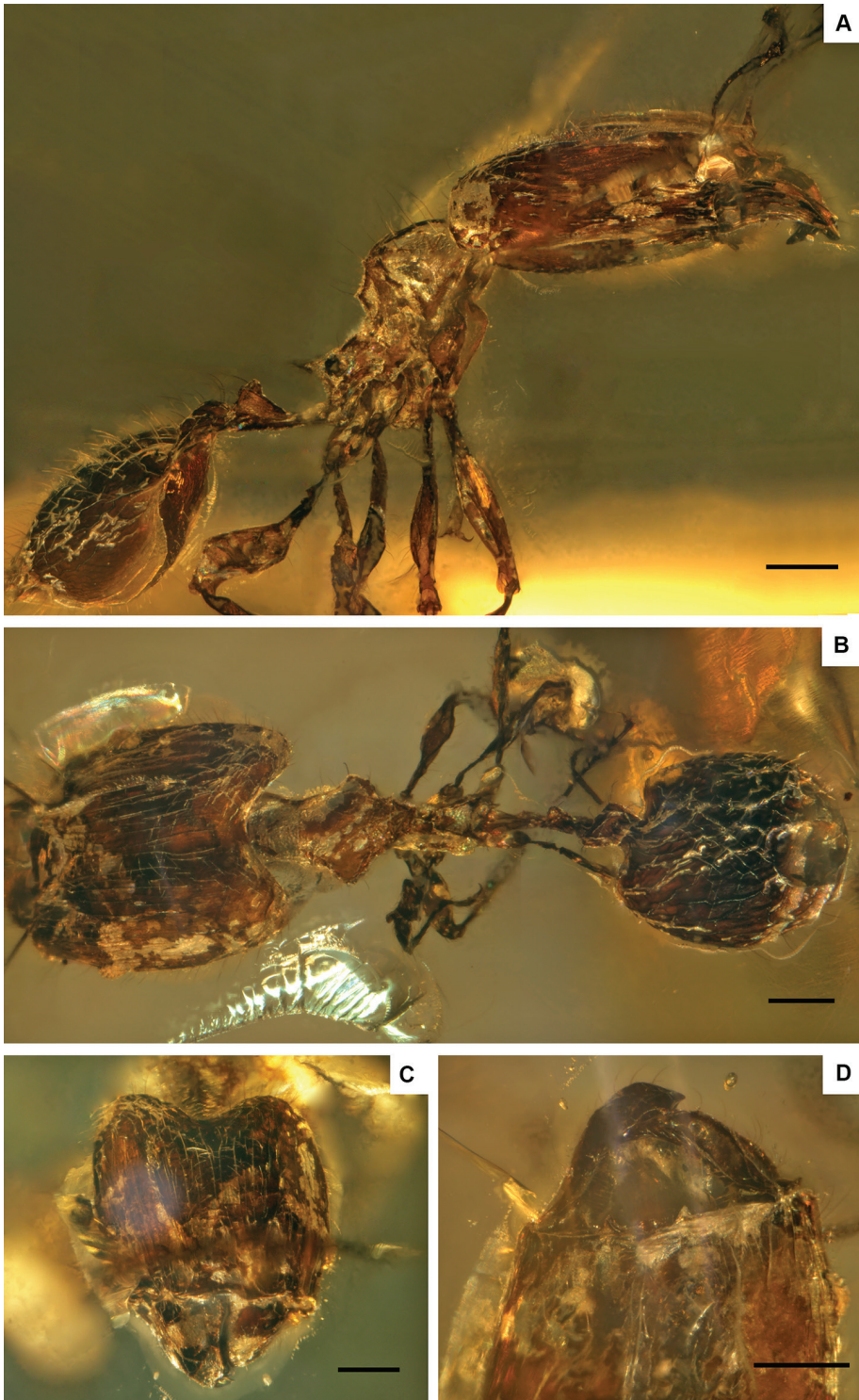
Figure 1. †*Pheidole anticua* sp. nov. **A** Lateral view **B** dorsal view **C** full face view and **D** hypostomal margin. Scale bars: 0.2 mm.
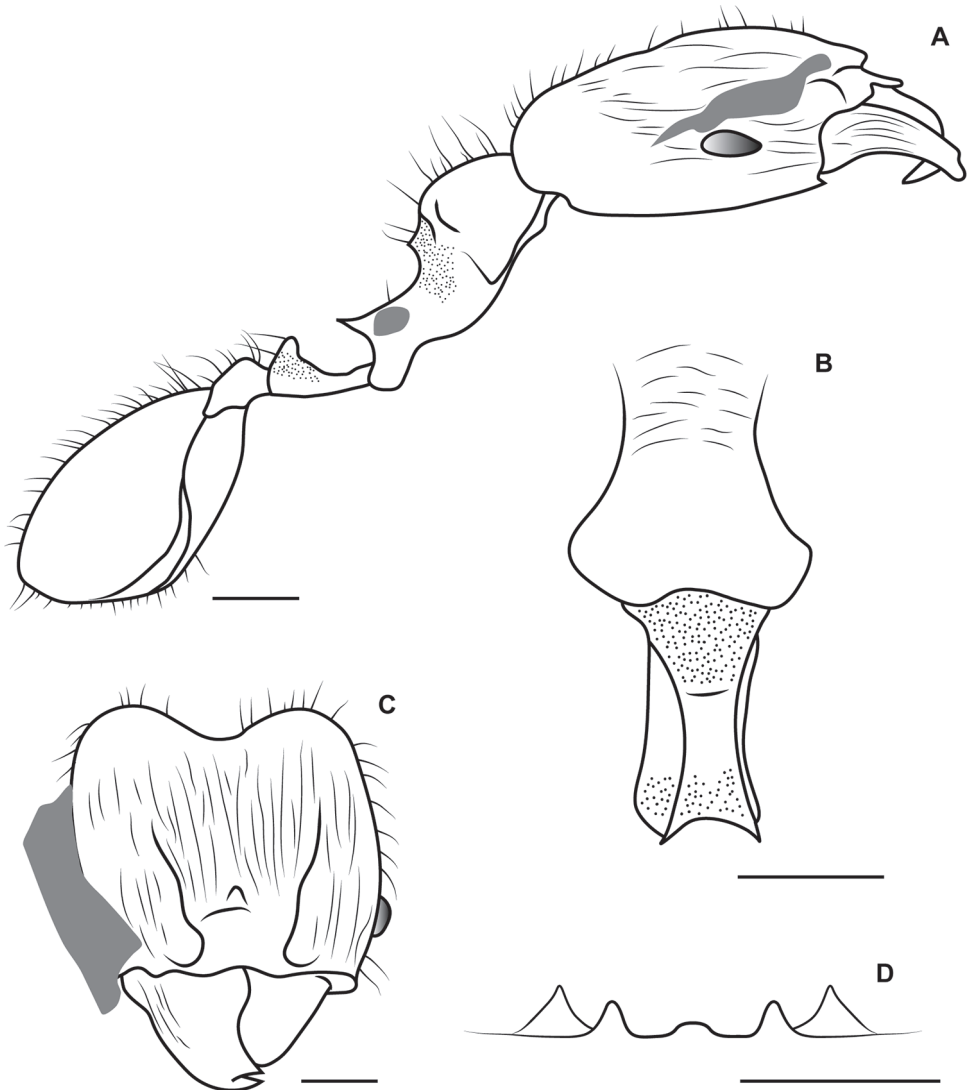
Figure 2. Illustrations of †*Pheidole anticua* sp. nov. **A** Lateral view **B** full face view **C** dorsal view and **D** hypostomal margin. Scale bars: 0.2 mm.

sents discrete to moderate distortions in the antennae, mesosoma (especially in the propodeum), legs, waist and gaster. Additionally, head vertexal margin and gaster present abundant compression wrinkles. The inclusion also presents several bubbles, and a smalls internal fractures on the matrix close to the right lateral margin of head which hamper prefect visualization.

Diagnosis. Among the extant *Pheidole* species, †*P. anticua* shares some features with members of the *flavens* group, which is characterized by small size, short antennal scape, thick antennal club, compact body, and vestigial or absent mesonotal convexity. Some of the extant and morphologically similar species are *Pheidole arhuaca* Forel, *Pheidole*

nitidicollis Emery, *Pheidole flavens* Roger, *Pheidole jamaicensis* Wheeler, W.M., *Pheidole schmalzi* Emery, and *Pheidole tambopatae* Wilson. However, all these species, except for *P. jamaicensis*, present shorter scapes when compared to †*P. anticua*. Additionally, unlike *P. flavens*, †*P. anticua* has a projecting and slightly angulate humerus (like *P. arhuaca, P. nitidicollis, P. jamaicensis, P. schmalzi,* and *P. tambopatae*). Compared with the other five species, †*P. anticua* has different mesosomal sculpture, with a smooth and shiny pronotum but sculptured mesonotum. †*P. anticua* cannot be assigned as the major worker of †*P. primigenia* and †*P. tethepa* due to the absence of humeral spines and the comparatively small body size (considering the average size proportion between *Pheidole* minor and major workers).

Measurements (holotype): HL 0.75, HW 0.71, SL 0.5, EL 0.11, ML 0.63, PSL 0.12, PTW 0.06, PPW 0.15, CI 95, SI 70.

Description. Lateral margins of head, in full face view, slightly convex; with abundant hairs extending laterally. Dorsum of mandible with basal area costate and the remaining surface smooth and shiny. Hypostomal margin straight; with median process vestigial and broad, submedian processes conspicuous, narrow and straight, distant from outer processes. Clypeus, in frontal view, with anterior notch; surface uniformly smooth and shiny. Scape length not surpassing the mid-height between the eyes and the fronto-vertexal lobes; with decumbent to erect hairs. Malar area, in full-face view, with some curved costae near antennal fossae, gradually becoming longitudinal near lateral margins of head. Frons, in full-face view, uniformly costate longitudinally. Antennal scrobe, in full-face view, shallow, internally costate longitudinally, not delimited posteriorly by a curved costulae. Vertexal margin deep, with narrow and strongly convex lobe; surface smooth and shiny.

Humerus, in dorsal-oblique view, projected and slightly angulate; with flexuous hair as long as the adjacent ones. Pronotal profile flat; surface completely smooth and shiny; with abundant long, flexuous and dark hairs. Mesonotum, in lateral view, projected and angulate, abruptly inclined posteriorly; with surface areolate. Katepisternum surface areolate. Propodeum, in lateral view, with long, narrow inclined projections; surface entirely areolate.

Petiolar peduncle, in lateral view, with dorsal margin gradually ascending posteriorly, so that the anterior margin of the node is inconspicuous. Petiolar node, in frontal view, with dorsal margin bilobed; with abundant, long and flexuous hairs, two of which are comparatively longer than the adjacent ones. Postpetiole, in dorsal view, with lateral margins rounded, surface smooth and shiny; with abundant, long and flexuous hairs. First gastral tergum uniformly smooth and shiny; dorsally with flexuous erect to decumbent hairs, less than 1.5× the eye length.

Etymology. From Latin *anticua* meaning old.

Discussion

†*Pheidole anticua* is the first fossil species of the genus for which the major worker is described. In Wilson's (2003) monograph 22 undescribed *Pheidole* fossil specimens are cited, including majors and minors, most of which are deposited in private collections.

In the same work is an image of a major worker from the Dominican amber owned by Elizabeth J. Romans and photographed by Frank M. Carpenter (his fig. 6 on p. 11). However, it is impossible to confirm if this specimen is the same as †*P. anticua,* due to low image resolution and not direct comparison.

Castes and subcastes pose a greater challenge to palaeomyrmecology than they do to the alpha-taxonomy of modern taxa. While discussing the taxonomy of extant groups one should refrain from describing a species based on a particular caste. The same procedure is advised for the description of fossil taxa, with specimens sometimes only tentatively associated to a given species (e.g., Baroni Urbani and de Andrade 2003). However, this is not always possible due to the rarity of the material and the difficulty of finding conspecific specimens in the same deposit (e.g., *Pachycondyla oligocenica* Dlussky et al. 2015, described from only a male specimen). *Pheidole* species yet to be discovered in the Dominican amber and from other relatively young New World deposits will most likely suffer from limitations in caste association. We encourage descriptions of majors and minors of *Pheidole*, but we do not recommend descriptions based on males and queens, which will potentially be conspecifics of species already described. Informal descriptions (e.g., "*Pheidole* sp." of Baroni Urbani 1995, p.12) are highly recommended, as these will add to the knowledge of fossil fauna diversity without artificially inflating the genus taxonomically.

The fossil species †*P. primigenia* and †*P. tethepa* are unique among New World *Pheidole* for having pronotal humeral spines (Wilson 1985; Baroni Urbani 1995), a trait never found in the extant members of the genus in this region. While Wilson (1985) suggested convergent evolution of pronotal spinescence in the Neotropics (and questioned the placement of †*P. tethepa* within *Pheidole*), Baroni Urbani (1995) concluded a relationship between †*P. primigenia* and †*P. tethepa* to Old World spinescent *Pheidole* lineages was more likely. Recent molecular phylogenies have shown that four extant Old-World lineages (*aristotelis*, *quadricuspis*, *quadrispinosa*, and *bifurcata* clades) have independently evolved pronotal spinescence (Sarnat et al. 2017). This suggests that this trait, although uncommon in the genus as a whole, has arisen repeatedly a sufficient number of times to justify Wilson's hypothesis of convergent evolution of spinescence in the Neotropics.

Among the extinct species of *Pheidole*, the most dubious fossil is †*P. cordata*. Its first record in the literature is Schweigger (1819). In this work, the author listed fossils from Baltic amber and described informally and illustrated an ant with a remarkably large head, showing triangular projections on the propodeum. These projections can be interpreted as propodeal spines or teeth. However, Schweigger did not name this specimen, and some years later, Holl (1829: 140) named it as †*Formica cordata*, using the same characters as Schweigger.

Mayr (1868) transferred it to *Pheidole* (Mayr 1868), even though he believed that Schweigger's sketch was not clear and Holl's description was somewhat crude. We conclude that Holl's decision to describe this species and Mayr's placement in *Pheidole* may have been hasty. The specimen studied by Schweigger is presumably lost, which

precludes its proper placement using current genus concepts in Formicidae (Mayr 1868; Antweb 2019). Dlussky (2008) suggested treating †*Formica cordata* as Formicidae *incertae sedis*, and we concur that there is no strong reason to assume it belongs to *Pheidole*, though it is certainly a myrmicine ant. Thus, we consider †*P. cordata* as *incertae sedis* in Myrmicinae.

Among the fossil ant genera known from Baltic amber, at least two can be associated with †*P. cordata:* †*Stiphromyrmex* Wheeler and *Aphaenogaster* Mayr. Both genera are morphologically very close to *Pheidole* and are characterized by an enlarged head, 12-segmented antenna with a club of three segments, presence of propodeal spines, and a two-segmented waist (Mackay and Mackay 2002; Radchenko and Dlussky 2017).

Pheidole was inferred to have originated in the Neotropics at 58 mya with a single colonization in the Old World around 20 mya (Moreau 2008; Economo et al. 2015). Therefore, the presence of a *Pheidole* species in Baltic amber would imply an unexpectedly early dispersal of the genus to the Old World, in the Eocene or earlier. It is also important to highlight that, except for †*P. cordata*, no *Pheidole* species are currently recognized for the Baltic amber, which corroborates the current hypothesis of a New World diversification of the genus with a single event of colonization in the Old Word. In this scenario, we consider †*P. cordata* cannot be safely assigned to any known genus, mostly due to the poor knowledge about its morphology. All definitive fossil records for *Pheidole* are restricted to the New World (Table 1).

A question remains regarding the identity of the fossil species *Pheidole rasnitsyni*. Dubovikoff (2011) proposed *Pheidole rasnitsyni* from pieces assumed to be truly Baltic amber, but he latter informed Perkovsky (2016: 117) that they were actually copal. Considering the putative young age of this inclusion (< 1 mya), it is possible that *P. rasnitsyni* is a junior synonym of a modern species. To accurately ensure the identity of this species, direct comparison with extant species would be necessary. However, in addition to the traditional limitations in observing details of morphology in resin inclusions, a second problem is that *P. rasnitsyni* is known only from minor workers. This makes it extremely difficult to determine the relationship between *P. rasnitsyni* and other extant species, since the morphology of minor workers in *Pheidole* is extremely conserved, especially in the Palaearctic species. In this scenario, although we think that *P. rasnitsyni* clearly belongs to *Pheidole*, we encourage a careful analysis of its identity in the future.

Table 1. Summary of the *Pheidole* species known from the fossil record.

Species	Deposit	Caste	Period
†*Pheidole cordata* (Holl, 1829), *incertae sedis* in Myrmicinae	Baltic amber (34–48 m.y.) (Seyfullah et al. 2018)	Minor worker	Eocene
†*Pheidole tertiaria* Carpenter, 1930	Florissant, Colorado (34.07 ± 10 m.y.) (Evanoff et al. 2001)	Queen	Oligocene
†*Pheidole tethepa* Wilson, 1985	Dominican amber (16–19 m.y.) (Seyfullah et al. 2018)	Minor worker	Miocene
†*Pheidole primigenia* Baroni Urbani, 1995	Dominican amber (16–19 m.y.) (Seyfullah et al. 2018)	Minor worker	Miocene
†*Pheidole rasnitsyni* Dubovikoff, 2011	Copal (<1 Ma) (Perkovsky 2016)	Minor worker	Holocene
†*Pheidole anticua* Casadei Ferreira, Chaul & Feitosa, 2019, sp. n.	Dominican amber (16–19 m.y.) (Seyfullah et al. 2018)	Major worker	Miocene

Acknowledgments

References

AntWeb (2019) AntWeb. https://www.antweb.org [Accessed 5 April 2019]

Barden P (2017) Fossil ants (Hymenoptera: Formicidae): ancient diversity and the rise of modern lineages. Myrmecological News 24: 1–30.

Baroni Urbani C (1995) Invasion and extinction in the West Indian ant fauna revisited: the example of *Pheidole* (Amber Collection Stuttgart: Hymenoptera, Formicidae. VIII: Myrmicinae, partim). Stuttgarter Beiträge zur Naturkunde. Serie B (Geologie und Paläontologie) 222: 1–12.

Baroni Urbani C, de Andrade ML (2003) The ant genus *Proceratium* in the extant and fossil record (Hymenoptera: Formicidae). Museo Regionale di Scienze Naturali Monografie (Turin) 36: 1–492.

Bolton B (2019) An online catalog of the ants of the world. http://antcat.org [Accessed 01 July 2019]

Dlussky, GM (2008) Ants of the Tribe Formicini (Hymenoptera, Formicidae) from Late Eocene Amber of Europe. Paleontological Journal 42(5): 500–513. https://doi.org/10.1134/S0031030108050055

Dlussky GM, Rasnitsyn AP, Perfilieva KS (2015) The ants (Hymenoptera: Formicidae) of Bol'shaya Svetlovodnaya (Late Eocene of Sikhote-Alin, Russian Far East). Caucasian Entomological Bulletin 11(1): 131–152. https://doi.org/10.23885/1814-3326-2015-11-1-131-152

Dubovikoff DA (2011) The first record of the genus *Pheidole* Westwood, 1839 (Hymenoptera: Formicidae) from the Baltic amber. Russian Entomological Journal 20: 255–257. https://doi.org/10.15298/rusentj.20.3.06

Economo, EP, Klimov P, Sarnat EM, Guénard B, Lecroq B, Knowles LL (2015) Global phylogenetic structure of the hyperdiverse ant genus *Pheidole* reveals the repeated evolution of macroecological patterns. Proceedings of the Royal Society Series B 282: 1–10. https://doi.org/10.1098/rspb.2014.1416

Evanoff E, Mcintosh WC, Murphey PC (2001) Stratigraphic summary and 40Ar/39Ar Geochronology of the Florissant Formation, Colorado. In Evanoff E, Gregory Wodzicki KM, Johnson KR (Eds) Fossil flora and stratigraphy of the Florissant Formation, Colorado. Proceedings of the Denver Museum of Nature and Science 4(1): 1–16.

Holl F (1829) Handbuch der Petrefactenkunde: eine Beschreibung aller bis jetzt bekannten Versteinerungen aus dem Thier- und Pflanzenreiche. Bd. 2 [part].: P. O. Hilschersche Buchhandlung, Dresden, 489 pp.

Mayr G (1868) Die Ameisen des baltischen Bernsteins. Beiträge zur Naturkunde Preussens 1: 1–102.

Moreau CS (2008) Unraveling the evolutionary history of the hyperdiverse ant genus *Pheidole* (Hymenoptera: Formicidae). Molecular Phylogenetics and Evolution 48(1): 224–239. https://doi.org/10.1016/j.ympev.2008.02.020

Perkovsky EE (2016) Tropical and holarctic ants in Late Eocene ambers. Vestnik Zoologii 50: 111–122. https://doi.org/10.1515/vzoo-2016-0014

Radchenko A, Dlussky GM (2017) New Species of the Extinct Ant Genus *Stigmomyrmex* Mayr and Designation of the Neotype of *Stiphromyrmex robustus* (Mayr) (Hymenoptera: Formicidae: Myrmicinae). *Annales Zoologici* Museum and Institute of Zoology, Polish Academy of Sciences, 67(4): 773–780. https://doi.org/10.3161/00034541ANZ2017.67.4.012

Sarnat EM, Friedman NR, Fischer G, Lecroq-Bennet B, Economo EP (2017) Rise of the spiny ants: diversification, ecology and function of extreme traits in the hyperdiverse genus *Pheidole* (Hymenoptera: Formicidae). Biological Journal of the Linnean Society 122(3): 514–538. https://doi.org/10.1093/biolinnean/blx081

Schweigger AF (1819) Beobachtungen auf naturhistorischen Reisen. Anatomisch-physiologische Untersuchungen über Corallen; nebst einem Anhange, Bemerkungen über den Bernstein enthaltend. Reimer, Berlin, 127 pp. https://doi.org/10.5962/bhl.title.14416

Seyfullah LJ, Beimforde C, Dal Corso J, Perrichot V, Rikkinen J, Schmidt AR (2018) Production and preservation of resins – past and present. Biological Reviews 93: 1684–1714. https://doi.org/10.1111/brv.12414

Wilson EO (1985) Ants of the Dominican amber (Hymenoptera: Formicidae). 1. Two new myrmicine genera and an aberrant *Pheidole*. Psyche (Cambridge) 92: 1–9. https://doi.org/10.1155/1985/17307

RESEARCH ARTICLE

Aprica: a new genus and life history for the pteridivore *Xanthia patula* Druce, 1898 (Lepidoptera, Noctuidae)

Paul Z. Goldstein[1], Daniel H. Janzen[2], Winnie Hallwachs[2]

1 *Systematic Entomology Laboratory, USDA, National Museum of Natural History, E-502, P.O. Box 37012, MRC 168, Washington, DC 20013-7012, USA* **2** *Department of Biology, University of Pennsylvania, Philadelphia, PA 19104, USA*

Corresponding author: *Paul Z. Goldstein* (paul.goldstein@ars.usda.gov)

Citation: Goldstein PZ, Janzen DH, Hallwachs W (2019) *Aprica:* a new genus and life history for the pteridivore *Xanthia patula* Druce, 1898 (Lepidoptera, Noctuidae). ZooKeys 866: 127–145. https://doi.org/10.3897/zookeys.866.27647

Abstract

Aprica Goldstein, **gen. nov.** is described to accommodate *Xanthia patula* Druce, 1898. Recent discovery of its larva, which has been recorded eating foliage of species in six families of leptosporangiate ferns, suggest a possible subfamily assignment within the Eriopinae, but this cannot be substantiated based on adult morphology. This species has no obvious close relatives either among the core noctuid pteridivore genera currently recognized in the Eriopinae (e.g., *Callopistria* Hübner, [1821]), nor among genera more recently discovered to be fern-feeders but which remain incertae sedis with respect to subfamily (e.g., *Leucosigma* Druce, 1908, *Lophomyra* Schaus, 1911). The recorded foodplant profile is similar to that of another ambiguously placed Nearctic species *Fagitana littera (*Guenée, 1852) (Noctuidae: Noctuinae: Xylenini, incertae sedis) with which it shares no obvious synapomorphies.

Keywords

Area de Conservacion Guanacaste (ACG), Costa Rica, fern-feeder, pteridivory

Introduction

Druce (1898: 486, pl. 94, fig. 14) described *Xanthia patula* (Noctuidae) from the holotype collected in the Santa Clara Valley, Costa Rica. The species has subsequently been collected in southern Mexico and Central America. *Xanthia* is otherwise considered a

holarctic genus feeding primarily on *Salix* and *Populus* (Salicaceae). The species *patula* was placed in in *Bagisara* by Poole (1989). In his treatment of New World Bagisarinae, a subfamily with larvae associated primarily with Malvaceae, Ferguson (1997: 348) acknowledged that the species' placement was not straightforward, and returned it to *Xanthia* by default, remarking "I could not place it to genus, but am sure that the species belongs somewhere in the large assemblage long known as the Amphipyrinae but now probably within the expanded concept of the Hadeninae of recent authors (e.g., Kitching & Rawlins [1998]." Kitching and Rawlins' (1999[1998]) circumscriptions of both Amphipyrinae and Hadeninae have since been modified considerably, and for the purpose of providing context we note that they included Eriopinae, which are currently the taxonomic core of noctuids that feed on ferns (pteridivores) as a tribe within the Hadeninae. The combination *Bagisara patula* reappeared only informally among determinations made by Poole in the course of a long-term caterpillar inventory of Area de Conservacion Guanacaste (ACG), northwestern Costa Rica (Janzen and Hallwachs 2016) where, importantly, it was discovered feeding on several species of ferns. Since pteridivory (fern-feeding) occurs in few noctuid groups and is unrecorded both for Bagisarinae and for the Xylenini, in which *Xanthia* resides, we wished to evaluate whether this species shares any of the primary features of the Eriopinae. The Eriopinae are not decisively circumscribed, but a combination of numerous adult and larval features have been articulated by Poole (1995), Fibiger and Lafontaine (2005), and Yen and Wu (2009).

Materials and methods

Pinned specimens were examined with an incandescent light source. Genitalic preparations follow Clarke (1941) in part and Lafontaine (2004) but were stained with chlorazol black and slide-mounted in Euparal. Vesicae were everted prior to fixation. Dissections followed either an overnight room-temperature soak in supersaturated sodium hydroxide or a brief 15-minute heated soak and were examined with stereomicroscopes prior to slide-mounting. Wing preparations followed the procedure modified from Jaeger (2017): Following an overnight soak in a small stender dish with enough 50% EtOH solution to cover the wings and 10 drops of 6% NaCl, ethanol and bleach were added as necessary, depending on the ease with which scales could be cleared. Wings were stained overnight in Eosin Y. Photographs were made using the Microptics and Visionary Digital imaging systems and images manipulated with Adobe Photoshop (Adobe Systems, Mountain View, CA). Images of vesicae were taken in glycerin, held in a sectioned plexiglass cylinder affixed to a slide. Measurements were made with the aid of an ocular micrometer. Forewing (FW) length was measured from the center of the axillary area to the apex of the forewing. Terminology generally follows Forbes (1954) and Lafontaine (1998, 2004). The fine description of characters such as coloration, vesica, and immature stages is confined to the species description; the remainder are included in that of the genus.

Repository abbreviations

The following abbreviations refer to collections from which specimens form the basis of this study:

AMNH   American Museum of Natural History, NY, USA
MNHUK   The Natural History Museum, London, UK
USNM   National Museum of Natural History [formerly, United States National Museum], Washington, District of Columbia, USA

Results

Although some of the larval characters that can be seen in *A. patula* are consistent with those in Eriopinae, including cephalic striping, oblique lateral striping and false eyespots on the first abdominal segment (Yen and Wu 2009), they are not diagnostic, and most of the larval characters that would corroborate the assignment of *Aprica* to Eriopinae (including setal characters and features of the spinneret) are not discernible from available images. Two features in the adults consistent with Eriopinae are the expression and configuration of M2 arising from the discal cell in the hind wing (Fig. 21) and non-uniform sclerotization of the phallus (Figs 24–27), which is primarily confined apically and ventrally (Yen and Wu 2009). Abdominal hair pencils and eversible coremata on the sacculus (Fibiger and Lafontaine 2005) typical of Eriopinae are lacking. *Aprica* also lacks the conspicuous genitalic and larval features that diagnose either Bagisarinae (Ferguson 1997) such as the fused valvae and the absence of the first two pairs of abdominal prolegs; nor can it be assigned to Xylenini or, thereby, *Xanthia* based on the characters summarized by Fibiger and Lafontaine (2005: 48).

Systematics

Aprica **Goldstein, gen. nov.**
http://zoobank.org/796AEA59-E454-495E-9109-D1BD667D1863

Type species. *Xanthia patula* Druce, 1898.
    Type locality. Costa Rica.
    Etymology. *Aprica* (feminine) derives from the Latin *apricus*, sunny, open to the light.
    Diagnosis. *Aprica* may be diagnosed readily both from the appearance of the forewing and by the male and female genitalia. The bisection of the golden-orange FW and similar thoracic coloration from the sunset-reddish HW and similar abdominal coloration is distinctive. Although the male genitalia are unremarkable, the valve simple with a rudimentary, hook-like clasper, the combination of this feature with the absence of abdominal coremata, and the presence of M2 on the HW, differentiates *Aprica* from

other genera with pteridivorous species in which either the clasper is absent and the coremata present (e.g., *Callopistria*, *Phuphena* Walker, 1858); from genera with the reverse condition (e.g., *Fagitana* Walker, 1865, in which coremata are absent but which bear a complex clasping apparatus and corresponding ridge on the female 8th sternite), or in which the hindwing M2 is not expressed (e.g., *Leucosigma*, *Lophomyra*). In both *Aprica patula* and *Fagitana littera,* the corpus bursae is elongate and the ductus seminalis arises from an appendix bursae located at the posterior (proximal) end of the corpus, a condition shared by several Eriopinae but usually uninformative at the generic level.

Description. *Head.* Antennae setose, biramous in males, uniramous in females; scaled above, cupreous. Labial palpi upturned, densely scaled. Eyes naked.

Thorax. Thoracic vestiture golden orange, concolorous with forewing. *Wings.* General "background" coloration sharply bisected between forewing and hind wing, the former predominantly orange (as the thoracic vestiture) and the latter a reddish russett (as the abdominal vestiture); M2 faintly but clearly expressed on hindwing. *Legs.* One pair mid-tibial spurs, two pair on hind-tibiae; three rows of tibial spines on legs.

Abdomen. Coremata absent; without brushes, pockets, or levers.

Male genitalia. Uncus heavily setose; dorsal edges of tegumen straight, angled ventrally at roughly 45°, tegumen widest supra-medially; valvae medially situated, articulating with the vinculum in its dorsal half, setose throughout, of more or less constant width with a minor constriction at the cucullus; corona well developed; baso-costal processes of sacculus robust; clasper medially situated in valve, elongate with a sharply sclerotized apical hook at the cucullus; pleurite fused; juxta shield-shaped; transtilla well developed and paratergal sclerite evident, well fused; sacculus gently rounded.

Female genitalia. Papillae anales flanged at postero-basal edge; posterior and anterior apophyses rod-like, not swollen apically, the anterior slightly shorter than the posterior. Antrum well developed; ductus seminalis arising from the appendix bursae, appendix bursae deriving dorsally from the posterior third of the ductus bursae; ductus bursae wide, elongate, tubular, with a 360° counter-clockwise torsion immediately posterior to the corpus bursae; corpus bursae, oblong, bearing a single transverse signum.

Immature stages. Known from images of *A. patula*; see description below.

Distribution. Mexico and Central America

Aprica patula (Druce, 1898), comb. nov.
Figs 1–53

Xanthia patula Druce, 1898 in Godman and Salvin 1898: 486, pl. 94, fig. 14; Hampson, 1908: 597, pl. 121, fig. 23; Ferguson, 1997: 348.
*Bagisara patula:* Poole, 1989: 154.

Holotype locality. Costa Rica, Santa Clara Valley [BMNH].

Material examined. 38♂, 16♀ **COSTA RICA** (34♂, 15♀): The following label data precede individual unique voucher codes of the format yy-SRNP-xxxxxx (SRNP

= Santa Rosa National Park, a unique identifier coined when the inventory was confined to Sector Santa Rosa of ACG in the early 1980's) on all reared and light-trapped specimens from ACG (24♂, 9♀): Voucher: D.H. Janzen & W. Hallwachs DB: http://janzen.sas.upenn.edu Area de Conservacion Guanacaste, COSTA RICA.

All records of "on" a given plant species refer definitively to "feeding on." Specimens lacking food plant records were light trapped in the forest and have a 6-digit suffix in their SRNP codes, while reared specimens have a 1–5-digit suffix.

Alajuela Province: Area de Conservacion Guanacaste (9♂, 4♀): *Males*: Sector Rincon Rain Forest: Estacion Caribe (melina), 10.8956, -85.29558, el. 391m: 11/09/2007, F. Quesada & R. Franco, collector, 07-SRNP-110152, USNMENT01463558; Sector Rincon Rain Forest: Estacion Caribe (melina), 10.8956, -85.29558, el. 391m: 11/10/2007, F. Quesada & R. Franco, collector, 07-SRNP-110402, USNMENT01463615; Sector Rincon Rain Forest: Jabalina, Manta Pizote, 10.97325, -85.31542, el. 288m: 09/30/2008, S. Rios & H. Cambronero, collector, 08-SRNP-107404, USNMENT01463664; Sector Rincon Rain Forest: Jacobo, 10.94076, -85.3177, el. 461m: larva on *Salpichlaena volubilis*: 06/16/2014, ecl. 07/19/2014, Edwin Apu, collector, 14-SRNP-80751, USNMENT01463658; Sector Rincon Rain Forest: Manta Hugo, 10.8811, -85.2677, el. 491m: 03/14/2009, H. Cambronero & R. Franco, collector, 10-SRNP-107506, USNMENT01463699; Sector Rincon Rain Forest: Protrero Chaves, 10.93868, -85.32167, el. 433m: 8/19/2009, F. Quesada & H. Cambronero, collector, 09-SRNP-107666, Dissection 148312, USNMENT01441902; Quebrada Bambu, 10.9301, -85.25205, el. 109m: larva on *Lomariopsis vestita*: 09/18/2012, ecl. 10/13/2012, Cirilo Umaña, collector, 12-SRNP-76932, USNMENT01463565; Sector San Cristobal: Estacion San Gerardo, 10.88009, -85.38887, el. 575m: 04/29/2006, H. Cambronero & S. Rios, collector, 06-SRNP-103767, USNMENT01463650; Sendero Carmona, 10.87621, -85.38632, el. 670m: larva on *Thelypteris nicaraguensis*: 05/16/2005, ecl. 06/07/2005, Gloria Sihezar, collector, 05-SRNP-2726, USNMENT01463665. *Females:* Sector Rincon Rain Forest: Sendero Rincon, 10.8962, -85.27769, el. 430m: larva on *Salpichlaena volubilis*: 03/23/2011, ecl. 04/23/2011, Jose Perez, collector, 11-SRNP-41357, USNMENT01463594; Sector Rincon Rain Forest: San Lucas, 10.91847, -85.30338, el. 320m: larva on *Thelypteris nicaraguensis*: 6/8/2011, ecl. 6/27/2011, Jorge Hernandez, collector, 11-SRNP-42773, Dissection 148174, USNMENT01463999; Quebrada Escondida, 10.89928, -85.27486, el. 420m: larva on *Thelypteris nicaraguensis*: 11/16/2010, ecl. 12/16/2010, Anabelle Cordoba, collector, 10-SRNP-44267, USNMENT01463798; Sector San Cristobal: Estacion San Gerardo, 10.88009, -85.38887, el. 575m: 04/30/2006, S. Rios & F. Quesada, collector, 06-SRNP-103899, USNMENT01463696. **Guanacaste Province**: Area de Conservacion Guanacaste (15♂, 7♀): *Males*: Sector Cacao: Cuesta Caimito, 10.8908, -85.47192, el. 640m: larva on *Pteris plumula*: 11/13/2007, ecl. 12/07/2007, Manuel Pereira, collector, 07-SRNP-47084, USNMENT01463600; Sector Cacao: Estacion Gongora, 10.88449, -85.47306, el. 557m: 09/12/2007, R. Franco & S. Rios, collector, 07-SRNP-111179, USNMENT01463585; Sector Cacao: Estacion Gongora, 10.88449, -85.47306, el. 557m: 09/12/2007, R. Franco &
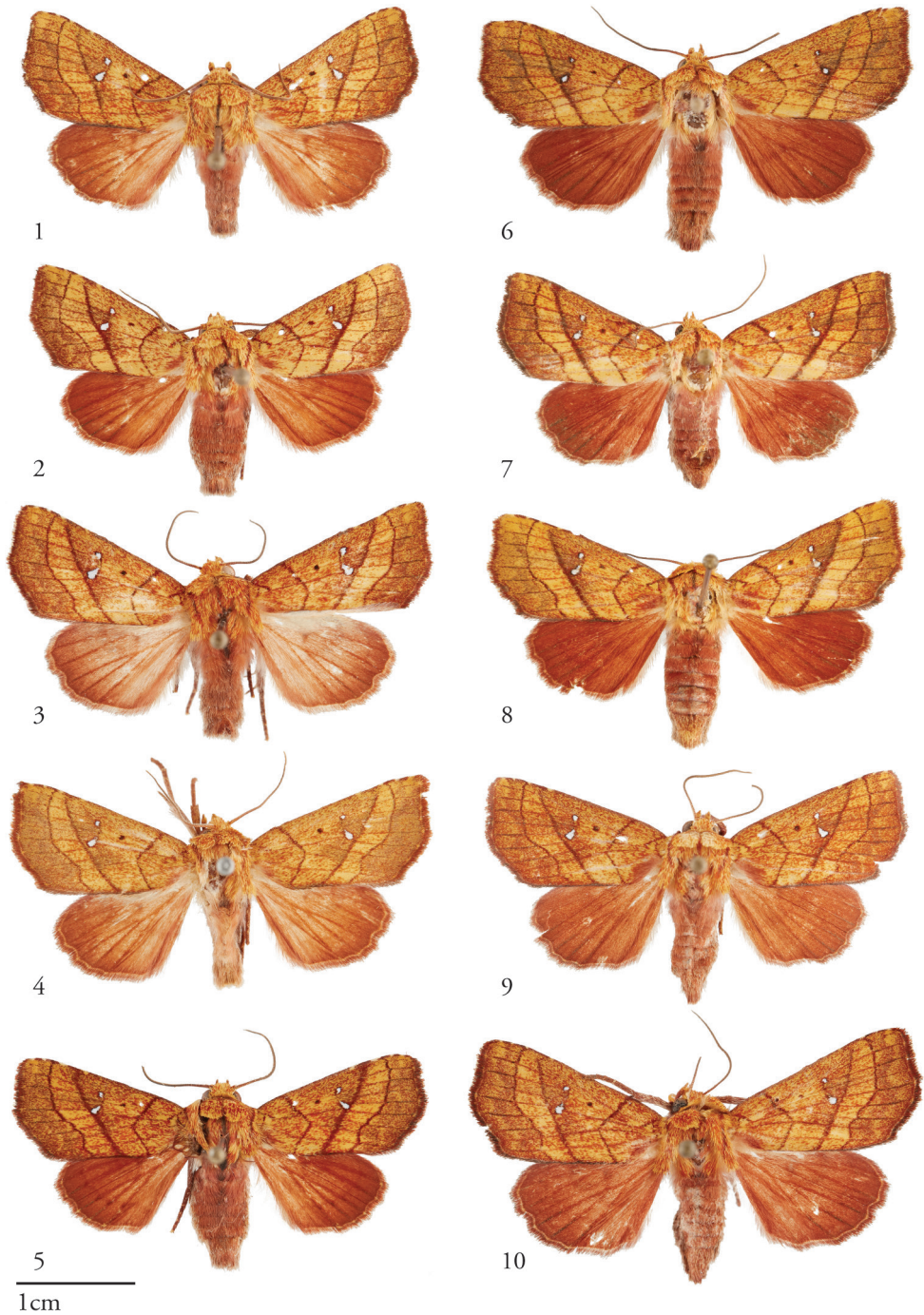
Figures 1–10. Dorsal habitus of *Aprica patula*, males (left, **1–5**) and females (right, **6–10**). **1** USN-MENT01463599, 05-SRNP-48763 **2** USNMENT01463665, 05-SRNP-2726 **3** USNMENT01463894 **4** USNMENT01463893 **5** USNMENT01463658, 14-SRNP-80751 **6** USNMENT01463798, 10-SRNP-44267 **7** USNMENT01463999, 11-SRNP-42773 **8** USNMENT01463895, 07-SRNP-46182 **9** USNMENT01463671, 08-SRNP-104889 **10** USNMENT01463571.
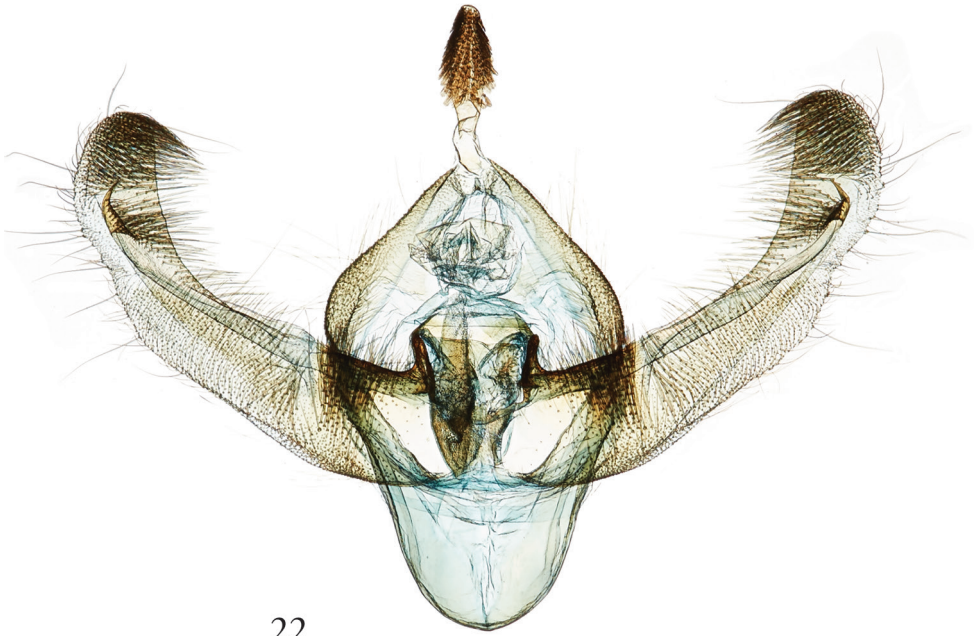
1cm
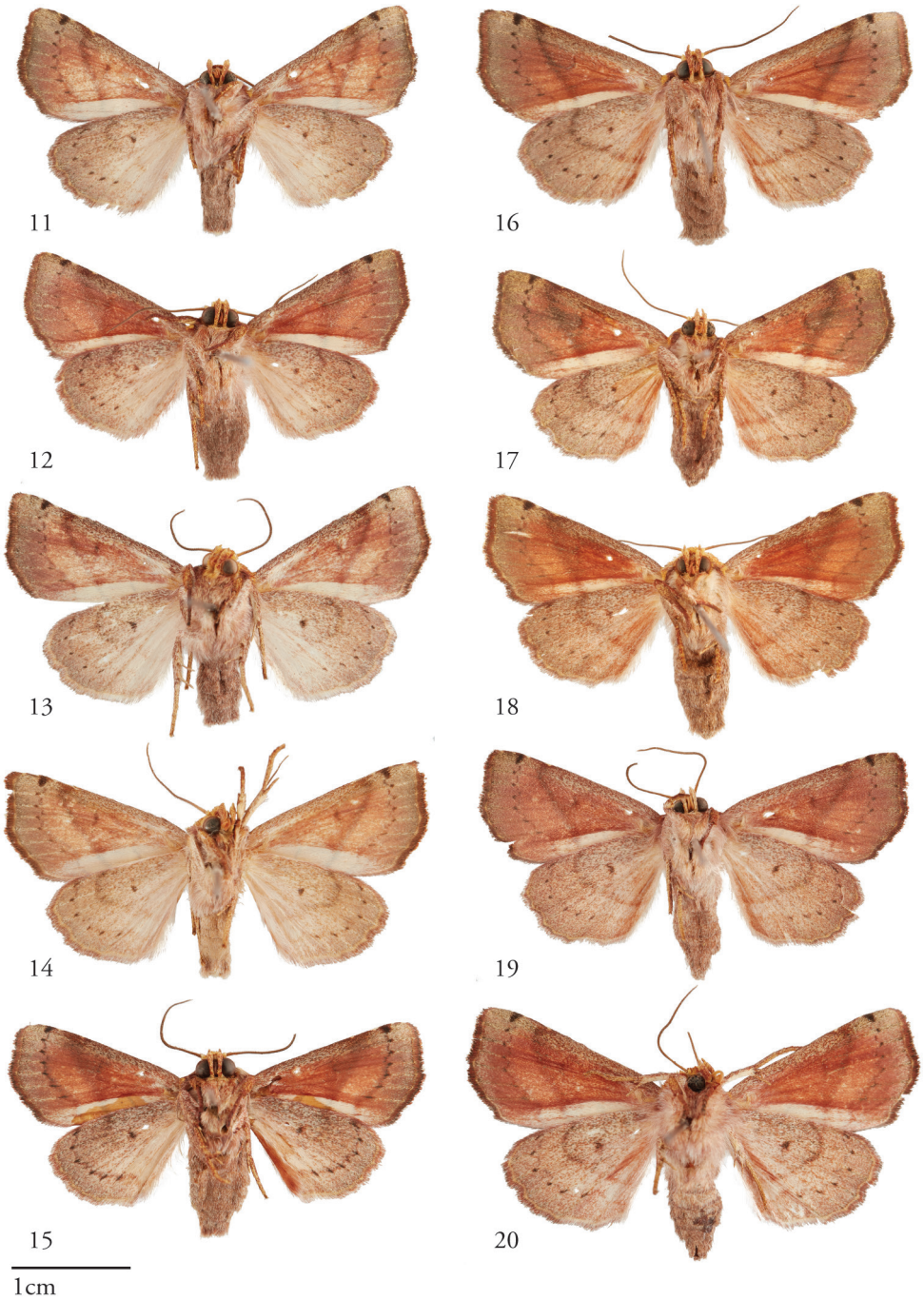
Figures 11–20. Ventral habitus of *Aprica patula*, males (left, **11–15**) and females (right, **16–20**). **11** USN-MENT0146359905-SRNP-48763 **12** USNMENT0146366505-SRNP-2726 **13** USNMENT01463894 **14** USNMENT01463893 **15** USNMENT01463658 14-SRNP-80751 **16** USNMENT01463798 10-SRNP-44267 **17** USNMENT01463999 11-SRNP-42773 **18** USNMENT01463895 07-SRNP-46182 **19** USNMENT01463671 08-SRNP-104889 **20** USNMENT01463571.

S. Rios, collector, 07-SRNP-111178, USNMENT01463617; Sector Cacao: Gongora Bananal, 10.88919, -85.47609, el. 600m: larva on *Pteris plumula*: 10/25/2005, ecl. 11/19/2005, Manuel Pereira, collector, 05-SRNP-48763, USNMENT01463599; Sector Cacao: Quebrada Otilio, 10.88996, -85.47966, el. 550m: larva on *Pteris plumula*: 09/17/2007, ecl. 10/11/2007, Manuel Pereira, collector, 07-SRNP-46183, USNMENT01463543; Sector Cacao: Quebrada Otilio, 10.88996, -85.47966, el. 550m: larva on *Pteris plumula*: 09/17/2007, ecl. 10/08/2007, Manuel Pereira, collector, 07-SRNP-46186, USNMENT01463693; Sector Cacao: Quebrada Otilio, 10.88996, -85.47966, el. 550m: larva on *Pteris plumula*: 09/17/2007, ecl. 10/07/2007, Dunia Garcia, collector, 07-SRNP-46181; Sector Cacao: Toma de Agua, 10.92956, -85.46512, el. 1160m: 08/09/2010, S. Rios & R. Franco, collector, 10-SRNP-112086, USNMENT01463590; Sector Pailas: Canopy Tours, 10.81262, -85.40248, el. 700m: 9/30/2016, H.Cambronero&R.Franco, collector, 16-SRNP-106142, USNMENT01464165; Sector Pailas: Canopy Tours, 10.81262, -85.40248, el. 700m: 06/11/2008, H. Cambronero & F. Quesada, collector, 08-SRNP-103411, USNMENT01463691; Sector Pitilla: Colocho, 11.0256, -85.41224, el. 390m: 03/19/2007, H. Cambronero & F. Quesada, collector, 07-SRNP-102458, USNMENT01463603; Sector Pitilla: Estacion Pitilla, 10.98931, -85.42581, el. 675m: 03/01/2006, S. Rios & R. Franco, collector, 06-SRNP-102362, USNMENT01463573; Sector Pitilla: Estacion Pitilla, 10.98931, -85.42581, el. 675m: 03/02/2006, R. Franco & F. Quesada, collector, 06-SRNP-102550, Dissection 148362, USNMENT01463556; Sector Pitilla: Estacion Quica, 10.99679, -85.39695, el. 487m: 08/29/2008, S. Rios & R. Franco, collector, 08-SRNP-105409, USNMENT01463651; Sector Pitilla: Estacion Quica, 10.99679, -85.39695, el. 487m: 08/29/2008, S. Rios & R. Franco, collector, 08-SRNP-105410, USNMENT01463621. *Females*: Sector Cacao: Quebrada Otilio, 10.88996, -85.47966, el. 550m: larva on *Pteris plumula*: 09/17/2007, ecl. 10/08/2007, Manuel Pereira, collector, 07-SRNP-46187, USNMENT01463536; Sector Cacao: Quebrada Otilio, 10.88996, -85.47966, el. 550m: larva on *Pteris plumula*: 9/17/2007, ecl. 10/8/2007, Manuel Pereira, collector, 07-SRNP-46182, USNMENT01463895; Sector Cacao: Quebrada Otilio, 10.88996, -85.47966, el. 550m: larva on *Pteris plumula*: 09/17/2007, ecl. 10/11/2007, Manuel Pereira, collector, 07-SRNP-46185; Sector Cacao: Quebrada Otilio, 10.88996, -85.47966, el. 550m: larva on *Pteris plumula*: 9/17/2007, ecl. 10/12/2007, Dunia Garcia, collector, 07-SRNP-46180, Dissection 148173, USNMENT01463897; Sector Cacao: Roca Verde, 10.89354, -85.43603, el. 835m: 08/12/2007, R. Franco & F. Quesada, collector, 07-SRNP-108036, USNMENT01463587; Sector Pitilla: Estacion Pitilla, 10.98931, -85.42581, el. 675m: 02/28/2006, S. Rios & H. Cambronero, collector, 06-SRNP-101627, USNMENT01463623; Sector Pitilla: Pasmompa, 11.02666, -85.41026, el. 400m: 07/31/2008, R. Franco & S. Rios, collector, 08-SRNP-104889, USNMENT01463671. **Other** (10♂,4♀): *Males*: COSTA RICA: Juan Vinas, Schaus & Barnes, coll., USNMENT01463893; COSTA RICA: Cartago, Orosi Estacion Tapanti Parque, 9 456' N, -83 471' W, 4062", July 7–9 2008, 1275m, J. Bolling Sullivan, collector, Dissection 148364, USNMENT01463654; same data, USNMENT01463683;
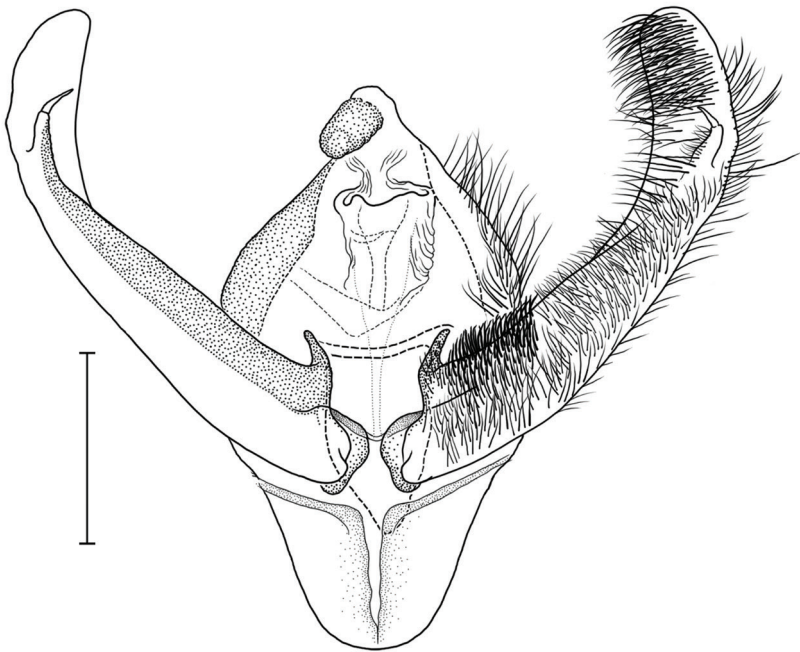
21

Figure 21. Forewing, hind wing. male, USNMENT01463577, Dissection #148371.

same data, USNMENT01463630; COSTA RICA: Cartago, Orosi Estacion, Tapanti Parque, LN-559900-194000, 1275 m, February 12–17, 2005, J. Bolling Sullivan, collector, USNMENT01463894; COSTA RICA: Cartago, Orosi Estacion, Tapani Parque, LN-559900-194000, 1275 m, February 12–17, 2005, J. Bolling Sullivan, collector, Dissection 148371, USNMENT01463577; same data, USNMENT01463681; COSTA RICA: Tuis, May 28–June 4, Schaus and Barnes, collectors, Collection WmSchaus, USNMENT01463564; COSTA RICA: Tuis, June, Schaus and Barnes, collectors, USNMENT01463648; COSTA RICA: San Jose 4000ft, Nov 06, Collection WmSchaus, USNMENT01463535. *Females*: COSTA RICA: Cartago, Orosi Estaction, Tapani Parque, LN-559900-194000, 1275 m, February 12–17, 2005, J. Bolling
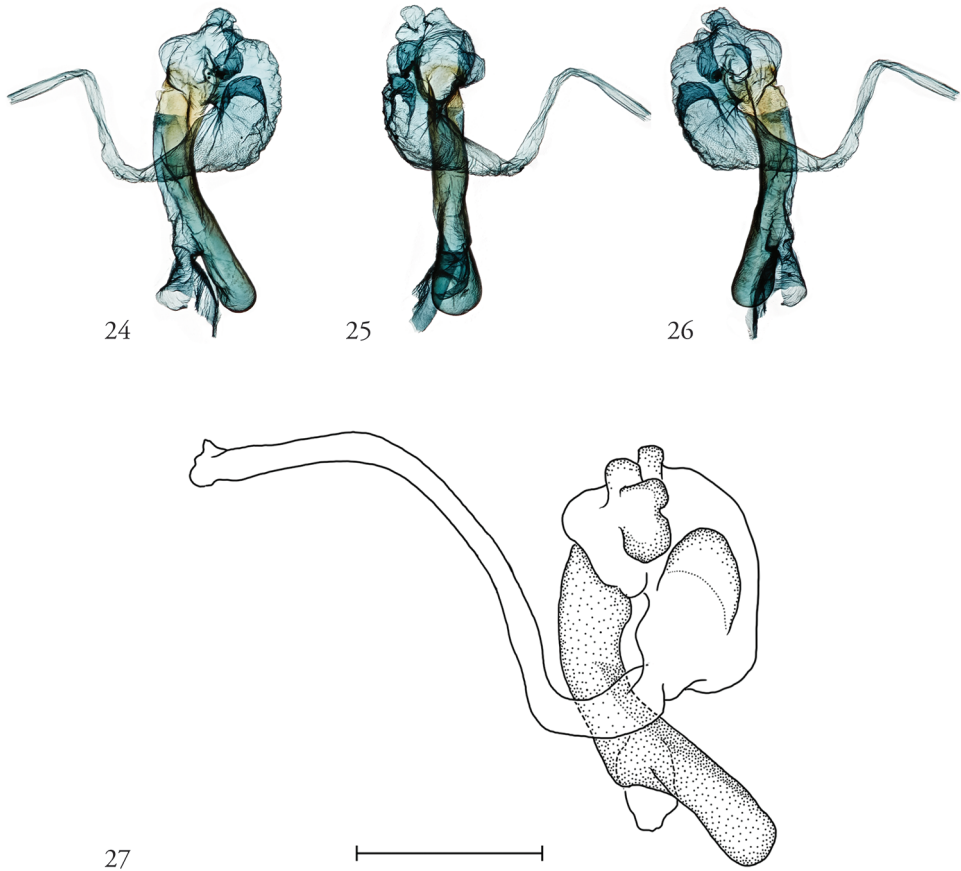
Figures 22, 23. Male genitalia. **22** Valvae, USNMENT01463556, 06-SRNP-102550, Dissection #148362 **23** Valvae (ink) USNMENT01441902, 09-SRNP-107666, Dissection #148312.

Figures 24–27. Male genitalia. **24–26** Vesica, from 3 angles, USNMENT01463556, 06-SRNP-102550, Dissection #148362 **27** Vesica (ink), USNMENT01441902, 09-SRNP-107666, Dissection #148312.

Sullivan, collector, USNMENT01463571; same data, USNMENT01463641; same data, USNMENT01463568; COSTA RICA: Carillo, Schaus and Barnes, collectors, USNMENT01463572. **GUATEMALA** (3♂,1♀): *Males*: GUATEMALA: Cayuga, May, Schaus and Barnes, collectors, USNMENT01463555; GUATEMALA: Cayuga, Sept, Schaus and Barnes, collectors, Dognin Collection, USNMENT01463529; GUATEMALA: Cayuga, Schaus and Barnes, collectors, Aug., Photo Noc.22, USNMENT01463672. *Female*: GUATEMALA: Retalhuleu, from L Thiel, S Sebastian, USNMENT01463544. **MEXICO** (1♂): Zacualpan [Veracruz] T21, USNM slide # 59037, USNMENT01463653.

Diagnosis. The apposition of the forewing and hind wing colors differentiates this species from several unrelated New World species (both tropical and extra-tropical) that share superficially similar orange forewing coloration. None of these has a deep reddish hind wing or the laterally bisected contrast in body coloration between thorax and abdomen. The combination of the expressed M2 on the hind wing, the absence of abdominal
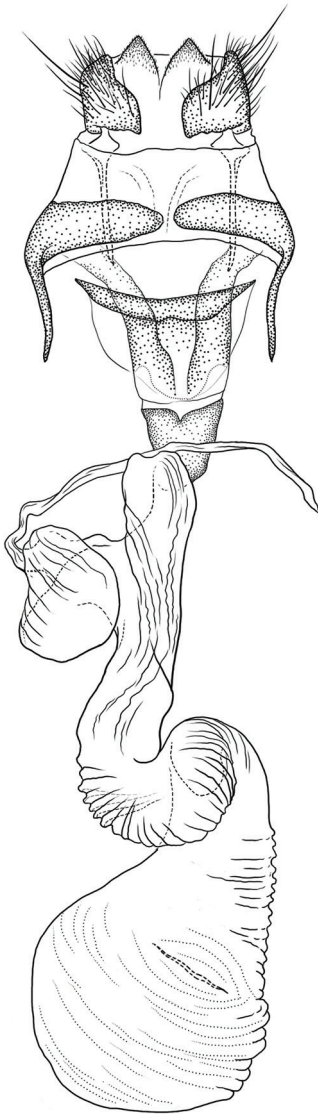
28   29

Figures 28–29. Female genitalia. **29** USNMENT01463999, 11-SRNP-42773, Dissection #148174 (ink) **30** USNMENT01463999, 10-SRNP-46180, Dissection #148173.

coremata, and the configuration of the male and female genitalia are summarized in the generic diagnosis *supra vide* as distinct from Eriopinae and other pteridivorous Noctuidae.

Description. *Head.* Eyes smooth; labial palpi upturned, apex level with antennal base; antennae setose, bifasciculate in males; frons and vertex mix of golden yellow and reddish-orange scales concolorous with those of forewings and thorax.

Thorax. Prothoracic vestiture as described for genus. *Wings*. Forewing length, males, 12.1 mm–15.0 mm (males, $n = 34$, $\bar{x} = 13.5$ mm, M = 13.2 mm); females, 12.1 mm–16.1 mm ($n = 17$, $\bar{x} = 14.2$ mm, M = 14.3 mm). FW not broadly rounded, outer margin convex; FW scaling golden yellow, suffused with reddish-orange scales, some lilacine at costa; postmedial area less heavily suffused with reddish-orange than antemedial or subterminal areas; antemedial, medial, and postmedial lines distinct and unbroken, the medial line ~2× as thick as others; baso-posterior russet patch; reniform spot constricted to form two white stigmata, the antero-costal stigma round and smaller than the other, j-shaped stigma; HW near-uniformly russet-orange, yellowish-orange terminal line unbroken. FW underside russet in center, bounded by paler shading along the costal and posterior margin below the anal vein; pm line jagged, dark gray, fading gradually from costal fascia to the anal vein. HW underside with discal spot present, pm line visible as a series of dark gray spots where it meets the veins; medial lines of both wings diffuse. *Legs*. As above, for genus. Scales the same mix of golden orange and reddish as on the head and thorax, but more uniformly reddish on the fore-femora.

Abdomen. As above, for genus. Vestiture paler than on thorax and concolorous with hind wing.

Male genitalia. As above, for genus. Phallus not uniformly sclerotized, weakly so towards the vesica; vesica without cornuti, with a complex of four bubble-like sub-basal diverticula and one larger basal diverticulum; vesica distended baso-medially, recurved clockwise over the phallus before narrowing and everting in a counter-clockwise twist (Figs 24–27).

Female genitalia. As above, for genus.

Immature stages. Known only from images of living larvae. Larvae are cylindrical, not tapered posteriorly, exhibiting green-brown polymorphism (in some cases the penultimate instar green, ultimate instar brown), and both bear false eyespots on the first abdominal segment; the spot is white postero-ventrally, the front half black with a white dot. In the brown form, the head bears a calico pattern, while in the green form the head is more uniformly green; both forms bear a lateral genal stripe. The brown form is predominantly rusty orange, a pair of subdorsal stripes formed by paler orange wedges. Larvae curl their heads under their abdomens when disturbed, emphasizing their false eyespots. This recall's Yen and Wu's (2009) remarks on the eriopine genus *Callopistria* which "when threatened...bend their abdominal segments A1 and A2 upwards," as do caterpillars in many families. The subdorsal lines in the green larval form comprise a series of irregularly shaped segmental yellow blotches through A6, beneath which runs a series of supra-spiracular spots; a small supra-spiracular black dash may is visible on A4 and A7 as well. The posterior segments, beginning with A7, bear scattered yellow markings.

Biology. Larvae collected in March, May, June, September, October, and November, with adults eclosing in each of the corresponding subsequent months. Recorded times from the onset of pre-pupa to eclosion 15–17 days. Pupation within a cocoon of leaves lightly silked together. Larvae have been collected feeding on the following ferns: *Pteris plumula* Desv. (= *Pteris quadriaurita* Retz., Pteridaceae),

Figures 30–37. Larvae, brown, last instar. **31** USNMENT01463599, 05-SRNP-48763 ♂ DHJ408116 **32** SNMENT01463665 05-SRNP-2726 ♂ DHJ402483 **33** USNMENT01463599, 05-SRNP-48763 ♂ DHJ408117 **34** USNMENT01463599, 05-SRNP-48763 ♂ DHJ408121 **35** USNMENT01463599, 05-SRNP-48763 ♂ DHJ408123 **36** USNMENT01463599, 05-SRNP-48763 ♂ DHJ408124 **37** US-NMENT01463599, 05-SRNP-48763 ♂ DHJ408125 **38** USNMENT01463599, 05-SRNP-48763 ♂ DHJ408126.

Figures 38–45. Larvae, green, penultimate instar. **39** 05-SRNP-48764 DHJ408129 **40** USN-MENT01463798, 10-SRNP-44267 ♀ DHJ478607 **41** 05-SRNP-48764 DHJ408127 **42** USN-MENT01463798, 10-SRNP-44267 ♀ DHJ478603 **43** USNMENT01463798, 10-SRNP-44267 ♀ DHJ478606 **44** USNMENT01463798, 10-SRNP-44267 ♀ DHJ478605 **45** USNMENT01463798, 10-SRNP-44267 ♀ DHJ478608 **46** 05-SRNP-48764 DHJ408128.

Figures 46–53. Young larvae, cocoon and pupa **46–49, 51–53** 14-SRNP-71583 **46** DHJ723850 **47** DHJ723852 **48** DHJ723855 **49** DHJ723892 **50** Ichneumonid cocoon, 11-SRNP-69437, DHJ804089 **51** DHJ723898 **52** DHJ723899 **53** DHJ723901.

Pteridium caudatum (L.) (Dennstaedtiaceae), *Thelypteris nicaraguensis* (E. Fourn.) C.V. Morton (Thelypteridaceae), *Salpichlaena volubilis* (Kauf.) J. Sm. (Blechnaceae), *Lomariopsis vestita* E. Fourn. (Lomariopsidaceae), and *Nephrolepis biserrata* (Sw.) Schott (Davailleaceae). Recorded hymeopteran parasitoids at ACG include *Enicospilus maculipennis* (Cameron, 1886) (Ichneumonidae: Ophioninae) and at least one undescribed ichneumonid (cocoon, Fig. 50). False eyespots on the first abdominal segment appear well developed by the third instar and conspicuous in the green fourth instar as well as the brown last instars. It may be no more than coincidence that all the brown last instars turned out to be males when reared, while all the green penultimate instars turned out to be females when reared.

Distribution. Mid-elevation rainforest Mexico, Guatemala, Costa Rica.

Discussion

Fern-feeding within the Noctuoidea is confined primarily to the Eriopinae, a small number of genera with uncertain placement, and several genera of Herminiinae (Erebidae). The degree to which fern-feeding is more generally conserved phylogenetically has yet to be rigorously tested but see Weintraub et al. (1995) for such an examination in the Lithinini (Geometridae). Within the Noctuidae *sensu stricto*, a precise determination of the number of fern-feeding origins is only now feasible, and enough phylogenetic information exists at least to imply its existence, if not its independent origin, outside the Eriopinae proper. Because of the uncertain placement of several noctuid genera, including *Leucosigma* (Goldstein et al. 2018a), *Lophomyra* (Goldstein et al. 2018b), and *Fagitana* Walker, the number of inferred origins of noctuid fern-feeding might increase with further study.

In addition to the exercise of circumscribing such genera as well as the Eriopinae, questions remain among the higher-level assignments of those with no obvious relatives, including *Aprica*. Although images of larvae reveal certain features common to many fern-feeding caterpillars (green-brown polymorphism, the presence of eyespots on A1, cephalic striping), most of the larval characters discussed by Beck (1960, 1999–2000), Poole (1995), Fibiger and Lafontaine (2005), and Yen and Wu (2009) that could potentially corroborate a higher taxonomic cannot be visualized from available habitus images of living larvae. Adult features considered diagnostic for Eriopinae (e.g., uniquely configured abdominal brushes, eversible saccular coremata, simple membranous corpus bursae without signa) are not observed in *Aprica patula*. Although fern-feeding is phylogenetically localized enough to have flagged this species for examination initially and cast further doubt on its placement in Bagisarinae or Xylenini, it should be noted that Ferguson (1997) removed it from *Bagisara* without the benefit of any life history information, and we detect insufficient evidence among the available data to place it with Eriopinae.

Provisional DNA barcode analyses suggest a possible kinship of *Aprica* with *Fagitana*, but these data are not adequate to corroborate their kinship in the absence

of other characters, particularly among the larvae. It warrants mention in part because, like *Aprica*, the phylogenetic placement of *Fagitana* is uncertain; it is a ditypic genus comprising the well-characterized North American species *littera* associated with ferns in at least three of the same families as hosts of *Aprica* (Blechnaceae, Thelypteridaceae, Dennstaedtiaceae) and a rather dissimilar Asian species *gigantea* (Draudt, 1950) with an unknown life history. While *Aprica* and *Fagitana* share the unusual larval fern-feeding behavior with known Eriopinae, this is insufficient to unite them given the absence of published diagnostic eriopine genitalic features. Although we find it less than ideal to have created a monotypic genus, *Aprica*, these discrepancies combined with the absence of larval characters and more extensive phylogenetic data render its placement elsewhere difficult to support, and its higher placement at best ambiguous.

Acknowledgments

References

Beck H (1960) Die Larvalsystematik der Eulen (Noctuidae).Akademie Verlag, Berlin, 406 pp.

Beck H (1999–2000) Die Larven der Europäischen Noctuidae. Vol. 1–4: Text (1); Illustrations (2–4). Herbipolitana. Buchreihe zur Lepidopterologie. Band 5/1: 859 pp.

Ferguson DC (1997) Review of the New World Bagisarinae with description of two new species from the Southern United States (Noctuidae). Journal of the Lepidopterists' Society 51(4): 344–357.

Fibiger M, Lafontaine JD (2005) A review of the higher classification of the Noctuoidea (Lepidoptera) with special reference to the Holarctic fauna. Esperiana Band 11: 7–92

Forbes WTM (1954) The Lepidoptera of New York and Neighboring States. III. Noctuidae. Memoir 329, Cornell University Agricultural Experiment Station, Ithaca, New York.

Godman FD, Salvin O (1898) Biologia Centrali-Americana; or Contributions to the Knowledge of the Fauna of Mexico and Central America. Zoology. Lepidoptera. Heterocera by H. Druce. Volume 2. Taylor and Francis, London, 692 pp. [pls 65–101]

Goldstein PZ, Janzen DH, Hallwachs W, Proshek B, Dapkey T (2018a) A review of *Leucosigma* Druce, 1908 (Lepidoptera, Noctuidae): A newly discovered case of fern-feeding and a description of three new species. ZooKeys 788: 87–133. https://doi.org/10.3897/zookeys.788.21222.figures105-110

Goldstein PZ, Janzen DH, Hallwachs W, Proshek B, Dapkey T (2018b) Review of *Lophomyra* Schaus, 1911 (Lepidoptera: Noctuidae): A new combination and re-descriptions of species newly associated with ferns (Polypodiaceae). ZooKeys 788: 135–165. https://doi.org/10.3897/zookeys.788.21235

Hampson GF (1908) On the moths collected during the cruise of the 'Valhalla' during winter 1905–6 by Mr. E.G.B. Meade-Waldo. Annals and Magazine of Natural History, series 8, 1: 474–492.

Jaeger CM (2017) Phylogeny of Tortricidae (Lepidoptera): A morphological approach with enhanced whole mount techniques. Masters Thesis, Mississippi State University, 117 pp.

Janzen DH, Hallwachs W (2011) Joining inventory by parataxonomists with DNA barcoding of a large complex tropical conserved wildland in northwestern Costa Rica. PLoS ONE 6 (8): e18123. https://doi.org/10.1371/journal.pone.0018123

Janzen DH, Hallwachs W (2016) DNA barcoding the Lepidoptera inventory of a large complex tropical conserved wildland, Area de Conservacion Guanacaste, northwestern Costa Rica. Genome 59: 641–660. https://doi.org/10.1139/gen-2016-0005

Kitching IJ, Rawlins JE (1999[1998]) The Noctuoidea [355–401]. In Kristensen NP (Ed.) Lepidoptera: Moths and Butterflies. Volume 1: Evolution, systematics, and biogeography. Handbook of Zoology/Handbuch der Zoologie. Walter de Gruyter, Berlin/New York, 491 pp.

Lafontaine JD (1998) The Moths of America North of Mexico (Fascicle 27.3.) – Noctuoidea, Noctuidae (part): Noctuinae, Noctuini. Wedge Entomological Research Foundation, Washington, DC, 348 pp.

Lafontaine JD (2004) The Moths of America North of Mexico (Fascicle 27.1.) – Noctuoidea, Noctuidae (part): Noctuinae, Agrotini. Wedge Entomological Research Foundation, Washington, DC, 385 pp.

Poole RW (1989) Lepidopterorum Catalogus (New Series, Fasc. 118 Noctuidae Part 1. EJ Brill, New York.

Poole RW (1995) Noctuioidea: Noctuidae (part), Cuculliinae, Stiriinae, Psaphidinae (Part). In RB Dominick et al. (Eds) The Moths of America North of Mexico Fasc. 26.: The Wedge Entomological Research Foundation, Washington, DC, 249 pp.

Weintraub JD, Lawton JH, Scoble MJ (1995) Lithinine moths on ferns: a phylogenetic study of insect-plant interactions. Biological Journal of the Linnean Society 55: 239–250. https://doi.org/10.1111/j.1095-8312.1995.tb01062.x

Yen S-H, Wu S (2009) Biota Taiwanica. Hexapoda: Lepidoptera, Noctuoidea, Noctuidae, Eriopinae. National Sun Yat-Sen University & National Science Council, 60 pp. [xvi, pls 1–20]